UNIVERSITAT DE BARCELONA

# Fenton and Photo-Fenton like at neutral pH for the removal of emerging contaminants in water and wastewater effluents

Antonella De Luca

UNIVERSITAT DE BARCELONA

Programa de doctorat d'*Enginyeria i Tecnologies Avançades*

# FENTON AND PHOTO-FENTON LIKE AT NEUTRAL PH FOR THE REMOVAL OF EMERGING CONTAMINANTS IN WATER AND WASTEWATER EFFLUENTS

**Antonella De Luca**

*Directors:*
Dr. Santiago Esplugas Vidal i Dr. Renato Falcao Dantas
Departament de Química Analítica i Enginyeria Química
Universitat de Barcelona

El Dr. SANTIAGO ESPLUGAS VIDAL, catedràtic del Departament de Química Analítica i Enginyeria Química de la Universitat de Barcelona i el Dr. RENATO FALCAO DANTAS,

CERTIFIQUEN QUE:

El treball d'investigació titulat "FENTON AND PHOTO-FENTON LIKE AT NEUTRAL PH FOR THE REMOVAL OF EMERGING CONTAMINANTS IN WATER AND WASTEWATER EFFLUENTS" constitueix la memòria que presenta la Enginyera Civil Antonella De Luca per a aspirar al grau de Doctor per la Universitat de Barcelona. Aquesta tesi doctoral ha estat realitzada dins del programa de doctorat "Enginyeria i Tecnologies Avançades", en el Departament de Química Analítica i Enginyeria Química de la Universitat de Barcelona.

I perquè així consti als efectes oportuns, signen el present certificat a Barcelona, 4 de Juliol 2016.

Dr. Santiago Esplugas Vidal i Dr. Renato Falcao Dantas

*Directors de la tesi doctoral*

*“[...] mantenendo intatto, sino all’ultimo,*

*l’interesse per la ricerca*

*intesa come strumento di conoscenza*

*e non come oggetto di competizione*

*e strumento di potere.[...]”*

*Rita Levi-Montalcini*

*“The science of today is the technology of tomorrow”*

*Edward Teller*

## Acknowledgements

The gratitude I feel in regard to all those who shared with me these five years cannot be summarized in only one page. I personally trust that no words are needed to prove love and affection and I like to think that you all know how grateful I am. Anyway, I will spend some words…

First at all, I would like to thank Prof. Santiago Esplugas for welcoming me in his research group, for believing in me and to make possible my personal and professional growth…without the opportunity he willed me, I would have not been who I am today! Thanks also to Dr. Renato F. Dantas for having been at the same time supervisor and friend.

I would like to thank Prof. Carme Sans from which enthusiasm and dedication, I could appreciate during our collaborations, I took the cue for loving the research. I cannot avoid also thanking Prof. Carmen Gonzalez, especially for the precious help and support she gave me in carrying the heavy weight of the bureaucracy. Thanks to Prof. Pilar Marco and Prof. Jaume Giménez for the help they never refused to give me.

I would also like to mention my gratitude to Prof. Dionysios D. Dionysiou and Dr. Xuexiang He for the incredible willingness they demonstrated during my stay at the University of Cincinnati. In the same way, thanks to Prof. Mohamed Gamal El-Din, Dr. Nikolaus Klamerth and Dr. Leonidas Perez-Estrada for kindly welcoming me at the Univerity of Alberta.

Un grazie speciale va a l'Ing. Giusy Lofrano, la mia mentore, che in tutti questi anni non ha mai smesso di rendermi consapevole dell'enorme fiducia che ripone nelle mie potenzialità.

Gracias de todo corazón a todos aquellos que durante aquestos años han sido mi familia aquí en Catalunya: a Mireia, amiga, confidente y casi podría decir hermana; a Roger y Nardi por escucharme y aconsejarme; a Angel, Ana, Núria, Oscar, Xavi y Isaac por estar siempre y cuando lo necesitara; gracias también a Marc, Meme, Mari, Albert, Vio, Dani, Maycoll, Sergi, Miriam, Sipi, Xavi y Anna porque estos años no habrían sido lo mismo sin todos vosotros. Los bonitos recuerdos de los momentos vividos juntos ocuparan siempre un lugar especial en mi corazón. Gracias también a Rodrigo y Daniel, cuyo cariño no sufre los kilómetros de mar y tierra que nos separan.

Grazie a Zia, Jenny, Sabrina, Ale, Laura, Roby e tutti i miei amici che nonostante lontani non mi hanno mai fatto mancare quell'affetto che ha il sapore di casa.

Thanks to Marc, my future, which presence and support gave me the motivation to be here today writing the last page of my PhD thesis.

Per ultimo ma sicuramente primo in ordine di importanza, il mio grazie più speciale. Grazie a mamma e papà, esempio di sacrificio e dedizione, umiltà e amore: tutto quello che sono è il vostro frutto. Grazie alle mie sorelline e il mio fratellone, i miei pilastri e il dono più grande e prezioso della mia vita. Grazie per aver sempre organizzato i vostri weekend in funzione dei miei biglietti aerei e per non avermi mai fatto mancare il sostegno e l'affetto che da trent'anni sono il motore di ogni mio successo. Infine, grazie a Emilia e Marco per essere parte di questa nostra "famiglia di pazzi" e a Miriam, la stellina che illumina la nostra famiglia.

I wish to thank the Ministry of Science and Innovation of Spain (projects CTQ2011-26258 and CTQ2014-52607-R and Consolider-Ingenio 2010 CSD2007-00055) for their financial support and the Spanish Ministry of Economy and Competitiveness (FPI research fellowship, Ref. BES-2012-053177).

## List of Contents

## List of Figures

## List of Tables

## ABSTRACT

In the last decades, the scientific community has been involved in the research of new kinds of contaminants generally known as of “emerging concern” (CECs). The harmfulness of CECs, even at small concentrations as well as, property of bioaccumulation and persistence, makes them extremely dangerous for the human health. The scientific community is constantly researching about novel treatments able to achieve the removal of these contaminants.

Advanced Oxidation Processes (AOPs) are considered one of the most useful treatments to achieve CECs degradation. Among the AOPs, Fenton and photo-Fenton processes are particularly powerful, cheap and easily managed. Nevertheless, some setting requirements of Fenton processes have limited their application at industrial scale. One of the most important limits is the necessity to operate a tight control of the pH in order to avoid iron precipitation (optimum pH~2.8). Unfortunately, the optimum pH for Fenton reaction is essentially far from the normal values of the wastewater treatment plant (WWTP) effluents. Scientific community is then working on the improvement of the operating conditions of Fenton processes in order to improve the applicability in wastewater treatment. These modifications are essentially focused on the possibility to perform the treatment at circumneutral pH (Fenton and photo-Fenton like processes). Fenton like processes can be carried out in heterogeneous or homogeneous way according to the phase of the catalyst into the solution.

In this study was firstly confirmed the suitability of Fenton based processes in recalcitrant compounds removal. Fenton, UV-A photo-Fenton and UV-C photo-Fenton were, in fact, applied for atrazine removal from secondary effluent (SE) of municipal wastewater treatment plant (MWWTP). UV-A and UV-C photo-Fenton allowed remove 50% and 100% of the initial atrazine content respectively.

The main objective of this thesis was then the assessment of photo-Fenton’s suitability for recalcitrant contaminant at circumneutral pH. Thus, homogeneous photo-Fenton like at neutral pH was applied for sulfamethoxazole (SMX) removal. In order to avoid iron precipitation, chelating agents were used to keep soluble the iron at circumneutral pH. The chelating ability of four chelating agents (ethylenediaminetetraacetic acid-EDTA, nitrilotriacetic acid-NTA, oxalic acid and tartaric acid) was tested. Then, once determined the optimum molar ratio L:Fe for iron chelation (1.5:1 for EDTA and NTA, 10:1 for tartaric acid and 20:1 for oxalic acid), their catalytic activity was evaluated when employed in photo-Fenton like for SMX removal. The highest SMX percentage removal, together with the minimum chelating agents required and the better property of biodegradability and low toxicity, demonstrated the suitability of NTA for the purpose.

A further study on the stability of the chelates under reaction was carried out. The operating conditions adopted for the treatment significantly influence the stability of the chelate solution. Thus, in order to proper control the parameter set up the behavior of chelates has been study under thermal, oxidative and photochemical stress. It was demonstrated as the temperature control can represent an interesting tool to extend the chelates lifetime under oxidative and photochemical stress. By adopting different $H_2O_2$ doses, a linear correlation

between doses and chelate decomposition could be identified. The better suitability of UV-A irradiation, against UV-C and Xe lamp, to preserve the iron chelate solution was demonstrated.

Moreover, the influence of the influent characteristics on the process efficiency needed to be also considered. Thus, different water matrices were used for the experiments. The efficiency of photo-Fenton like catalyzed by Fe(III)-NTA has been compared when applied to different aqueous matrixes (Milli-Q water, tap water, secondary effluent wastewater and well water. it was demonstrated as the ions content, especially $Ca^{2+}$ and $Mg^{2+}$, significantly compromise the process of chelation. High alkalinities and organic matter, instead, mainly influenced the phase of process, when acting as radicals scavengers, reduced the amount available for SMX oxidation. Iron chelate dosage was performed in order to limit the interference due to the water composition but in the conditions adopted, this strategy did not succeed. Other strategies were then adopted to promote SMX removal. Between them, $Mn^{2+}$ mediated photo-Fenton like showed somehow possibility for improvement. Highest removal rate was in fact exhibited in the first minutes of reaction when adding $Mn^{2+}$ to the solution in ratio molar Mn:Fe 0.5:1.

Finally, the conclusive study of the thesis regarded the assessment of the $Br^-$ presence on the efficiency achievable in recalcitrant compounds removal when applying UV/PS/$Fe^{2+}$ for removal of benzophenone-4 (BZ4), nitrobenzene (NB), nitrobenzoic acid (NBA), atrazine (ATZ) and ampicilline (AMP). $Br^-$ demostrated to be a strong inhibitor in the removal of all the considered contaminants except for NB. In this case, the removal was significantly enhanced in bromide containing water.

# THESIS DIRECTOR'S REPORT AND LIST OF PUBLICATIONS

Departament de Química Analítica i Enginyeria Química
Facultat de Química
Universitat de Barcelona
C/Martí i Franquès, 1
08028 Barcelona, España

Dr. SANTIAGO ESPLUGAS VIDAL, Professor from the Chemical Engineering Department of the University of Barcelona, and Dr. RENATO FALCAO DANTAS, Professor at the University of Campinas (Brazil), and both directors of the PhD thesis of Antonella De Luca, issues the following report related with her participation in the publications derived from this PhD thesis:

The experimental work and results discussion included in the publications and Congresses communications included in this thesis was mainly developed in the Chemical Engineering Department of the University of Barcelona by Antonella De Luca, under the supervision of her PhD directors. Part was also developed at the University of Cincinnati under the supervision of Prof. Diounysiou. The publications included in this thesis were not presented in other doctoral thesis or a thesis presented as a summary of publications.

I. De Luca, A., Dantas, R.F., Simoes, A.S.M., Toscano, I.A.S., Lofrano, G., Cruz, A., Esplugas, S., 2013. *Atrazine removal in municipal secondary effluents by Fenton and photo-Fenton treatments*. Chemical Engineering and Technology, 36 (12), 2013, 2155-2162. doi: 10.1002/ceat.201300135

II. De Luca, A., Dantas, R.F., Esplugas, S., *Assessment of iron chelate efficiency for photo-Fenton at neutral pH.* Water Research, 61, 2014, 232-242. doi:10.1016/j.watres.2014.05.033

III. De Luca, A., Dantas, R.F., Esplugas, S., *Study of Fe(III)-NTA chelates stability for applicability in photo-Fenton at neutral pH*. Applied Catalysis B: Environmental., 179, 2015, 372–379. doi:10.1016/j.apcatb.2015.05.025

IV. De Luca, A., He, X., Dionysiou, D.D., Dantas, R.F., Esplugas, S., *Effects of Bromide on the Degradation of Organic Contaminants with UV and $Fe^{2+}$ Activated Persulfate.* Chemical Engineering Journal, In press, doi:10.1016/j.cej.2016.06.066

Below, a detailed list including the impact factor (IF) and subject categories of the journals were the author of this thesis published her works is presented (data obtained from *Journal Citation Report®*, 2015).

- Applied Catalysis B: Environmental (IF: 8.328)

| Category Name | Quartile in Category |
|---|---|
| Chemistry, Physical | Q1 |
| Engineering, Environmental | Q1 |
| Engineering, Chemical | Q1 |

- Water Research (IF: 5.991)

| Category Name | Quartile in Category |
|---|---|
| Engineering, Environmental | Q1 |
| Environmental Sciences | Q1 |
| Water resources | Q1 |

- Chemical Engineering Journal (IF: 5.310)

| Category Name | Quartile in Category |
|---|---|
| Engineering, Environmental | Q1 |
| Engineering, Chemical | Q1 |

- Chemical Engineering and Technology (IF: 2.385)

| Category Name | Quartile in Category |
|---|---|
| Engineering, Chemical | Q2 |

Dr. Santiago Esplugas Vidal and Dr. Renato Falcao Dantas

Barcelona, 4rd of July 2016

# NOMENCLATURE

| | |
|---|---|
| AOPs | Advanced Oxidation Processes |
| AMP | Ampicillin |
| ATZ | Atrazine |
| BLB | Black light blue lamps |
| $BOD_5$ | Biochemical Oxygen Demand at 5 days ($mgO_2\ L^{-1}$) |
| CECs | Contaminants of Emerging Concern |
| COD | Chemical Oxygen Demand ($mgO_2\ L^{-1}$) |
| CPC | Compound parabolic collector |
| DOC | Dissolved Organic Carbon ($mg\ L^{-1}$) |
| E | Energy |
| $E_{E,mix}$ | Electrical energy for mixing ($Wh\ L^{-1}$) |
| $E_{E,pro}$ | Electrical energy for irradiation ($Wh\ L^{-1}$) |
| $E_{E,\ chem}$ | Cost of reagents converted to energy ($Wh\ L^{-1}$) |
| $E_{E,tot}$ | Total electrical energy ($Wh\ L^{-1}$) |
| $E_{EO,rx}$ | Electrical energy for irradiation per order of magnitude ($Wh\ (L{\cdot}order)^{-1}$) |
| $E_{EO,tot}$ | Total electrical energy per order of magnitude ($Wh\ (L{\cdot}order)^{-1}$) |
| $EC_{50}$ | The median effective concentration |
| hv | Radiation |
| HPLC | High Performance Liquid Chromatograph |
| $k_{obs}$ | Observed pseudo-first order kinetic constant ($min^{-1}$) |
| LOD | Limit of Detection |
| LOQ | Limit of Quantification |
| LP-UV | Low Pressure UV |
| MP-UV | Middle Pressure UV |
| NB | Nitrobenzene |
| NBA | Nitrobenzoic acid |

| | |
|---|---|
| NOM | Natural Organic Matter |
| NPOC | Non-purgeable Organic Carbon (mg $L^{-1}$) |
| POC | Particulate Organic Carbon (mg $L^{-1}$) |
| pKa | Dissociation constant |
| PMS | Peroxymonosulfate |
| PR | Photo-reactor |
| PS | Persulfate |
| P-UV | Pulsed UV |
| $Q_{UV}$ | Accumulated energy for UV irradiation(kJ$L^{-1}$) |
| RH | Organic compounds |
| SAE | Solar accumulative energy |
| SE | Secondary Effluent |
| SMX | Sulfamethoxazole |
| THMs | Trihalomethanes |
| TOC | Total Organic Carbon (mg $L^{-1}$) |
| UV | Ultraviolet light |
| UV-A | Ultraviolet light range 315-400 nm |
| UV-B | Ultraviolet light range 280-315 nm |
| UV-C | Ultraviolet light range 200-280 nm |
| UV-Vis | Ultraviolet visible |
| VUV | Vacuum ultraviolet |
| WW | Wastewater |
| WWTP | Wastewater Treatment Plant |
| ZVI | Zerovalent iron |

Greek letters

| | |
|---|---|
| $\phi$ | Quantum yield |

| | |
|---|---|
| λ | Irradiation wavelength (nm) |

Acronyms

| | |
|---|---|
| CAS | Chemical Abstract Service |
| ECO-CMX | Council of the States-Cross Media Committee |
| EPA | Environmental Protection Agency |
| EU | European Union |
| UNESCO | United Nations Educational, Scientific and Cultural Organization |
| UNICEF | United Nations Children's Fund |
| US | United States |
| WHO | World Health Organization |
| WWAP | World Water Assessment Programme |
| WTD | Water Framework Directive |

# 1 INTRODUCTION

## 1.1 Water resources

*"There is a water crisis today. But the crisis is not about having too little water to satisfy our needs. It is a crisis of managing water so badly that billions of people - and the environment - suffer badly."* (World Water Council).

Since 1990, almost 2 billion people globally have gained access to improved sanitation, and 2.3 billion have gained access to drinking-water from improved sources. Some 1.6 billion of these people have piped water connections in their homes or compounds, according to a new WHO/UNICEF report which also highlights a narrowing disparity in access to cleaner water and better sanitation between rural and urban areas (WHO/UNICEF 2014). More than half of the global population lives in cities, and urban areas are still better supplied with improved water and sanitation than rural ones. But the gap is decreasing. In 1990, more than 76% people living in urban areas had access to improved sanitation, as opposed to only 28% in rural ones. In 1990, 95% people in urban areas could drink improved water, compared with 62% people in rural ones. By 2012, 96% people living in towns and 82% of those in rural areas had access to improved water (WHO/UNICEF 2014).

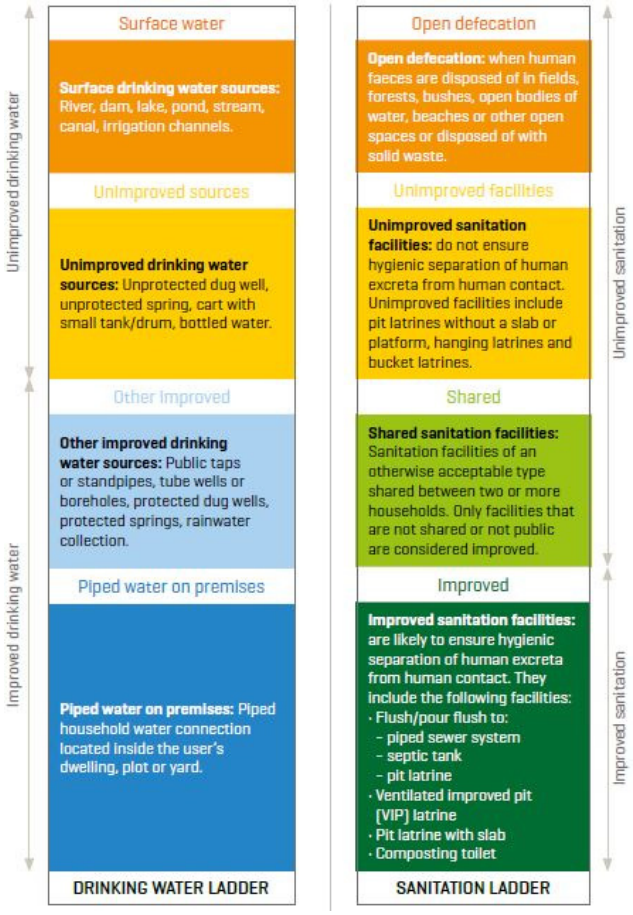


**Figure 1 Progresses and gap in water sanitation and drinking water access (WHO/UNICEF 2014)**

Despite this progress, sharp geographic, socio-cultural, and economic inequalities in access to improved drinking water and sanitation facilities still persist around the world. In addition to

the disparities between urban and rural areas, there are often also striking differences in access within towns and cities. People living in low-income, informal or illegal settlements or on the outskirts of cities or small towns are less likely to have access to an improved water supply or better sanitation (Figure 1, (WHO/UNICEF 2014).

Moreover, 884 million people still live without safe drinking water and 2.6 billion (two in five) do not have adequate sanitation. Poor sanitation and contaminated water are linked to transmission of diseases such as cholera, diarrhea, dysentery, hepatitis A, and typhoid. In addition, inadequate or absent water and sanitation services in health care facilities put already vulnerable patients at additional risk of infection and disease (3.5 million people die prematurely each year from water-related diseases) (World Water Council 2015).

The difficult scenario of water accessibility is aggravated by the scarcity of available water (Figure 2) due to the climate change and the growing exploitation of the available resources. The global population is projected to reach 9 billion by 2050 – an increase of 4 billion over the level in 1990. Water use has been growing at more than twice the rate of population increase in the last century, and, although there is no global water scarcity as such, an increasing number of regions are chronically short of water. Water scarcity is both a natural and a human-made phenomenon. There is enough freshwater on the planet for seven billion people but it is distributed unevenly and too much of it is wasted, polluted and unsustainably managed. Population growth and accelerating economies mean greater demand for energy and food, further increasing the pressure on limited water and land, while creating the opportunity for new technology to use water more efficiently (World Water Council 2015).

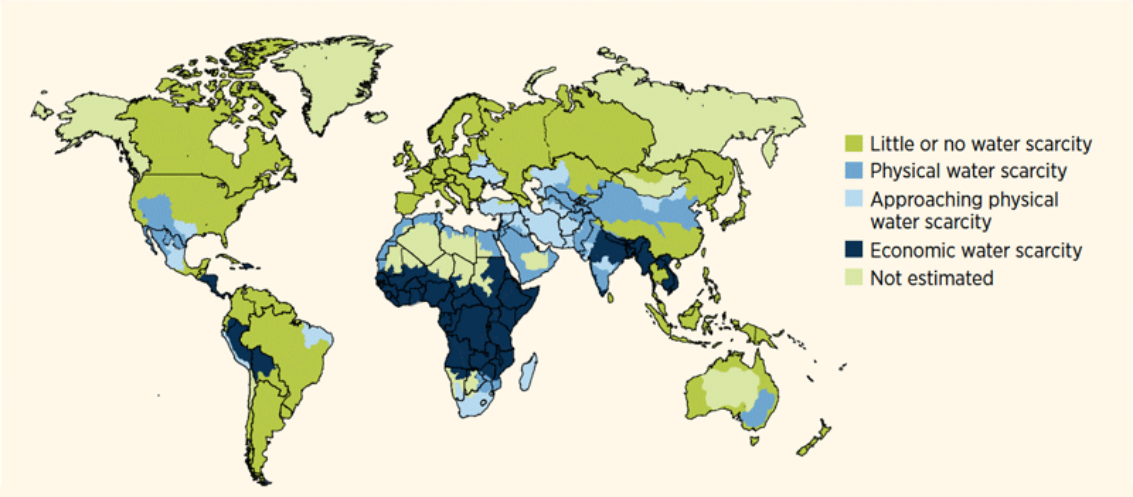


**Figure 2 Water stress versus water scarcity (UNESCO and WWAP 2012)**

Big efforts are required to face the problem of water scarcity around the world. There is no winning solution, only the combined effort from different sectors can help to find the solution or eventually to, at least, reduce the pressure and build a path toward a different future.

## 1.2 Contaminated water and water reuse

In the field of Environmental Engineering a possible contribution to facing the problem of water scarcity is the implementation of adequate treatment able to reduce the impact on the water system and eventually make possible the reutilization of sanitized water.

Additionally to the global water scarcity, the release of pollutants with potential to harm both humans and the environment into water bodies is the biggest threat to the world's freshwater supplies. In this context, wastewater treatment plants (WWTPs) are finalized to minimize the environmental impact of discharging untreated water into natural water systems (Meneses et al. 2010). However, the complexity of the affluent to a wastewater treatment plants, makes impossible the definition of an univocal scheme of treatment. Thus, sometimes a conventional process' scheme for water treatment might not be proper to remove the pollution charge. Then the risk of contact of humans and living beings with contaminated effluent might result increased. In other words, when there are no adequate treatments units, wastewater treatment plants could be identified as a major source of these compounds to the environment (Glassmeyer et al. 2005; Clara et al. 2005). To prevent this, a specific assessment of the influent quality should be done. Consequently, it could be necessary to provide WWTPs of specific treatments able to degrade recalcitrant contaminant that can't be removed by conventional treatments, especially when reuse is aimed.

The conventional WWTPs consist of two levels of treatment: preliminary and primary (physical and chemical), and secondary (biological) treatment. These treatments may reduce: suspended solids, biodegradable organics, pathogenic bacteria and nutrients. Besides, as sustainability is promoted within the water cycle, the functions of WWTPs also should be to recover: water resources (reclaimed water), energy (methane from anaerobic digestion) and materials (biosolids and nutrients). This treated wastewater is usually discharge into the sea or rivers but not used for reuse purposes. Also a WWTP may get a resource from wastewater carrying out a tertiary treatment on the treated wastewater which can be, then, reused (Meneses et al. 2010).

The main objective of wastewater reclamation and reuse projects is to produce water of sufficient quality for all non-potable uses (uses that do not require drinking water quality standards). Using reclaimed water for these applications would save significant volumes of freshwater that would otherwise be wasted (Iglesias Esteban and Ortega de Miguel 2008; Meneses et al. 2010). Reclaimed water can replace freshwater in traditional practices such as agricultural and landscape irrigation, industrial applications, environmental applications (surface water replenishment, and groundwater recharge), recreational activities, urban cleaning, firefighting, construction, etc. (Petala et al. 2006; Yang and Abbaspour 2007; Meneses et al. 2010).

Spain Royal Decree 1620/2007 is nowadays the principal water reuse regulation for Spain. It established the legal regime for the reuse of treated water, including the basic conditions for reuse of treated water, quality standards and the proceedings for initiatives or plans from public authorities' initiatives. It represented an important advance to standardize water reuse practices despite the large cost of implementation. It contributed to the consolidation of water reuse inside the global water resources management (Iglesias et al. 2010). Central and autonomic governments have been doing noticeably efforts to spread the reuse of reclaimed water for the last two decades. These initiatives were finally recognized, reunited and organized in 2009 under a nationwide project entitled: "Plan Nacional de Reutilización de Aguas". The objectives of the plan were both strategic and environmental. The main strategic aims were: achieve "zero discharge" objective in coastal areas; replace inland areas pre-

potable water concessions by reclaimed water for uses where feasible; promote good practices of reuse of reclaimed water, estimate future reusability, etc. As environmental objectives, the plan envisaged the change from the traditional approach of "supply", founded on the basis of large hydraulic infrastructures, to new strategies of water resources "on demand management" and the protection of inland and coastal estuaries ecosystems (Agriculture Ministry of Spain). The plan covered the entire Spanish territory and its application reached horizon until 2015. However, after the change of government in late 2011 and the economic crisis, the plan seems to have stopped. More detailed information on the legal framework of water will be given afterwards.

## 1.3 General legal framework of water

### *1.3.1 Directive 2000/60/CE*

To protect our water resources and the water environment since 2000 the Water Framework Directive (WFD) has been in place as the main European legislation. It requires managing the water so that its quality and quantity does not affect the ecological services of any specific water body.

The purpose of this Directive is to establish a framework for the protection of inland surface waters, transitional waters, coastal waters and groundwater, which:

- Prevents further deterioration and protects and enhances the status of aquatic ecosystems.
- Promotes sustainable water use based on a long-term protection of available water resources.
- Aims at enhanced protection and improvement of the aquatic environment.
- Ensures the progressive reduction of pollution of groundwater and prevents its further pollution.
- Contributes to mitigating the effects of floods and droughts.

Member States shall identify the individual river basins lying within their national territory and, for the purposes of this Directive, shall assign them to individual river basin districts. Small river basins may be combined with larger river basins or joined with neighboring small basins to form individual river basin districts where appropriate. Member States shall ensure the establishment of a register or registers of all areas lying within each river basin district which have been designated as requiring special protection. The European Parliament and the Council shall adopt specific measures against pollution of water by individual pollutants or groups of pollutants presenting a significant risk to or via the aquatic environment, including such risks to waters used for the abstraction of drinking water (European Commission, 2000).

Other Directives at European level:

- Commission Directive 2009/90/EC, of 31 of July 2009, laying down, pursuant to Directive 2000/60/EC of the European Parliament and of the Council, technical
- specifications for chemical analysis and monitoring of water status (European Commission, 2009a).

- Directive 2008/105/EC of the European Parliament and of the Council of 16 December 2008 on environmental quality standards in the field of water policy, amending and subsequently repealing Council Directives 82/176/EEC, 83/513/EEC, 84/156/EEC, 84/491/EEC, 86/280/EEC and amending Directive 2000/60/EC of the European Parliament and of the Council (European Commission, 2008).

Concerning the Spanish legislation, as basic texts related to water could be cite:

- Real Decreto Legislativo 1/2001, de 20 de Julio, por el que se aprueba el texto refundido de la ley de aguas (in Spanish, Spanish Goverment, 2001).
- Real Decreto Legislativo 606/2003, de 23 de Mayo, por el que se modifica el Real Decreto 849/1986, de 11 de abril, por el que se aprueba el Reglamento del Dominio Público Hidráulico, que desarrolla los Títulos preliminar, I, IV, V, VI y VIII de la Ley 29/1985, de 2 de Agosto, de aguas (in Spanish, Spanish Goverment, 2003).
- Real Decreto 60/2011, de 21 de Enero, sobre las normas de calidad ambiental en el ámbito de la política de aguas. Ministerio de Medio Ambiente y Medio Rural y Marino. Transpone: Directiva 2009/90/CE, de 31 de julio de 2009, Directiva 2008/105/CE, de 16 de diciembre, de conformidad con la Ley de Aguas, texto refundido aprobado por Real Decreto Legislativo 1/2001, de 20 de julio (in Spanish, Spanish Goverment, 2011).
- Real Decreto 670/2013, de 6 de Septiembre, por el que se modifica el Reglamento del Dominio Público Hidráulico aprobado por el Real Decreto 849/1986, de 11 de Abril, en materia de registro de aguas y criterios de valoración de daños al dominio público hidráulico (in Spanish, Spanish Goverment, 2013a).

### *1.3.2 Persistent organic pollutants and emerging contaminants regulations*

In the EU, the commitments made under both the Stockholm Convention and the CLRTAP persistent organic pollutants (POPs) protocol are translated into directly applicable law by the POPs Regulation.

- Regulation (EC) No 850/2004 of the European Parliament and of the Council of 29 April 2004 on persistent organic pollutants and amending Directive 79/117/EEC (European Commission, 2004b).
- 2006/507/EC: Council Decision of 14 October 2004 concerning the conclusion, on behalf of the European Community, of the Stockholm Convention on Persistent Organic Pollutants (European Commission, 2006a).

Regarding to emerging contaminants the NORMAN Project is based on (Brack et al. 2012):

- A more rapid and wide-scope exchange of data and information on the occurrence and effects of emerging substances,
- Better data quality and comparability via validation and harmonisation of common measurement methods (chemical and biological) and monitoring tools.
- More transparent information.
- The establishment of an independent and competent forum for the technical/scientific debate on issues related to emerging substances.

Concerning to United States legislation:

Recommendations and regulations have been purposed for the Emerging Contaminants Environmental Council of the States -Cross Media Committee (ECOS-CMC) in cooperation with the U.S. Environmental Protection agency (EPA) Office in order to prevent environmental contamination due to these chemicals (ECOS Green Report 2010; state experiences with emerging contaminants: recommendations for federal action (Environmental Council of the States, 2010). The Department of Defense has incorporated key elements in Directive 4715.18 of June 11, 2009 entitled "Emerging Contaminants" (Department of Defense, 2009).

## 1.4 Emerging contaminants

It has generally been assumed that possible polluting agents are eliminated through sewage treatment. However, not all polluting agents are removed through standard treatments (Ginebreda et al. 2010; Teijon et al. 2010). A number of compounds are known to persist through WWTPs in an unaltered form having then been identified in municipal effluents and in receiving waters (Kolpin et al. 2002; Phillips et al. 2010). Between these persistent compounds is the emergent polluting agent group, constituted by chemicals of a highly diverse origin, characterized by its high production and consumption entailing its continuous presence in the environment (Ginebreda et al. 2010; Teijon et al. 2010). These compounds are generally known as emerging contaminants or contaminants of emerging concern (CECs), including a large group of substances that have been recently characterized as contaminants (Lapworth et al. 2012) or newer substances that recently were discovered in the environment (Lindsey et al. 2001; Petrovic and Barceló 2006; Richardson and Ternes 2011). Among them, drugs, diagnosis products, steroids and hormones, antiseptics, personal care products, petrol additives, heavy metals and metalloids, surfactants endocrine disruptors, etc. are covered by this term. Table 1 summarizes the sources of the major categories of micropollutants in the aquatic environment (Luo et al. 2014).

**Table 1 Sources of micropollutants in the aquatic environment (Luo et al. 2014)**

| Category | Important subclasses | Major sources | |
|---|---|---|---|
| | | Distinct | Nonexclusive |
| Pharmaceuticals | NSAIDs*, lipid regulator, anticonvulsants, antibiotics, β-blockers and stimulants | Domestic wastewater; Hospital effluents; Run-off from CAFOs**; aquaculture | Sources that are not exclusive to individual categories include: Industrial wastewater (from product manifacturing discharges); Landifill leachate (from improper disposal of used, defective or expired items) |
| Personal care products | Fragrances, disinfectants, UV filters and insect repellents | Domestic wastewater (from bathing, shaving, spraying, swimming etc.) | |
| Steroid hormones | Estrogens | Domestic wastewaters (from excretion); Run-off from CAFOs; aquaculture | |
| Surfactants | Non-ionic surfactants | Domestic wastewater (from bathing, laundry, dishwashing etc.); Industrial wastewater (from industrial cleaning discharges) | |

**Table 1** ***(continued)***

| Category | Important subclasses | Major sources | |
|---|---|---|---|
| | | **Distinct** | **Nonexclusive** |
| Industrial chemicals | Plasticizers, fire retardants | Domestic wastewaters (by leaching out of the materials) | |
| Pesticides | Insecticides, herbicides and fungicides | Domestic wastewaters (from improper cleaning, run-off from gardens, lawns and roadways etc.); Agricultural run-off | |

*NSAIDs: Non-steroidal Anti-Inflammatory Drugs

**CAFOs: Concentrated Animal Feeding Operations

Although the low concentration in which they can be found in the environment, concern related to these contaminants is essentially due to their bioaccumulation and persistence (Kim et al. 2007; Hernando et al. 2007; Richardson 2008; Kasprzyk-Hordern et al. 2008; Miranda-García et al. 2010) as well as their resistance to conventional wastewater treatments (Planas et al. 1997; Brooks et al. 2003; Crane et al. 2006; Nentwig 2007; Quinn et al. 2008; Dantas et al. 2008; Schultz et al. 2010).

Although risk assessment seems to indicate that trace concentration of pharmaceuticals in drinking water are very unlikely to pose risk to human health, the World Health Organization pointed out as knowledge gaps still exist in terms of assessing risks associated with long-term exposure to low concentrations of pharmaceuticals and the combined effects of mixtures of pharmaceuticals (World Health Organization (WHO)).

A great diversity of trace pollutants can be found in treated effluents from urban waste-water treatment plants. The Table 2 reviews the occurrence of pharmaceuticals (emerging pollutants) present in WWTP effluents around the world.

**Table 2 Occurrence of emerging and priority pollutants in wastewater effluents. (extracted (Muñoz et al. 2009))**

| Compound | Effluent concentration Medium-maximum (ng $L^{-1}$) | Country |
|---|---|---|
| **PHARMACEUTICALS** | | |
| **Analgesics/anti-inflamatories** | | |
| Diclofenac | 680-5500 | France, Greece, Italy, Sweden |
| | 60-80 | USA |
| Ibuprofen | 50-320 | USA |
| Naproxen | 300-3200 | USA |
| | 1100-5200 | France, Greece, Italy, Sweden |
| Acetaminophen | 10-19 | South Korea |
| Ketoprofen | 318-620 | Croatia |
| N-acetyl-4-amino-antipiryne | 2900-7000 | Germany |
| (4-AAA) (Dipirone metabolite) | 3600-59600 | Canada |
| Codoine | 900-8100 | Spain |
| Mefenamic | 7-10 | Croatia |

**Table 2** ***(continued)***

| Compound | Effluent concentration Medium-maximum (ng $L^{-1}$) | Country |
|---|---|---|
| **Antibiotics** | | |
| Trimethoprim | 550-1900 | USA |
| | 320-660 | Germany |
| | 58-188 | South Korea |
| Ciprofloxacin | 239-514 | Italy |
| | 170-860 | USA |
| | 120-400 | Canada |
| Ofloxacin | 562-1081 | Italy |
| | 130-294 | South Korea |
| | 17-30 | Croatia |
| Sulfamethoxazole | 390-820 | Croatia |
| | 400-2000 | Germany |
| | 136-407 | South korea |
| **β-blockers** | | |
| Metoprolol | 730-2200 | Germany |
| | 60-160 | USA |
| | 80-390 | France, Greece, Italy, Sweden |
| Propanolol | 290-470 | Croatia |
| | 20-50 | USA |
| Atenolol | 400-1150 | Croatia |
| Sotalol | 185-210 | Croatia |
| **Lipid Regulators** | | |
| Bezafibrate | 10-10 | Croatia |
| | 2200-4600 | Germany |
| | 50-200 | Canada |
| Gemfibrozil | 120-320 | Croatia |
| | 920-5500 | USA |
| Clofibric acid (metabolite) | 28-30 | Croatia |
| | 360-1600 | Germany |
| | 30-80 | Canada |
| Fenofibric acid (metabolite) | 380-1200 | Germany |
| **Psychiatric drugs** | | |
| Diazepam | 30-40 | Germany |
| Fluoxetine | 50-140 | Canada |
| Carbamazepine | 70-1200 | France, Greece, Italy, Sweden |
| | 110-2300 | Canada |
| | 2100-6300 | Germany |
| **Hormones** | | |
| Estrone | 30-80 | Spain |
| | 42-48 | Italy |
| Diethylstilbestrol | 9-30 | Spain |
| Estriol | 16-25 | South Korea |
| **Anti-ulcer agent** | | |
| Ranitidine | 135-200 | Croatia |
| | 298-610 | Italy |

**Table 2 *(continued)***

| Compound | Effluent concentration Medium-maximum (ng $L^{-1}$) | Country |
|---|---|---|
| **PRIORITY POLLUTANTS** | | |
| Pesticides | | |
| Diurion | 40-400 | Germany |
| Atrazine | 40-40 | Germany |
| Isoproturon | 40-320 | Germany |
| Hexachlorobenzene | 1.7-15 | Greece |

Thus, when there are no adequate treatments units, wastewater treatment plants could be identified as a major source of these compounds to the environment (Glassmeyer et al. 2005; Clara et al. 2005) and specific treatments able to eliminate CECs, especially when reuse is aimed, might be provided. An interesting alternative is to install a tertiary treatment. Among them, advanced oxidation processes (AOPs) can be a useful option to remove recalcitrant contaminants.

### *1.4.1 Atrazine*

Atrazine (2-chloro-4-ethylamine-6-isopropylamino-s-triazine, ATZ) has been the most widely used herbicide, mainly applied to remove broadleaf and grassy weeds in corn or crops. The solubility of atrazine is 30 mg $L^{-1}$ in water (Ward and Weber 1968), and the half-life of atrazine is 283 days in groundwater without light (Navarro et al. 2004). Although atrazine was banned from the European Union (EU) in 2004, its considerable use in the past, its moderate solubility and good stability have meant that it is frequently detected in the atmosphere, surface water, groundwater and soil, leading to environmental problems (Marchini et al. 1988; Bottoni and Funari 1992; Gfrerer et al. 2002; Ma et al. 2003; Gavrilescu 2005). The problem of atrazine contamination of surface and ground water are often results from agricultural runoff. Nevertheless, contamination by atrazine is also due to point sources such as pesticide manufacturing industry, dumped site of pesticide wastes, etc. (Kearney and Roberts 1998; Ghosh and Philip 2006). Very few reports are available on the occurrence of atrazine in domestic or industrial wastewater probably due to the absence of regular monitoring mechanisms for pesticides in wastewater. In addition, it's common in the people to throw out the unused pesticide and allow the water after washing pesticide container, into existing sewer systems. Thus, atrazine can get mixed with domestic wastewater (Monteith et al. 1995; Ghosh and Philip 2006). Indeed, atrazine concentration was monitored in the effluent from existing wastewater treatment plants in Switzerland and it was found that in many cases concentration was more than the permissible limit (Gerecke et al. 2002; Ghosh and Philip 2006). Atrazine is considered a potential contaminant that can cause cancer and harm the human endocrine system (Min et al. 2008; Sathiakumar and Delzell 2010).

### *1.4.2 Sulfamethoxazole*

Sulfamethoxazole (SMX) is an antibiotic widely used for human and veterinary animals (Segura et al. 2009), among the most frequently detected antibiotics in the aquatic environment (Heberer 2002). The main use has been in the treatment of acute urinary tract infections. It has also been used against gonorrhea, meningitis and serious respiratory tract infections

(Pneumocystis carinii) and prophylactically against susceptible meningococci. Despite its relatively unfavourable pattern of tissue distribution, it is the sulfonamide most commonly used around the world in combination with trimethoprim or pyrimethamine for the treatment of various systemic infections. The combination with trimethoprim is used mainly for the treatment of urinary tract infections; with pyrimethamine, it is used in the treatment of chloroquine-resistant Plasmodium falciparum malaria (Schnitzer 1978; Gennaro 1995). SMX is slight soluble (0.5 g $L^{-1}$) and hydrophilic (octanol water partition coefficient: log $K_{ow}$ = 0.27). Due to its poor metabolism and slow degradation, recently the persistence of SMX in the environment has been of great concern. Furthermore, this antibiotic in the environment may cause adverse effects to the microbial communities, hence imposing great risk to the non-target species in the ecosystems (Boxall et al. 2012; Bouki et al. 2013). It is well known to bioaccumulate up the food chain and trigger acute as well as chronic adverse effects (Göbel et al. 2005). Studies from scientific literauture indicate that simultaneous exposure to multiple antibiotics could result in the enhanced toxic effects (Park and Choi 2008). A general concern for public health is the development of antibiotic resistance from chronic exposure to antibiotic contaminated water.

## 1.5 Advanced Oxidation Processes

Advanced oxidation processes (AOPs) were first proposed for potable water treatment in the 1980s (Glaze 1987; Glaze et al. 1987), which are defined as the oxidation processes involving the generation of hydroxyl radicals (OH·) in sufficient quantity to effect water purification. Later, the AOP concept has been also extended to the oxidative processes with sulfate radicals ($SO4^{\cdot-}$). Thus, more in general, AOPs can be defined as all those chemical treatment procedures based on the production of very reactive species (especially hydroxyl radicals) generated in atmospheric or sub-supercritical conditions of temperature and pressure with or without catalyst and/or reactive energy (electrochemical, UV-Vis or ultrasounds). AOPs can oxidize and mineralize several organic molecules to yield $CO_2$ and inorganic ions as final products (Gogate and Pandit 2004; Ikehata and El-Din 2006; Miranda-García et al. 2010; Gozzi et al. 2012).

On the basis of the source of the oxidizing species or the method employed for its production, one possible AOPs' classification can be:

- Based on **photolysis**:
    - UV Photolysis;
    - V-UV Photolysis;
- Based on **ozone**:
    - Ozonation (alkaline conditions);
    - Ozonation + UV and/or $H_2O_2$;
    - Ozonation + catalyst;
- Based on **hydroxil radicals**:
    - Fenton;
    - Fenton-like;
    - Photo-Fenton;
    - UV/ $H_2O_2$;
    - Electro-Fenton ;

    - Photocatalysis;
- Based on **sulfate radical** species:
    - UV/PS and UV/PMS;
    - Catalyst/PS and Catalyst/PMS;
    - Heat/PS and Heat/PMS;
- **Thermal** processes:
    - Supercritical wet oxidation;
    - Wet oxidation;
    - Wet oxidation + $H_2O_2$;
- **High energy** processes:
    - Ultrasound technologies;
    - Electrochemical oxidation;
    - Electron beam oxidation;
    - Microwaves enhanced processes;
    - Hydrocavitation;
    - Non thermal plasma.

Advanced oxidation involves several steps schematized in the figure below (Figure 3) and explained as follows:

1) Formation of strong oxidants (e.g. hydroxyl radicals).
2) Reaction of these oxidants with organic compounds in the water producing biodegradable intermediates.
3) Reaction of biodegradable intermediates with oxidants referred to as mineralization (i.e. production of water, carbon dioxide and inorganic salts).

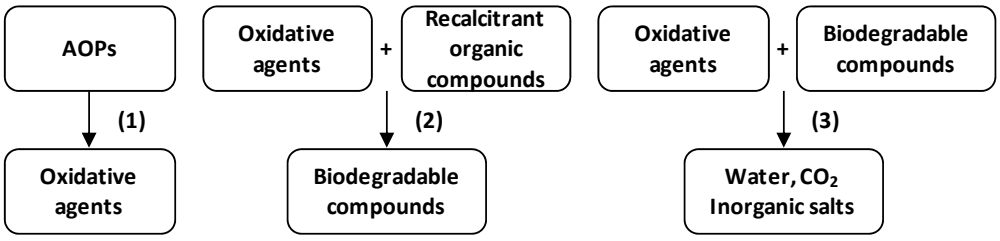


**Figure 3 Steps involved in an AOPs treatment of wastewater**

Some of the types of AOPs mentioned before result more efficient depending on the target solution. The effectiveness of AOPs is in fact strongly dependent of some aspects such as: the composition and concentration load of the stream in question and the treatment aim itself.

The extent of pollution removal needed influences treatment performance. Thus, coupling various processes can be sometimes convenient in order to enhance the global efficiency removal optimizing implementation of AOPs at the right place to limit costs. Treatment performance can be enhanced through coupling various processes as follow (Comninellis et al. 2008):

- Simultaneous application of different AOPs to promote the rates of organics oxidation (i.e. UV/$H_2O_2$, UV/$H_2O_2$/$TiO_2$, UV/Fenton and Ultrasound/UV/$TiO_2$, etc.). These types of

combinations may lead to synergetic effects when treatment efficiencies are greater than the sum of efficiencies that could be achieved by the individual treatments alone.

- Sequential application of various AOPs to treat effluents containing a mixture of organics. This approach is useful for treating effluents characterized by the mixtures that present different levels of reactivity towards different AOPs (industrial effluents.
- Application of separation treatment prior to AOP treatment to transfer pollutants to another phase so that they can be treated more easily. Such separation treatment includesstripping, coagulation-flocculation, sedimentation, filtration, adsorption etc.
- Application of AOPs as a pre-treatment stage to enhance biodegradability and reduce toxicity, followed by biological post-treatment. This approach is based on the fact that biological treatment is perhaps less costly and more environmentally friendly than other destructive treatments and that complete mineralization by AOPs incurs excessive treatment costs.

AOPs can be installed at different stages of wastewater (or drinking also) treatment plants depending on influent composition and desired effluent quality. AOPs can be installed either as tertiary treatment after the biological (secondary) treatment of wastewater, or as pre-treatment stage in order to enhance the biodegradability of trace organic contaminants (Figure 4) (Petrovic et al. 2011).

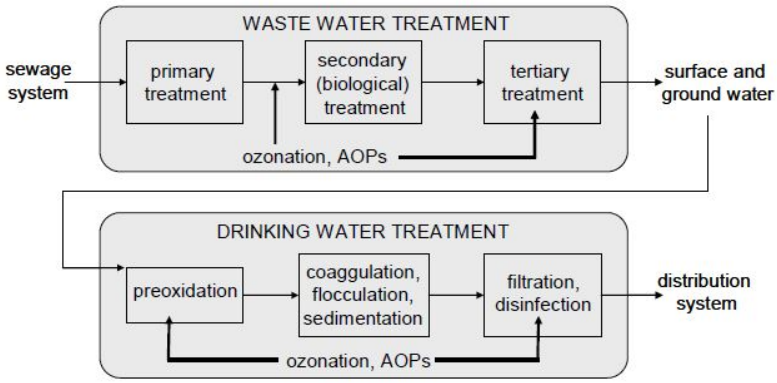


**Figure 4 Possible applications of AOPs in wastewater and drinking water treatment (Petrovic et al. 2011).**

More in general, optimal treatment scheme may be decided after considering the level of water quality it wants to be achieved. This is usually dictated by the purpose of the treatment, the national or international environmental regulations and then by the type of waste it has to be treated. A part from these, some others aspects might be taken into account when deciding the strategies to adopt for implementing the treatment scheme, such as (Comninellis et al. 2008):

- If the wastewater is biodegradable, a biological treatment would be the more convenient (unless discharge limits are already fulfilled regarding organic carbon content, toxicity and other physicochemical parameters, which is an unlikely case for industrial wastewaters). Classical biological treatments are, in fact, the cheapest and most environmentally compatible option.

- If the wastewater is not biodegradable and its organic content is high (TOC > 0.1 g $L^{-1}$), a pre-treatment by means of an AOP followed by a biological post-treatment could be the more suitable option. The monitoring of the effluent quality would be in this case unavoidable to check it complies with legal requirements for effluent discharge.
- If the wastewater is not biodegradable, its organic content is low (TOC < 0.1 g $L^{-1}$) but toxicity is still high, AOP treatment would help in reducing the toxicity. However, in this case, subsequent biological treatment would not be recommended due to the little metabolic value for the micro-organisms of the effluent. Very often this wastewater could be disposed of to the environment or sent to a public sewage treatment system for further polishing.
- If the wastewater is not biodegradable, its TOC content and toxicity are low but other physicochemical requirements are not met (i.e. the effluent is coloured), an AOP treatment without subsequent bio-treatment could also be suitable. In this case, after the AOP treatment, the effluent quality has to be assessed before discharge.

### *1.5.1 Water Quality Impacts*

As briefly mentioned before, considering the water quality parameters is really important in order to define the better treatment's strategy. These, in fact, can significantly influence the efficiency of the treatment. For example, an excessive presence of dissolved organic matter would determine the establishment of competition for hydroxyl radicals. Thus, at the end, the removal efficiency on the target compound would be reduced by defect of HO· available for degradation (Hoigné 1998).

The most important parameters that can influence the effectiveness of the AOPs are synthetized below:

- Alkalinity: as already mentioned, the hydroxyl radical is nonselective and, thus, can be exhausted by the presence of organic or inorganic compounds other than the contaminants of concern. Both carbonate and bicarbonate will scavenge hydroxyl radicals to create carbonate radicals (see reaction below, (Morel and Hering 1993)) which, in turn, react with other organic or inorganic compounds present, albeit at a much slower rate (Hoigné and Bader 1976; Peyton et al. 1998).

$$HO\cdot + HCO_3^- \rightarrow CO_3\cdot + H_2O \qquad (1)$$

  The rate constant for reactions of the hydroxyl radicals with carbonate and bicarbonate are much slower compared to the reaction with several recalcitrant compounds ($k_{HO\cdot/CO32-}$=3.9 x $10^8$ $M^{-1}$ $s^{-1}$; $k_{HO\cdot/HCO3-}$=8.5 x $10^6$ $M^{-1}$ $s^{-1}$, (Buxton et al. 1988)). However, for these second order reactions, the actual reaction rate, r, is a function of both the rate constant and the concentration of the reactant. Then, considering that water with medium to high alkalinities (>100 mg $L^{-1}$ as $CaCO_3$) likely contain carbonate and bicarbonate ions at concentrations several orders of magnitude greater than target compounds they want to be removed by AOPs, the reaction of hydroxyl radicals with carbonate and bicarbonate can proceed as fast or faster than their reaction with the target compound. In this case, a possible strategy to reduce the negative effect of radical scavenging can be lowering the alkalinity, for example by means of pH

adjustment or carbon dioxide stripping, before treating with AOPs (Peyton et al. 1998). Alternatively, higher doses of oxidant and higher reaction time may be provided.

- TOC and NOM. TOC measurement incorporates all organic compounds present in the water, both dissolved organic carbon (DOC) and particulate organic carbon (POC) and include naturally occurring compounds and anthropogenic compounds (e.g., pesticides, gasoline components, and chlorinated compounds). NOM, a subset of TOC, is commonly used to describe large macromolecular organic compounds present in water including humic substances, proteins, lipids, carbohydrates, fecal pellets, or biological debris (Stumm and Morgan 2012). Though not highly reactive, NOM often contains reactive functional groups (Hoigné 1998). Both TOC and NOM will scavenge hydroxyl radicals limiting the effectiveness of AOPs ($k_{NOM}$=1.9 x $10^4$ to 1.3 x $10^5$ $(mgL^{-1})^{-1}s^{-1}$, (Peyton et al. 1998)). The effects of high concentrations of NOM may be mitigated by the addition of higher dosages of oxidant and longer reaction times.
- Nitrates and Nitrites. Any constituent present in the water that adsorbs UV light will decrease the formation of hydroxyl radicals when formed by photo dissociation of hydrogen peroxide. Nitrates and nitrites adsorb UV light in the range of 230 to 240 nm and 300 to 310 nm and, consequently, high nitrate or nitrite concentrations can limit the effectiveness of UV technologies.
- Phosphates and Sulfates. These compounds, with the potential to scavenge hydroxyl radicals, are commonly present in low concentrations in source waters. However, they are extremely slow in reacting with HO·, and their scavenging effect can usually be neglected (Hoigné 1998) for ozone/peroxide/UV systems. For $TiO_2$ systems, sulfates have been noted to significantly decrease the destruction rate of organic contaminants at concentrations above approximately 100 mg $L^{-1}$ (Crittenden et al. 1996).
- Turbidity. Turbidity lowers the transmittance of the source water and, thus, lowers the penetration of the UV radiation into the source water. Thus, in systems where UV irradiation is employed for the dissociation of $H_2O_2$, a decrease in efficiency as turbidity increases.

## 1.6 Radical driven oxidation

As previously described AOPs can be considered as all those procedures based on the production of very reactive species such as highly reactive free radicals. The high effectiveness of hydroxyl radicals (HO·) in destroying organic chemicals is justifiable by their nature of reactive electrophiles (electron preferring) that react rapidly and nonselectively with nearly all electron-rich organic compounds. They have an extremely high oxidation potential (between 2.8 V at pH 0 and 1.95 V at pH 14, Table 3) and exhibit faster rates of oxidation reactions comparing to conventional oxidants such as $H_2O_2$ or $KMnO_4$ (Gogate and Pandit 2004).

**Table 3 Oxidation potential of various oxidants.**

| Oxidant | Oxidation potential (V) |
|---|---|
| Fluorine | 3.03 |
| Hydroxyl radical | 2.80 |
| Sulfate radical | 2.60 |
| Atomic oxygen | 2.42 |
| Ozone | 2.07 |

**Table 3 *(continued)***

| Oxidant | Oxidation potential (V) |
|---|---|
| Hydrogen peroxide | 1.78 |
| Perhydroxyl radical | 1.70 |
| Permanganate | 1.68 |
| Hypobromous acid | 1.59 |
| Chlorine dioxide | 1.57 |
| Hypochlorous acid | 1.57 |

Once generated, the hydroxyl radicals can attack organic chemicals by radical addition, hydrogen abstraction and electron transfer (SES 1994). The general reactions in which HO· are involved can be summarized as following (where R is used to describe the organic reacting compound):

1. **Radical addition:** the electrophilic addition to double bound C=C constitutes the most common mechanisms of oxidative degradation of organics by HO· :

$$R + HO\cdot \rightarrow ROH \quad (2)$$

2. **Hydrogen abstraction:** This reaction generates organic radicals which by addition of molecular oxygen yield peroxide radicals. These intermediates initiate chain reactions of oxidative degradation, leading to carbon dioxide, water and inorganic salts:

$$R + HO\cdot \rightarrow R\cdot + H_2O \quad (3)$$

$$R\cdot + O_2 \rightarrow RO_2\cdot \quad (4)$$

3. **Electron transfer**:

$$R^n + HO\cdot \rightarrow R^{n-1} + OH^- \quad (5)$$

The amount of radicals formed is the limiting factor for the process efficiency. Moreover, due to their no selectivity, there is a competition between compounds and the hydroxyl radicals. A wide variation of background substances can be present in the water matrix. These, scavenging the hydroxyl radicals can reduce significantly the amount of them available to oxidize the recalcitrant compounds.

In Table 4 are synthetized the main substances and/or influents which act as hydroxyl radical scavenger (Wols and Hofman-Caris 2012).

**Table 4 Main hydroxyl radicals scavengers (extracted from (Wols and Hofman-Caris 2012))**

| Name | | Ref. |
|---|---|---|
| Hydrogen peroxide ($H_2O_2$) | (k= $2.7 \times 10^7$ $M^{-1}$ $s^{-1}$) | (Buxton et al. 1988) |
| Hydrogen peroxide anion ($H_2O^-$) | (k= 7.5 $M^{-1}$ $s^{-1}$) | (Christensen et al. 1982) |
| Carbonate ($CO_3^{2-}$) | (k= $3.9 \times 10^8$ $M^{-1}$ $s^{-1}$) | (Buxton et al. 1988) |
| Bicarbonate ($HCO_3^-$) | (k= $8.5 \times 10^6$ $M^{-1}$ $s^{-1}$) | (Buxton et al. 1988) |
| Hydrogen phosphate ion ($HPO_4^{2-}$) | (k= $1.5 \times 10^5$ $M^{-1}$ $s^{-1}$) | (Maruthamuthu and Neta 1978) |
| Dihydrogen phosphate ion ($H_2PO_4^-$) | (k= $2.0 \times 10^4$ $M^{-1}$ $s^{-1}$) | (Maruthamuthu and Neta 1978) |
| Nitrite ($NO_2^-$) | (k= $1.0 \times 10^{10}$ $M^{-1}$ $s^{-1}$) | (Coddington et al. 1999) |
| Bromide ion ($Br^-$) | (k= $1.1 \times 10^{10}$ $M^{-1}$ $s^{-1}$) | (Buxton et al. 1988) |

The main fundamentals of the treatments applied in this thesis are now described in the following sections.

### *1.6.1 UV-photolysis*

Direct photolysis involves the interaction of light with molecules (in addition to water) to bring about their dissociation into fragments, with the following mechanistic pathway:

$$R + h\upsilon \rightarrow intermediates \quad (6)$$

$$intermediates + h\upsilon \rightarrow CO_2 + H_2O + R^- \quad (7)$$

This process is far to be particularly effective especially if compared to other where radiation is combined with hydrogen peroxide or ozone, or if catalyst is additionally employed. The most common sources of UV light are continuous wave low pressure mercury vapor lamps (LP-UV), continuous wave medium pressure mercury vapor lamps (MP-UV), and pulsed-UV (P-UV) xenon arc lamps. Both LP-UV and MP-UV mercury vapor lamps produce a series of line outputs, whereas the xenon arc lamp produces continuous output spectra.

### *1.6.2 UV/$H_2O_2$*

UV/$H_2O_2$ processes generally involve generation of HO· radical through UV photolysis of $H_2O_2$. Then, the degradation of the organic compound can be carried out by means of photon attack (direct UV photolysis) and hydroxyl radical reactions (Wols et al. 2013).

The photolysis of hydrogen peroxide occurs when UV radiation (hv) is applied, as shown in the following reaction:

$$H_2O_2 + h\upsilon \rightarrow 2HO\cdot \quad (8)$$

The maximum absorbance of $H_2O_2$ is near 220 nm and its molar absorptivity at 253.7 nm is low (20 $M^{-1}$ $cm^{-1}$). Thus HO· radicals are formed per incident photon absorbed. The quantum yield of hydroxyl radical formation is really low ($\varphi_{HO\cdot}$=0.5) due to the rapid reconversions of the radicals in the solution. This technique requires a relatively high dose of $H_2O_2$ or eventually a much longer UV-exposure time. However, too high concentration of $H_2O_2$ scavenges the hydroxyl radicals, reducing the efficacy of the process. Again, the absorptivity of hydrogen peroxide may be increased by using UV lamps characterized by lower wavelengths emissions.

The main reactions of the system are showed in Table 5:

**Table 5 Major reactions occurring in UV/$H_2O_2$**

| Reactions | | Ref. | Eq. |
|---|---|---|---|
| **Initiation** | | | |
| $\boldsymbol{H_2O_2 \overset{h\upsilon}{\rightarrow} 2HO\cdot}$ | Φ= 0.5 at 253.7 nm | (De Laat et al. 1999) | (9) |
| $\boldsymbol{H_2O_2 \rightarrow H_2O + ½O_2}$ | | | (10) |
| **Propagation** | | | |
| $\boldsymbol{HO\cdot + H_2O_2 \rightarrow HO_2\cdot + H_2O}$ | (k= 2.7 × $10^7$ $M^{-1}$ $s^{-1}$) | (Buxton et al. 1988) | (11) |

**Table 5** ***(continued)***

| Reactions | | Ref. | Eq. |
|---|---|---|---|
| $HO_2 \cdot + H_2O_2 \rightarrow HO \cdot + H_2O + O_2$ | (k= 1.1 - 3.7 $M^{-1} s^{-1}$ ) | (Bielski et al. 1985) | (12) |
| $HO_2 \cdot + HO_2^- \rightarrow HO \cdot + HO^- + O_2$ | | | (13) |
| **Termination** | | | |
| $HO \cdot + HO_2 \cdot \rightarrow H_2O + O_2$ | (k= 6.6 × $10^9$ $M^{-1} s^{-1}$) | (Buxton et al. 1988) | (14) |
| $HO \cdot + HO \cdot \rightarrow H_2O_2 + O_2$ | (k= 5.2 × $10^9$ $M^{-1} s^{-1}$) | (Buxton et al. 1988) | (15) |

Between the advantages of using UV/$H_2O_2$ there are:

- possibility of adding high amount of hydrogen peroxide due to its high solubility;
- no potential for bromate formation;
- MP-UV and pulsed UV-irradiation can be used as disinfectant as well;
- No off-gas treatment is required;
- The process is not limited by mass transfer as it instead happens for $O_3$ processes.

Between the disadvantages, can be instead enumerated:

- The interference with UV light penetration in case of high turbidity of the effluent to be treated;
- Less stoichiometric efficiency in HO· production than $O_3$/UV process;
- The presence of interfering compounds (i.e. nitrate) can compete with $H_2O_2$ for absorbing the light;
- Potential increase in THM formation when combined with pre and/or post-chlorination.

### *1.6.3 Conventional Fenton and Photo Fenton*

#### *Fenton*

The Fenton reagent, a mixture of hydrogen peroxide and Fe(II) salt, has been discovered by Henry J.H. Fenton who discovered the high enhancement of HO· production employing iron salts as catalyst of hydrogen peroxide decomposition (Fenton process).

Until now, more than 1700 rate constants have been determined for reaction of Fenton oxidation of organic and inorganic compounds in aqueous solution. Fenton process is considered as a process potentially convenient and economic due to the generation of oxidizing species for the degradation of several compounds. Moreover, the cheapness of hydrogen peroxide together with the harmless of potential residual on the environment make the application of $H_2O_2$ based processes particularly convenient. Additionally, the extra benefit due to the enhanced production of hydroxyl radicals when employing iron species (really cheap and not toxic as well) point more out these advantages.

Fe(II) and Fe(III) ions, when no complexed by organic agents, exist in several hydrolyzed species and/or as inorganic complexes depending of the pH value of the solution. In solution characterized by a pH range of 2-7, Fe(II) would be mainly present as $Fe^{2+}_{(aq)}$ while Fe(III) would present as $Fe^{3+}_{(aq)}$ for pH<3, $FeOH^{2+}$ at pH=3 and $Fe(OH)_2^+$ for pH in the range 3-7 (see Figure 5).

At circumneutral pH, then, $Fe^{3+}$ would be present as $Fe(OH)_{3(s)}$ that will precipitate (Huston and Pignatello 1999). Hence, to avoid Fe(III) precipitation, an acidic pH environment is required by the standard Fenton reaction (Pérez et al. 2002).

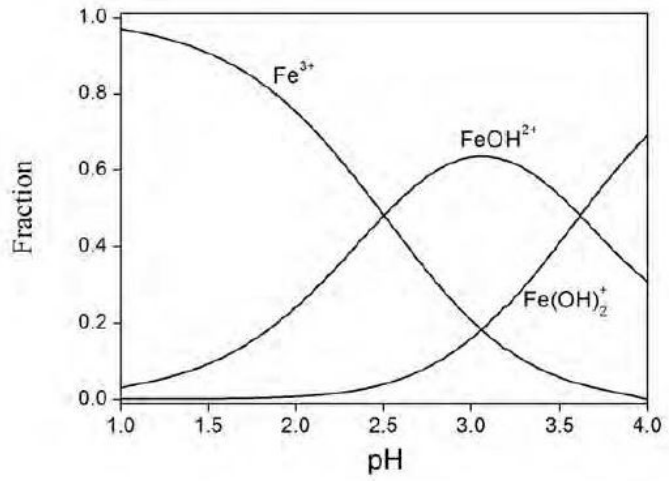


**Figure 5 Fe(III) speciation between pH 1 and 4 at 25 °C**

In Fenton, $Fe^{2+}$ catalyzes the $H_2O_2$ decomposition starting a complex series of chain radical reactions in which the iron cyclically passes from the oxidation state 2 to 3 and vice versa.

The main reaction's mechanism of the $H_2O_2$ decomposition in acid solution and in presence or iron ions is described by the following reactions (Table 6):

**Table 6 Major reactions occurring in Fenton**

| Reactions | | Ref. | Eq. |
|---|---|---|---|
| **Initiation** | | | |
| $Fe^{2+} + H_2O_2 \rightarrow Fe^{3+} + HO^- + HO\cdot$ | (k = 76 $M^{-1}$ $s^{-1}$) | (Rigg et al. 1954) | (16) |
| $Fe^{3+} + H_2O_2 \rightarrow FeOOH^{2+} + H^+ \leftrightarrow Fe^{2+} + HO_2\cdot + H^+$ | (k= 0.001 – 0.01 $M^{-1}$ $s^{-1}$) | (Walling and Goosen 1973) | (17) |
| $H_2O_2 \rightarrow H_2O + \frac{1}{2}O_2$ | | | (18) |
| **Propagation** | | | |
| $HO\cdot + H_2O_2 \rightarrow HO_2\cdot + H_2O$ | (k= 2.7 × $10^7$ $M^{-1}$ $s^{-1}$) | (Buxton et al. 1988) | (19) |
| $HO_2\cdot + H_2O_2 \rightarrow HO\cdot + H_2O + O_2$ | (k= 1.1 - 3.7 $M^{-1}$ $s^{-1}$ ) | (Bielski et al. 1985) | (20) |
| **Termination** | | | |
| $Fe^{2+} + HO\cdot \rightarrow Fe^{3+} + HO^-$ | (k= 3.2 × $10^8$ $M^{-1}$ $s^{-1}$) | (Buxton et al. 1988) | (21) |
| $Fe^{3+} + HO_2\cdot \rightarrow Fe^{2+} + H^+ + O_2$ | (k= 1.2 × $10^6$ $M^{-1}$ $s^{-1}$) | (Bielski et al. 1985) | (22) |
| $Fe^{2+} + HO_2\cdot + H^+ \rightarrow Fe^{3+} + H_2O_2$ | (k= 1.3 × $10^6$ $M^{-1}$ $s^{-1}$) | (Bielski et al. 1985) | (23) |
| $HO\cdot + HO_2\cdot \rightarrow + H_2O + O_2$ | (k= 6.6 × $10^9$ $M^{-1}$ $s^{-1}$) | (Buxton et al. 1988) | (24) |
| $HO\cdot + HO\cdot \rightarrow + H_2O_2$ | (k= 5.2 × $10^9$ $M^{-1}$ $s^{-1}$) | (Buxton et al. 1988) | (25) |
| $HO_2\cdot + HO_2\cdot \rightarrow + H_2O_2 + O_2$ | (k= 1.3 × $10^6$ $M^{-1}$ $s^{-1}$) | (Buxton et al. 1988) | (26) |

From the set reactions, it is observable as $H_2O_2$ can act as HO· scavenger as well as initiator of the chain reaction (Eq. 19 and 16). It has been demonstrated that acidic pH levels near 3 are usually optimum for Fenton oxidations (Arnold et al. 1995). The reaction rate of the $H_2O_2$ decomposition by means the catalytic effect of $Fe^{2+}$ and $Fe^{3+}$ is clearly lower in presence of the last one. The reduction of $Fe^{3+}$ to $Fe^{2+}$ (Eq. 17) is, then, the limiting step in the overall reaction (Pignatello et al. 2006). Though, the superoxide/hydroperoxy radicals ($HO_2\cdot/O_2\cdot^-$) plays an important role in the redox cycle of iron in aqueous phase, the generation of hydroperoxide anion $HO_2\cdot$ may be neglected at neutral pH (Bielski et al. 1985). Thus, although chemically efficient for the removal of organic pollutants, Fenton reaction slows down appreciably after the initial conversion of $Fe^{2+}$ to $Fe^{3+}$. Thus, the addition of relatively large amounts of $Fe^{2+}$ may be required in order to enhance the degradation of the pollutant of interest.

In the presence of organic substrates (RH), excess ferrous ion, and at low pH, hydroxyl radicals can add to the aromatic or heterocyclic rings (as well as to the unsaturated bonds of alkenes or alkynes). Figure 6 shows a typical interaction between HO· and an aromatic ring, similar to the interaction would also be established between the hydroxyl radical and aliphatic hydrocarbon.

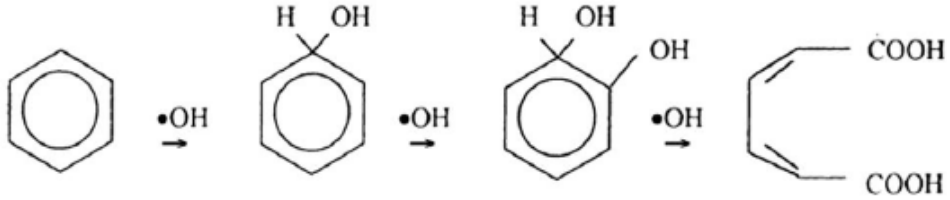


**Figure 6 Degradation of an aromatic ring by hydroxyl radical attack (Neyens and Baeyens 2003).**

Hydroxyl radical attack can also involve hydrogen atom abstraction, initiating the following radical chain oxidation (Walling 1975; Lipczynska-Kochany et al. 1995):

$$RH + HO\cdot \rightarrow H_2O + R\cdot \quad (27)$$

$$R\cdot + H_2O_2 \rightarrow ROH + HO\cdot \quad (28)$$

$$R\cdot + O_2 \rightarrow ROO\cdot \quad (29)$$

The organic free radicals, produced in the first of the set reaction, may then be oxidized by $Fe^{3+}$, reduced by $Fe^{2+}$, or dimerized according to the following reactions (Tang 1997):

$$R\cdot + Fe^{3+} \rightarrow R^+ + Fe^{2+} \quad \text{(oxidation)} \quad (30)$$

$$R\cdot + Fe^{2+} \rightarrow R^- + Fe^{3+} \quad \text{(reduction)} \quad (31)$$

$$R\cdot + R\cdot \rightarrow R - R \quad \text{(dimerization)} \quad (32)$$

The competition for hydroxyl radical reaction between $Fe^{2+}$, $Fe^{3+}$ and organic compounds represent a limiting factor for the oxidation of these last ones. It appears clear, then, as the ratio between these three components need to be the proper to maximize the oxidation of the organic compounds (Neyens and Baeyens 2003). However, an important limitation of Fenton reaction is also the formation of recalcitrant intermediates that inhibit the complete

mineralization. Particularly noteworthy is the formation of oxalic acid, a poisonous and persistent product of many degradation reactions.

Other point of strength and disadvantages of the process can be synthesized as following. Between the advantages of using Fenton process there are:

- no potential for bromate formation;
- No off-gas treatment is required;
- Its simplicity and the almost null energy requirements made it really cheap and easily manageable.

Between the disadvantages, can be instead enumerated:

- Requires iron extraction system with consequent production of high volumes of iron sludge waste;
- Very low pH is required (≈2.8) to keep the iron soluble in solution;
- pH adjustment increases the operation and maintenance cost.

Even though Fenton process is able to destroy the toxic organic compounds in a relatively short time, it cannot lead to complete mineralization of organic compounds. The extent of mineralization can achieve values of around 40–60%, depending on the amount of reagents employed.

***Photo-Fenton***

Photo-Fenton (Fe(II)/$H_2O_2$/UV) is a Fenton based process in which irradiation with sunlight or an artificial light source is employed to enhance the contaminant removal rate by promoting the reduction of Fe(III) to Fe(II). Photo-Fenton process is basically the combination of Fenton reagents and UV-vis radiation (λ<600 nm). The photo-reduction of $Fe^{3+}$ to $Fe^{2+}$ ions for λ<580 nm (Faust and Hoigné 1990) and the photolysis of $H_2O_2$ via shorter wavelength (λ<310 nm) ensures, in fact, extra HO· radicals production.

Irradiating the system with UV or visible light the photoassisted Fenton's process produces ferric ions as a by-product of the reaction between Fe(II) and $H_2O_2$ and then it is photochemically transformed back into ferrous ions (Table 7). The additional reactions involved in the process are:

**Table 7 Major reactions occurring in Photo-Fenton**

| Reactions | | Ref. | Eq. |
|---|---|---|---|
| $Fe^{2+} + H_2O_2 \rightarrow Fe^{3+} + HO^- + HO\cdot$ | (k = 76 $M^{-1}$ $s^{-1}$) | (Rigg et al. 1954) | (33) |
| $Fe^{3+} + H_2O \xrightarrow{h\nu} Fe^{2+} + HO\cdot + H^+$ | Φ= 0.07 at 253.7 nm<br>Φ= 0.14 at 314 nm<br>Φ= 0.017 at 360 nm | (De Laat et al. 1999)<br>(Zepp et al. 1992; Sun and Pignatello 1993) | (34) |
| $H_2O_2 \xrightarrow{h\nu} 2HO\cdot$ | Φ= 0.5 at 253.7 nm | (De Laat et al. 1999) | (35) |

The hydroxyl radical production is determined by the $H_2O_2$ concentration and by the availability of irradiation at the proper wavelength as well. In fact, as it is observable from the

second of the set reaction, irradiation of the Fenton reaction not only regenerates the $Fe^{2+}$, but also produces an additional hydroxyl radical. Moreover, since $Fe^{2+}$ is regenerated by light with decomposition of water rather than $H_2O_2$, the Photo-Fenton process consumes less $H_2O_2$ and requires only catalytic amount of $Fe^{2+}$. Consequently, another important advantage that characterizes Photo-Fenton process is that the production of the sludge waste is reduced respect to the original Fenton process. However, similarly to dark Fenton, the pH control of the medium is strictly required. Again, differently to UV/$H_2O_2$, Photo-Fenton can use sunlight (Litter and Quici 2010; Carra et al. 2014) instead of UV light. This represents a very important advantage of the process being making the process significantly more suitable from the economic point of view.

The effectiveness of photo-Fenton for the degradation of recalcitrant compounds has been largely demonstrated. Some studies in which recalcitrant compound have been treated by means of Photo-Fenton process have been reviewed by RahimPouran et al. (2015) (Table 8):

**Table 8 Efficiency of photo-Fenton treatment of some organic compounds in recalcitrant effluents (Rahim Pouran et al. 2015)**

| Compound | Initial value ($mg\ L^{-1}$) | Operational condition | | | | | Optimal performance | Ref |
|---|---|---|---|---|---|---|---|---|
| | | [H2O2] ($mg\ L^{-1}$) | Iron ($mg\ L^{-1}$) | pH - | [Ox] ($mg\ L^{-1}$) | T (°C) | | |
| ***Pharmaceuticals*** | | | | | | | | |
| **Pharmaceutical wastewater** | $TOC_0$: 125 | 5250 | 55 | 3 | 325 | 32 | 84% TOC removal within 115 min at $H_2C_2O_4$:$Fe^{3+}$ ratio of 3 | (Monteagudo et al. 2013) |
| **Penicillin G** | 200 | 680 | 55 | 3.5 | – | – | 83.3% Pen-G degradation within 30 min | (Gogate and Pandit 2004) |
| **Amoxicillin**<br>**Ampicillin**<br>**Cloxacillin** | 104<br>105<br>103 | $H_2O_2$/COD 1.5 | 5.2<br>5.25<br>5.15 | 3 | – | – | Complete degradation within 2 min; COD and DOC removal of 80.8% and 58.4% at 50 min | (Elmolla and Chaudhuri 2009b) |
| **Amoxicillin**<br>**Cloxacillin** | 138<br>84 | $H_2O_2$/COD 2.5 | 6.9<br>4.2 | 3 | – | – | Complete degradation within 1 min; 89% COD removal and complete nitrification with combined photo-Fenton-SBR | (Elmolla and Chaudhuri 2011) |
| **Lincomycin (LCM)** | 25 | 170 | 11.17 | – | – | – | DOC removal of 65% for LCM and 80% for DZP within 60 min irradiation | (Bautitz and Nogueira 2010) |
| **Diazepam (DZP)** | 25 | | | | | | | |
| **Hospital wastewater** | | COD:$H_2O_2$:$Fe^{2+}$ 1:4:0.1 | | 3 | – | – | Increasing $BOD_5$/COD ratio from 0.3 to 0.52 and oxidation degree from −1.14 to +1.58 | (Elmolla and Chaudhuri 2011) |
| **Amoxicillin** | 50 | 120 | 2.8 | 2.5–2.8 | – | – | 73–81% TOC removal after 240 min, AMX removal after 5–15 min using Fe-Ox and $FeSO_4$respectively | (Trovo' et al. 2011) |
| **Nalidixic acid** | 45 | 300 | 20 | 2.6– 2.8 | – | – | 15% DOC and 100% NXA removal after 210 min | (Sirtori et al. 2011) |

**Table8** ***(continued)***

| Compound | Initial value (mg $L^{-1}$) | Operational condition | | | | | Optimal performance | Ref |
|---|---|---|---|---|---|---|---|---|
| | | [$H_2O_2$] (mg $L^{-1}$) | Iron (mg $L^{-1}$) | pH - | [Ox] (mg $L^{-1}$) | *T* (°C) | | |
| **Dichlorodiphenylamine (DCDPA), Diclofenac sodium salt (NaDCF), meclofenamic acid sodium salt (NaMCF)** | Each 5 | 10 | 10 | 3.5 | – | – | 99% DCF and MCF and 96% DCDPA degradation within 120 min; rate constant order of $k_{DCDPA} < k_{DCF} < k_{MCF}$ | (Miró et al. 2013) |
| **Sulfamethoxazole [SMX]** | 200 | >300 | 10 | 2.8 | – | 25 | 98% SMX removal, $BOD_5$/COD improvement from 0.0 to 0.3, 2.4–79.9% TOC removal with $H_2O_2$ doses from 50 to 1000 mg $L^{-1}$ | (González et al. 2007) |
| **Paracetamol** | 157.5 | 200 | 20 | – | – | – | 83.33% reduction in reagent cost, 79.11% reduction in costs of reaction time (from 3.4502 \$/$m^3$ to 0.7392 \$/$m^3$) | (Santos-Juanes Jordá et al. 2011) |
| **Sulfadiazine (SDZ)** | 25 | 170 | – | 2.5 | 17.6 | – | Complete degradation after 8 min irradiation, 92% and 90% mineralization of SDZ and STZ after 42 min of irradiation | (Batista and Nogueira 2012) |
| **Sulfathiazole (STZ)** | 25 | | | | | | | |
| **Mitoxantrone (MTX)** | 31.11 | 640 | 30 | 3 | 47.5 | – | 60%, 77% and 82% mineralization using $Fe^{2+}$, $Fe^{3+}$ and Fe-Ox respectively within 140 min | (Cavalcante et al. 2013) |
| ***Agrochemicals*** | | | | | | | | |
| **Malathion** | 10 | 1000 | 25 | 3 | – | – | Malathion removal to desired level (0.1 mg $L^{-1}$) after 135 min | (Zhang and Pagilla 2010) |
| **Diuron and Linuron** | $TOC_0$: 50 | 202 | 15.9 | 2.8 | – | 25 | Herbicides degradation within 60 min irradiation with UV-A, 30% TOC removal by ph-F alone and 87% by ph-F-SBR | (Farré et al. 2006) |
| **Lindane (γ-HCH)** | 1.01 | 1000 | 125 | 3 | – | – | 95% and 99.91% TOC removal after 2 and 4 h of irradiation | (Nitoi et al. 2013) |
| **Laition, Metasystox, Sevnol and Ultracid** | Each 50 | 100 | 20 | 2.8 | – | 30 | Up to 80% mineralization of the mixture after 45 min, 31% DOC removal with only ph-F within 140 min and 90% with ph-F-SBR after 7 h | (Ballesteros Martín et al. 2009) |
| **Alachlor, atrazine, chlorfenvinphos, diuron, isoproturon, pentachlorophenol** | Each 50 | 100 | 20 | 2.8 | – | – | Degradation of the all pesticides into intermediates, 90% TOC removal after <15 min | (Monteagudo et al. 2011) |
| **Methomyl** | 20 | 34 | 28 | 3 | – | – | 100% methomyl removal within 30 min | (Tamimi et al. 2008) |

**Table8** ***(continued)***

| Compound | Initial value ($mg\ L^{-1}$) | Operational condition | | | | | Optimal performance | Ref |
|---|---|---|---|---|---|---|---|---|
| | | $[H_2O_2]$ ($mg\ L^{-1}$) | Iron ($mg\ L^{-1}$) | pH - | [Ox] ($mg\ L^{-1}$) | *T* (°C) | | |
| **Linuron** | 10 | 13.6 | 2.2 | 4 | – | 25 | Complete linuron degradation after 20 min, 90% TOC removal after 25 h with formation of chloride, nitrate and ammonium ions | (Katsumata et al. 2005) |
| **Abamectin** | 9 | 204 | 28 | 2.5 | – | – | 70% Abamectin degradation within 60 min, 60% mineralization after 180 min | (Matos et al. 2012) |
| **Metalaxyl** | 150 | 80 | 2 | 2.8 | – | – | 96.3% metalaxyl degradation after 180 min | (Silva et al. 2012) |
| ***Petroleum refinery*** | | | | | | | | |
| **Oxalates** | 182 | 1020 | $[Fe^{2+}]$ 280 | 3.9 | – | – | Faster degradation of formates than oxalates, $^{a}EEC_{TOC=15}$( UV-C) = 1.30 €$m^{-3}$, $EEC_{TOC}$=15(UV-A) = 2.37 €$m^{-3}$ | (Simunovic et al. 2011) |
| **Formats** | 92 | | $[Fe^{3+}]$ 447 | | | | | |
| **Sourwater from refinery plant** | – | 4000 | 400 | – | – | – | 87% DOC removal with ph-F within 60 min | (Coelho et al. 2006) |
| **Diesel oil** | – | 1700 | 5.6 | 3 | – | – | 99% TOC removal within 30 min | (Galvão et al. 2006) |
| **Petroleum extraction wastewater** | 1.6 | 16,500 | 0.93 | 3 | – | – | 92% and 96% polycyclic aromatic hydrocarbons and aromatic removal within 7 h sunlight exposure | (Rocha et al. 2013) |
| **Phenol** | 200 | 1080 | 5 | 3 | 10 | – | 98% COD removal within 120 min, 90% phenol degradation at 10 min | (Huang et al. 2010) |
| **Phenol** | 100 | >18.2% | AMKC[b] 2.23 g | 5.4 | – | – | 99.15% phenol degradation within 5 min | (Ayodele et al. 2012) |
| **Xylene** | 15 | 5100 | 14.5 | 2.5–3.0 | – | – | 94.5% xylene removal after 60 min, 100% TOC removal within 90 min | (da Silva et al. 2012) |
| **Phenol** | $DOC_0$500 | 6400 | 22 | 3 | – | – | 95.1% DOC removal after 180 min under solar irradiation, | (Nogueira et al. 2008) |
| ***p*-Nitroaniline (PNA)** | 25 | 340.15 | 2.8 | 3 | – | 20 | >98% degradation efficiencies of PNA within 30 min solar irradiation | (Sun et al. 2008) |
| **Protocatechuic acid (PCA), p-coumaric acid (p-CA), Gallic acid (GA),** | 20 | 400 | 20 | 4 | 60 | 25–39 | 100% PCA removal within 4 min, 100% p-CA degradation within 2 min, 100% GA degradation (within 3 min, 94% TOC removal after 194 min | (Monteagudo et al. 2011) |

[a] $EEC_{TOC=15}$:electrical energy costs required to achieve reference value of 15 mg C $L^{-1}$.
[b] AMKC: acid modified kaolin clay supported ferric-oxalate catalyst.

***Operative parameters***

Several components can influence the rate and the stoichiometry of Fenton reaction, from the quality of the treating water to the operative parameters set for the treatment. The first group of components has been already mentioned in section 1.5.1. Concerning the second group, we can mention:

- the concentration of $Fe^{2+}$ and $Fe^{3+}$;
- the concentration of $H_2O_2$;
- the ratio $Fe^{2+}/H_2O_2$;
- the pH;
- the temperature.

**$Fe^{2+}/Fe^{3+}$ concentration** is fundamental to allow the start of the radicals' catalytic mechanism of Fenton's process. The optimum dosage is characteristic for Fenton's process and it generally depends of the water quality of the influent. it has important to take into account that:

- The optimum concentration generally depends of the concentration of organic matter (RH) present in the aqueous matrix;
- Minimum doses (2-20 mg $L^{-1}$) allow the system to progress independently of the charge in terms of organic substrate;
- Iron concentration lower than 25-50 mg $L^{-1}$ can entail to long reactions time for the achievement of significant removals;
- A ratio Fe/RH (indicative) of 1:10 - 1:50 ensure good oxidation achievements.

In photo-Fenton, by the way, significantly lower concentration of iron can allow the achievements of higher efficiency of treatment due to the faster reconversion of $Fe^{3+}$ to $Fe^{2+}$ due to the irradiation of the solution.

**$H_2O_2$ concentration** is fundamental to ensure the HO· production. The oxidation of the transformation products of the main contaminants can require high concentration of oxidant for the achievements of significant mineralization of the solution. In Fenton, the concentration of $H_2O_2$ generally required change between 100 and 10000 mg$H_2O_2$ $L^{-1}$. Also in this case, the oxidant concentration can significantly be reduced when irradiating the solution (photo-Fenton) because the extra contribution in HO· production.

Hydroxyl radical is not only involved in the reaction with the organic compounds but in several other reactions, included those one in which Fenton reagents participate. Thus, **the ratio $Fe^{2+}/H_2O_2$** is really important in order to ensure the adequate production of radicals available for the oxidation, avoiding scavenging effects.

As already mentioned, the key features of Fenton system are its reagents conditions. These parameters determine the overall reaction efficiency and the ratio between them (**$Fe^{2+}/H_2O_2$**) represent an important key to understand the development of the reaction. When the ratio is ***high ($Fe^{2+}/H_2O_2 \geq 2$)*** and in absence of organics, the consumption ratio of ferrous ion to hydrogen peroxide ($\Delta Fe^{2+}/\Delta H_2O_2$) becomes about two and radical chain reactions are quickly terminated. In fact the radicals produced from the chain initiation's reaction (Eq. 16) mainly react with ferrous ions (Eq. 21) and not with hydrogen peroxide (Eq. 19), as it is also

observable from the rate constant for the reactions. On the other hand, the presence of organics, mainly affect the behavior of the ferrous ions because the competition for HO·. Thus, the presence of organics, significantly reduce the ratio $\Delta Fe^{2+}/\Delta H_2O_2$ suggesting as ferrous ions is utilized more as reactant than not as catalyst of the reaction. In case of **medium ratio *($Fe^{2+}/H_2O_2$ =1)*** when in presence of organics, the hydrogen peroxide quickly converts $Fe^{2+}$ in $Fe^{3+}$ (eq. 16). Hydrogen peroxide decomposes under the effect of $Fe^{3+}$ induced chain reactions showing a decomposition rate significantly lower. It is then possible to identify two possible systems (ferrous system and ferric system) depending of the major oxidation stage of the iron present. In this condition, an excessive presence of RH can strongly hinder the reaction between HO· and $Fe^{2+}$. Hydrogen peroxide slower consumption is then observable due to the reaction of this with the remaining $Fe^{3+}$. Finally, with a **low ratio *($Fe^{2+}/H_2O_2$ «1),*** after a first rapid depletion of hydrogen peroxide, follows a slow decomposition of the same occurred by ferric ion. On the other hand, in presence or organics, the initial hydrogen peroxide decomposition induced by ferrous ion is lower than in the absence of organics. HO· mainly reacts with $H_2O_2$ producing $HO_2$· which participate in propagating radical chain reaction producing ferrous ions trough reduction of ferric ions. The consumption of hydrogen peroxide results larger than in absence of organics ($\Delta Fe^{2+}/\Delta H_2O_2$«1) (Neyens and Baeyens 2003).

Fenton's reaction rate is maximum for **pH** values around 3-4 (optimum 2.8) while significantly decrease for pH higher than 6. At this pH, in fact, $Fe^{2+}$ is oxidized producing no reactive oxyhydroxide iron species that are useless for the catalysis of Fenton reaction. During the reaction the pH can also change due to the production of reaction's by-products requiring then a constant adjustment of the pH. The addition of chelating agent has been demonstrated useful to increase the efficiency of the process at circumneutral pH.

Increasing the **temperature**, higher rate of the reactions can be obtained. This effect is especially noticeable for temperature higher than 20 °C. However, for temperatures between 40 and 50 °C, the effect of enhanced rate of the reaction cannot compensate the negative effect of the hydrogen peroxide decomposition. The hydrogen peroxide available for the radical production would be then significantly reduced. The optimum range of temperature for Fenton applications is then variable in the range of 20-40 °C. Higher temperatures could be considered when applying heterogeneous treatment.

### *1.6.4 Photo-Fenton at neutral pH: Chelate based Photo-Fenton like*

Among the AOPs, Fenton and photo-Fenton technologies have been widely studied and reported as interesting alternatives to be employed as specific treatments to achieve CECs removal. Nevertheless, some not negligible disadvantages related to them, make difficult their applicability, including the narrow pH range of work (pH 2-3). To overcome several disadvantages associated to conventional photo-Fenton operational conditions and to take advantage of its good performance, the process should be modified. Allow a wider pH range of work by developing modified Fenton like processes (at neutral/circumneutral pH) is indispensable for the real application of the treatment. Fenton-like reactions make use of various iron compounds including complexes of iron with organic ligands or solid supports. Fenton and photo-Fenton like at neutral pH can be performed in two different modes, homogenous and heterogeneous (Garrido-Ramírez et al. 2010; Sun et al. 2014).

Heterogeneous photo-Fenton like at neutral pH can be carried out by means of support materials such as neutral organic polymers, ion exchanges membranes or resins and inorganic materials (clay, zeolites, etc.). Homogeneous Fenton like at neutral pH could be carried out using substances able to solubilize iron in a wider range of pH than conventional photo-Fenton. These substances are named chelating agents and are able to form photoactive species ($Fe^{3+}L$) suitable to maintain the iron soluble. Chelation is useful to extend the pH range over which iron is soluble because the chelating ligand competes favorably with hydroxide ion for coordination and chelated complexes are typically soluble (Pignatello et al. 2006). Less catalytic activity is generally expected when catalyzing Fenton-like reaction by means of iron chelate. Chelating process, in fact, imply a reduction of the metal ion activity having this been one of the most common use of chelating agents (Means et al. 1980). However the possibility of reducing the production of iron sludge and avoiding the requirement of influent acidification could make the application advantageous.

Although the mechanism of Fe(III)-chelates catalyzed Fenton-like reaction has not yet been clarified, it is generally accepted that HO· radical dot plays a major role in the degradation of contaminants (Dao and De Laat 2011; Sun et al. 2013; Huang et al. 2013).

Chelating agents can bind iron, then the initiation of Fenton-like reactions takes place as described by the following reactions (Xue et al. 2009):

$$Fe^{3+} + L \rightarrow Fe(III)L \quad (36)$$

$$Fe(III)L + H_2O_2 \rightarrow Fe(II)L + H^+ + HO_2 \cdot \quad (37)$$

$$Fe(III)L + HO_2 \cdot \rightarrow Fe(II)L + H^+ + O_2 \quad (38)$$

$$Fe(III)L + O_2^- \cdot \rightarrow Fe(II)L + O_2 \quad (39)$$

$$Fe(II)L + H_2O_2 \rightarrow Fe(III)L + HO \cdot + OH^- \quad (40)$$

Similarly to what happens in conventional photo-Fenton, under UV irradiation, the radicals production results significantly enhanced. The most likely explanation of this enhancement is the photo-dissociation of the chelates by ligand-to-metal charge-transfer excitation (Sun and Pignatello 1993) with consequent reduction of iron to form ferrous ion:

$$Fe(III)L \overset{h\nu}{\rightarrow} Fe^{2+} + L \cdot \quad (41)$$

The ligand-free radical is able to react with dissolved oxygen in water to form superoxide radical (Stasicka 2011):

$$L \cdot + O_2 \rightarrow O_2^- \cdot + L' \quad (42)$$

The $O_2^{-}\cdot$ radical and its conjugated form $HO_2\cdot$ (eq. 43) can participate in further reactions generating $H_2O_2$ (eq. 44-46, Table 9):

**Table 9 Reactions involving $HO_2\cdot$/ $O_2^-\cdot$**

| Reactions | | Ref. | Eq. |
|---|---|---|---|
| $\boldsymbol{O_2^-\cdot + H^+ \leftrightarrow HO_2\cdot}$ | $pK_a$=4.8 | (Bielski et al. 1985) | (43) |
| $\boldsymbol{Fe^{2+} + HO_2\cdot/O_2^-\cdot + H^+ \rightarrow Fe^{3+} + H_2O_2}$ | (k= 1.2±0.5 × $10^6$ $M^{-1}$ $s^{-1}$) | (Bielski et al. 1985) | (44) |
| $\boldsymbol{HO_2\cdot + HO_2\cdot \rightarrow H_2O_2 + O_2}$ | (k= 8 × $10^5$ $M^{-1}$ $s^{-1}$) | (De Laat et al. 1999) | (45) |
| $\boldsymbol{HO_2\cdot + HO_2\cdot \rightarrow H_2O_2 + O_2}$ | | | (46) |
| $\boldsymbol{Fe^{2+} + H_2O_2 \rightarrow Fe^{3+} + HO^- + HO\cdot}$ | (k = 76 $M^{-1}$ $s^{-1}$) | (Rigg et al. 1954) | (47) |

Finally, as a consequence of the radical chain reaction, hydroxyl radical can be additionally formed by Fenton reaction by oxidizing Fe(II) with $H_2O_2$ (eq . 47).

Eventually, two additional reactions could also be considered:

$$Fe(III)L - OH \xrightarrow{h\nu} Fe(II)L + OH\cdot \quad (48)$$

$$Fe(II)L - O_2H \xrightarrow{h\nu} Fe(II)L + HO_2\cdot \quad (49)$$

To be useful, a Fe(III) chelate must (Sun and Pignatello 1992):

- have catalytic activity toward oxidation of the waste component, i.e., be capable of generating hydroxyl radical or other reactive oxidant from $H_2O_2$;
- be resistant to oxidation in the medium;
- be environmentally safe.

Several compounds have been largely considered as potentials iron chelators in photo-Fenton like processes at neutral pH (Sun and Pignatello 1992; Klamerth et al. 2013) forming strong complexes with $Fe^{3+}$. Sun and Pignatello (1992) evaluated many chelating agents to solubilize $Fe^{3+}$ at pH 6 and mineralize 2,4-dichlorophenoxyacetic acid in the $Fe^{3+}/H_2O_2$ system. Their study indicated that several ligands (such as dipicolinic acid, oxalic acid, and gallic acid) could complex with $Fe^{3+}$ to form soluble chelates which had the ability to oxidize pesticide waste, proving also that some of them have a low capability to decompose $H_2O_2$ without UV light (i.e. Fe(III)-citrate). The chelating agents considered by Sun and Pignatello (1992) are listed in Table 10. Later, they chose picolinic acid, gallic acid, and rhodizonic acid as chelating agents to mineralize pollutants in the $Fe^{3+}$-chelate $H_2O_2$ system (at pH 6) with or without UV irradiation (Sun and Pignatello 1993).

**Table 10 Chelate ability of ligands of Iron(III) at pH 6 and activity of the chelate with respect to the oxidation of 2,4-D by $H_2O_2$ (extracted from (Sun and Pignatello 1992))**

| Ligand | Activity |
|---|---|
| ***Aminopolycarboxylates*** | |
| **EDTA** | Inactive |
| **HEDTA** | Inactive |
| **EDDHA** | Inactive |
| **EGTA** | Inactive |
| **NTA** | High |
| **HEIDA** | High |
| ***Policaboxylates*** | |
| **Citric acid** | Low |
| **Mucic acid** | Moderate |
| **Malonic acid** | Moderate |
| **L-malic acid** | Inactive |
| **Ketomalonic acid** | Low |
| **DL_tartaric acid** | Low |
| **Oxalic acid** | Low |
| ***Hydroxamates*** | |
| **Acetoxydroxamic acid** | Inactive |
| ***N-heteroclycic carboxylates*** | |
| **Picolinic acid** | High |
| **Dipicolinic acid** | Moderate |
| ***Polyhydroxy aromatics*** | |
| **Catechol** | Moderate |
| **1,2-dihydroxybenzoic acid** | Moderate |
| **Gallic acid** | High |
| **Quercertin** | Moderate |
| **Rutin** | Inactive |
| **Pyrocatechol violet** | Moderate |
| **Alizarin red** | Low |
| ***Porphyrins*** | |
| **Hemin** | Inactive |
| **Hematin** | Inactive |
| **Hematoporphirine X** | Inactive |
| ***Phosphates*** | |
| **Pyrophosphate** | Inactive |
| **Hypophosphate** | Inactive |
| **Tripolyphosphate** | Inactive |
| **Trimetapolyphosphate** | Inactive |
| **Phytate** | Inactive |
| **imidodiphosphate** | Inactive |
| **Carbamylphosphate** | Inactive |
| **Phosphonoformate** | Inactive |
| **Adenosine 5'-diphosphate** | Inactive |
| **Adenosine 5'-triphosphate** | Inactive |
| ***Miscellaneous*** | |
| **Rhodizonic acid** | High |
| **Tetrahydroxy-1,4-quinone** | High |

**Table10 *(continued)***

| Ligand | Activity |
|---|---|
| **Ascorbic acid** | Moderate |
| **Hexaketocyclohexane (HKCK)** | High |

The generation of reactive species depends greatly on the properties of chelates (e.g., type and number of functional groups), the molar ratio of chelates to Fe(III), $H_2O_2$ and Fe(III) concentrations, and the pH (Sun and Pignatello 1992; De Laat et al. 2011).

A measure of the strength of the interaction between the ligand and the metal ions is expressed through the **stability constant** (formation constant or binding constant) of the complexes. This represents the equilibrium of the substitution reaction of the formation between the metal ion (M) and the ligand (L) and it can express as following:

$$K_{M-L} = \frac{[ML]}{[M][L]} \tag{50}$$

In Table 11 are listed the stability constant of some suitable complexes (extract from (Furia 1973)):

**Table 11 Stability constants (log $K_{M-L}$) of cations with several ligands (Furia 1973)**

| | Al(III) | Ba | Ca | Co(II) | Cu | Fe(II) | Fe(III) | Hg | Mg | Mn | Ni | Sr | Zn |
|---|---|---|---|---|---|---|---|---|---|---|---|---|---|
| **Acetic acid** | | 0.39 | 0.53 | 2.24 | | | | 3.7 | 0.51 | | 0.74 | 0.43 | 1.03 |
| **Adipic acid** | | 1.92 | 2.19 | | 3.35 | | | | | | | | |
| **ADP** | | 2.36 | 2.82 | 3.68 | 5.90 | | | | 3.11 | 3.54 | 4.50 | 2.50 | 4.28 |
| **Alanine** | | 0.80 | 1.24 | 4.82 | 8.18 | | | | | 3.24 | 5.96 | 0.73 | 5.16 |
| **β-Alanine** | | | | | 7.13 | | | | | | 4.63 | | 4 |
| **Albumin** | | | 2.20 | | | | | | | | | | |
| **Arginine** | | | | | | 3.20 | | | | 2.0 | | | |
| **Ascorbic acid** | | | 0.19 | | | | | | | | | 0.35 | |
| **Asparagine** | | | 0 | | | | | | | | | 0.43 | |
| **Aspartic acid** | | 1.14 | 1.16 | 5.90 | 8.57 | | | | 2.43 | 3.74 | 7.12 | 1.48 | 2.90 |
| **ATP** | 9.58 | 3.29 | 3.60 | 4.62 | 6.13 | | | | 4.0 | 3.98 | 5.02 | 3.03 | 4.25 |
| **Benzoic acid** | | | | | 1.6 | | | | | | 0.9 | | 0.9 |
| **n-Butyric acid** | | 0.31 | 0.51 | | 2.14 | | | | 0.53 | | | 0.36 | 1.00 |
| **Casein** | | | 2.23 | | | | | | | | | | |
| **Citraconic acid** | | | 1.3 | | | | | | | | | 1.3 | |
| **Citric acid** | 11.7 | 2.3 | 3.5 | 4.4 | 6.1 | 3.2 | 11.85 | 10.9 | 2.8 | 3.2 | 4.8 | 2.8 | 4.5 |
| **Cysteine** | | | | 9.3 | 19.2 | 6.2 | | 14.4 | <4 | 4.1 | 10.4 | | 9.8 |
| **Dehydracetic acid** | | | | | 5.6 | | | | | | 4.1 | | |
| **Desferri-ferrychrysin** | | | | | | | 29.9 | | | | | | |
| **Desferri-ferrichrome** | | | | | | | 29.0 | | | | | | |
| **Desferri-ferrioxamin E** | | | | 11.8 | 13.7 | | 32.5 | | | | 12.2 | | 12 |
| **3,4-Dihydroxybenzoic acid** | | | 3.71 | 7.96 | 12.79 | | | | 5.67 | 7.22 | 8.27 | | 8.91 |
| **Dimethylglyoxime** | | | | | 11.94 | | | | | | 14.6 | | 7.7 |
| **O,O-Dimethylpurpurogallin** | | | 4.5 | 6.6 | 9.2 | | | | 4.9 | | 6.7 | | 6.8 |
| **EDTA** | 16.13 | 7.78 | 10.70 | 16.21 | 18.8 | 14.3 | 25.7 | 21.5 | 8.69 | 13.56 | 18.56 | 8.63 | 16.5 |
| **Formic acid** | | 0.60 | 0.80 | | 1.98 | | 3.1 | | | | | 0.66 | 0.60 |
| **Fumaric acid** | | 1.59 | 2.00 | | 2.51 | | | | | 0.99 | | 0.54 | |
| **Gluconic acid** | | 0.95 | 1.21 | | 18.29 | | | | 0.70 | | | 1.00 | 1.70 |
| **Glutamic acid** | | 1.28 | 1.43 | 5.06 | 7.85 | 4.6 | | | 1.9 | 3.3 | 5.9 | 1.37 | 5.45 |
| **Glutaric acid** | | 2.04 | 1.06 | | 2.4 | | | | 1.08 | | | 0.6 | 1.60 |
| **Glyceric acid** | | 0.80 | 1.18 | | | | | | 0.86 | | | 0.89 | 1.80 |
| **Glycine** | | 0.77 | 1.43 | 5.06 | 7.85 | 4.6 | | | 1.9 | 3.3 | 5.9 | 1.37 | 5.45 |
| **Glycolic acid** | | 0.66 | 1.11 | 1.60 | 2.81 | | 4.7 | | 0.92 | | | 0.80 | 1.92 |

**Table11 *(continued)***

| | Al(III) | Ba | Ca | Co(II) | Cu | Fe(II) | Fe(III) | Hg | Mg | Mn | Ni | Sr | Zn |
|---|---|---|---|---|---|---|---|---|---|---|---|---|---|
| **Glycylcglycine** | | | 1.24 | 3.00 | 6.7 | 2.62 | 9.1 | | 1.34 | 2.19 | 4.18 | | 3.91 |
| **Glycylsarcosine** | | | | 3.91 | 6.50 | | | | | 2.29 | 4.44 | | |
| **Guanosine** | | | | 3.2 | 6 | 4.3 | | | 3.0 | | 3.8 | | 4.6 |
| **Histamine** | | | | 6.16 | 9.55 | 9.60 | 3.72 | | | | 6.88 | | 5.96 |
| **Histidine** | | | | 7.30 | 10.60 | 5.89 | 4.00 | | | 3.58 | 8.69 | | 6.63 |
| **β-Hydroxybutyric** | | 0.43 | 0.60 | | | | | | 0.60 | | | 0.47 | 1.06 |
| **3-Hydroxyflavone** | | | | 9.91 | 13.20 | | | | | | | | 9.70 |
| **Inosine** | | | | 2.6 | 5 | 3 | | | | | 3.3 | | |
| **Inosine triphosphate** | | | 3.76 | 4.74 | | | | | 4.04 | 4.57 | | | |
| **Isovaleric acid** | | | 0.20 | | 2.08 | | | | | | | | |
| **Itaconic acid** | | | 1.20 | | 2.8 | | | | | | 1.8 | 0.96 | 1.9 |
| **Kojic acid** | 7.7 | | 2.5 | 7.11 | 6.6 | | 9.2 | | 3.0 | | 7.4 | | 4.9 |
| **Lactic acid** | | 0.55 | 1.07 | 1.89 | 3.02 | | 6.4 | | 0.93 | 1.19 | 2.21 | 0.70 | 1.86 |
| **Leucine** | | | | 4.49 | 7.0 | 3.42 | 9.9 | | | 2.15 | 5.58 | | 4.92 |
| **Lysine** | | | | | | | 4.5 | | | 2.18 | | | |
| **Maleic acid** | | 2.26 | 2.43 | | 3.90 | | | | | 1.68 | 2.0 | 1.1 | 2.0 |
| **Malic acid** | | 1.30 | 1.80 | | 3.4 | | | | 1.55 | 2.24 | | 1.45 | 2.80 |
| **Methionine** | | | | | | 3.24 | 9.1 | | | | 5.77 | | 4.38 |
| **Methylsalicylate** | | | | | 5.90 | | 9.77 | | | | | | |
| **NTA** | >10 | 4.82 | 6.41 | 10.6 | 12.68 | 8.84 | 15.87 | | 5.41 | 7.44 | 11.26 | 4.98 | 10.45 |
| **Orotic acid** | | | | 6.39 | | | | | | | 6.82 | | 6.42 |
| **Ornithine** | | | | 4.02 | 6.90 | 3.09 | 8.7 | | | <2 | 4.85 | | 4.10 |
| **Oxalic acid** | 7.26 | 2.31 | 3.0 | 4.7 | 6.3 | >4.7 | 9.4 | | 2.55 | 3.9 | 5.16 | 2.54 | 4.9 |
| **β-Phenylalanine** | | | | | 7.74 | 3.26 | 8.9 | | | | | | |
| **Pimelic acid** | | | | | | | | | | 1.08 | | | |
| **Pivalic acid** | | | 0.55 | | 2.19 | | | | | | | | |
| **Polyphosphate** | | | 3.0 | | 3.5 | 3.0 | | | 3.2 | 5.5 | 3.0 | | 2.5 |
| **Proline** | | | | | | 4.07 | 10.0 | | | 3.34 | | | |
| **Propionic acid** | | 0.34 | 0.50 | | 2.2 | | 3.45 | | 0.54 | | | 0.43 | 1.01 |
| **Purine** | | | | | 6.90 | | | | | | 4.88 | | |
| **Pyrophosphate** | | | 5.0 | | 6.7 | | 22.2 | | 5.7 | | 5.8 | | 8.7 |
| **Pyruvic acid** | | | 0.8 | | 2.2 | | | | | | | | |
| **Riboflavin** | | | | 3.9 | <6 | | | | | 3.4 | 4.1 | | <4 |
| **Salicylaldehyde** | | | | 4.67 | 7.40 | 4.22 | 8.70 | | 3.69 | 3.73 | 5.22 | | 4.50 |
| **Salicylic acid** | 14.11 | | | 6.72 | 10.60 | 6.55 | 16.36 | | 4.7 | 2.7 | 6.95 | | 6.85 |
| **Sacrosine** | | | | 4.34 | 7.83 | 3.52 | 9.7 | | | | 5.41 | | |
| **Serine** | | | 1.43 | | | 3.43 | 9.2 | | | | 5.44 | | |
| **Succinic acid** | | 1.57 | 1.20 | 2.08 | 3.3 | | 7.49 | | 1.2 | 2.11 | 2.36 | 0.9 | 1.78 |
| **(±)- tartaric acid** | | 1.95 | 1.80 | | 3.2 | | 7.49 | | 1.36 | | 3.78 | 1.94 | 2.68 |
| **Tetrametaphosphate** | | 4.9 | 5.2 | | 3.18 | | | | 5.17 | | 4.95 | 2.8 | |
| **Threonine** | | | | | | 3.30 | 8.6 | | | | | | |
| **Transferrin** | 12.3 | | | | | | | | | | | | |
| **Trimetaphosphate** | | | 2.50 | | 1.55 | | | | 1.11 | 3.57 | 3.22 | 1.95 | |
| **Triphosphate** | | 6.3 | 6.5 | | 9.8 | | | | 5.8 | | | 3.80 | 9.7 |
| **Tryptophan** | | | | | | | 9.0 | | | | | | |
| **Uridine diphosphate** | | | | | | | | | 3.17 | | | | |
| **Uridine triphosphate** | | | 3.71 | 4.55 | | | | | 4.02 | 4.78 | | | |
| **n-Valeric acid** | | 0.20 | 0.30 | | 2.12 | | | | | | | | |
| **Valine** | | | | | 7.92 | 3.39 | 9.6 | | | 2.84 | 5.37 | | 5.0 |
| **Xanthosine** | | | | 2.8 | 3.4 | <2 | | | | | 3.0 | | 2.4 |

However, it cannot be neglected that chelating agents are organic compounds that are generally absent into the municipal wastewater treatment plans (MWWTP). They have to be added into the solution to create soluble complexes with Fe(III). For this purpose, consider the stability constant is also a valid tool for choosing the chelating agent that would imply the less requirement of ligand for the chelation of the catalyst.

The definition of the (ligand:Fe) **L:Fe molar ratio** is fundamental to endure the complete chelation of the catalyst required for the reaction. In first approximation it can be determined according to the stoichiometry of the substitution reaction. Indeed, the molar ratio for chelation can be theoretically determined for a certain pH by observing the number of available sites for chelation of the ligand (i.e. numbers of the carboxyl groups). However, at neutral pH a certain amount of iron can equally precipitate implying a lower rate of Fenton reaction due to the major requirement of ligand (Sun and Pignatello 1992).

Even though most of the chelating agents studied over the years are able to be used as iron chelators, several are the concerns of the faith related to their usage. The eventually poor **biodegradability** and the increase of **toxicity** due to the formation of complexes with heavy metals should be carefully evaluated. While chelates are used because their powerful metal-binding properties, it is this same characteristic which may have undesirable environmental consequences if allowing the mobilization of heavy metals. Since it is important avoiding pollute the environment and increase the toxicity of the effluent to keep iron soluble for the treatment, chelate speciation assumes a fundamental importance. In fact, the biodegradability and the toxicity of a chelate not only depend of the chelating agent itself but they are strictly dependent on the metal bound to them (Pirkanniemi et al. 2003). The suitability of the chelating agents in terms of biodegradability and low toxicity is, then, one of the assessment's standard to choose the proper ligand.

On the other hand, the **stability of the chelate under reaction stress** is really important for the efficiency of the process since they are also sensitive to the attack of the radical species available for the reaction. Under oxidation, the chelate degradation can be divided into three categories (Means et al. 1980):

- **Ultimate degradation** occurs when the elements constituting the original compound are released in inorganic form (e.g., $CO_2$, mineralization of the chelate solution);
- **Primary degradation** refers to when the characteristic properties (e.g. chelating ability) of the compound are no longer evident;
- **Secondary degradation** indicates breakdown into compounds possessing similar primary characteristic to the original compound (e.g., degradation of chelate into compounds which still have complexing ability).

The resistance of the chelating agents under the attack of the hydroxyl radicals has to endure enough to ensure iron solubility for the catalysis of the ultimate decomposition of hydrogen peroxide. The choice of the chelating agents can not overlook the evaluation of all these aspects.

Between the most used chelating agents, aminopolycarboxylic acids are probably the most effective. They are generally used as sequestering agents in industrial cleaning, household detergents, photographic industry, pharmaceuticals, textile and paper manufacturing (Abida et al. 2006). Among them, EDTA (ethylenediaminetetraacetic acid), NTA (nitrilotriacetic acid), DTPA (diethylenetriaminepentaacetic acid), etc. are still commonly used (Guenter Kari et al. 1995). They are multidentate compounds, containing several carboxyalkyl groups bound to one or more nitrogen atoms, able to form covalent coordination bonds with the central metal ion (Sillanpää et al. 2011). These are really well known because their versatility and ability to

form stable, water-soluble complexes with a wide range of metal ions. Due to their remarkable complexation properties, synthetic APCAs have been used for domestic and industrial applications to control the solubility and precipitation of metallic ions (Egli 2001; Bucheli-Witschel and Egli 2001).

In this study four chelating compounds were studied, two of them belong to the family of the aminopolycarboxylic acids (EDTA and NTA). Oxalic acid and tartaric acid (polycarboxylic acids) were also studied.

***Ethylenediaminetetraacetic acid: EDTA***

Consisting in four carboxylic and two amino groups, EDTA poses six donor atoms (hexadentate chelating agent) to form a maximum of five chelate rings due to the stability of the two tertiary amino groups (Figure 7).

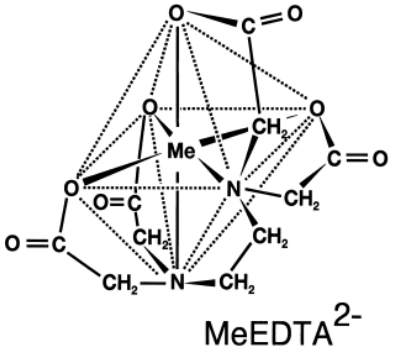


**Figure 7 Ideal octahedral structure of metal-EDTA complex (Bucheli-Witschel and Egli 2001)**

The ability to form stable complexes with metal ions (log K=27.5 for Fe(III)-EDTA complexes) made this chelating agents one of the most used ever. The high value of the stability constant of EDTA with Fe(III) confirms as the species Fe(III)-EDTA is the most predominant species of EDTA in surface water (Nowack and Stone 2002). The different species of Fe(III)-EDTA along the pH scale are shown in Figure 8.

It has been demonstrated that EDTA is resistant to biodegradation (Sillanpää and Oikari 1996) and chemically stable under oxidizing conditions (Sillanpää et al. 2003). However, Ramö and Sillanpää (2001), showed as alkaline environmental was favorable for the degradation of EDTA by $H_2O_2$. Because of its poor biological degradation, EDTA persists in surface waters where transformation by microorganism is also insignificant. Here, EDTA is to be found in considerable concentrations, being one of the highest ever determined for a single anthropogenic, widely distributes substance (Guenter Kari et al. 1995). Though it has been said that Fe(III)-EDTA is the predominant species in surface water other metal speciation is also possible, causing a strongly enhance of toxicity.

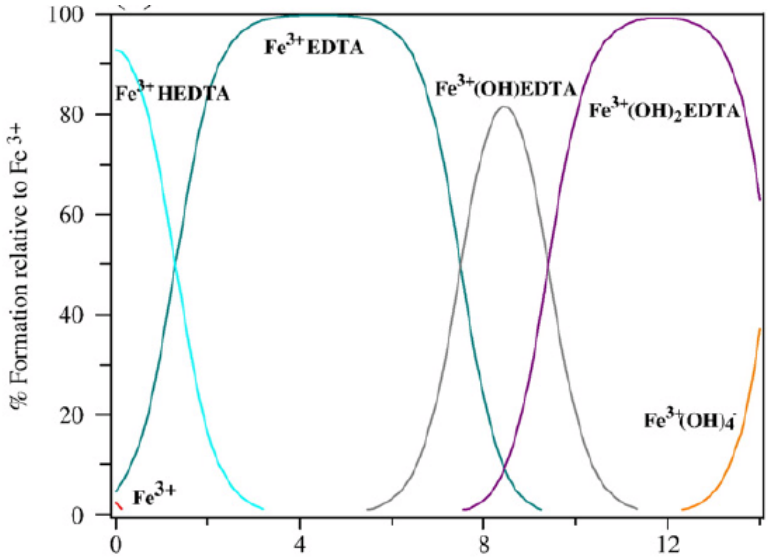


**Figure 8 Dissolved iron and EDTA species in water system at different pH (EDTA:Fe 1:1). 1= $Fe^{3+}$; 2= FeHEDTA; 3= $FeEDTA^{-}$; 4= $Fe(OH)EDTA^{2-}$; 5= $Fe(OH)_2EDTA^{3-}$; 6= $Fe(OH)_4^{-}$ (Guenter Kari et al. 1995)**

It is also important to mention that when EDTA finally degrades in water system, it releases remarkable amount of nitrogen. Finally considering the strongly enhance of toxicity dependent on metal speciation, the use of EDTA as iron chelate to perform Photo-Fenton like at neutral pH should be carefully considered.

***Nitrilotriacetic acid: NTA***

NTA it is a tripodal tetradentate trianionic ligand also belonging to the family of the aminopolycarboxylic acids. An ideal octahedral structure of metal-NTA complex is showed in Figure 9.

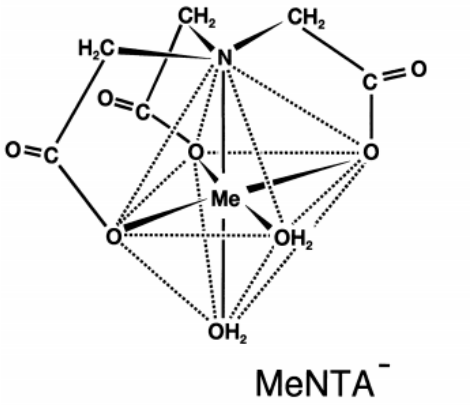


**Figure 9 Ideal octahedral structure of metal-NTA complex (Bucheli-Witschel and Egli 2001)**

The strong ability of NTA as iron chelator represented by its stability or equilibrium constant (log K=15.9 for Fe(III)-NTA complexes) makes it a reasonable candidate to be employed in this process (Furia 1973; Howsawkeng et al. 2001). The speciation of Fe(III)-NTA existing along the pH scale are shown in Figure 10:

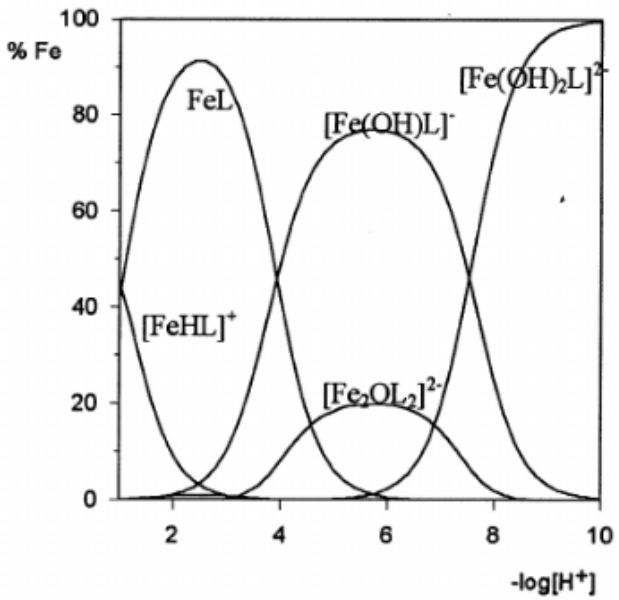


**Figure 10 Dissolved iron and NTA species in water system at different pH (NTA:Fe 1:1) (Sanchiz et al. 1999)**

Its higher biodegradability compared to other strong chelator as well as its supposed good stability under irradiation make this compound particularly competitive in its usage (Means et al. 1980; Svenson et al. 1989). The biodegradability of NTA as free chelator has been already demonstrated and the concern related to the fate of NTA release in the environment after treatment can be almost denied. The capacity biodegrade NTA appears to be high in most environmental compartments and the key to the "environmentally friendly" behavior of this complexing agent is the ubiquitous existence of a variety of different NTA-degrading microorganism in high numbers (Egli 2001; White and Knowles 2003). Moreover, the worry about the toxicity of NTA has been also disproved especially if compared to other chelating agents such as EDTA and if considering the low concentration hypothesized for its application. Sillanpää et al. (2003), in fact, carried out a study in which the acute toxicity of some chelates was analyzed. The toxicity as $LC_{50}$ and $EC_{50}$ of NTA was calculated and a very low toxicity exhibited by NTA was showed. However, the toxicity and the biodegradability of the chelates are strongly dependent on the metal speciation (Sillanpää et al. 2003; Pirkanniemi et al. 2003). On certain occasion, the toxicity of the chelate can be even lower than of the free chelator. In presence of Mn-NTA an enhancement in the algal growth was in fact also observed (Sillanpää et al. 2003). Perhaps an increment of the acute toxicity can be expected in case of heavy metal chelation. Nevertheless, considering the higher value exhibited by the equilibrium constant of Fe-NTA chelates, the exchange of iron for others heavy metals might be underdog.

***Oxalic acid***

Oxalic acid is a carboxylic acid which typically occurs as the dihydrate with the formula $C_2H_2O_4 \cdot 2H_2O$. it is a reducing agent and its conjugate base, known as oxalate ($C_2O_4^{2-}$), is a chelating agent for metal ions.

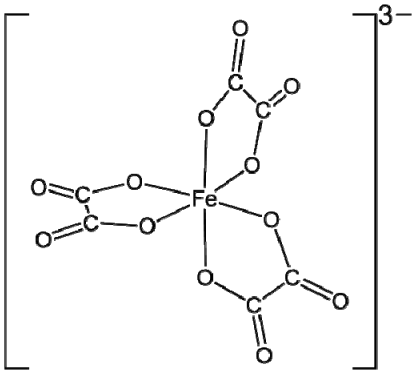


**Figure 11 Ideal octahedral structure of metal-OA complex**

Although oxalate contains four atoms which have lone pairs of electrons, it is a bidentate ligand (Figure 11). The planarity of the ion, in fact, makes impossible the establishment of four bonds with the metal ion. The speciation of ferrioxalate complexes is shown in Figure 12.

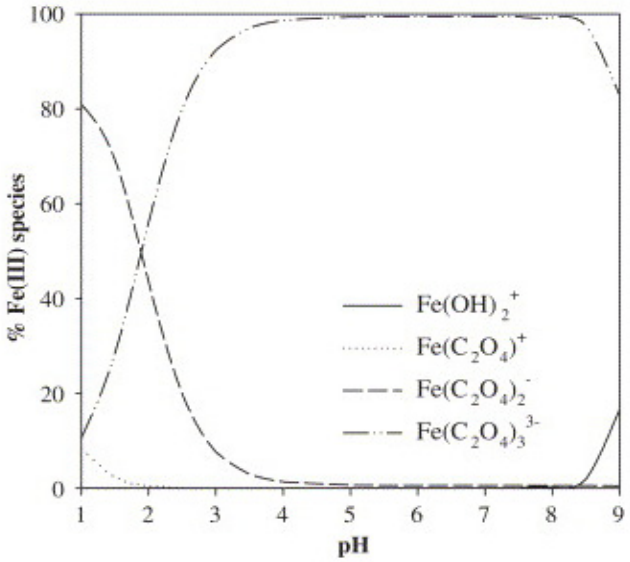


**Figure 12 Simulation of Fe(III)-OA speciation (Jeong and Yoon 2005)**

Ferrioxalate is a photosensitive complex that is able to expand the usage of solar spectrum range up to 450 nm (18 % of solar irradiation) improving the oxidation efficiency of the solar-Fenton process (Pupo Nogueira and Guimarães 2000; Emilio et al. 2002; Nogueira et al. 2005b). Due to its high photosensitivity, it has widely used a chemical actinometer for light intensity measurements. Ferrioxalate photochemistry provides extra sources of oxidant $H_2O_2$ and catalyst $Fe^{2+}$ for the Fenton reaction to yield more HO· radicals (Cooper and DeGraff 1972; Sedlak and Hoigné 1993; Selvam et al. 2005) according to the following reactions:

$$[Fe(C_2O_4)_3]^{3-} \xrightarrow{h\nu} Fe^{2+} + 2{C_2O_4}^{2-} + {C_2O_4}^{-}\cdot \quad (51)$$

$${C_2O_4}^{-}\cdot + [Fe(C_2O_4)_3]^{3-} \rightarrow Fe^{2+} + 3{C_2O_4}^{2-} + 2CO_2 \quad (52)$$

$${C_2O_4}^{-}\cdot + O_2 \rightarrow 2CO_2 + O_2^{-} \quad (53)$$

$$O_2^{-} + H^{+} \rightarrow HO_2\cdot \quad (54)$$

$$HO_2 \cdot + HO_2 \cdot \rightarrow H_2O_2 + O_2 \quad (55)$$

$$H_2O_2 + Fe^{2+} \rightarrow Fe^{3+} + HO \cdot + OH^- \quad (56)$$

The high quantum yield of $Fe^{2+}$ generation ($\Phi_{Fe2+}$=1.24 at 300 nm) (Hatchard and Parker 1956a) has been pointed out as one of the main reasons for the high efficiency of ferrioxalate in photo-Fenton process (Eq. 51 and 52)) when compared to $Fe^{3+}/H_2O_2$.

Despite the advantages related to the possibility of using the solar irradiation to catalyze the process, there is the disadvantage related to the requirement of a high molar ratio for iron chelate formation. Oxalic acid, is in fact, a relatively weak chelating agent (log K=9.4 for Fe(III)-OA complexes) and previous studies have indicated molar ratio of 10:1 OA:Fe to carry out photo-Fenton like at neutral pH (Sun and Pignatello 1992). Thus, the addition of oxalate has been considered as disadvantageous due to the increase of carbon load in the system.

***Tartaric acid***

Tartaric acid is a diprotic acid also belonging to the family of the polycarboxylates compounds. TA forms relatively weak chelates with Fe(III) (log K=7.49).

Not many information related to the use of tartaric acid as chelating agent for Fe(III) are reachable in scientific literature. Sun and Pignatello (1992) describe its low activity in the application of chelate based Fenton like at neutral pH when adopting 1:1 TA:Fe molar ratio for 2,4-dichlorophenoxyacetic acid (2,4-D). In Figure 13 it is represented the tartaric acid speciation at different pH.

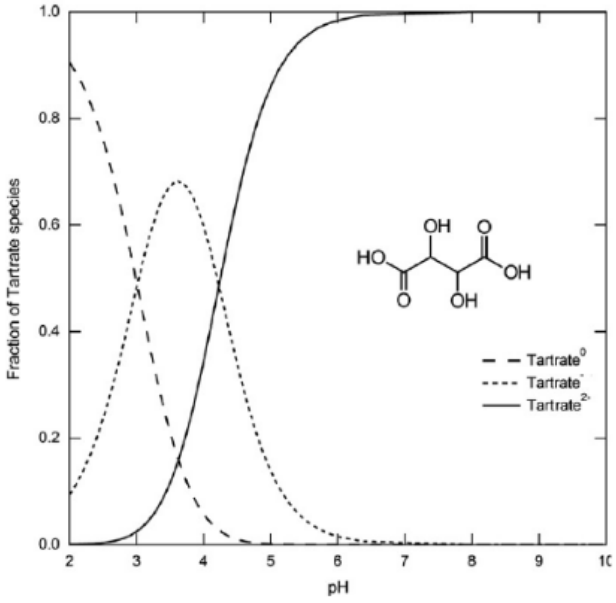


**Figure 13 Tartaric acid speciation at different pH (Ukrainczyk et al. 2013)**

Some studies of chelate based photo-Fenton applications have been rewieved by RahimPouran et al. (2015) (Table 12):

**Table 12 Effect of chelating agents on degradation efficiency of photo-Fenton system (Rahim Pouran et al. 2015)**

| Probe molecule/ Concentration (mg $L_{-1}$) | Chelating ion/ (mM) | Operational condition | | | | | Optimal performance | Ref |
|---|---|---|---|---|---|---|---|---|
| | | $[H_2O_2]$ (mg $L^{-1}$) | Fe (mg $L^{-1}$) | pH - | [a]SAE/λ ($Wm^{-2}$/nm) | reactor | | |
| **Indigo-dye/ 33.33 (BOD5/COD = 0.20)** | Oxalate 3.4 ($C_2O_4 2^-$/ $Fe^{2+}$:35) | 257 | 1.87 | 5–6 | 290 nm | bCPC | 69% TOC removal within 180 min, Significant increase in biodegradability ratio | (Vedrenne et al. 2012) |
| **Bisphenol A (BPA)** | EDDS 0.1 | 3.4 | 5.6 | 6.2 | 530 (340 nm) | Simple Pyrex-[c]PR | 92% BPA degradation within 120 min irradiation, complete BPA removal with 1 mmol $L^{-1}$ $H_2O_2$ within 10 min | (Huang et al. 2012) |
| **Antibiotic solution/ 300 (amoxicillin:150 cloxacillin:150)** | Oxalate $H_2O_2$/ $C_2H_2O_4$ 37.5 | $H_2O_2$/ COD 2.75 | $H_2O_2$/ $Fe^{3+}$ 75 | 3.0 | 850 | SolSim solar reactor | COD, TOC and $NH_3$-H of 78.37, 52.30 and 45.94% respectively within 90 min, biodegradability ratio improvement from 0 to 0.35 | (Monteagudo et al. 2013) |
| **Pharmaceutical wastewater/ (TOC: 125)** | Oxalate 5.8 | 5250 | 120 | 3.0 | 34 | CPC solar reactor | 84% TOC removal within 115 min, 3.57 mol $H_2O_2$ for 1 mole TOC removal; cost of treatment 0.0157 €/g TOC | (Monteagudo et al. 2013) |
| **Methyl Violet (MV)/(12.24)** | EDTA, 0.4 NTA ,0.6 | 680 | 50 | 5.0 | Vis >420 nm | Simple Pyrex | 49.8% MV removal within 120 min in the dark, increased degradation up to 92% within 120 min in presence of light; 3.47 times increase in rate constants in ph-F compared to Fenton | (An et al. 2013) |
| **Rhodamine B (RhB)/(4.8)** | EDTA, 0.4 | 340 | 50 | 5.0 | Vis >420 nm | Simple Pyrex | 70% RhB removal within 40 min in the dark; 1.95 times increase in rate constants in ph-F compared to Fenton | (An et al. 2013) |
| **Phenol/(282)** | NTA ,0.6 | 2040 | 50 | 3.0 | Vis >420 nm | Simple Pyrex-PR | 2.07 times increase in rate constants in ph-F compared to Fenton | (An et al. 2013) |

[a] SAE:solar accumulative energy
[b] CPC: compound parabolic collector.
[c] PR: photo reactor

### *1.6.5 Sulfate radical based oxidation*

As already mentioned, processes based on Fenton reaction represent one of the most traditional and environmentally friendly AOPs used since 1960s (Neyens and Baeyens 2003). However, because some technical gaps of Fenton reaction based treatments such as the use of a low pH, the scientific community is searching for proper modifications capable of making these treatments more adequately applicable. Another suitable modification considers replacing $H_2O_2$ with peroxymonosulfate (PMS) or persulfate (PS), from which both sulfate and hydroxyl radicals can be generated after activation. Activation can be accomplished by a

variety of reactions, including heat (Huang et al. 2005; Yang et al. 2010), ultraviolet (UV) or vacuum ultraviolet (VUV) light irradiation (Yang et al. 2010; Gu et al. 2013), alkaline pH (Furman et al. 2010), transition metals (e.g., aqueous Fe(II), Fe(III), Ag(I), Cu(II), Co(II) and Ru(III))(Anipsitakis and Dionysiou 2004; Ahmad et al. 2012; Jiang et al. 2013), iron oxides (Jo et al. 2014), or zero-valent iron (ZVI, Fe(0)) (Liang and Guo 2010). Due to its cheapness, high activity and environmental friendly nature, iron species have been commonly selected as the activator to produce sulfate radical.

PS/$Fe^{2+}$ has similarity with a Fenton system in the propagation of a series of reactions generating active radical species (Kolthoff et al. 1951). The molar extinction coefficients of PS at 248, 308, and 351 nm were 27.5 ± 1.1, 1.18 ± 0.05, and 0.25 ± 1.01 $mol^{-1}$ $cm^{-1}$, respectively, suggesting the high energy of short wavelength UV (Herrmann 2007). UV-254 nm/PS has in fact shown a high sulfate radical quantum yield of 1.4-1.8 as compared to the hydroxyl radical quantum yield of 1.0 in UV-254 nm/$H_2O_2$ (Baxendale and Wilson 1957; Mark et al. 1990). The inter-conversion of sulfate radicals into hydroxyl radicals, a non-selective and highly active oxidant, may increase the treatment efficiency of the UV-254 nm/PS process (Table 13, (Neta et al. 1988)). Consequently, the use of UV-254 nm/PS/$Fe^{2+}$ may show a synergistic effect, such as by a fast regeneration of $Fe^{2+}$ via UV-254 nm reduction of $Fe^{3+}$ and subsequently radical generation, as demonstrated by its higher effectiveness than UV-254 nm/PS/$Fe^{3+}$ and UV-254 nm/$H_2O_2$/$Fe^{3+}$ systems in the removal of certain organic contaminants (Shah et al. 2015).

**Table 13 Major reactions occurring in UV/PS/$Fe^{2+}$.**

| Reaction | | Ref. | Eq. |
|---|---|---|---|
| $S_2O_8^{2-} \xrightarrow{h\upsilon} 2SO_4^{\cdot-}$ | Φ=1.4-1.8 | (Mark et al. 1990) | (57) |
| $SO_4^{\cdot-} + SO_4^{\cdot-} \rightarrow S_2O_8^{2-}$ | k=5.0 x $10^8$ $M^{-1}$ $s^{-1}$ | (Neta et al. 1988) | (58) |
| $SO_4^{\cdot-} + S_2O_8^{2-} \rightarrow SO_4^{2-} + S_2O_8^{\cdot-}$ | k=1.2 x $10^6$ $M^{-1}$ $s^{-1}$ | (Neta et al. 1988) | (59) |
| $Fe^{2+} + S_2O_8^{2-} \rightarrow Fe^{3+} + SO_4^{2-} + SO_4^{\cdot-}$ | k=2.7 x $10^1$ $M^{-1}$ $s^{-1}$ | (Bennedsen et al. 2012) | (60) |
| $SO_4^{\cdot-} + Fe^{2+} \rightarrow SO_4^{2-} + Fe^{3+}$ | k=3.0 x $10^8$ $M^{-1}$ $s^{-1}$ | (Rastogi et al. 2009) | (61) |
| $SO_4^{\cdot-} + OH^- \rightarrow SO_4^{2-} + HO^{\cdot}$ | k=(6.5 ± 1.0) x $10^7$ $M^{-1}$ $s^{-1}$ | (Neta et al. 1988) | (62) |
| $SO_4^{\cdot-} + H_2O \rightarrow SO_4^{2-} + HO^{\cdot} + H^+$ | k<60 $M^{-1}$ $s^{-1}$ | (Neta et al. 1988) | (63) |
| $HO^{\cdot} + SO_4^{\cdot-} \rightarrow HSO_5^-$ | k=(0.95±0.08) x $10^{10}$ $M^{-1}$ $s^{-1}$ | (Klaning et al. 1991) | (64) |
| $HO^{\cdot} + S_2O_8^{2-} \rightarrow OH^- + S_2O_8^{\cdot-}$ | k<1.0 x $10^6$ $M^{-1}$ $s^{-1}$ | (Buxton et al. 1988) | (65) |
| $Fe^{2+} + HO^{\cdot} \rightarrow Fe^{3+} + OH^-$ | k=3.2 x $10^8$ $M^{-1}$ $s^{-1}$ | (De Laat et al. 1999) | (66) |
| $Fe^{3+} + h\nu \rightarrow Fe^{2+} + HO^{\cdot}$ | Φ≈0.07 | (De Laat et al. 1999) | (67) |
| $Fe^{3+} + HO_2^{\cdot} \rightarrow Fe^{2+} + O_2 + H^+$ | k<1.0 x $10^3$ $M^{-1}$ $s^{-1}$ | (De Laat et al. 1999) | (68) |

Despite the well-known effectiveness of AOPs for water remediation, counter-productive effects can also take place. Depending on the characteristics of the treatment conditions, higher levels of toxicity can be occasionally generated (Homem and Santos 2011; Fatta-Kassinos et al. 2016). In fact, due to their high reactivity with both hydroxyl and sulfate radicals Table 14), the presence of chloride and bromide, for example, may influence not only the

degradation efficiency of the targeted organic contaminants but also the potential generation of toxic halogenated byproducts.

**Table 14 Additional reactions occurring in UV/PS/$Fe^{2+}$ in the presence of bromide.**

| Reaction | | Ref. | Eq. |
|---|---|---|---|
| $Br^- + SO_4^{\cdot-} \rightarrow Br^{\cdot} + SO_4^{2-}$ | k=3.5 x $10^9$ $M^{-1}$ $s^{-1}$ | (Redpath and Willson 1975) | (69) |
| $HO^{\cdot} + Br^- \rightarrow BrOH^{\cdot-}$ | k=1.1 x $10^{10}$ $M^{-1}$ $s^{-1}$ | (Buxton et al. 1988) | (70) |
| $Br^{\cdot} + Br^- \rightarrow Br_2^{\cdot-}$ | k=1.0 x $10^{10}$ $M^{-1}$ $s^{-1}$ | (Zehavi and Rabani 1972) | (71) |
| $Br_2^{\cdot-} \rightarrow Br^{\cdot} + Br^-$ | 6.6 x $10^3$ $s^{-1}$ | (Matthew and Anastasio 2006) | (72) |
| $Br^{\cdot} + OH^- \rightarrow BrOH^{\cdot-}$ | k=1.3 x $10^{10}$ $M^{-1}$ $s^{-1}$ | (Neta et al. 1988) | (73) |
| $BrOH^{\cdot-} \rightarrow Br^{\cdot} + OH^-$ | 4.2 x $10^6$ $s^{-1}$ | (Zehavi and Rabani 1972) | (74) |
| $BrOH^{\cdot-} + H^+ \rightarrow Br^{\cdot} + H_2O$ | k=4.4 x $10^{10}$ $M^{-1}$ $s^{-1}$ | (Zehavi and Rabani 1972) | (75) |
| $Br^- + BrOH^{\cdot-} \rightarrow Br_2^{\cdot-} + OH^-$ | k=1.9 x $10^8$ $M^{-1}$ $s^{-1}$ | (Zehavi and Rabani 1972) | (76) |
| $Br_2^{\cdot-} + OH^- \rightarrow Br^- + BrOH^{\cdot-}$ | k=2.7 x $10^6$ $M^{-1}$ $s^{-1}$ | (Mamou et al. 1977) | (77) |
| $Br_2^{\cdot-} + Br_2^{\cdot-} \rightarrow Br^- + Br_3^{\cdot-}$ | k=1.8 x $10^9$ $M^{-1}$ $s^{-1}$ | (Neta et al. 1988) | (78) |
| $Br_3^{\cdot-} \leftrightarrows Br^- + Br_2$ | k=1.5 x $10^9$ $M^{-1}$ $s^{-1}$ | (Beckwith et al. 1996) | (79) |
| $Br_2^{\cdot-} + HO^{\cdot} \rightarrow HOBr + Br^-$ | k=1.0 x $10^9$ $M^{-1}$ $s^{-1}$ | (Wagner and Strehlow 1987) | (80) |
| $HOBr + HO^{\cdot} \rightarrow BrO^{\cdot} + H_2O$ | k=2.0 x $10^9$ $M^{-1}$ $s^{-1}$ | (Neta et al. 1988) | (81) |
| $Br_2 + H_2O \leftrightarrows HOBr + Br^- + H^+$ | k=1.6 x $10^{10}$ $M^{-1}$ $s^{-1}$ | (Beckwith et al. 1996) | (82) |
| $HOBr \leftrightarrows BrO^- + H^+$ | pKa=8.8 | (Haag and Hoigne 1983) | (83) |
| $BrO^- + Br_2^{\cdot-} \longrightarrow BrO^{\cdot} + 2Br^-$ | k=8±0.7 x $10^7$ $M^{-1}$ $s^{-1}$ | (Buxton and Dainton 1968) | (84) |
| $BrO^- + Br^{\cdot} \longrightarrow BrO^{\cdot} + Br^-$ | k=4.1 x $10^9$ $M^{-1}$ $s^{-1}$ | (Kläning and Wolff 1985) | (85) |
| $2BrO^{\cdot} + H_2O \longrightarrow BrO^- + BrO_2^- + 2H^+$ | k=4.9±1 x $10^9$ $M^{-1}$ $s^{-1}$ | (Buxton and Dainton 1968) | (86) |
| $BrO_2^- + BrO^{\cdot} \rightarrow BrO^- + BrO_2^{\cdot}$ | k=3.4±0.7 x $10^8$ $M^{-1}$ $s^{-1}$ | (Buxton and Dainton 1968) | (87) |
| $BrO_2^- + Br_2^{\cdot-} \longrightarrow Br^- + BrO^{\cdot} + BrO^-$ | k=8.0±0.8 x $10^7$ $M^{-1}$ $s^{-1}$ | (Buxton and Dainton 1968) | (88) |
| $BrO^- + HO^{\cdot} \rightarrow BrO^{\cdot} + OH^-$ | k=4.5 x $10^9$ $M^{-1}$ $s^{-1}$ | (Neta et al. 1988) | (89) |
| $2BrO_2^{\cdot} \leftrightarrows Br_2O_4$ | k=1.4 x $10^9$ $M^{-1}$ $s^{-1}$ | (Buxton and Dainton 1968) | (90) |
| $2BrO_2^{\cdot} + H_2O \rightarrow BrO_2^- + BrO_3^- + 2H^+$ | k=4.2 x $10^7$ $M^{-1}$ $s^{-1}$ | (Buxton and Dainton 1968) | (91) |

Bromate, which is classified as a B2 probable human carcinogen (US EPA National Center for Environmental 1986), is known to be formed from bromide containing waters treated with ozone and HO· based AOPs (Von Gunten and Oliveras 1998; Von Gunten 2003). The $SO_4^{\cdot-}$, though more selective than HO·, is also a strong oxidant ($E°_{SO4^{\cdot-}}$=2.5 - 3.1 V (Neta et al. 1988); $E°_{HO^{\cdot}}$=2.4 - 2.7 V at acidic pH, $E°_{HO^{\cdot}}$=1.9 - 2.0 V at alkaline pH (Buxton et al. 1988)).

Unfortunately, likewise Fenton based processes, activation of PS process by means of iron species has some intrinsic drawbacks related to the use of iron as activator of the PS decomposition. In order to give a response to this limitation and then enhance the efficiency and the applicability of the process, iron chelate have been also employed in Fe(II/III) activation of PS system. Ahmad et al. (2012) showed as both Fe(II)-EDTA and Fe(III)-EDTA were effective for activating persulfate decomposition and generating reductants, whereas Fe(III)-

EDTA was somewhat more effective than Fe(II)-EDTA in generating sulfate and hydroxyl radical. Surprisingly they also showed that the dominant oxidant in the iron-EDTA activated persulfate systems was hydroxyl radical, rather than sulfate radical (Ahmad et al. 2012).

Some studies have demonstrated the effectiveness of the sulfate radical based process activated by iron species for removal of organic compounds. Some examples are given in Table 15:

**Table 15 Efficiency of sulfate radical based oxidation activated by iron chelates**

| PS activator | Compound (mM) | Operational condition | | | | Optimal performance | Ref |
|---|---|---|---|---|---|---|---|
| | | $[S_2O_8^{2-}]$ (mM) | Iron (mM) | pH _ | t (hours) | | |
| **Fe(III)-EDTA 1:1 EDTA:Fe** | TCE (0.3 mM) | 40 | 3.58 | 10 | 9 | Almost 90% of TCE removal after 9 hours of treatment. | (Liang et al. 2009) |
| **Fe(III)-EDTA Fe(II)-EDTA 1:1 EDTA:Fe** | TCE (2 μM) | 500 | 10 | 5 | 3 | 87% of TCE removal was obtained in PS treatment activated by Fe(II)-EDTA. 88 % of removal was obtained when activated by Fe(III)-EDTA | (Ahmad et al. 2012) |
| **Fe(II)-CA* 1:2 CA:Fe** | TCE (0.15 mM) | 2.25 | 0.30 | 5.62 to 3.98 | 1 | Complete degradation of the probe compound was obtained after 60 min of treatment | (Wu et al. 2014) |

* CA= citricacid

# 2 OBJECTIVES

AOPs are generally known to be really effective processes in the treatment of recalcitrant contaminant making eventually possible water reutilization for several purposes. The aim of this thesis was the assessment of AOPs applied to different water matrixes for the removal of recalcitrant compound. In particular, special attention was given to the set up of homogeneous Photo-Fenton like at neutral pH catalyzed by iron chelate. The effectiveness of conventional Photo-Fenton makes really interesting the possibility of extend its application in a wider range of water treatments when avoiding the acidification of the influent and following neutralization.

The above discussed objectives were divided in the following specific goal:

- ✓ The assessment of the suitability of Photo-Fenton process as strategy for recalcitrant compound degradation by comparison of Fenton and photo-Fenton (with UV-A and UV-C irradiation) en acidic media. Once determined the suitability of the process the possibility of performing some modification for applications at neutral pH might be considered.

- ✓ The assessment of some specific agents application in iron chelation and the identification of the more convenient iron specie to employ for the purpose. Find out the optimum molar ratio L:Fe for the achievement of the total chelation of the iron content with the chelating agents chosen (ethylenediaminetetraacetic acid-EDTA, nitrilotriaceticacid-NTA, oxalic acid and tartaric acid). Finally, assess the application of these chelating agents in photo-Fenton like at circumneutral pH for the degradation of one target compound (sulfamethoxazole-SMX) in order to distinguish the catalytic activity of each one.

- ✓ The achievement of a deep knowledge of the stability of the more suitable iron chelate among all those tested (Fe(III)-NTA). The complexes behavior under thermal, oxidative and photochemical strain was monitored all over the treatment.

- ✓ Assessment of Fe(III)-NTA chelates based photo-Fenton like a circumneutral pH for application in the treatment of several aqueous matrixes. Analysis of the influence of water composition on the efficiency of the treatment.

- ✓ Consider the possibility of process' optimization in order to reduce the influence of the water composition on the iron chelate process. Additional strategies to enhance SMX removal can be taken into account (iron chelate dosage; addition of $Mn^{2+}$ which is supposed to enhance the production of $O_2 \cdot^-$ radicals and to promote the reduction of $Fe^{3+}$ chelates to $Fe^{2+}$ chelates; addition of persulfate to produce $SO_4^{\cdot-}$ radicals in order to enhance the oxidation rate of SMX).

# 3 MATERIALS, ANALYTICAL METHODS AND PROCEDURES

## 3.1 Chemicals and reagents

### *3.1.1 Model compound A: Atrazine*

Atrazine was purchased from Fluka with a purity of 98%. The most important chemical data are shown in Table 16:

**Table 16 Chemical data of Atrazine**

| **Atrazine (ATZ)** | |
|---|---|
| **Chemical formula** | $C_8H_{14}ClN_5$ |
| **Chemical structure** | 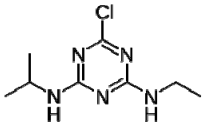 |
| **Molar mass** | 215.68 g/mol |
| **CAS number** | 1912-24-9 |

### *3.1.2 Model compound B: Sulfamethoxazole*

Sulfamethoxazole (SMX) was purchased from Sigma-Aldrich (Spain). The most important chemical properties of the antibiotic used as model compound for the experiments are summarized in Table 17:

**Table 17 Chemical data of Sulfamethoxazole**

| **Sulfamethoxazole (SMX)** | |
|---|---|
| **Chemical formula** | $C_{10}H_{11}N_3O_3S$ |
| **Chemical structure** | 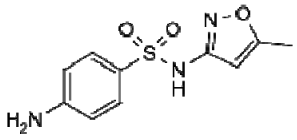 |
| **Molar mass** | 253.28 g/mol |
| **CAS number** | 723-46-6 |

### *3.1.3 Chelating agents*

The chelating agents tested in this study were (see Table 18):

- Nitrilotriacetic acid (NTA), purchased from Alfa Aesar (Spain);
- Ethylenediaminetetraacetic acid (EDTA), purchased from Panreac Quimica Inc (Spain);
- Oxalic acid (in the hydrate form), purchased from Panreac Quimica Inc (Spain);
- DL-tartaric acid, purchased from Alfa Aesar (Spain).

**Table 18 Chemical data of the chelating agents used in this study**

| **Nitrilotriacetic acid (NTA)** | |
|---|---|
| **Chemical formula** | $C_6H_9NO_6$ |
| **Chemical structure** | 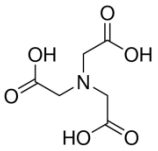 |
| **Molar mass** | 191.12 g/mol |
| **CAS number** | 139-13-9 |
| **Ethylenediaminetetraacetic acid (EDTA)** | |
| **Chemical formula** | $C_{10}H_{16}N_2O_8$ |
| **Chemical structure** | 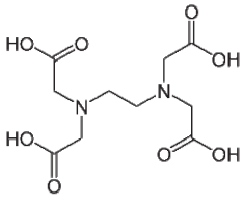 |
| **Molar mass** | 292.24 g/mol |
| **CAS number** | 60-00-4 |
| **Oxalic acid dehydrate** | |
| **Chemical formula** | $C_2H_2O_4{\cdot}2H_2O$ |
| **Chemical structure** | 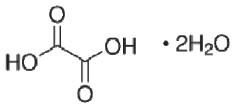 |
| **Molar mass** | 126.07 g/mol |
| **CAS number** | 6153-56-6 |
| **DL-Tartaric acid** | |
| **Chemical formula** | $C_4H_6O_6$ |
| **Chemical structure** | 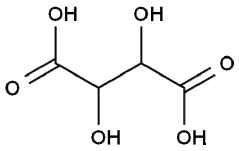 |
| **Molar mass** | 150.09 g/mol |
| **CAS number** | 133-37-9 |

### *3.1.4 Others*

All reagents used for chromatographic analyses, acetonitrile and ultrapure water (Milli-Q) were HPLC grade. Chemicals used as the mobile phase for HPLC (acetonitrile), catalysts (anhydrous Iron(III) chloride ($FeCl_3$), ferrous sulfate ($FeSO_4{\cdot}7H_2O$)), oxidants (hydrogen peroxide solution ($H_2O_2$), 30% w/v), hydrochloric acid (HCl), auxiliary chemicals for initial pH value adjustment (sodium hydroxide (NaOH)) were purchased from Panreac Quimica (Spain).

The filters used were Chmlab Group 0.45 µm (pore size) PVDF membrane filters and Minisart-RC 0.20 µm (pore size) nylon membrane filters.

## 3.2 Main techniques and analytical instruments

### *3.2.1 High Performance Liquid Chromatography*

***Determination of Atrazine concentration***

Due to the low atrazine concentration, solid phase extraction (SPE) was applied before the HPLC-UV measurement, using an extraction vacuum chamber (Manifold) and 30 µm Oasis HBL cartridges. To perform the SPE, a two-liter water sample was passed through the multi-walled carbon nanotube-packed cartridge (which was washed with 6 mL dichloromethane methanol, 6 mL acetonitrile and 6 mL acidified purified water (pH=3 with $H_2SO_4$)) at a flow-rate of 4 mL $min^{-1}$ by a vacuum pump. Afterwards, the cartridge was kept at reduced pressure for 5 min to remove any residual water. The matter retained on the cartridge was eluted by 4.5 mL of acetonitrile and 4.5 mL of methanol at the flow-rate of 1 mL $min^{-1}$. The effluents were collected in a test tube and condensed to dryness under a gentle flow of nitrogen at room temperature. They were then re-dissolved with 1 mL of acetonitrile/water (60% v/v) and filtered through a 0.45 µm disc filter before analysis with an HPLC system supplied by Waters Corporation. The HPLC column used was a Teknokroma C-18 Tracer Extrasil ODS2 (250 mm x 4.6 mm) and the mobile phase consisted of a 60:40 solution of acetonitrile and water, respectively. The wavelength of the UV detector was set at 221 nm and the flow rate kept at 1 mL $min^{-1}$.

***Determination of SMX concentration***

The concentration of SMX was quantified by HPLC-UV supplied by Agilent. The HPLC column used was a Teknokroma C-18 Tracer Extrasil ODS2 (250 mm x 4.6 mm) and the mobile phase consisted of a 60:40 solution of acetonitrile and water, respectively. The wavelength of the UV detector was set at 270 nm and the flow rate kept at 1 mL $min^{-1}$.

### *3.2.2 Dissolved iron measurement*

The iron content was determined according to the 1,10-phenantroline standardized procedure (ISO 6332) (International Organization for Standardization 1988). Ferrous iron Fe (II) forms a red colored complex with 1.10-phenantroline. The absorption of this complex measured at 510 nm, by spectrophotometer Hach Lange DR 3900, is proportional to ferrous iron concentration. Total iron can be measured after ferric iron Fe(III) reduction with ascorbic acid to ferrous iron Fe (II). Consequently, ferric iron concentration Fe(III) can be eventually calculated as the difference between total iron and ferrous iron.

### *3.2.3 Determination of the hydrogen peroxide consumption*

Hydrogen peroxide ($H_2O_2$) determination was followed through metavanadate spectrophotometric procedure (Nogueira et al. 2005a) in order to know $H_2O_2$ consumption during photodegradation reactions.

The procedure is based on the reaction of $H_2O_2$ with ammonium metavanadate in acidic medium (as described by the reaction below), which results in the formation of a red-orange

color peroxovanadium cation, with maximum absorbance at 450 nm. The measurement was carried out by means of a spectrophotometer Hach Lange DR 3900.

$$VO_3^- + 4H^+ + H_2O_2 \rightarrow VO_2^{3+} + 3H_2O \quad (92)$$

The spectrophotometric analysis was also confirmed using the colorimetric method with test strips (Peroxide Test, Merk).

### *3.2.4 Determination of Total organic carbon (TOC)*

TOC determination was performed with a Shimadzu 5055 TOC-VCSN analyzer by means of catalytic combustion at 680 °C according to Standard Method 5220D procedures (APHA et al. 2012). The device was equipped with an ASI-V Autosampler (Shimadzu). Samples of 12 mL were filtered (0.45 µm) previous to being injected in the device. Thus, in this work, TOC identifies Dissolved Organic Carbon (DOC). TOC was more properly determined as NPOC (non-purgeable organic carbon). For this reason inorganic carbon had to be previously removed bubbling air throughout the sample after acidification with HCl. Total Notrogen (TN) content was also measured by means of the specific module TNM-1 (Shimadzu) coupled to the installation.

### *3.2.5 Determination of Chemical Oxygen Demand (COD)*

COD analysis give and indirect measure of the organic compounds contained in the water sample. The test determines the amount of oxygen required to oxidize organic matter of a solution by means of strong oxidant agents. These tests were carried out following the Standard Method 5220 D: closed reflux and colorimetric method (APHA et al. 2012). The method consists of heating at high temperature (150 °C) a known volume of sample with an excess of potassium dichromate in presence of $H_2SO_4$ over a period of 2 hours in a hermetically sealed glass tube. The dichromate was in excess, and thus, the organic matter was oxidized and dichromate was reduced to $Cr^{3+}$. Furthermore, to avoid possible interference of chloride in the sample, silver sulfate was also added. The residual chrome IV was then colorimetrically measured in a spectrophotometer (Hach Odyssey DR/2500) at 420 nm (low COD method).

### *3.2.6 Determination of Biochemical Oxygen Demand (BOD)*

Biochemical oxygen demand is determined by incubating a sealed sample of water for five days ($BOD_5$) and measuring the loss of oxygen from the beginning to the end of the test.

$BOD_5$ was determined according to Standard Method 5210 by respirometric method using OxiTop equipment during five days under constant stirring and controlled temperature (20 ± 1 °C). The microorganism-seed (lyophilized capsules 5466-00, Cole-Parmer) were aerated during 2 hours before inoculation.

### *3.2.7 Aromaticity*

Aromatic organics can be detected using the UV 254 nm wavelength because of the strong absorption properties that these double bond organics have at that wavelength. Ultraviolet absorbance (UV-A) procedure requires that the sample be passed through a 0.45 µm filter and

transferred to a quartz cell. It is then placed in a spectrophotometer and reported in $cm^{-1}$. The spectrophotometer used was in this work was Perkin Elmer UV/VIS Lambda 20.

### *3.2.8 Ion-Exchange Chromatography*

Inorganic anions and cations were detected by means of ion-exchange chromatography. This technique allows the separation of ions and polar molecules based on their change and on their coulombian interaction with the stationary phase. The liquid sample is injected in the device and passes through a column where the stationary phase retains the electrolytes according with its charge and affinity. The device used for the detection was a 861 Advanced Compact IC supplied by Metrohm.

### *3.2.9 Alkalinity*

Alkalinity is a measure of the buffering capacity of a water or wastewater to neutralize acids. The buffering capacity of a wastewater is mainly related to the bicarbonate ($HCO_3^-$) and carbonate ($CO_3^{2-}$) content. However the presence of other buffering substances such as hydroxide, borate, silicates, phosphates, ammonium, sulphides and organic ligands can also provide alkalinity to the wastewater. The alkalinity was measured with an automatic titration device (CRISON pH Burette 24) equipped qith a pH meter (CRISON Basic 20).

### *3.2.10 Biological Assay A: Microtox*

Acute toxicity of the different effluents was measured by Microtox$^R$ toxicity test, using luminescent *Vibrio fischeri* bacteria. Analysis was conducted according to the standard Microtox$^R$ test procedures recommended by the manufacturer (Azur Environmental, Delaware, USA). Toxicity is expressed as Effective Concentration that reduces the bioluminescence to 50% ($EC_{50}$) value, the concentration of sample that causes a 50% reduction in light emission after 15 min of contact.

### *3.2.11 Biological Assay B: Luminotox*

To assess toxicity, LuminoTox was used. The LuminoTox SAPS test kit consisted of a fluorometer biosensor that used stabilized aqueous photosynthetic activity. SAPS are algae that fluoresce when photosynthesis is triggered by light absorption. The absorbed energy is emitted as fluorescence, which is the signal measured by the LuminoTox device. Decreases in fluorescence measurements produced by blank and test samples containing toxic contaminants were expressed as percentage inhibition. An incubation period of 15 minutes was started when 100 µL of SAPS solution were added to 2 mL of sample using an amber syringe. Following this exposure period, the content of the syringe was added to a cuvette within the LuminoTox device to determine toxicity. The samples were analyzed after residual hydrogen peroxide quenching using catalase solution.

### *3.2.12 Actinometric measures*

The photon flow incidents the experiment's volume was determined by means of actinometric experiments according to the range of emission wavelengths of the lamps. For solarbox and black light blue lamps reactors the incident photon flow was measured by actinometry based

on o-Nitrobenzaldehyde (o-NB) reaction (Kuhn et al. 2004; De la Cruz et al. 2013). This actinometry fits well with the emission of the Xenon and black light blue lamps, because actinometer absorbs in the range from 290 to 400 nm. o-NB actinometry was carried out adapting the method proposed by Willet and Hites (Willett and Hites 2000).

Other actinometric experiments were then carried out to determine the characteristic photon flow of the UV-C reactor (Kuhn et al. 2004).

## 3.3 Experimental devices

### *3.3.1 UV-A Photo-reactor*

UV-A Photo-Fenton-like experiments were carried out in a 2L Pyrex jacketed stirred vessel (inner diameter 11 cm, height 23 cm), equipped with three black-light blue lamps (Philips TL 8W, 08 FAM) wrapped in three Duran glass tubes. The lamps were axially arranged to the reactor and the emitted radiation was between 350and 400 nm and maximum at 365 nm. The photon flows supplied to the solution, periodically measured with o-nitrobenzaldehyde actinometry (Kuhn et al. 2004; De la Cruz et al. 2013), was 5.05 µEinstein $s^{-1}$ at 365 nm.
The vessel was covered with aluminum foil to avoid loss of photons and personal damage. During the runs, the temperature was kept at 25.0 ± 0.8 °C with a thermostatic bath (Haake C-40) by circulating the water through the jacket around the reactor. Good mixing was provided using a magnetic stirrer. When hydrogen peroxide was added, UV-A lamps were switched on.
In Figure 14 is shown a schematic design of the UV-A Photo-device.

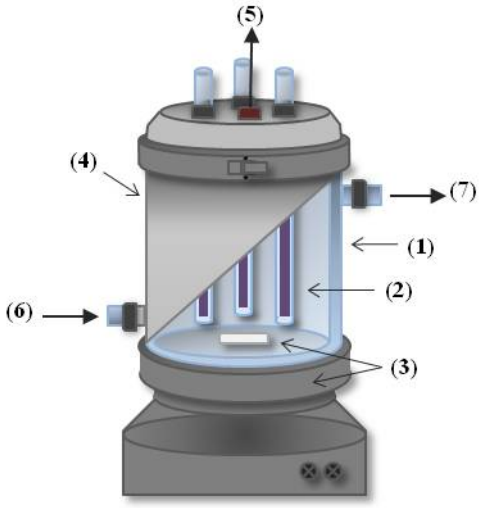


**Figure 14 UV-A Photo-Reactor scheme. (1) 2L Jacketed reactor, (2) Black-light blue lamps, (3) Magnetic stirrer, (4) Alumina foil, (5) Sampling orifice, (6) Thermostatic bath (IN), (7) Thermostatic bath (OUT).**

### *3.3.2 UV-C Photo-reactor*

UV-C light was supplied in a photochemical reactor quite similar to the previous but with different lamps. Thus, three fluorescent lamps (Philips TUV 8W, G8T5) wrapped in three quartz tubes, with emitted radiation between 200 and 280 nm, with a maximum of 254 nm were used. The photon flow was measured by chemical actinometry (Kuhn et al. 2004) and was 9.4 µEinstein $s^{-1}$ at 254 nm.

Figure 15 shows a schematic design of the UV-C photo-reactor.

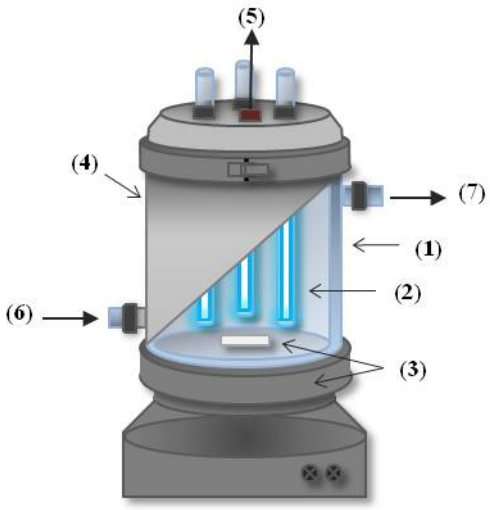


**Figure 15 UV-C Photo-Reactor scheme. (1) 2L Jacketed reactor, (2) Fluorescent lamps, (3) Magnetic stirrer, (4) Alumina foil, (5) Sampling orifice, (6) Thermostatic bath (IN), (7) Thermostatic bath (OUT).**

### *3.3.3 Solar light simulator*

Solar light was simulated with a solar simulator (Solarbox Co.Fo.Me.Gra, 220 V, 50 Hz). The solution was continuously pumped (peristaltic pump Ecoline VC-280II, Ismatec) into the Solarbox and recirculated back to the reservoir jacketed thermostatic 1 L stirred tank. Inside the Solarbox, aDuran tubular photoreactor (24 cm length, 2.11 cm diameter, 0.078 L) was irradiated by a Xe-lamp of 1 kW (Philips XOP 15-OF 1CT). As for the UV-A photo reactor, the photon flow was measured with o-Nitrobenzaldehyde actinometry (Kuhn et al. 2004; De la Cruz et al. 2013) and was 2.68 µEinstein $s^{-1}$.

A scheme of the solar simulator is depicted in Figure 16.

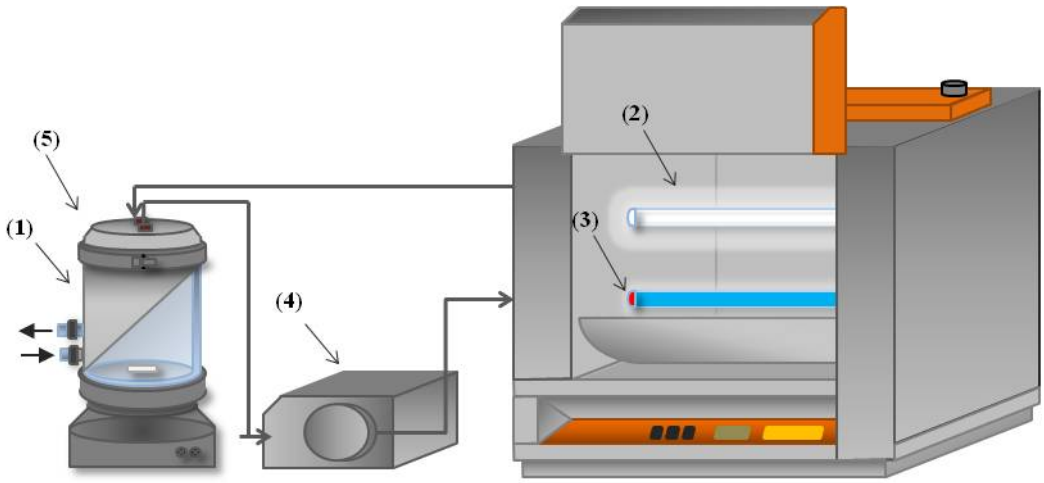


**Figure 16 Solar simulator scheme. (1) 1L Jacketed thermostatic stirred tank, (2) Xenon lamp, (3) tubular photo-reactor (24 cm length, 2.11 cm diameter, 0.078 L), (4) Peristaltic pump, (5) Access for sampling.**

# 4 Atrazine removal in municipal secondary effluents by means of Fenton and photo-Fenton treatments

## 4.1 Introduction

Atrazine degradation has been extensively studied under Fenton and Fenton-like processes (Huston and Pignatello 1999; Gallard 2000). It has been shown that advanced oxidation processes based on the Fenton's reaction allow atrazine removal. Huston and Pignatello showed that 98.8% of atrazine degradation was obtained after 30 minutes of treatment (Huston and Pignatello 1999). Gallard and De Laat obtained up to 80% removal of atrazine in optimum operating conditions (Gallard 2000). However, Chan and Chu showed that, depending on the initial doses and ratio of Fe(II) and $H_2O_2$, about 15-98% of atrazine was removed after 5-10 minutes of reaction (Chan and Chu 2003). Chu et al. compared the removal of atrazine by conventional Fenton's processes with stepwise Fenton's processes, in which the total dose of $H_2O_2$ was split and inputted into the system at different times and/or quantities (Chu et al. 2007).They found that this technique significantly improved the performance of Fenton's processes (in terms of atrazine decay) by about 10%. Kassinos et al. compared TOC removals for atrazine by dark Fenton and Photo-Fenton showing as the maximum TOC removal achieved for atrazine was 57% after 2 hours of Photo-Fenton reaction (Kassinos et al. 2009). It was also proven as combine these technologies with electrochemistry promoting Electro-Fenton process could be an alternative solution to remove micropollutants (Rosales et al. 2012). All of these studies were carried out to evaluate atrazine degradation in synthetic solutions. The treatment performance in wastewater may be lower, due to the interference of natural organic and inorganic compounds in the effluent.

The main results presented in this chapter have been published in Chemical Engineering and Technology (section 4.5 Appendix). Here, they are discussed the results of the assessment of the suitability of Fenton's reaction based process for successfully remove atrazine from the secondary effluents (SE) of a municipal wastewater treatment plant (MWTP) that uses activated sludge. Thus, through this study, it wanted to be demonstrated the removal's potentiality of the treatment. Then, the process' modification fit to the purpose of improving its applicability even in neutral aqueous matrixes will be discussed in the following chapters. It represents, then, a preliminary study to the following chapters in which photo-Fenton was applied in circumneutral pH conditions.

In this study, the SE with total organic carbon (TOC) between 11 and 18 mg $L^{-1}$ was spiked with 0.1 mg $L^{-1}$ of atrazine. The treatments tested were: Fenton, UV-A photo-Fenton and UV-C photo-Fenton. All the experiments were performed at pH 2.8 ± 0.1 and the analyzed parameters were atrazine concentration, TOC, chemical oxygen demand (COD), $UV_{254}$ absorbance, $H_2O_2$ concentration and toxicity (using LuminoTox®). Atrazine removal percentages were around 20% for Fenton, 60% for UV-A photo-Fenton and 70% for UV-C photo-Fenton treatments, respectively. Organic matter mineralization by Fenton treatment was monitored and no significant reduction was observed. However, organic matter oxidation (in terms of COD reduction) of around 30% and 40% were achieved by Fenton and photo-

Fenton processes, respectively. It can be stated that the photo-Fenton process with UV-C is a useful technique for atrazine degradation. The use of UV-C light leads to higher degradation than UV-A. Nevertheless, the higher costs related to the use of UV-C light must be considered in order to perform an adequate cost-benefit analysis.

## 4.2 Materials and methods

### *4.2.1 Wastewater characterization*

All experiments were carried out with SE spiked with atrazine to evaluate its degradation in a real matrix. The SE was taken downstream of the MWTP secondary biological treatment in Gavà-Viladecans (Barcelona, Spain). The MWTP serves a population of 300,000 equivalent inhabitants and uses the classical activated sludge processes. In addition, it serves industrial users, which justifies the variability of chemical parameters over time. After collection, samples were transported to the laboratory and stored at 4 °C.

The most important chemical parameters of the effluent were: COD (chemical oxygen demand) between 36.3 and 73.6 mg $L^{-1}$ and TOC (total organic carbon) between 11 and 18 mg $L^{-1}$. In order to eliminate solids that could interfere with the lamps' irradiation and analytical analysis, the effluent was filtered with a 10 µm filter paper. The chemical characteristics of the untreated water (after filtration) are summarized in Table 19:

**Table 19 SE from MWTP characterization after 10 µm filtration.**

| Parameter | |
|---|---|
| **pH** | 7.85 |
| **Turbidity (NTU)** | 0.90 |
| **TOC (mg $L^{-1}$)** | 11-18 |
| **COD (mg$O_2$ $L^{-1}$)** | 33-34 |
| **$BOD_5$ (mg$O_2$ $L^{-1}$)** | 8.5 |

Due to the high porosity with which the filtration was carried out, no significant variation for TOC values was obtained (<1%).

### *4.2.2 Sample preparation and experimental set up*

Taking into consideration that typical micropollutant concentrations in the effluent are in the 0.1–20.0 µg $L^{-1}$ range, we decided to work at 100 µg $L^{-1}$ of atrazine, which is a compromise between (i) a high enough concentration to characterize kinetics using conventional analytical techniques, and (ii) a low enough concentration to simulate real conditions.

The initial pH of secondary effluent was between 7.6 and 7.9, which is far from the optimum of 2.8 for the Fenton and photo-Fenton treatments. Thus, we used sodium hydroxide (NaOH) and sulfuric acid ($H_2SO_4$) for the pH adjustment.

When the pH had been adjusted, $Fe^{2+}$ as $FeSO_4 \cdot 7H_20$ was added (1 mg $L^{-1}$ for the Fenton and UV-C photo Fenton treatments, and 5 mg $L^{-1}$ for the UV-A photo Fenton treatment). The different iron concentration used for UV-A photo-Fenton and UV-C photo-Fenton can be explained taking into account that atrazine has a high UV-C direct photolysis rate, so its removal by UV/$H_2O_2$ can be promoted by simultaneous effect of HO· oxidation and UV-C

photolysis. For this reason, in order to reduce the system cost as well as to ensure the environmental safeguard, a lower concentration of iron was used for UV-C photo-Fenton.

After 15 min of stirring, the solution was well homogenized, and atrazine (0.1 mg $L^{-1}$) and hydrogen peroxide (5 mg $L^{-1}$) were added. Considering that high $H_2O_2$ concentration increases treatment costs and $H_2O_2$ in excess can have radical scavenging activity that reduces treatment efficiency, the $H_2O_2$ concentration used was such as to obtain a molar ratio of $H_2O_2$/TOC equal to 0.1. The experiments of UV-A and UV-C photo-Fenton were carried out making use of the photo-reactores described in the sections 3.3.1 and 3.3.2 respectively.

## 4.3 Results and discussion

### *4.3.1 Atrazine removal*

Atrazine was used as a model microcontaminant to verify the efficiency of the Fenton and photo-Fenton treatments to remove micropollutants from SE. For this purpose, atrazine was spiked in SE and the samples were subjected to both treatments. Photo-Fenton using UV-C radiation was also performed to observe the influence of a more energetic radiation source on the treatment.

***Fenton***

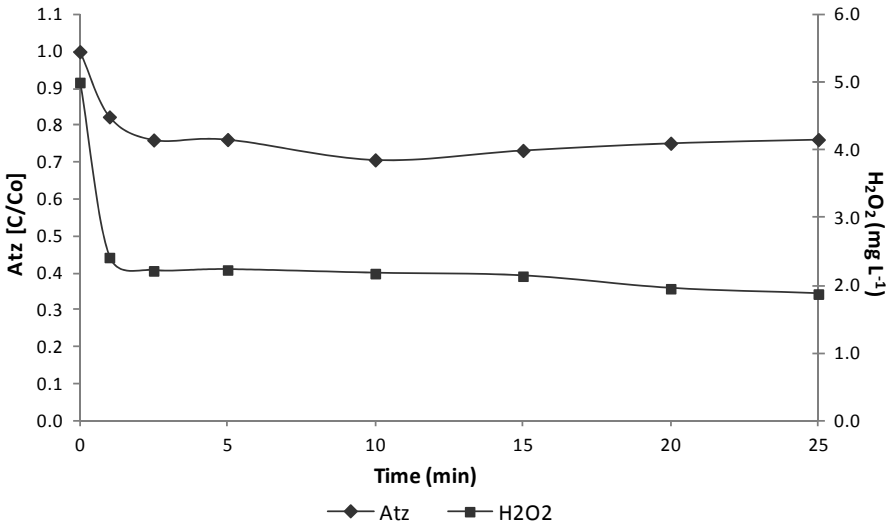


**Figure 17 Atrazine removal by Fenton reaction: $[ATZ]_0$ = 0.1 mg $L^{-1}$; $[H_2O_2]_0$ = 5 mg $L^{-1}$; $[Fe^{2+}]_0$ = 1 mg $L^{-1}$; pH = 2.7 ± 0.1.**

The first method tested was the Fenton reaction. Although this method is very effective for large quantities of organic contaminants, it could only remove about 20% of atrazine from SE (Figure 17). The reaction rate was high in the first minute of the reaction in which it fits well to first-order kinetics, and then it decreased at around 3 minutes and remained constant until the end of the reaction time. This behavior can be explained by the reduction of the Fenton reaction observed with the $H_2O_2$ decay curve. In this case, $H_2O_2$ consumption was very low after 3 minutes of reaction. After this point, $H_2O_2$ consumption was very low, proving that no significant HO· oxidation took place after 2 minutes of reaction. Iron availability plays an important role in the reaction rate reduction, since the formation of iron complexes was

observed. This phenomenon is augmented by the presence of SE organic matter. Therefore, it seems that iron availability is the limiting factor for the Fenton reaction in SE.

***UV-A Photo-Fenton***

It is well known that the $Fe^{2+}$ recovery rate strongly increases in the presence of UV-A radiation (Pignatello 1992; Pera-Titus et al. 2004). Since the Fenton reaction could not achieve significant atrazine removal from SE, the system was irradiated with UV-A (365 nm) to promote the photo-Fenton reaction and increase HO· formation. As can be seen in Figure 18, also in this case, the atrazine degradation rate fits well to first-order kinetics, however it was considerably increased and atrazine continued to be degraded until the end of the 120 minutes of treatment. The $H_2O_2$ consumption measurements show that consumption during the reaction time was higher, which indicates that more HO· was formed. The photo-Fenton reaction occurred throughout the reaction time and led to atrazine degradation of almost 60%.

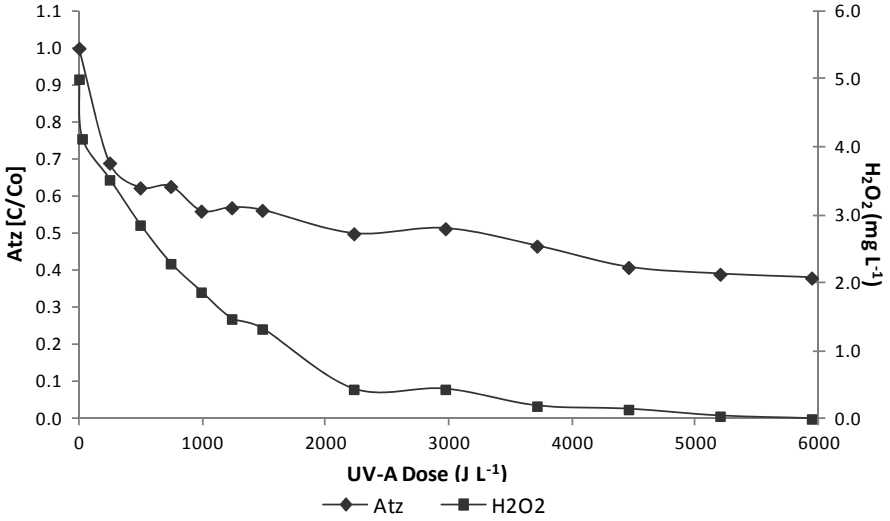


**Figure 18 Atrazine removal by photo-Fenton (UV-A): $[ATZ]_0$ = 0.1 mg $L^{-1}$; $[H_2O_2]_0$ = 5 mg $L^{-1}$; $[Fe^{2+}]_0$ = 5 mg $L^{-1}$; pH = 2.7 ± 0.1.**

About 90% of $Fe^{2+}$ was rapidly converted to $Fe^{3+}$ in the first few minutes of the reaction (Figure 19). However, the remaining $Fe^{2+}$ concentration promoted the photo-Fenton reaction until the end of the reaction time. Therefore, the degradation rate of atrazine in SE is higher in the photo-Fenton process than in the Fenton reaction, as photo-Fenton promotes $Fe^{2+}$ reconstitution with subsequently higher HO· formation. Under the experimental conditions, the light incidence was sufficient to convert a suitable quantity of $Fe^{3+}$ to $Fe^{2+}$. However, the best results may be achieved with higher light intensity.

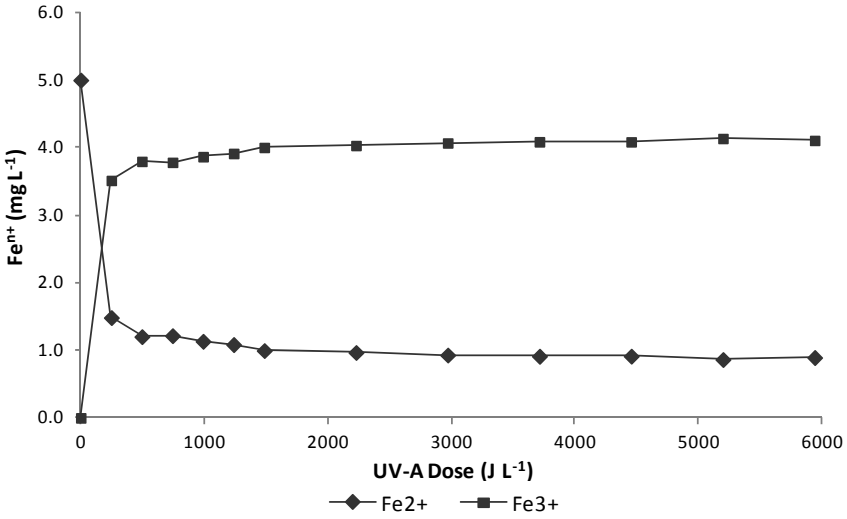


**Figure 19 Iron content: $[ATZ]_0$ = 0.1 mg $L^{-1}$; $[H_2O_2]_0$ = 5 mg $L^{-1}$; $[Fe^{2+}]_0$ = 5 mg $L^{-1}$; pH = 2.7 ± 0.1.**

***UV-C Photo-Fenton***

Another source of UV, UV-C (254 nm) radiation, was used to test the influence of wavelength on the photo-Fenton reaction and to try to improve the system efficiency. The use of UV-C promoted a faster atrazine degradation rate than the photo-Fenton with UV-A and the Fenton reaction. Complete atrazine removal was achieved after 20 minutes of reaction which rate fits well to first-order kinetic (Figure 20). It is important to consider that atrazine has a high UV-C direct photolysis rate. Thus, HO· oxidation and direct UV-C photolysis act simultaneously and promote a synergic effect on ATZ removal. It is also known that $H_2O_2$ in the presence of UV-C is directly photolysed in HO·. Thus, in this method, the degradation was also influenced by the UV/$H_2O_2$ process.

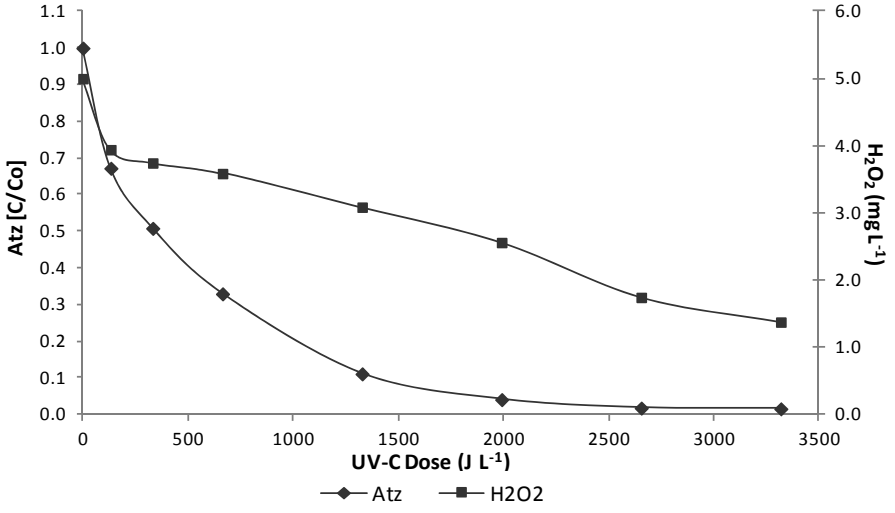


**Figure 20 Atrazine removal by photo-Fenton (UV-C): $[ATZ]_0$ = 0.1 mg L-1; $[H_2O_2]_0$ = 5 mg L-1; $[Fe^{2+}]_0$ = 1 mg $L^{-1}$; pH = 2.7 ± 0.1.**

In Table 20 are summarized the effiency in terms of ATZ removal achieved by means of the technologies considered in this study.

**Table 20 Percentage of atrazine removal achieved by means of the technologies adopted in this study**

| | time | UV Dose | ATZ(*) | $H_2O_2$ (**) |
|---|---|---|---|---|
| | min | kJ $L^{-1}$ | % | % |
| **Fenton** | 25 | - | 23.8 | 62.5 |
| **UV-A photo-Fenton** | 120 | 6 | 62 | 100 |
| **UV-C photo-Fenton** | 25 | 3.3 | ≈100 | 72.5 |

(*) removal
(**) consumption

### *4.3.2 Mineralization, oxidation and aromaticity removal*

Once it had been proved that the tested methods could remove atrazine from SE, organic matter oxidation, mineralization and aromaticity removal were also studied.

***Fenton***

Since the Fenton reaction was the weakest treatment method for removing atrazine from SE, low transformation of the organic matter was expected from this method. This is confirmed in Figure 21. The graph shows that the Fenton system cannot promote the mineralization of SE, due to the low quantity of HO· formed during the reaction. Slight oxidation (almost 10%) of SE was observed at the end of the 120 minutes of reaction. However, the oxidation cannot be attributed to aromatic content reduction, since $UV_{254}$ nm measurements indicate the absence of aromaticity removal after 120 minutes of reaction.

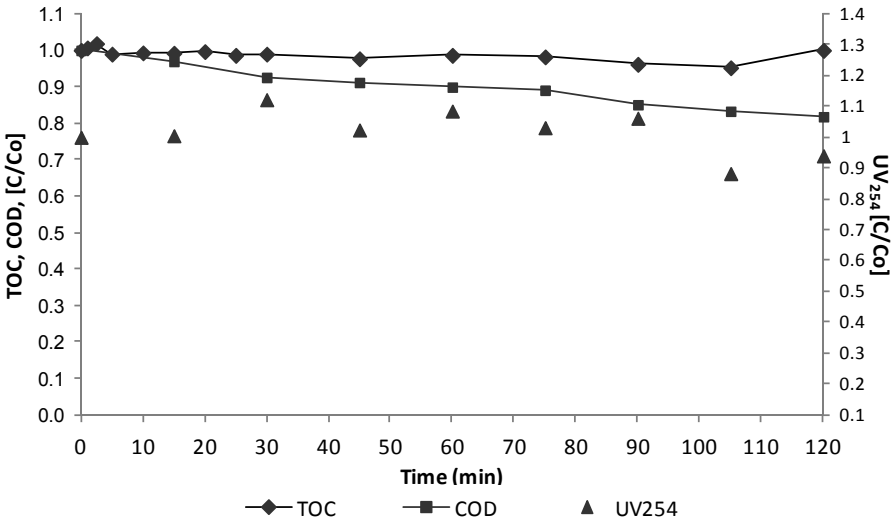


**Figure 21 Mineralization (TOC), oxidation (COD) and aromaticity removal ($UV_{254}$ nm) promoted by Fenton reaction: $[ATZ]_0$ = 0.1 mg $L^{-1}$; $[H_2O_2]_0$ = 5 mg $L^{-1}$; $[Fe^{2+}]_0$ = 1 mg $L^{-1}$; pH = 2.7 ± 0.1.**

***UV-A Photo-Fenton***

The photo-Fenton reaction promoted low mineralization of the organic matter content by almost 18% at the end of the reaction time. The oxidation of intermediates was also increased, which proves that this method can remove atrazine and promote some transformation of SE organic matter (Figure 22). More than 20% of oxidation was reached by the SE treatment using photo-Fenton. In addition, a slight (about 16%) destruction of aromatic compounds was obtained.

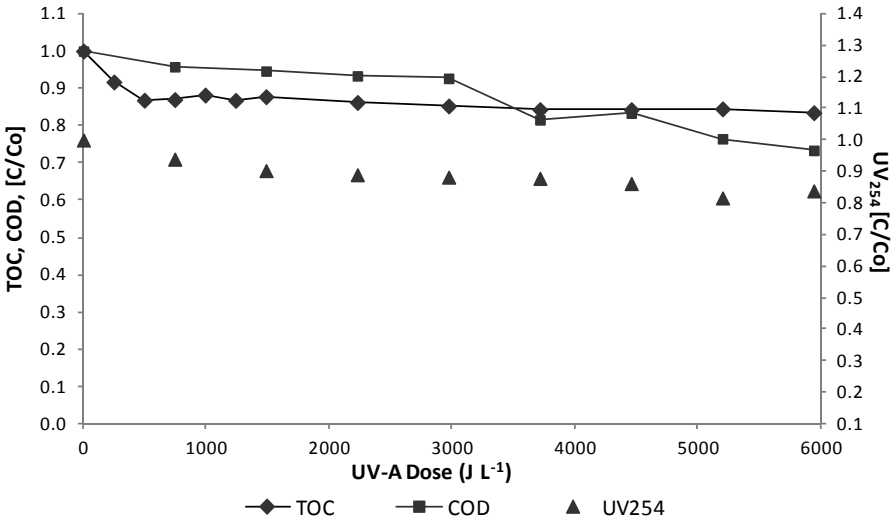


**Figure 22 Mineralization (TOC), oxidation (COD) and aromaticity removal ($UV_{254}$ nm) promoted by photo-Fenton reaction (UV-A): $[ATZ]_0$ = 0.1 mg $L^{-1}$; $[H_2O_2]_0$ = 5 mg $L^{-1}$; $[Fe^{2+}]_0$ = 5 mg $L^{-1}$; pH = 2.7 ± 0.1.**

Some organic matter was oxidized and this oxidation could change the biodegradability and toxicity of the final effluent. However, Figure 23 shows that the biodegradability and toxicity of the SE during treatment were not affected by the photo-Fenton process. On the one hand, the toxicity results were positive since it is evident that more toxic products were not formed. On the other hand, the organic matter transformation caused by oxidation did not change the biodegradability of the effluent. Thus, bacterial regrowth was not favored by the photo-Fenton UV-A treatment.

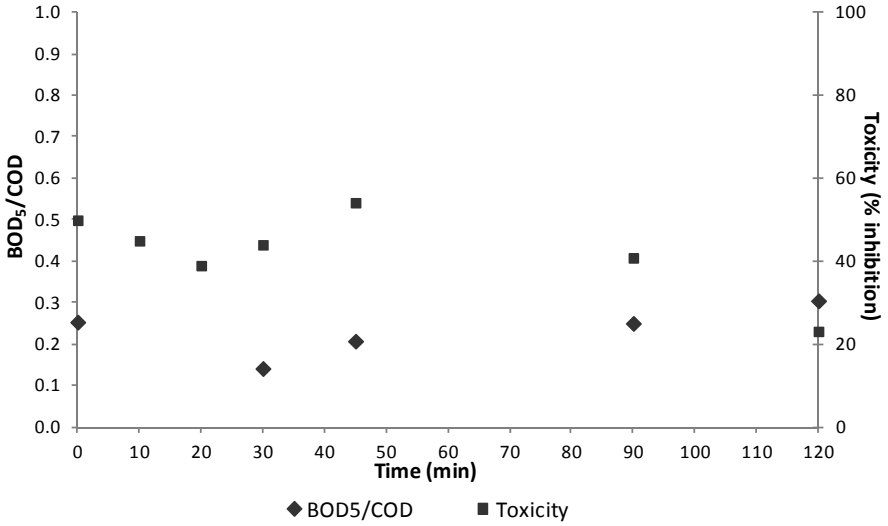


**Figure 23 Biodegradability and toxicity promoted by photo-Fenton reaction (UV-A): $[ATZ]_0$ = 0.1 mg $L^{-1}$; $[H_2O_2]_0$ = 5 mg $L^{-1}$; $[Fe^{2+}]_0$ = 5 mg $L^{-1}$; pH = 2.7 ± 0.1.**

***UV-C Photo-Fenton***

With the use of more energetic radiation, higher mineralization was expected. In fact, UV wavelength can significantly influence the TOC removal ratio, so that TOC removal is usually higher in the presence of UV-C than UV-A. This is because UV light with a shorter wavelength can significantly influence the direct formation of HO· radicals as well as the photo-reduction rate of $Fe^{3+}$ to $Fe^{2+}$. In fact, the quantum yield of photo-reduction for $Fe^{3+}$ to $Fe^{2+}$ significantly

increases as the UV light wavelength decreases (Feng et al. 2003). Despite that, Figure 24 shows that no mineralization was obtained. This behavior is due to the fact that the effluent used in the experiment with UV-C light had the lowest organic matter content and may have contained recalcitrant organic compounds that resisted mineralization by HO·. The MWTP used to collect the effluent samples serves both municipal and industrial users, which explains the considerable variation in chemical parameters over time. The low mineralization of organic matter content obtained by photo-Fenton using UV-A may have been caused by more reactive compounds present in the previous effluent. Unlike the TOC, the oxidation of intermediates was higher than in the photo-Fenton using UV-A. Almost 40% of the organic content was oxidized when UV-C was used. In addition, the use of more energetic radiation promoted the reduction of $UV_{254}$ absorbance by about 80%. Apart from increasing the atrazine oxidation rate, the use of UV-C promotes the oxidation of organic matter and the cleavage of aromatic compounds in the effluent. Definitely, the high removal efficiencies obtained using UV-C Photo-Fenton and the lower costs involved in the use of it, make this treatment the most attractive among those tested.

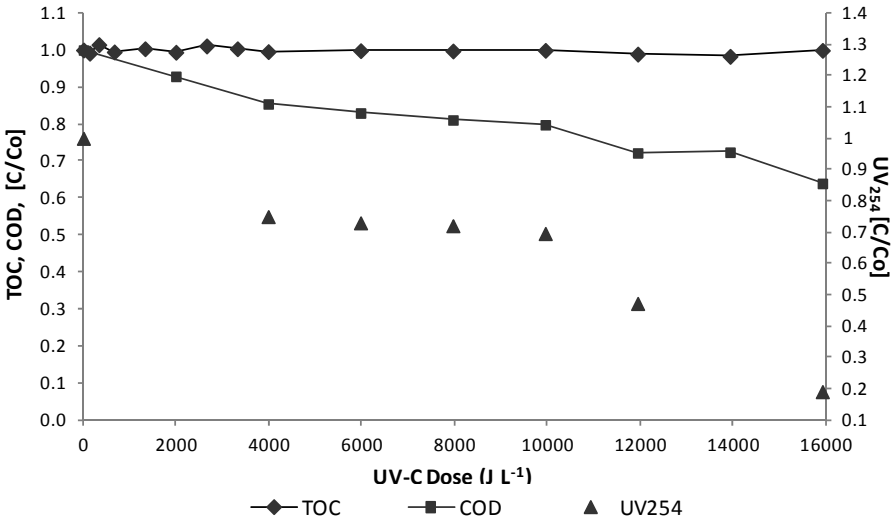


**Figure 24 Mineralization (TOC), oxidation (COD) and aromaticity removal ($UV_{254}$ nm) promoted by photo-Fenton reaction (UV-C): $[ATZ]_0$ = 0.1 mg $L^{-1}$; $[H_2O_2]_0$ = 5 mg $L^{-1}$; $[Fe^{2+}]_0$ = 1 mg $L^{-1}$; pH = 2.7 ± 0.1.**

In Table 21 are summarized the main results of mineralization, oxidation and aromaticity removal described in this section.

**Table 21 Removal efficiencies achieved by means of the technologies adopted in this study**

| | time | UV Dose | $H_2O_2^{(*)}$ | $TOC^{(**)}$ | $COD^{(**)}$ | $UV_{254}^{(**)}$ |
|---|---|---|---|---|---|---|
| | min | kJ $L^{-1}$ | % | % | % | % |
| **Fenton** | 120 | - | 65.6 | 0 | 18.2 | 6.0 |
| **UV-A photo-Fenton** | 120 | 6 | 100 | 16.5 | 26.6 | 16.1 |
| **UV-C photo-Fenton** | 120 | 16 | 100 | 0 | 36 | 80.8 |

(*) consumption
(**) removal

### *4.3.3 Economical consideration*

As it was previously said, in this study different energetic radiation were used to evaluate their contribution to atrazine removal in SE. To assess the suitability of these methods for real applications, cost estimation was carried out in order to compare them from an economic point of view. The calculation was based in the work published by Bolton to normalize the efficiency of the AOPs (Bolton et al. 2001). Thus, the electrical energy per order of magnitude (EEO) was calculated taking into account electricity costs of irradiation, mixing and chemical costs, all of them normalized to the reactor volume (Bolton et al. 2001). Only operational costs and not capital or maintenance costs were considered, as these are difficult to compare. Finally, technical-scale commercial prices were taken for chemical reagents used and converted to energy values of Catalonia (Spain) in 2013 (0.139 € $kWh^{-1}$)(Generalitat de Catalunya). Table 22 shows the conversion of the commercial prices of the chemical substances to energy values:

**Table 22 Commercial chemical substances and the conversion of their price to energy values.**

| Chemical | Company | Volume (L) | % | *d* (*) (g $mL^{-1}$) | Price (€) | (kg) | (€ $kWh^{-1}$) | (€ $kg^{-1}$) | (Wh $g^{-1}$) |
|---|---|---|---|---|---|---|---|---|---|
| $H_2O_2$ | PANREAC | 1 | 30 | 1.11 | 21.25 | 0.3 | 0.139 | 70.8 | 510.9 |
| $FeSO_4 \cdot 7H_2O$ | PANREAC | - | 99 | - | 26.38 | 0.99 | 0.139 | 26.6 | 192.2 |
| $H_2SO_4$ | PANREAC | 5 | 96 | 1.84 | 27.79 | 8.83 | 0.139 | 3.15 | 22.7 |

(*) chemical density

The electrical energy per order of magnitude ($E_{EO}$) for the percentage of atrazine removal achieved within 25 minutes of treatment was calculated trough the definition of the following figure of merit (Bolton et al. 2001):

| | | |
|---|---|---|
| $E_{E,mix}$ | [Wh $L^{-1}$] | electrical energy for mixing |
| $E_{E,pro}$ | [Wh $L^{-1}$] | electrical energy for irradiation |
| $E_{E,chem}$ | [Wh $L^{-1}$] | cost of reagents converted to energy |
| $E_{E,tot}$ | [Wh $L^{-1}$] | total electrical energy |
| $E_{EO,rx}$ | [Wh (L·order)$^{-1}$] | electrical energy for irradiation per order of magnitude |
| $E_{EO,tot}$ | [Wh (L·order)$^{-1}$] | total electrical energy per order of magnitude |

The order of magnitude for atrzine removal at 25 minutes was calculated as:

$$order\ of\ magnitude\ OM = \frac{[ATZ]_0 - [ATZ]_{25}}{[ATZ]_0} \quad (93)$$

In Table 23, the energetic requirements of Fenton, UV-A Photo-Fenton and UV-C Photo-Fenton are detailed:

**Table 23 Energetic requirements of Fenton, UV-A Photo-Fenton and UV-C Photo-Fenton**

| Treatment | Time (min) | OM (-) | $E_{E,mix}$ (Wh $L^{-1}$) | $E_{E,pro}$ (Wh $L^{-1}$) | $E_{E,chem.}$ (Wh $L^{-1}$) | $E_{E,tot}$ (Wh $L^{-1}$) | $E_{EO,rx}$ (Wh (L·order)$^{-1}$) | $E_{EO,tot}$ (Wh (L·order)$^{-1}$) |
|---|---|---|---|---|---|---|---|---|
| Fenton | 25 | 0.24 | 6.25 | - | 4.51 | 11 | 19 | 45 |
| UV-A Photo Fenton | 25 | 0.40 | 6.25 | 5 | 4.51 | 16 | 12.6 | 39.6 |
| UV-C Photo Fenton | 25 | 1.00 | 6.25 | 5 | 5.29 | 17 | 10.3 | 16.5 |

## 4.4 Conclusions

From the results obtained from this study, the following compulsion can be highlight:

- The Fenton reaction could not remove a significant quantity of atrazine from the secondary effluent. Additionally, this treatment could not promote the mineralization and oxidation of the SE organic matter. Low, insufficient $Fe^{2+}$ recovery may be the reason for the low efficiency of this method, since iron complex formation was observed.

- Photo-Fenton processes removed atrazine from SE. However, only about 50% of the atrazine was removed at the end of 120 minutes of reaction, with an initial molar ratio of $H_2O_2$/TOC equal to 0.1.

- When the same initial molar ratio of $H_2O_2$/TOC was used in the Fenton and photo-Fenton processes, more energetic radiation (UV-C) increased the atrazine removal and almost 100% of the atrazine was remove in 20 minutes of reaction. However, the contribution of direct UV-C photolysis cannot be neglected. The use of UV-C also promoted higher oxidation and aromaticity removal.

- The photo-Fenton (UV-C) was the most powerful of the tested methods. It did modify biodegradability and did not produce more toxic compounds.

- Photo-Fenton can be considered an optional method for the removal of pesticides from SE due its capacity to remove micropollutants with the minimum amount of organic matter transformation. However, further research should be carried out to improve the treatment (i.e. perform the treatment at neutral pH).

## 4.5 Appendix

Chemical Engineering & Technology



Antonella De Luca[1]
Renato F. Dantas[1]
Anderson S. M. Simões[2]
Ilda A. S. Toscano[2]
Giusy Lofrano[3]
Angel Cruz[1]
Santiago Esplugas[1]

[1] Department d' Enginyería Quimica, Universitat de Barcelona, Barcelona, Spain.
[2] Department of Chemistry, Universidade Federal da Paraiba, Cidade Universitária, João Pessoa, Brazil.
[3] Department of Environment, Salerno Province, Salerno Italy.

Research Article

# Atrazine Removal in Municipal Secondary Effluents by Fenton and Photo-Fenton Treatments

Alternative water sources, including effluents from municipal wastewater treatment plants (MWTP) are necessary to meet increasing water demand. Advanced oxidation processes based on the Fenton reaction were applied to remove atrazine from the secondary effluents of a MWTP that uses activated sludge. Fenton, UV-A photo-Fenton, and UV-C photo-Fenton treatments were tested. Atrazine removal percentages were around 20 % for Fenton, 60 % for UV-A photo-Fenton and 70 % for UV-C photo-Fenton treatments, respectively. Organic matter mineralization by Fenton treatment was monitored and no significant reduction was observed. However, organic matter oxidation in terms of COD reduction of around 30 and 40 % were achieved by Fenton and photo-Fenton processes, respectively. The photo-Fenton process with UV-C is a useful technique for atrazine degradation, leading to higher degradation than with UV-A while also being more attractive in an economic point of view.

**Keywords:** Advanced oxidation processes, Fenton, Pesticide, Photo-Fenton, Wastewater reuse

*Received:* February 22, 2013; *revised:* July 15, 2013; *accepted:* August 29, 2013

**DOI:** 10.1002/ceat.201300135

# 5 Chelate based photo-Fenton at circumneutral pH: catalytic efficiency and suitability evaluation of four iron chelates

## 5.1 Introduction

In this chapter they are showed the results of applying homogeneous photo-Fenton like at neutral pH to remove sulfamethoxazole (SMX) from water. The process was performed using chelating agents in order to solubilize iron in a neutral water solution. The main aim of this research was the study and the comparison of the efficiencies achieved by homogenous photo-Fenton processes when using different chelating agents. Four chelating agents were selected: two aminopolycarboxylicacids (EDTA, NTA), oxalic acid and DL-tartaric acid.

To ensure the desired iron content, specific amount of each chelating agent had to be used. At this purpose, a study of the chelation process was carried out in order to find out the proper Ligand:Fe (L:Fe) molar ratio to ensure the complete chelation of the added iron content. Once determined the concentration of chelating agent required for chelation, the effectiveness of the process was determined. The catalytic activity of the chelates strongly depends of the substance used for iron complexion.

The iron leaching was monitored over reaction time to evaluate the chelates stability and their resistance to HO· and UV-A radiation. Total Organic Carbon (TOC) analyses were also performed to evaluate the contribution in terms of solution contamination related to the use of chelating agents. Sulfamethoxazole was chosen as model compound to represent the presence of contaminant of emerging concern in wastewater in order to analyze the efficiencies of the chelating agents. All experiments were carried out in Milli-Q water in order to avoid interferences into the chelation process.

The main results showed in this chapter have been published in Water research (section 5.6 Appendix).

## 5.2 Chelating agents

Chelating agents are substances that are normally absent into the municipal wastewater treatment plant effluents, thus if they have to be employed as reactant, they have to be added during the treatments (Sillanpää and Oikari 1996; Sorvari and Sillanpää 1996; Sillanpää et al. 2003; Klamerth et al. 2013). Then, it is easy to understand that properties such as biodegradability and toxicity have to be evaluated in order to choose the correct chelating agent to form Fe(II) and Fe(III) complexes. The strength of the ligand to form complexes (chelating ability), that substantially depends on the chemical structure, is also important to limit the quantity of chelating agents that needs to be added to the solution in order to reduce the contribution of TOC. The most important ligands properties that have to be taken into account are the stability conferred to the complex, strength of the formed bond, biodegradability, toxicity of the ligand and the toxicity of the chelates which formation is expected. In general, chelating agents have several carboxylate groups linked to a number of tertiary nitrogen atoms. The functional groups form a stable and water-soluble complex with a

donor atom such as metals. The metal cation is centered in the complex, while being coordinately bound either to nitrogen or to oxygen atom as the anchoring site. Unlike regular ligands, chelating agents can form multiple coordination bonds to a single metal ion (Sillanpää et al. 2011).

The chelation ratio can be theoretically determined for a certain pH by observing iron concentration and the chemical structure and concentration of the ligand (i.e. numbers of carboxyl groups). However, at neutral pH a certain amount of iron can precipitate, thus the real rate needed to perform Fenton reaction can be very different due to the need of higher concentration of the ligand (Sun and Pignatello 1992).

The four chelating agents used to perform the experiments were:

- Ethylenediaminetetracetic acid (EDTA);
- Nitrilotriacetic acid (NTA);
- Oxalic acid (OA);
- Tartaric acid (TA).

Both EDTA and NTA are aminopolycarboxylicacids (APCAs) which are substances able to form very stable and strong bond with metals. Ethylenediaminetetraacetic acid (EDTA) is a hexadentate chelating ligand characterized by the higher chelating strength. In the past, due to its effectiveness, EDTA was used in a variety of industrial applications, but although it is non-toxic to mammals at environmental concentration, there are many concerns about the potential of EDTA to remobilize toxic heavy metals out of sewage sludge and sediments (Kari and Giger 1996). In 1984, Dufková studied the interaction of EDTA with photosynthetic organism and found that EDTA is toxic, although, it is interesting to note that the same concentration of EDTA chelated with micronutrients did not present toxic effect. This behavior is able to confirm as the chelator toxicity is strongly dependent of the chelated element. EDTA could be, also, responsible in eutrophication water processes (Sillanpää 1997). Besides, there are concerns related to its recalcitrant nature and poor biodegradability (Sillanpää and Oikari 1996) which made it a persistent organic pollutant. Actually, the alarm connected to these aspects has limited its applicability and it is being replaced by other chelating agents more environmental friendly such as nitrilotriacetic acid (NTA) (Tuulos-tikka et al. 2000; Sillanpää et al. 2011). It belongs to the same group and it is a tripodal tetradentate trianionic ligand. NTA biodegradability in sewage treatments was studied for the first time in the 1967, when Swisher et al. concluded that it was substantially completely biodegraded in a short time, which was subsequently confirmed (Means et al. 1980). Oxalic acid (OA) and DL-tartaric acid (TA) were also tested. Oxalic acid (OA), which belongs to the polycarboxylates, is a reducing agent and is its conjugate base, the oxalate acts as a chelating agent. OA is naturally present in many plants (Libert and Franceschi 1987) as well as TA, which is also a natural product, generally not bioaccumulable and not toxic for the aquatic fauna.

## 5.3 Sample preparation and experimental set up

Ferric ion solution 17.9 mM was prepared fresh daily dissolving anhydrous $FeCl_3$ in 0.1 M HCl to minimize iron(III) hydrolysis and polymerization (Flynn 1984). Iron chelate solution 0.089 mM of $Fe^{3+}$, was prepared by directly mixing the ferric ion solution with a solution of the

corresponding chelating agent in Milli-Q water. Then, after approximately 15 minutes of stirring, the pH of solution of oxalic and tartaric acid was slowly adjusted to 7.0 with NaOH, while the pH solution of EDTA and NTA was slowly adjusted to 8.0 to allow the chelating agent's dissolution. This procedure is necessary due to the low solubility of these carboxylic acids at acidic pH. Finally, SMX in concentration of 0.079 mM (20 mg $L^{-1}$, TOC= 12.3 mg $L^{-1}$, COD= 25.2 mg $L^{-1}$) was added after 1 hour of stirring approximately. When SMX was completely dissolved a further pH correction was needed to adjust it 7.0. Hydrogen peroxide was added into the solution in concentration of 0.294 mM (10 mg $L^{-1}$) immediately before to start the experiment.

The catalytic efficiency of the four iron chelates considered for this study was assess under UV-A irradiation. At this purpose the experimental device used to carry out the experiment was the UV-A Photo-reactor described in the Chapter 3 (Section 3.3.1). In Table 24 are summarized the most important experimental conditions adopted:

**Table 24 Operating condition adopted in Photo-Fenton like at circumneutral pH for SMX removal**

| | |
|---|---|
| **Reaction volume** | 2 L |
| **Temperature or reaction** | 25 °C |
| **$[SMX]_0$** | 0.079 mM (20 mg $L^{-1}$) |
| **$[H_2O_2]_0$** | 0.294 mM (10 mg $L^{-1}$) |
| **$[Fe^{3+}]$** | 0.089 mM (5 mg $L^{-1}$) |

## 5.4 Results and discussions

### *5.4.1 Chelation process*

To carry out a correct metal chelation it is important to set some parameters that control the process of chelates formations. The key operational conditions of chelation process are: oxidative state of iron ions, pH of iron chelate solution and Ligand:Fe molar ratio (L:Fe). Concerning the oxidative state of iron ions, it is well known that among the several reactions that govern conventional Fenton and photo-Fenton processes the ones in which $Fe^{2+}$ catalyzes the $H_2O_2$ decomposition led to the production of more reactive radicals than those catalyzed by $Fe^{3+}$. However, the behavior of the complexes could be different and more aspects have to be evaluated. When the iron species as $Fe^{2+}$ and $Fe^{3+}$ in solution are in the chelated form, it is important to ensure the stability of the complex in order to avoid iron release and its precipitation as well as to ensure Fe-complexes formation when competing ions are present. The "stability constant" of a complex can give important information about the complex formed by combining metal ion and chelating agent. This determines whether the complex will be formed in the presence of competing anions and can give us indication about the strength of the bond metal-ligand. The stability or equilibrium constant (K), expressed as log K, has been determined for many metals and chelating agents. The higher the log K values, the more tightly the metal ion will be bound to the chelating agent and the more probable that the complex will be formed. The stability constants of Fe(III)-EDTA and Fe(II)-EDTA are respectively 25.7 and 14.3, while of Fe(III)-NTA and Fe(II)-NTA are 15.9 and 8.9 respectively (Furia 1973). This is maybe due to the number of bonds that could be established and also to the ion dimension, in fact, the smaller dimension of Fe(III) probably make possible a closer chelate structure that make it less exposed to the external interaction and thus more stable. $Fe^{3+}$ has

been used as the ideal oxidation state to form complexes of iron to use as Fenton and photo-Fenton catalyst. However, no faster kinetic was observed when $Fe^{2+}$ was used to form the complexes.

The pH of the solution prepared to form iron complexes is another important factor for the chelation efficiency. There is a hyperbolic relationship between the pH and the log K that give us information about the minimum pH required to obtain a satisfactory chelation. For EDTA, this minimum pH values for $Fe^{3+}$ is below 2.0, while for the $Fe^{2+}$ it is higher (≈5.0). Nevertheless, the importance of this parameter is essential due to the chelating ability of chelating agent to form bond with metal ions in the solution, however it mainly depends on the solubility of the chelating agents. Due to addition of the acidic ferric ion solution, the pH of the chelate solution drops at acidic values. EDTA and NTA are slightly soluble in acidic water, which solubility can be only improved by addition of a base. For this reason, it is necessary to raise the solution pH to solubilize the chelating agent and allow the chelation. Instead, oxalic acid and tartaric acid are very soluble in acidic water which already allows the beginning of the chelation process in lower pH. Thus, for EDTA and NTA it is preferable let mixing the solution at neutral/alkaline pH for almost 1 hour to ensure good chelation efficiency while for oxalic acid and tartaric acid the initial pH adjustment is not tightly required to solubilize the ligand and to start the chelation process. The pH adjustment have to be performed slowly in order to avoid too quickly change that could result in catalyst loss due to iron precipitation.

The Ligand:Fe (L:Fe) molar ratio is another important parameter that has to be determined in order to achieve the better operating conditions of work. The molar ratio of the ligand has to be stoichiometric correct and it must be at least 1:1, nevertheless it can be higher than this. Although the molar ratio can be theoretically identified, experimentally a greater ratio is needed to yield adequate chelation efficiency. In fact, if the quantity of ligand is inadequate for the quantity of metal to be chelate, the chelation process will be limited, thus this quantity should be determined experimentally. The chelation process is quite complex and more factors could interfere in it such as the consumption of a portion of chelating agent by non-selective complexion with mineral cations (Tsang et al. 2012). Moreover, the process could be faster and more complete when ratio was increased due to the increased presence of free chelators. Perhaps, free chelators act recapturing the iron ions released from the destroyed Fe-L chelate, thus avoiding iron precipitation. However, this aspect cannot lead to an unconditional use of these compounds due to negative side-effects involved such as the increase of effluent's TOC and the risk of heavy metals remobilization.

In this study, the amount of chelating agent employed in the chelation process was decided after a study carried out for each ligand to find out the real L:Fe molar ratio that allowed obtaining the best percentage of iron chelation with the minimum quantity of chelant, to make available the necessary $Fe^{2+}$ or $Fe^{3+}$ to catalyze the reaction and then to correctly perform Fenton and photo-Fenton processes. Several chelating molar ratios were tested. The test was performed preparing iron chelate solutions with the same concentration of $Fe^{3+}$ and different amount of chelating agent. The solution was let stirring to allow the complexes formation then the pH was adjusted to neutral values. The solutions characterized for an inadequate L:Fe molar ratio presented uncomplexed iron precipitate, the soluble chelate iron could be measured with the spectrophotometric method of phenantroline. To avoid measurement

errors due to the disorder of the precipitate's fraction, the total iron content was measured after filtration with 0.2 µm pore size syringe filters.

The chemical structure of the chelating agent is also a determining factor to define the molar ratio required. Aminopolycarboxylates compounds, such as EDTA and NTA could almost chelate all the iron into the solution with a 1:1 L:Fe molar ratio, although for NTA, which chemical structure is simpler than EDTA, 2:1 L:Fe ratio could be required. It essentially means that NTA is characterized by a less Fe-chelating ability than EDTA as it is possible to observe by the stability constants of Fe(III)-EDTA and Fe(III)-NTA. Chelating agents for which Fe-chelating ability is lower than aminopolycarbolylates need a higher L:Fe molar ratio. However, several are the authors that used the theoretical 1:1 stoichiometric molar ratio. Sun and Pignatello, for example, used 1:1 L:Fe molar ratio for almost all fifty chelating agent tested, including EDTA, NTA and tartaric acid. Other compounds characterized by a less chelating strength, such as oxalic acid, citric acid, sulfur compounds, phosphates and others, required 10:1 L:Fe molar ratio (Sun and Pignatello 1992).

Experimental results shown in Figure 25 confirmed that, following the chelation procedure previously reported by Sun and Pignatello (1992), theoretical stoichiometric ratio could be not enough to obtain the complete Fe(III) chelation. EDTA and NTA (aminopolycarboxylates compounds) needed a smaller chelating molar ratio than tartaric acids and oxalic acid (polycarboxylates) to chelate the $Fe^{3+}$ content. Furthermore, higher Fe(III)-NTA molar ratio is required respect to the EDTA due to its less Fe-chelate ability. In fact, with 0.5:1 L:Fe molar ratio, around 50% of Fe(III) chelate was achieved with EDTA while less than 40% was achieved using NTA. Besides, using NTA as chelating agent, molar ratios equal or higher than 1.5:1 should be used to achieve 100% of Fe(III) chelation. Only EDTA can achieve almost 100% of chelation with 1:1 L:Fe molar ratio.

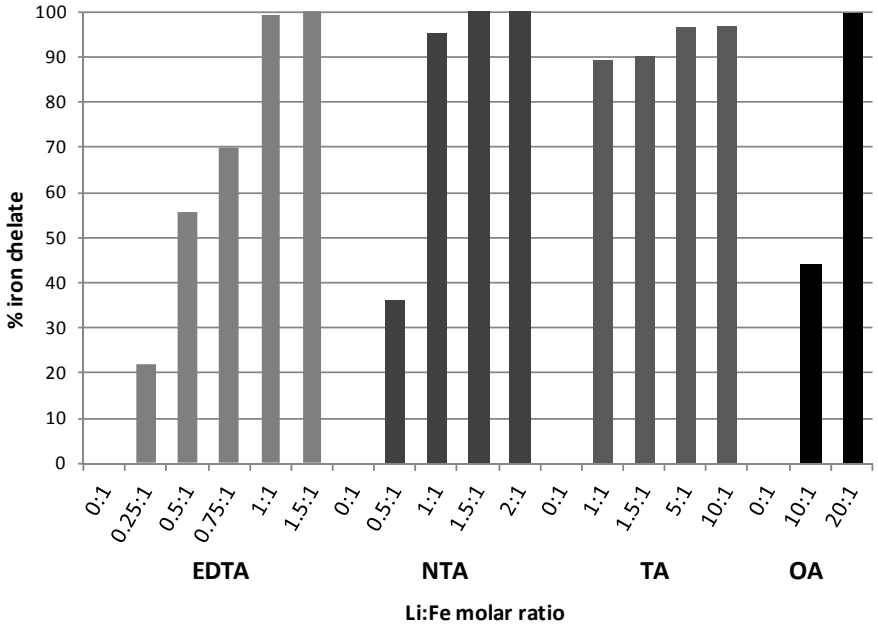


**Figure 25 Percentage of iron chelates formed with several L:Fe(III) molar ratio adopted**

When tartaric acid was tested, it was observed that even though the increase of L:Fe molar ratio, it was very difficult to achieve to complete Fe(III) chelation and only about the 97% of iron chelate was obtained with a 10:1 molar ratio. In particular, the increase of chelation efficiency obtained between the molar ratio of 1:1 and 10:1 is only 8%. However, as it will be shown in this work, a great improvement of the kinetic rate could be obtained using the 10:1 L:Fe molar ratio. Concerning Fe(III) chelation with oxalic acid, differently than what it can be found in scientific literature, when oxalic acid was used, 10:1 molar ratio was not even sufficient to achieve 50% of Fe(III) chelate. Total chelation was obtained with 20:1 ratio.

Comparing tartaric and oxalic acid, it is possible to observe that at 10:1 molar ratio the dissolved $Fe^{3+}$ percentage is higher using tartaric acid (96%) than using oxalic acid (44%). These results are in accordance to what has been also described by Xue et al. (2009) nonetheless as well as they also observed, it is unexpectedly that Fe-chelating ability do not correlate with the stability constant (log $K_{Fe(III)-L}$) which, instead, follows this order: oxalate>tartrate (Manning and Ramamoorthy 1973; Ramamoorthy and Manning 1974; Blesa et al. 1984; Hanna et al. 2005; Xue et al. 2009).

Table 25 presents the L:Fe molar ratio needed to ensure the complete iron chelation together with the stability constant if the respective chelates. These molar ratios were then used to perform the photo-Fenton at neutral pH and verify the efficiency of HO· formation and consequent organic pollutant removal.

**Table 25 L:Fe molar ratio used to perform Photo-Fenton like at circumneutral pH and stability constants of the chelates**

| | L:Fe molar ratio | log $K_{Fe(III)-L}$ (*) |
|---|---|---|
| **Fe(III)-EDTA** | 1.5:1 | 25.7 |
| **Fe(III)-NTA** | 1.5:1 | 15.9 |
| **Fe(III)-TA** | 10:1 | 7.5 |
| **Fe(III)-OA** | 20:1 | 9.4 |

(*) (Furia 1973)

The optimum L:Fe molar ratio that allows the higher percentage of iron chelate may not be the optimum choice to perform Fenton based treatments if complementary aspects are taken into account. It is also important considering the environmental impact and the added costs connected with a higher use of chemicals. For this reason, these aspects were considered in this study in order to demonstrate as these molar ratios could represent the overall optimum from different point of view.

In order to assess the photo-Fenton performance at neutral pH using different chelating agents, SMX degradation was used as a model contaminants and it was monitored during the reaction time. Pseudo-first order kinetic constants were calculated to compare the reaction rate obtained by the use of the different chelating agents.

### *5.4.2 Efficiency of iron chelates in SMX degradation*

In order to compare the chelating agents previously introduced in respect to the catalytic activity, their effect on SMX degradation has been studied. As observable looking at the absorption spectrum of SMX reported in several studies, there is no absorption at the wavelength investigated (Hişmioğullari and Yarsan 2009). The reaction between SMX and HO·

is estimated to have a rate constant of 3.7±0.1 x $10^9$ $M^{-1}$ $s^{-1}$ (Lam and Mabury 2005). The SMX degradation curves obtained with photo Fenton at neutral pH catalyzed by the Fe(III) chelates tested in this study have been represented in Figure 26(a). The degradation curve of the target compound, obtained by conventional photo-Fenton has also been represented to make clearer the different kinetic order rate of photo-Fenton like performed using chelating agents. During the reaction, as represented in Figure 26(b), the oxidant consumption and the iron content were monitored in order to evaluate the effective stability of the chelating agents tested as well as to be able to better understand the reaction rates obtained.

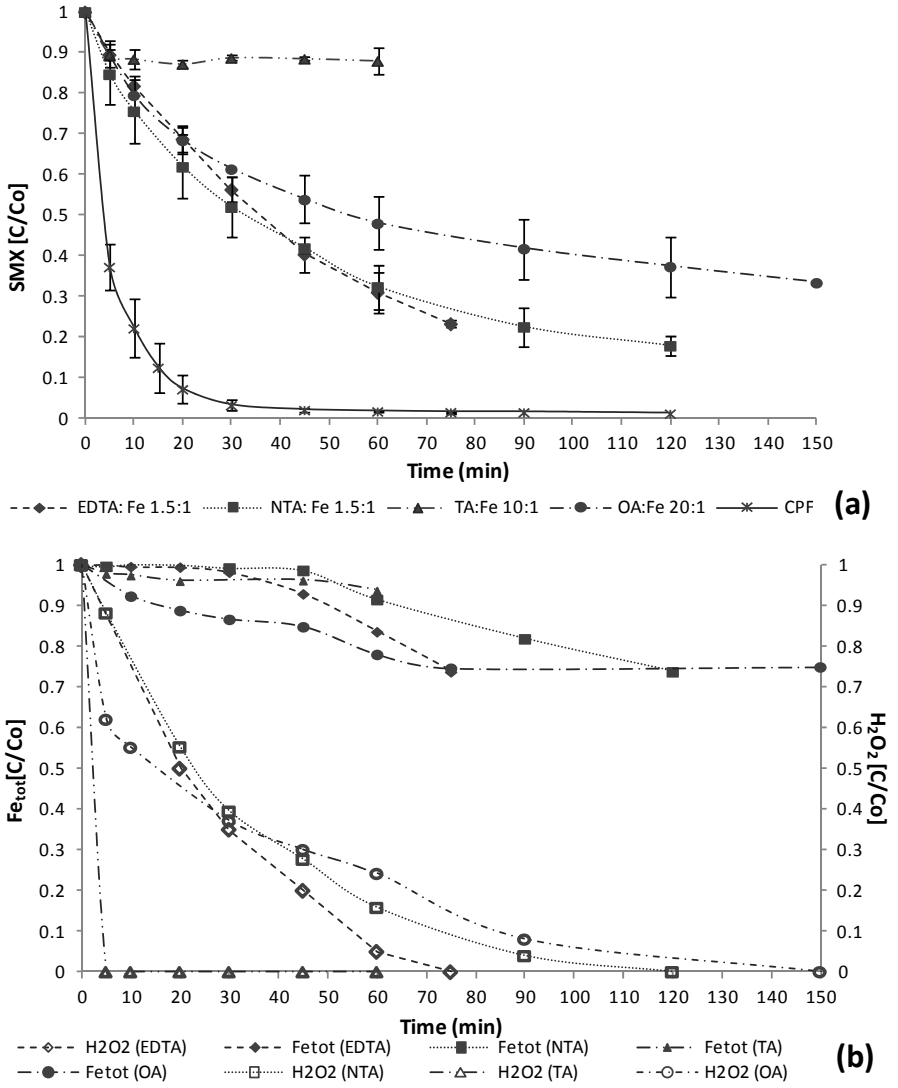


**Figure 26 (a) SMX removal by photo-Fenton like at neutral pH with Fe(III)-L chelates ($Fe^{3+}$ 0.089 mM as Fe(III)-L, pH= 7.0 ±0.7) compared with SMX removal by means of conventional photo-Fenton (CPF) ($Fe^{2+}$ 0.089 mM as $Fe_2SO_4 \cdot 7H_2O$, pH= 2.8 ±0.1); (b) trend of Fe content and $H_2O_2$ during reaction of Photo-Fenton like with Fe(III)-L chelates**

Due to the well-known characteristics of stronger chelating agent, EDTA was the first chelator tested as iron chelator to catalyze Fenton reaction. Among the various metal complexes of EDTA, Fe(III)-EDTA with its stability constants of log $K_{Fe(III)\text{-}EDTA}$=25.7 is the most predominant form present in surface water (Nowack and Stone 2002).

As it was expected (Pignatello et al. 2006), the kinetic of photo-Fenton like at neutral pH catalyzed by Fe(III)-EDTA chelates (1.96 x $10^{-2}$ $min^{-1}$) was significantly slower than in conventional photo-Fenton (1.26 x $10^{-1}$ $min^{-1}$) and complete SMX degradation was obtained after 75 minutes of reaction. When photo-Fenton like at neutral pH with Fe(III)-EDTA chelates was performed, the reaction lasts until hydrogen peroxide consumption in 75 minutes of reaction time when 76.6% of SMX degradation was achieved. During the reaction, no relevant change of pH was observed and its value did not drop below 6.3. This result can be probably justified taking into account the presence in solution of free ligands which provide alkalinity that is the buffering capacity to neutralize the acids produced. Therefore, it was demonstrated that Fe(III)-EDTA chelates were suitable to catalyze the hydrogen peroxide decomposition although the SMX degradation reaction was slower than in conventional photo-Fenton at pH=2.8. It has to be taken into account that when conventional photo-Fenton is performed, Fe(II) is generally used to initiate Fenton reaction being well-known its faster kinetic in respect to Fe(III). At neutral pH, the necessity to ensure a better stability of the chelates let to prefer Fe(III) ions (which have higher stability constant) to form iron complexes that could imply the reaction rate reduction.

During the reaction, HO· attacked both SMX and Fe(III)-EDTA chelate which involves the breaking of complexes with iron releasing in the solution. Thus, iron released precipitated reducing the catalytic activity. For this reason, the reactivity of the chelate with HO· is fundamental to control the efficiency of the treatment since higher reactivity means faster destruction of the complex. Figure 26(b) shows that during the first 30 minutes of reaction, the chelates resisted to the radical attack and no loss of iron was observed. This could be explained by the high stability conferred to the complexes by the EDTA. After that point, a gradual release of the iron content was observed until a value around 26%, which also represents the percentage of the chelates destroyed during the reaction.

Due to the higher biodegradability such as the analogue high chelating strength of Fe(III)-NTA chelates (log $K_{Fe(III)-NTA}$=15.9), NTA could represent an ideal alternative to replace EDTA and similar behaviors in terms of degradation efficiency and chelates stability were expected by its use.

Figure 26(a) also shows that neither by the use of NTA it was possible to achieve the same kinetic rate obtained by conventional photo-Fenton process, being the reaction rate at neutral pH much slower (2.51 x $10^{-2}$ $min^{-1}$ against the 1.26 x $10^{-1}$ $min^{-1}$ of the conventional photo-Fenton). However, at 120 minutes of reaction when hydrogen peroxide was totally consumed, Fe(III)-NTA chelates allowed to obtain a higher SMX reduction (82.2%) than what was achieved by the use of Fe(III)-EDTA. Despite the higher reaction time when compared to Fe(III)-EDTA, this result demonstrates a greater catalytic activity of NTA chelates than EDTA. This evidence could be also confirmed by the faster SMX degradation kinetic constant registered in the first minutes of reaction (2.51 x $10^{-2}$ $min^{-1}$), than when EDTA chelates were employed (1.96 x $10^{-2}$ $min^{-1}$). In particular, when NTA chelates were used, two different rates of degradation can be individuated, being the reaction faster in the first 45 minutes (2.51 x $10^{-2}$ $min^{-1}$) and then slower (1.39 x $10^{-2}$ $min^{-1}$) until the total consumption of the hydrogen peroxide. Although the lower reaction time of photo-Fenton like with EDTA chelates may seem an advantage, observing half time of SMX obtained, it can be observed how this is

slightly lower when NTA is used ($t_{½,EDTA}$=35 min; $t_{½,NTA}$=32 min) that again confirms the better effectiveness of NTA. No significant change in pH was observed until the end of the experiments (±0.7).

Regarding the complex reactivity toward HO· during the reaction, when NTA was used, complexes destruction began after 45 minutes of reaction. After this moment, a gradual reduction of iron content was observed until 26.1% (Figure 26(b)). The iron loss starting at 45 minutes of reaction justifies the reduction of the kinetic constant observed for the SMX, registering a connection between iron releasing and catalytic activity.

The OA chelates are generally characterized by low stability constants, which for the Fe(III)-OA chelates (log $K_{Fe(III)-OA}$=9.4) (Furia 1973) suggests that high quantity of ligand should be added into the solution to complex all iron required to catalyze the reaction. Moreover, as it is shown in Figure 26(a), when a polycarboxylate compound as oxalic acid was tested a lower catalytic activity was observed and only 66.6% of SMX removal was achieved. Furthermore, the less catalytic activity of oxalic acid can be observed also taking into account the most long duration of the reaction (150 minutes to consume all $H_2O_2$). This behavior is due to the low stability of the chelates along with the higher reactivity with HO·. In fact, in the first 30 minutes, the kinetic constant in terms of SMX degradation was 1.75 x $10^{-2}$ $min^{-1}$, no much smaller than when EDTA chelates were employed (1.96 x $10^{-2}$ $min^{-1}$). Afterwards, a strong reduction of the kinetic constant was observed (from 1.75 x $10^{-2}$ $min^{-1}$ to 0.44 x $10^{-2}$ $min^{-1}$) which could be related to the destruction of Fe(III)-OA complexes by HO·, thus releasing iron in the solution during the reaction time.

Figure 26(b) shows that the Fe(III) chelates formed with oxalic acid had a weak stability which led to an iron releasing that started from the beginning of the reaction until reach a loss of 25.2% after 150 minutes. This behavior is not surprising when you consider the high photosensitivity of the ferrioxalate that, in fact, is also used as the basis of a chemical actinometer (Hatchard and Parker 1956b). All these considerations as well as, the long reaction time observed in photo Fenton reaction catalyzed by Fe(III)-OA complexes let think that, without the use of UV radiation, a very slow reactivity could be obtained. Obviously, the optimum amount of reagent might be fixed, nevertheless due to the weak stability of the chelator, impractical concentration of oxalic acid should be used.

It is important to mention that the weak stability of complexes allows the reduction of Fe(III) to Fe(II) leading to the release of the ion, and then to the breaking of the complex (Hislop and Bolton 1999). This phenomenon is also responsible for the progressive reduction of the catalytic activity of the chelates. The breaking of the complexes bonds, which is followed by the iron precipitation also reduces the amount of photons available for the reaction. Differently from what was observed during the use of others chelating agents tested, a slight increase of pH was observed (+0.15), that confirms what was already registered in previous studies (de Lima Perini et al. 2013). This pH increment could be attributed to the poor stability of the complex and also its photo sensibility, which led to a great release of iron and then to the presence in solution of a great amount of chelator in its ionic form that free of the Fe(III), may establish acid-base reactions.

Finally, when tartaric acid (TA) was tested, its relative weakness as chelating agent expected by the knowledge of the stability constants of Fe(III)-TA chelates (log $K_{Fe(III)-TA}$=7.49) (Furia 1973) has been confirmed. Moreover, when TA was tested, an unexpected behavior was observed. After only 5 minutes of reaction, no hydrogen peroxide presence was detected and thus no more SMX degradation was registered. In fact, only 14.3% of SMX removal was achieved after 60 minutes (Figure 26(a)), which was practically obtained in the first 10 minutes of reaction when the degradation rate registered was of 2.22 x $10^{-2}$ $min^{-1}$. This result could be due to an excess of chelating agent into the solution which, due to its relatively high reaction rate with hydroxyl HO· radicals (1.4x$10^{9}$ $M^{-1}s^{-1}$) can act as scavenger of hydroxyl radicals (Pignatello et al. 2006; Xue et al. 2009). It is a plausible assumption considering the low improvement in Fe(III) chelation obtained by increasing the amount of chelating agent, thus a large amount of free TA was expected to be in solution. No changes in pH values were observed, which remained constant along the time. The shutdown of the reaction can be also observed in Figure26(b) when is shown that a small loss of iron has occurred (only 6.2%) due to the absence of radicals responsible for the attack to chelates and their breaking.

In Table 26 are summarizes the main results described in this section:

**Table 26 Fe(III)-L based photo-Fenton like at neutral pH: experimental results**

| | time<br>min | $Fe_{tot,0}$<br>% | $Fe_{lost}$<br>% | $k_{obs}$<br>$min^{-1}$ | SMX<br>% |
|---|---|---|---|---|---|
| **Fe(III)-EDTA 1.5:1(*)** | 75 | 100 | 26.1 | 1.96 x $10^{-2}$ | 76.6 |
| **Fe(III)-NTA 1.5:1(*)** | 120 | 100 | 26.1 | 2.51 x $10^{-2}$ | 82.2 |
| **Fe(III)-OA 20:1(*)** | 150 | 96 | 6.2 | 1.75 x $10^{-2}$ | 11.7 |
| **Fe(III)-TA 10:1(*)** | 10 | 100 | 25.2 | 2.22 x $10^{-2}$ | 66.6 |
| **CPF** | 60 | 100 | 0 | 1.26 x $10^{-1}$ | 98 |

(*) L:Fe molar ratio

### *5.4.3 Catalytic activity improvement*

Concerning the appropriate L:Fe molar ratio for the catalytic process, increasing the amount of ligand the chelation process and SMX degradation are better due to the presence of free chelators in solution. Figure 27 shows that although the 1:1 EDTA:Fe molar ratio could ensure a percentage of Fe(III) chelate very close to 100% (Figure 25), increasing this ratio to 1.5:1 (100% of iron chelate) a faster degradation was obtained (1.96 x $10^{-2}$ $min^{-1}$ against 1.18 x $10^{-2}$ $min^{-1}$ of 1:1 molar ratio). Perhaps, an explication of this behavior is that free chelators act recapturing the iron ions released from the destroyed Fe-L chelate, thus avoiding iron precipitation. However, this aspect cannot lead to an unconditional use of these compounds due to negative side-effects involved such as the increase of effluent's TOC and the risk of heavy metals remobilization.

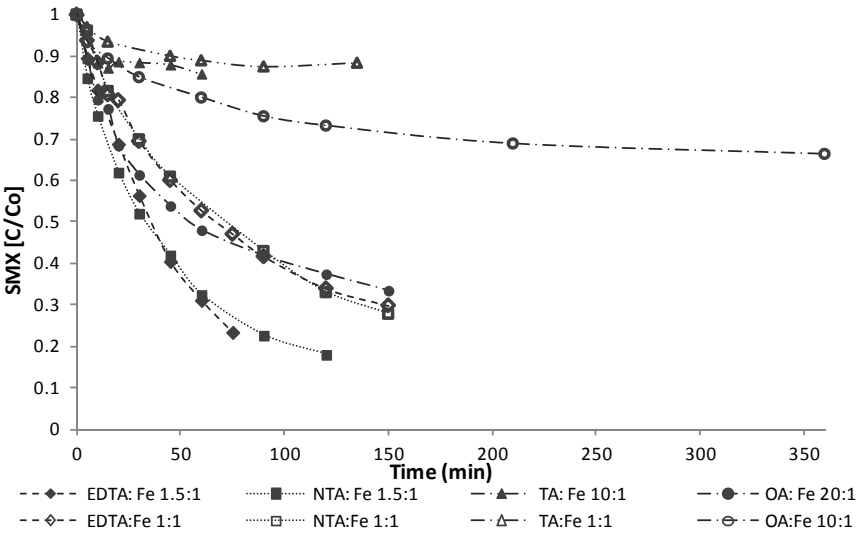


**Figure 27 Evaluation of the catalytic improvement of SMX removal by means of Photo-Fenton like at neutral pH when adopting different L:Fe(III) molar ratio**

It is important to take into account the environmental impact that could result from the higher EDTA:Fe molar ratio used. However, despite the obvious drawback due to TOC increase, a great reduction of electrical consumption can be obtained adjusting the molar ratio to the optimum for the complete iron chelation.

Scientific studies also reported tests of photo-Fenton like at neutral pH using NTA chelates in the 1:1 molar ratio (Sun and Pignatello 1992). Nonetheless, similarly to what happened with EDTA chelates, the 1.5:1 NTA:Fe showed a better catalytic activity of the complexes being the reaction rate associated considerably higher ($2.51 \times 10^{-2}$ $min^{-1}$ respect the $1.14 \times 10^{-2}$ $min^{-1}$ obtained when NTA was added in 1:1 molar ratio). Although the 1:1 molar ratio achieve a chelation near 100%, the catalytic activity in highly improved by the presence of free ligand. The presence of free chelator may play an important role on the maintenance of the catalytic activity of the Fe-L complex.

For what that concern OA, the L:Fe molar ratio generally reported in scientific studies (L:Fe 10:1 in this case) was tested in order to confirm the improvement of the catalytic effect resulting by the use of a correct molar ratio.

The lower efficiency of the 10:1 molar ratio was demonstrated by the drastic reduction of the catalytic activity along the reaction time of the OA chelates which could only allow a reaction rate of $0.81 \times 10^{-2}$ $min^{-1}$. A high increase on the SMX removal was observed with 20:1 OAFe molar ratio.

Finally, some authors indicated 1:1 as L:Fe molar ratio to employ tartaric acid as chelating agent (Sun and Pignatello 1992). However, as Figure 27 also shows, a better efficiency of chelation as well as slightly better catalytic activity of the complexes could be obtained with higher quantities of TA. In fact, despite the small improvement of Fe(III) chelate obtained by the use of TA chelates in a 10:1 molar ratio, the reaction showed a kinetic ratio much faster than the reaction in which chelates was formed in a molar ratio of 1:1 ($2.22 \times 10^{-2}$ $min^{-1}$ with 10:1 L:Fe molar ratio and $0.91 \times 10^{-2}$ $min^{-1}$ with 1:1 L:Fe molar ratio). Differently of what was

observed when 10:1 molar ratio was used, when 1:1 was employed no immediate disappearance of hydrogen peroxide was observed. The presence of an excessive amount of free tartaric acid into the solution may act as hydrogen peroxide scavenger. These results confirm the very low catalytic activity of the TA that made it an impractical option for the desired goals.

Discussing about the possibility of improve the catalytic activity of iron chelates, when performing photo-Fenton at neutral pH using Fe-L, one can also doubt if use iron III because of the stability of the complex or iron II due to the known faster kinetics in regular photo-Fenton. Nevertheless experimental results demonstrated that the use of Fe(II) ions did not allow to obtain a higher level of SMX degradation (Figure 28). This result confirms that when chelating agents are used to solubilize the iron, the use of Fe(II) ions, that in conventional photo-Fenton represent the more active species from the catalytic point of view, does not present significant differences from experiments using Fe(III) ions. In fact, as it can be observed in Figure 28, up to 60 minutes of reaction the chelates of Fe(II)-NTA proved to be characterized for a little better catalytic activity than the chelates of Fe(III) while for longer reaction time this tendency overturned because of the better stability of the Fe(III)-NTA and finally, no improvement of SMX degradation was achieved by the use of the Fe(II) ions.

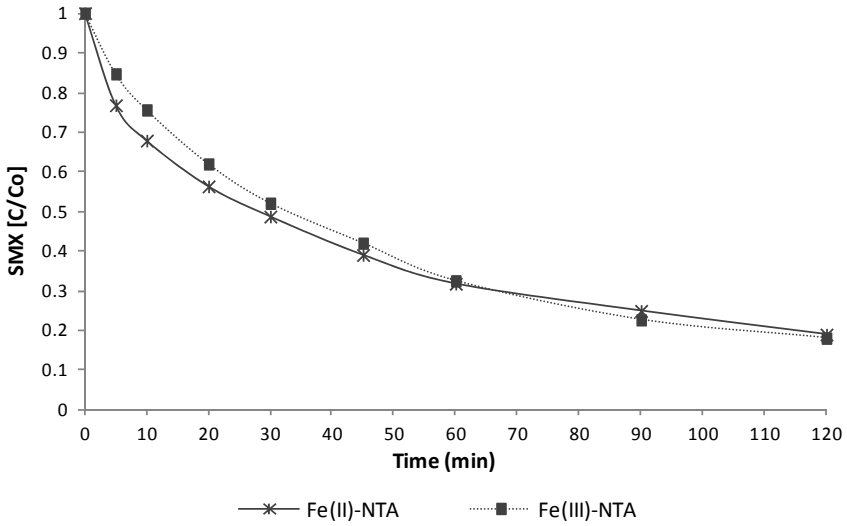


**Figure 28 SMX removal by means of Photo-Fenton like at neutral pH catalyzed by 1.5:1 molar ratio of Fe(III)-NTA and Fe(II)-NTA chelates**

The oxidation of iron inside the complex is a subject that was not deeply studied and no paper in literature reports such oxidation. The mechanism of the better catalytic performance of complexed Fe(II) should be better studied in the future. However, the catalytic activity improvement when Fe(II) is used should be observed. Thus, this result points out the importance of using $Fe^{3+}$ in order to ensure the better stability of the complexes which determine lower iron release during the reaction. It also demonstrates the ineffectiveness of the $Fe^{2+}$ form to improve the reaction rate in this type of system.

### *5.4.4 Comparison*

To select the correct chelator to perform photo-Fenton at neutral pH, it is important to observe not only at the efficiencies obtained by its utilization. The chelating agents are compounds which have to be added into the solution with consecutive increase of costs and TOC. Then, the best option is represented by the compound capable to allow the best efficiencies with minimal costs and TOC increase. For this purpose, the cost estimation is presented. The calculation was based in the work of Bolton et al., which normalizes the efficiency of the treatments carried out with all the chelators tested. Thus, the electrical energy per order of magnitude ($E_{EO}$) was calculated taking into account electricity costs of irradiation, mixing and chemical costs (only chelating agents), all of them normalized to the reactor volume (Bolton et al. 2001). The number of orders of magnitude was calculated from the percentage of SMX degradation. Technical-scale commercial prices were taken for chemical reagents used (EDTA=108.5 € $kg^{-1}$, NTA=84 € $kg^{-1}$, OA=87.23 € $kg^{-1}$, TA=116 € $kg^{-1}$) and converted to energy values of Catalonia (Spain) in 2013 (0.139 € $kWh^{-1}$).

Table 27 shows the conversion of the commercial prices of the chemical substances to energy values:

**Table 27 Commercial chemical substances and the conversion of their price to energy values.**

| Chemical | Company | Price (€) | (kg) | (€ $kWh^{-1}$) | (€ $kg^{-1}$) | (Wh $g^{-1}$) |
|---|---|---|---|---|---|---|
| EDTA | PANREAC | 54.3 | 0.5 | 0.139 | 0.11 | 0.78 |
| NTA | PANREAC | 42.0 | 0.5 | 0.139 | 0.08 | 0.61 |
| OA | PANREAC | 43.6 | 0.5 | 0.139 | 0.09 | 0.63 |
| TA | Alfa-Aesar | 58.0 | 0.5 | 0.139 | 0.12 | 0.84 |

The electrical energy per order of magnitude ($E_{EO}$) for the percentage of SMX removal achieved within the correspondent reaction time was calculated trough the definition of the following figure of merit (Bolton et al. 2001):

| | | |
|---|---|---|
| $E_{E,mix}$ | [Wh $L^{-1}$] | electrical energy for mixing |
| $E_{E,pro}$ | [Wh $L^{-1}$] | electrical energy for irradiation |
| $E_{E,chem}$ | [Wh $L^{-1}$] | cost of reagents converted to energy |
| $E_{E,tot}$ | [Wh $L^{-1}$] | total electrical energy |
| $E_{EO,rx}$ | [Wh (L·order)$^{-1}$] | electrical energy for irradiation per order of magnitude |
| $E_{EO,tot}$ | [Wh (L·order)$^{-1}$] | total electrical energy per order of magnitude |

The order of magnitude for atrzine removal at 25 minutes was calculated as:

$$order\ of\ magnitude\ OM = \frac{[SMX]_0 - [SMX]_t}{[SMX]_0} \quad (93)$$

In Table 28, the energetic requirements for SMX removal when applying the four chelating agents in the molar ratio required for iron chelation are shown:

**Table 28 Energetic requirements of photo-Fenton like at neutral pH catalyzed by Fe(III)-L chelates**

| L:Fe X:1 | Time (min) | OM (-) | $E_{E,mix}$ (Wh $L^{-1}$) | $E_{E,pro}$ (Wh $L^{-1}$) | $E_{E,chem.}$ (Wh $L^{-1}$) | $E_{E,tot}$ (Wh $L^{-1}$) | $E_{EO,rx}$ (Wh (L·order)$^{-1}$) | $E_{EO,tot}$ (Wh (L·order)$^{-1}$) |
|---|---|---|---|---|---|---|---|---|
| **EDTA-Fe 1.5:1** | 75 | 0.77 | 18.8 | 15 | 0.03 | 34 | 20 | 44 |
| **EDTA-Fe 1:1** | 150 | 0.70 | 37.5 | 30 | 0.02 | 68 | 43 | 96 |
| **NTA-Fe 1.5:1** | 120 | 0.82 | 30 | 24 | 0.02 | 54 | 29 | 66 |
| **NTA-Fe 1:1** | 150 | 0.72 | 37.5 | 30 | 0.01 | 68 | 42 | 94 |
| **OA-Fe 20:1** | 150 | 0.67 | 37.5 | 30 | 0.14 | 68 | 45 | 102 |
| **OA-Fe 10:1** | 360 | 0.34 | 90 | 72 | 0.07 | 162 | 214 | 482 |
| **TA-Fe 10:1** | 10 | 0.12 | 2.5 | 2 | 0.11 | 5 | 18 | 40 |
| **TA-Fe 1:1** | 135 | 0.13 | 33.8 | 27 | 0.01 | 61 | 216 | 486 |

Figure 29 presents the costs expressed in terms of total energy requirements per order of magnitude along with the percentage of TOC contribution due to the additionof chelating agents.

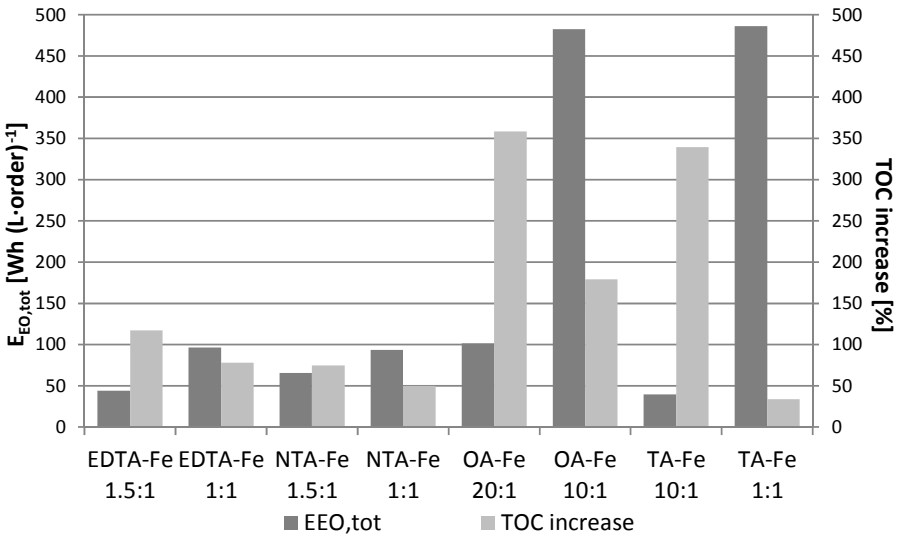


**Figure 29 Draft cost estimation for Photo-Fenton like at neutral pH with the chelating agents tested versus percentage of TOC contribution.**

Due to the less L:Fe molar ratio required and their better chelating activity, the costs incurred for the achievement of high efficiencies obtained with the use of EDTA and NTA were generally lower than those incurred with the use of tartaric and oxalic acid. Using EDTA at 1.5:1 molar ratio instead of 1:1, about 46% of energy is saved with a low increase of TOC (from ≈80% to ≈120%). Employing NTA chelates in the molar ratio of 1.5:1 in comparison to the 1:1 as it was suggested in some scientific studies, the costs could be reduced (≈30% of costs reduction) with a low increase of TOC contribution (from ≈50% to ≈75%). Concerning OA, using 20:1 molar

ratio, the strong increase of the degradation rate allowed obtaining a great reduction of costs (≈80% of reduction). However it also involved a high increase of TOC (≈350%) which contribution was already elevated in the 10:1 molar ratio (≈180%). Peculiar is the case of TA that in the two studied conditions implied two particularly different scenarios. When TA was increased the high increase of catalytic activity of the chelates allowed to greatly reduce the operative costs (≈90% of costs reduction) producing, however, a TOC increase of about 300%. The higher costs associated with the use of TA and OA are even less justifiable if one takes into account the high contribution of TOC.

In particular, it is important to emphasize that NTA, above all in the 1.5:1 molar ratio, appears to be the chelator that better defines a balance between benefits and negatives effects.

## 5.5 Conclusions

From the experimental results the following conclusions have been drawn.

- To perform photo-Fenton at neutral pH using chelating agent in order to solubilize the Fe(II) or Fe(III) is important to know that the stoichiometric 1:1 L:Fe molar ratio is generally not enough to ensure the complete chelation of the iron. The optimum ratio L:Fe has to be established observing the balance between chelation efficiency, environmental protection and lower costs.

- The use of iron in the oxidative form of $Fe^{2+}$ did not allow obtaining an improvement of the kinetic reaction respect the $Fe^{3+}$ which the use, instead, is preferable to ensure the stability of the complexes.

- Photo-Fenton like at neutral pH with EDTA and NTA could remove a significant quantity of SMX. Furthermore, due to the high strength of chelation that characterizes them, the use of these chelating agents allow the achievement of high efficiencies with minimal contribution of TOC.

- Using OA in a photo-Fenton like at neutral pH, which chelating strength and catalytic activity are significantly lower, could only allow the achievement of discreet efficiencies with an elevate L:Fe molar ratio that involves high TOC contribution.

- TA, with its minimal catalytic activity could represent, among the chelating agents tested, the least suitable option for the intended purpose.

- Taking into account the better properties of biodegradability respect of EDTA as well as the better efficiencies obtained with the smallest TOC contribution, NTA could represent a useful option to perform photo-Fenton process at neutral pH. In addition, photo-Fenton like at neutral pH performed with NTA chelates in 1.5:1 molar ratio appears to be the most cost-effective process among all tested.

## 5.6 Appendix

WATER RESEARCH 61 (2014) 232–242

Available online at www.sciencedirect.com

ScienceDirect

journal homepage: www.elsevier.com/locate/watres

# Assessment of iron chelates efficiency for photo-Fenton at neutral pH

*Antonella De Luca, Renato F. Dantas*, Santiago Esplugas*

*Department of Chemical Engineering, University of Barcelona, Martí i Franques 1, 08028 Barcelona, Spain*

ARTICLE INFO

*Article history:*
Received 19 February 2014
Received in revised form
15 May 2014
Accepted 19 May 2014
Available online 29 May 2014

*Keywords:*
Chelating agent
AOPs
Photo-fenton
Neutral pH
Water treatment
Sulfamethoxazole

ABSTRACT

In this study, homogeneous photo-Fenton like at neutral pH was applied to remove sulfamethoxazole from water. The process was performed using different chelating agents in order to solubilize iron in a neutral water solution. The chelating agents tested were: ethylenediaminetetraacetic acid (EDTA); nitrilotriacetic acid (NTA); oxalic acid (OA) and tartaric acid (TA). The iron leaching was monitored over reaction time to evaluate the chelates stability and their resistance to HO· and UV-A radiation. Chelates of EDTA and NTA presented more stability than OA and TA, which also confirmed their higher efficiency. Total Organic Carbon (TOC) analyses were also performed to evaluate the contribution in terms of solution contamination related to the use of chelating agents. The better properties of biodegradability in respect of EDTA combined with better efficiency in terms of microcontaminant removal and the smallest TOC contribution indicate that NTA could represent a useful option to perform photo-Fenton processes at neutral pH.

# 6 Fe(III)-NTA chelates: stability and applicability in Photo-Fenton at neutral pH

## 6.1 Introduction

The efficiency of Fe(III)-NTA as photo-Fenton like catalyst has been already demonstrated in the previous chapter. Nevertheless, the assessment of the durability of chelate stability over reaction is fundamental in order to better perform the treatment and to make it competitive in water decontamination compared with others advanced oxidation processes (AOPs).

The catalytic activity of the chelates is strongly dependent of their stability. In fact, the pH operating condition (circumneutral pH) makes impossible to keep soluble the iron content if released from the chelators structure. Chelates decomposition should be avoided not only in order to elude the reaction rate decrease but also to prevent large amount of $Fe(OH)_3$ concentrated waste. In fact, as already discussed in the case of conventional photo-Fenton, a great amount of iron precipitate would mean the necessity of providing the plant of an additional unit for sludge separation. Thus, the knowledge of the influence of the operating condition adopted for photo-Fenton at neutral pH is absolutely important to predict the efficiency of the treatment. Furthermore, the control of the parameter set up is really important to extend the chelates lifetime until the achievement of the required level of quality.

Ferric nitrilotriacetate Fe(III)-NTA , whose absorption spectrum shows a tail up to the visible domain, will undergo transformation upon irradiation (especially when adding oxidants species into the solution). In this regard, it is of great importance to have a thorough understanding of the chelate solution behaviour under UV light irradiation (Andrianirinaharivelo et al. 1993). The monitoring of the spectrum modification over reaction can supply useful information if overreaction instability phenomena will arise. In fact, the absorbance of the solution in correspondence of the spectrum peak has been demonstrated to be directly proportional to the chelates concentration. Thus, peak reduction over time represents a clear sign of the complexes breakage and subsequent decrement of the catalyst content.

In this chapter, the stability of Fe(III)-NTA chelates by monitoring the absorption spectrum during the reaction under different operating conditions will be discussed. Various factors have been taken into account and the stability of Fe(III)-NTA was studied under thermal, oxidative and photochemical stress and the effect of aging was considered as well. More in detail, Fe(III)-NTA solution stability was monitored under different temperature conditions (T=10-30 °C), in presence and absence of UV-A irradiation and by adding three different concentrations of $H_2O_2$. The additional effect on chelate stability caused by different irradiation source (UV-A, UV-C and Xenon lamps) was also evaluated. The entire study was performed at neutral pH.

The main results discussed in this chapter have been published in Applied Catalysis B: Environmental (section 6.7 Appendix).

## 6.2 Sample preparation

Ferric ion solution 71.6 mM was prepared fresh daily dissolving anhydrous $FeCl_3$ in 0.1 M HCl to minimize iron(III) hydrolysis and polymerization (Flynn 1984). Iron chelate solution 0.36 mM of $Fe^{3+}$ (20 mg $L^{-1}$), was prepared by directly mixing the ferric ion solution with a solution of the NTA in Milli-Q water. Thus, after approximately 15 minutes of stirring, the pH of solution was slowly adjusted to 8.0 to allow the chelating agent's dissolution. Then it was let stirring during one extra hour to ensure the complete chelation of iron content. The amount of chelating agent required was determined monitoring the absorbance at 258 nm of $Fe^{3+}$ solution by progressively addition of NTA. Increasing the chelator concentration, in fact, the absorbance grew until showing a plateau which coincided with the molar ratio of 1.5:1 (NTA:Fe(III)). This ratio, which correspond to a small excess in NTA was necessary to ensure the complete chelation of the iron content in the condition adopted for chelation process (De Luca et al. 2014). The concentration of iron chelate used to carry out the present study is significantly higher than what previously proposed for treatment of SMX in Milli-Q water (Chapter 5). The reason of that is uniquely connected with practical purpose of measurement.

When required, hydrogen peroxide was added into the solution immediately before to switch on the reactor lamps.

## 6.3 Analytical determination

Fe(III)-NTA stability was determined registering the absorbance of the 0.20 μm filtered samples at 258 nm using a UV/Vis Spectrophotometer (Perkin Elmer Lambda 20). During the reaction the instability phenomena arisen were monitored registering the evolution of the solution absorption spectrum. Because the decomposition of the complexes due to the stress caused by the applied conditions, iron was released from the chelator structure and a reduction of the absorbance was observed as shown in the Figure 30.

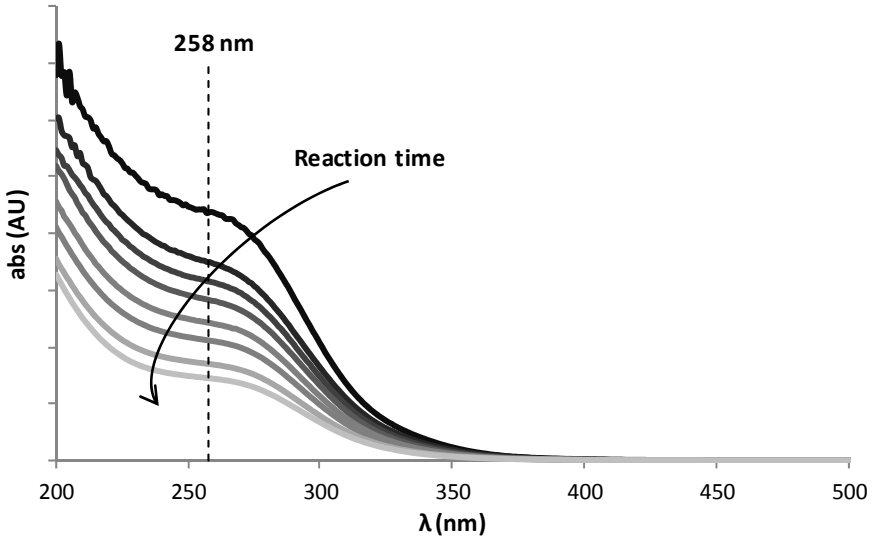


**Figure 30 Evolution of the Fe(III)-NTA absorption spectrum over time reaction.**

Total organic carbon determination (as NPOC) and hydrogen peroxide concentration were also monitored over reaction using the technique and the methods described in Chapter 3. It has to be pointed out as hydrogen peroxide absorbance also has a contribution at 258 nm. However, the contribution at the considered concentration was totally insignificant compared to the intensity of the peak registered for Fe(III)-NTA chelates (0.2% of the initial absorbance exhibited by the chelates solution). In this regard, it can be considered that the presence of oxidant did not compromise the monitoring of chelates solution stability.

## 6.4 Methodology

The effects produced on chelate solution stability by the variation of different operating parameters have been evaluated separately as well as synergistic effects.

The parameters that have been varied were:

- The temperature in dark as well as during the irradiation with UV-A and also after addition of hydrogen peroxide (0.59 mM, 20 mg $L^{-1}$);
- The hydrogen peroxide doses (0.59 mM, 1.18 mM and 2.94 mM corresponding to 20 mg $L^{-1}$, 40 mg $L^{-1}$ and 100 mg $L^{-1}$ respectively) at standard temperature (25 °C) and under UV-A irradiation;
- The source of irradiation during oxidation by adding specific hydrogen peroxide dose (0.59 mM) and at standard temperature (25 °C).

Effects on chelates solution stability could be also produced depending of the concentration of iron and NTA adopted. However, these two concentrations should be fixed in order to establish a good compromise between process efficiency and environmental safeguard. In Chapter 5 (De Luca et al. 2014), $Fe^{3+}$ was fixed to 0.089 mM (5 mg $L^{-1}$) to ensure a considerable reaction kinetic even if lower than conventional photo-Fenton as consequence of the effect of chelation. This concentration was also considered the optimum to make possible the reuse of the effluent in agriculture without excessive requirement of NTA content. The amount of chelator was instead determined to ensure the complete chelation of the iron content (1.5:1 NTA:Fe(III)). Under photochemical stress the stability would be probably compromised as much as lower is the concentration of the chelates. The moles of photons available are in fact independent of the characterization of the solution. Thus, the moles of photons per mol of chelates in the unit time will be lower when increasing the concentration of chelates. Under photochemical and oxidative stress, instead, the worse scenario would occur in correspondence of the higher concentration of chelates used. In this condition, the amount of Fe(III)-NTA would influence the stability of the chelate solution in reason of the more or less enhancement of the kinetic order rate of the photo-Fenton reaction.

In this study, pseudo-first order kinetic constants have been calculated for all the curves of absorbance reduction in order to better compare the obtained results.

## 6.5 Results and discussions

### *6.5.1 Effect of Temperature, UV-A exposure and $H_2O_2$*

The effect that heating can produce on metal chelate solution, reflected in the change of the stability constant value, is attributable to the structural change of the functional groups. Since the heating is not enough to change the ionic type of reaction no significant effects would be observed. On the other hand, ionic or coulombic effect will be observed in charge and charge distribution of the anions, and in the charge and the radius of cations. When that happens the most profound change is in the nature of the double bond of the carbons. Then, the mesomeric effect of resonance structure can be responsible of catalyst decomposition and losing of its activity (Calvin and Wilson 1945; Gojković et al. 1999).

The knowledge of the effects produced by the temperature on the stability of the iron chelate solution is important for correctly determine the set up of experimental temperature as also for an adequate control during the storage of the solution before its utilization.

As Figure 31 shows, during two hours in which the solution was kept at constant temperature, no changes of absorbance were registered. These results are able to demonstrate as in the tested range, the temperature did not produce the arisen of instability phenomena.

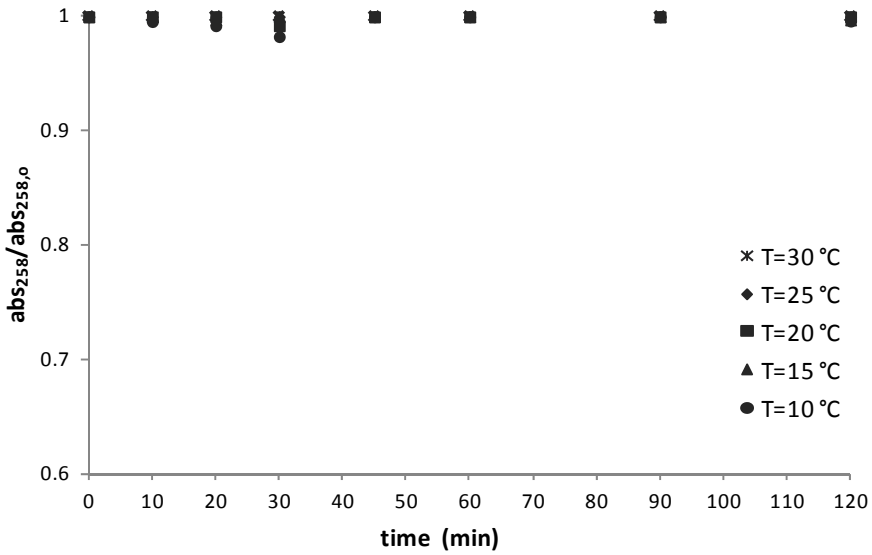


**Figure 31 Variation of the intensity of the absorption peak during two hours at different temperatures (T=10-30 °C).**

More interesting could be the monitoring of the solution stability under combined effect of aging and inconstant temperature. This information is, in fact, very useful in order to better implement the wastewater treatment plant's management system. In this regard, the evolution of the absorption spectrum was monitored during 9 days of storage at room temperature without specific control of temperature (T=23-32 °C).

In Figure 32 the absorption spectrums shows as, the reduction of the absorbance registered at 258 nm after 9 days of storage without temperature control was completely insignificant (≈3% absorbance reduction). The results obtained were able to demonstrate as, under natural

conditions of temperature any system of temperature control is not required to keep stable the chelate solution during the storage.

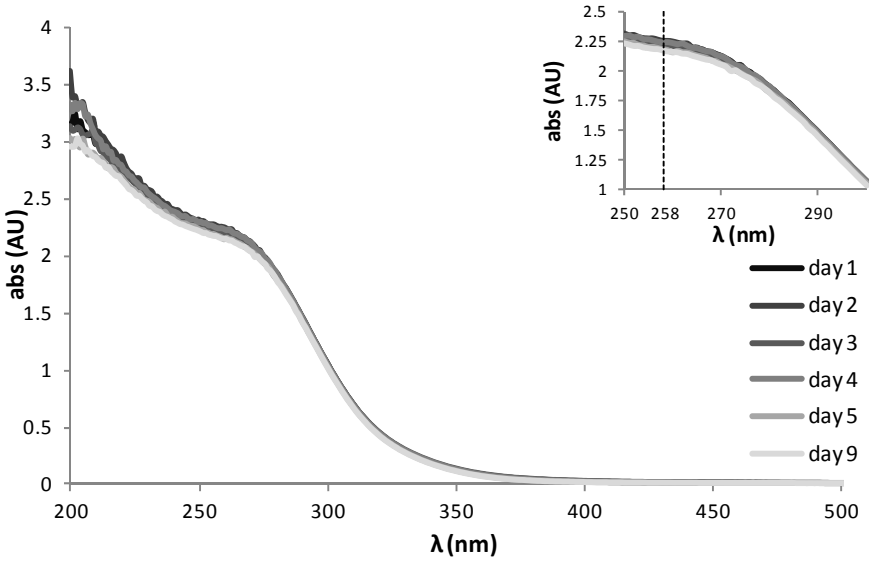


**Figure 32 Monitoring of the iron chelate stability of the solution kept at room temperature during 9 days.**

Different response in stability was expected under irradiation strain. Thus, the stability of iron chelate solution was monitored during two hours under UV-A irradiation and temperature control. The changes in absorbance at 258 nm exhibited by the solution under UV-A irradiation and constant temperature are shown in Figure 33. The results highlight as under photons transfer the role of the temperature control completely changes. In fact, when UV-A radiation was applied, keeping the temperature in the lower values tested allowed to extend the chelates lifetime.

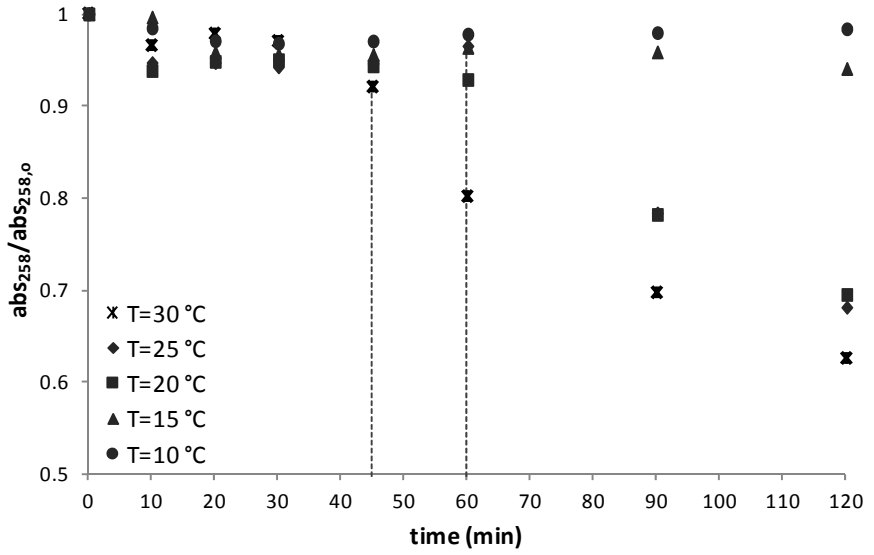


**Figure 33 Assessment of iron chelate stability under UV-A irradiation and different temperatures (T=10-30 °C).**

When temperature was kept between 10-15 °C, no reduction of chelate content was essentially arisen during two hours of irradiation. The curve of absorbance reduction, in fact,

showed a pseudo-first order kinetic constant almost null ($k_{obs}$=(0.69±0.06) x $10^{-3}$ $min^{-1}$). On the other hand, when under irradiation the temperature of the solution was kept between 20-25 °C it was possible to observe two different steps in the stability of the cheletes. Until 60 minutes of irradiation, in fact, the absorbance of the solution at 258 nm was almost constant ($k_{obs}$ =(0.93±0.05) x $10^{-3}$ $min^{-1}$). Since this moment and during one more hour of irradiation, the trend radically changed. Thus, a reduction in chelate content was gradually registered revealing the beginning of the complexes damage. This evidence was also confirmed by the appreciable increment of the pseudo-first order kinetic constant calculated for the second segment of the curve ($k_{obs}$ =2.53 x $10^{-3}$ $min^{-1}$). Similarly to this behavior, when the temperature was risen at 30 °C, instability phenomena were sooner arisen. The second segment of the curve of absorbance reduction was, in fact, recognizable earlier than what observed a lower temperature. Thus, also in this case two different segments could be clearly identified, the first one corresponding to the first 45 minutes of irradiation ($k_{obs}$ =0.90 x $10^{-3}$ $min^{-1}$) and the second one representative of the last 75 minutes of irradiation ($k_{obs}$ =2.59 x $10^{-3}$ $min^{-1}$). Thus, even if the temperature cannot directly influence the achievement of instability phenomena in chelate solution, its control allows extending the lifetime of the catalyst. The release of iron will start as sooner as higher the temperature is. Since it starts, the chelates solution's decay followed a similar trend. This similarity is remarkable for the almost parallel curves of absorbance reduction which, in the second segment, showed almost the same pseudo-first order kinetic constants. Under the considered condition no instability phenomena was achieved before 45 minutes of UV-A radiation. Nevertheless, no more than approximately 40% of the chelates resulted decomposed under the considered operating conditions.

The effect of direct photolysis on solution mineralization was also monitored (Figure 34).

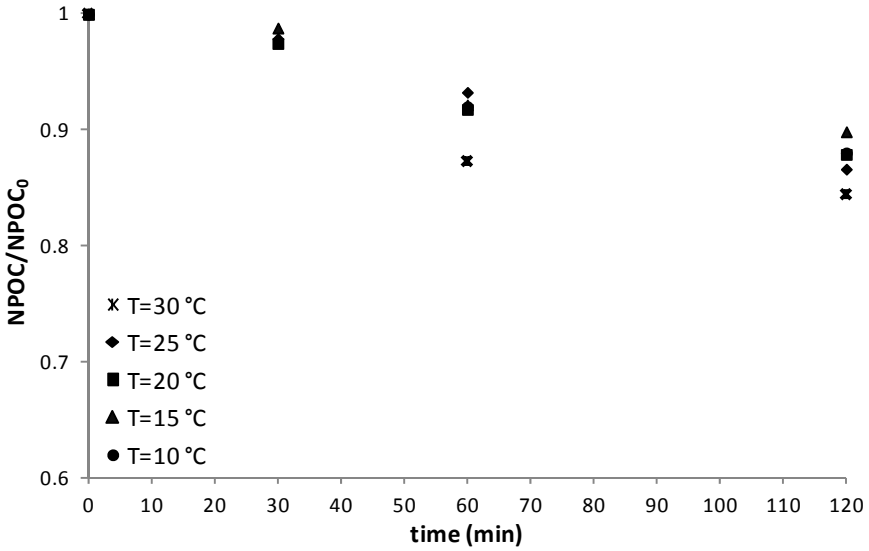


**Figure 34 Effect on mineralization by direct photolysis of iron chelate solution under UV-A irradiation and different temperatures (T=10-30 °C).**

The mineralization achieved was almost the same under all the considered conditions being efficiency variable between 11-16%. The trend was practically the same in the whole range of temperatures tested. All the curves showed a first step in which the mineralization was not yet started followed by a second one in which a small NPOC removal was gradually achieved. After

correlation of this result with what shown in the previous figure, additional discussion can be done. During the first part of the reaction the photons transferred, in almost all the temperature test range, were not able to produce the breakage of the chelates bonds and no NPOC removals could be achieved. Then, by an intramolecular photoredox process, which leads to the chelates destruction, ferrous ion and organic radicals from the ligands were formed (Balzani and Carassiti 1970). A small mineralization of the solution could be then achieved (Balzani and Carassiti 1970; Abida et al. 2006). Because the APCAs like NTA do not absorb light in the range of study, the direct photolysis might be negligible (Bunescu et al. 2008). Thus the mineralization obtained can be entirely ascribable to the organic radicals produced. By knowledge obtained by published works about the photochemical degradation of Fe(III) nitrilotriacetate solution, the mayor photoproducts expected are Fe(II), iminodiacetic acid (IDA), formaldehyde and $CO_2$ (Stolzberg and Hume 1975). At lower temperatures, even if minimum reduction in absorbance was observed, almost 10% of mineralization was obtained. This result can be explained taking into account the greater content of free chelator due to the different molar concentration adopted for NTA and $Fe^{3+}$ (1.5:1 NTA:$Fe^{3+}$). Thus, the minor production of organic radicals could be equally responsible of the attack to free ligands already present, which degradation was observable in NPOC removal but did not produce any effect in absorbance reduction.

The effect of the temperature was also evaluated under UV-A irradiation of iron chelate solution by adding 0.59 mM of hydrogen peroxide. As extra effect, due to the oxidative stress, a much higher contribution on chelate decomposition was expected.

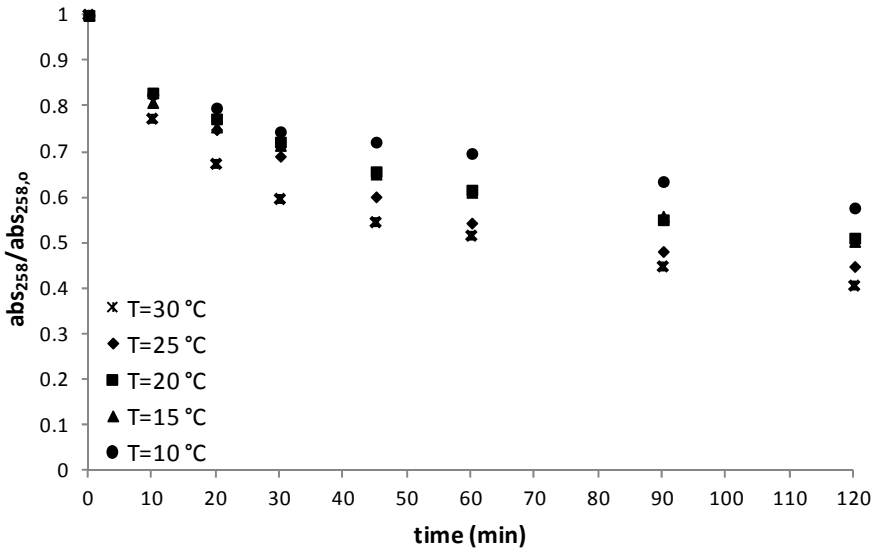


**Figure 35 Evaluation of the iron chelate stability under oxidation with UV-A irradiation and different temperatures ($[H_2O_2]_0$=0.59 mM, T=10-30 °C).**

Looking at the results showed in the Figure 35 solution, the presence of $H_2O_2$ involved the chelates decomposition since the beginning of the irradiation. An initial faster reduction in chelate content was already achieved in the first 30 minutes of reaction when the registered drop in absorbance was between 26% at 10 °C and 40% at 30 °C. Finally, after 120 minutes of reaction, the global reduction of ligand content was variable between 42% and 60% at 10 °C and 30 °C respectively. Thus, it seems clear as after the addition of the oxidant, an adequate

control of the temperature could be really useful to extend the lifetime of the chelates. Remarkable is the experimental evidence of total $H_2O_2$ consumption achieved after only 10 minutes of reaction for the whole analyzed conditions. The kinetics exhibited in chelates decomposition make possible identifying three range of temperature within which the trend was comparable. The calculated pseudo-first order kinetic constants were, in fact, respectively $k_{obs}$ =5.60 x $10^{-3}$ $min^{-1}$ for temperature set at 10 °C, $k_{obs}$ =(6.5±0.35) x $10^{-3}$ $min^{-1}$ for T=15-25 °C and $k_{obs}$ =9.12 x $10^{-3}$ $min^{-1}$ for T=30 °C.

The mineralization of Fe(III)-NTA solution obtained under UV-A irradiation and after adding 0.59 mM of $H_2O_2$ are shown in Figure 36.

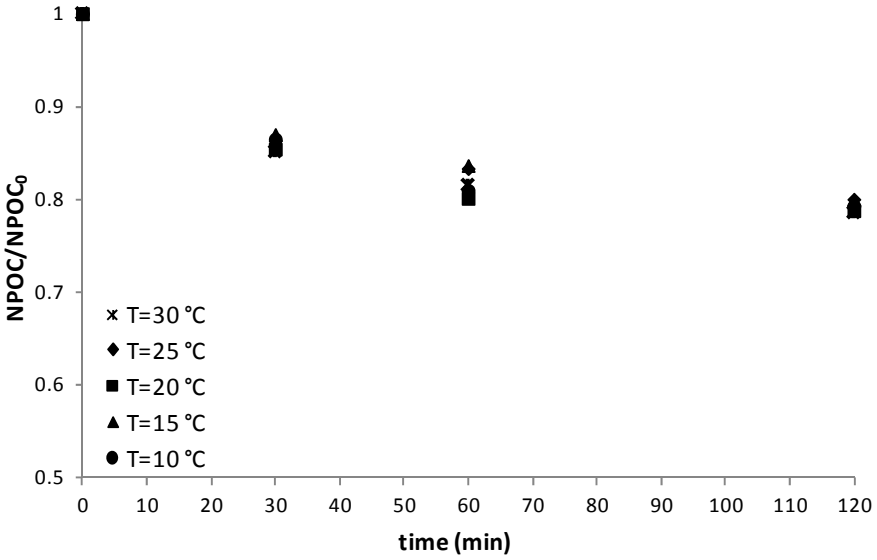


**Figure 36 Mineralization of iron chelate solution under oxidation with UV-A irradiation and different temperatures ($[H_2O_2]_0$=0.59 mM, T=10-30 °C).**

As effect of the $H_2O_2$ addition, the mineralization of the solution is also appreciable since the beginning of the reaction. The hydroxyl radicals produced quickly attacked the chelates molecules producing the breakage of the bonds of the Fe(III)-NTA complexes. As effect of the chelates decomposition, confirmed by the reduction of the absorbance at 258 nm, the correspondent amount of free chelator obtained was made available for mineralization. Differently from what registered in absence of oxidant, the mineralization curve of the solution did not show any initial segment essentially horizontal confirming the instantaneous occurrence of breakage and then mineralization of the chelates. It appears also clear as the amount of oxidant was totally inadequate to achieve high levels of efficiencies. After 30 minutes of reaction only the 15% of mineralization was achieved. Taking into account the total $H_2O_2$ consumption at 10 minutes of reaction and comparing this data with the much more smaller efficiency obtained under the same irradiation dose in absence of oxidant (≈1%), it is reasonable to ascribe this efficiency to the oxidative hydroxyl radicals activity. Since this time and until the end of the experiment, the extra contribution on mineralization was fixed at 5-6% of total carbon removal. This additional removal can be then ascribable to the presence of organic radicals originated from the oxidation of the free NTA. In fact, at wavelength longer than 345 nm, a redox process between Fe(III) and the carboxylate group of the ligand takes place. This process gave way to the production of Fe(II) and $R'CH_2CO_2\cdot$ which in turn undergone

a decarboxylation giving rise to $R'CH_2\cdot$. This radical chain, united with the direct photolysis of the solution, was supposed to be the responsible of the additional mineralization achieved (Abida et al. 2006).

In Table 29 are summarized the main experimental results in terms of Fe(III)-NTA decomposition described in this section:

**Table 29 Effects of irradiation and irradiation/oxidation strains on Fe(III)-NTA chelates decomposition**

| | T<br>°C | $k_{obs}$<br>$min^{-1}$ | $Fe_{lost}$ (*)<br>% |
|---|---|---|---|
| **UV-A** | 10-15 | $(0.69\pm0.06) \times 10^{-3}$ | 1.6-5.9 |
| | 20-25 | $(0.93\pm0.05) \times 10^{-3}$ | 30.5-31.9 |
| | 30 | $0.90 \times 10^{-3}$ | 37.5 |
| **UV-A /$H_2O_2$ $[H_2O_2]_0$=0.59 mM** | 10 | $5.60 \times 10^{-3}$ | 42.2 |
| | 15-25 | $(6.50\pm0.35) \times 10^{-3}$ | 48.8-55.1 |
| | 30 | $9.12 \times 10^{-3}$ | 59.4 |

(*) after 120 minutes

### *6.5.2 Effect of $H_2O_2$ doses*

At standard temperature (T=25 °C) the effect of hydrogen peroxide concentration was evaluated. In order to quantify the effect of the $H_2O_2$ dose on the instability of iron chelates solution, different $Fe^{3+}$:$H_2O_2$ ratios were adopted. In Figure 37 is shown the reduction of chelates content occurred into the irradiated solution with UV-A light using the $Fe^{3+}$:$H_2O_2$ ratios of 1:1, 1:2 and 1:5 respectively.

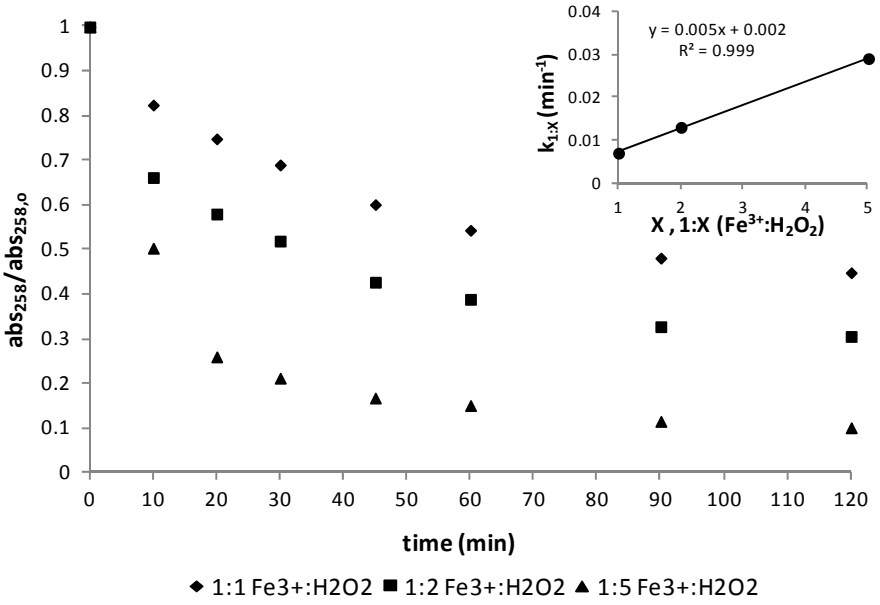


**Figure 37 Evaluation of the iron chelate stability under oxidation with UV-A irradiation at standard temperature (T=25 °C) and different $Fe^{3+}$:$H_2O_2$ ratios $[Fe^{3+}]_0$=0.36 mM; $[H_2O_2]_0$=0.59 mM, 1.18 mM, 2.94 mM).**

Obviously, the effect on chelate stability was much destructive as higher was the concentration of oxidant employed. The knowledge of the full extent of this effect could help

in prediction of the efficiency reduction of Fe(III)-NTA as catalyst. As previously occurred, the complete hydrogen peroxide consumption was obtained in the first 10 minutes of reaction for all the conditions analyzed. As observable in the top of the figure, in this period when the curves showed a considerably higher slope, the pseudo-first order kinetic constants appeared almost proportionally to the increasing of oxidant concentrations ($k_{obs,1:1}$=0.07 x $10^{-1}$ $min^{-1}$, $k_{obs,1:2}$=0.13 x $10^{-1}$ $min^{-1}$, $k_{obs,1:5}$=0.29 x $10^{-1}$ $min^{-1}$). The quick complete consumption of the oxidant for the whole doses employed could have been occurred for the insufficient amount of oxidant as well or, in some cases, for its excess by reducing the oxidation rate of the Fenton's process (Ku et al. 1998; Sillanpää et al. 2011). Anyway, since the hydrogen peroxide was completely exhausted, a stronger reduction in chelates content was still observed and it was much more significant as higher the initial hydrogen peroxide concentration was. Once again, this result could be related with the higher production of organic radicals generated for decomposition of the Fe(III)-NTA chelates. Finally, after almost 20 minutes from the beginning of the reaction, the kinetic reaction drastically dropped as obviousness of the consumption of the organic radicals produced. The final reduction in chelates content (after 120 minutes of reaction) settled at 90%, 69%, and 55% of the initial value for the $Fe^{3+}$:$H_2O_2$ ratios of 1:5, 1:2 and 1:1 respectively.

In the previous study of the authors, photo-Fenton like at neutral pH catalyzed by Fe(III)-NTA chelates was applied for SMX removal. Using the same NTA:$Fe^{3+}$ molar ratio adopted in the present study (1.5:1 NTA:$Fe^{3+}$) but by adding 0.29 mM of $H_2O_2$ (1:2 $Fe^{3+}$:$H_2O_2$), the reduction of iron content started only after 45 minutes of irradiation. This different result can be explained taking into account the effect of the competition established between the compounds for reaction with the available non-selective HO· radicals (De Luca et al. 2014). Thus, the amount of radicals made really available for reaction with the chelates was reduced and the lifetimes of the chelates could be extended. Finally, even though the response of the chelates can change according with the complexity of the system, the information got in the present study is able to make more understandable how the parameters influence the stability of the catalyst.

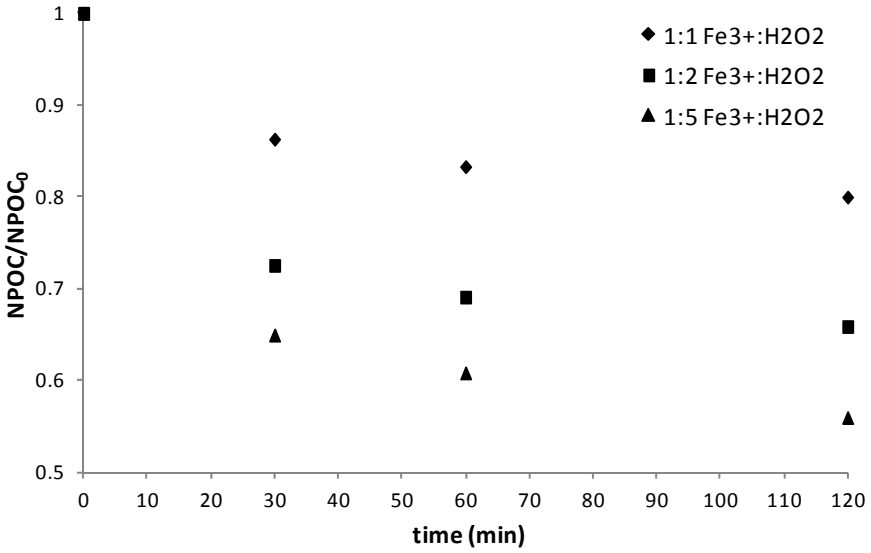


**Figure 38 Mineralization of iron chelate solution under oxidation with UV-A irradiation at standard temperature (T=25 °C) and different $Fe^{3+}$:$H_2O_2$ ratios (mg $L^{-1}$ : mg $L^{-1}$)[$Fe^{3+}$]$_0$=0.36 mM; [$H_2O_2$]$_0$=0.59 mM, 1.18 mM, 2.94 mM).**

In Figure 38 are shown the curves of NPOC removal obtained by adding the tested $H_2O_2$ doses. The efficiency achieved for solution mineralization showed a progressive increment according to the increment of the hydrogen peroxide dose applied (from 20% to 44% when increasing $H_2O_2$ by five times). Besides, the curves showed a changes in the rate of the reaction occurred at the total consumption of the hydrogen peroxide allowing identify two different steps of the reaction. In the first one, hydroxyl radicals and organic radicals were both responsible for the mineralization of the solution followed by another step in which the extra efficiency was ascribable to the action of the only organic radicals.

In Table 30 are summarized the results in terms of Fe(III)-NTA decomposition under UV-A irradiation and different doses of $H_2O_2$ (T= 25 °C):

**Table 30 Effect of $H_2O_2$ load on Fe(III)-NTA chelates decomposition under UV-A irradiation**

| | **1:X(*)** $Fe^{3+}:H_2O_2$ | **$k_{obs}$** $min^{-1}$ | **$Fe_{lost}$(**)** % |
|---|---|---|---|
| **UV-A /$H_2O_2$** | 1:1 | $0.07 \times 10^{-1}$ | 55.1 |
| | 1:2 | $0.13 \times 10^{-1}$ | 69.3 |
| | 1:5 | $0.29 \times 10^{-1}$ | 89.8 |

(*) mg $L^{-1}$ : mg $L^{-1}$ (**) after 120 minutes

### *6.5.3 Effect of UV-light exposure*

Because the maximum absorption of chelate solution was registered at 258 nm, the range of wavelength of radiation emitted from the lamp implies effects strongly different. Thus, the contribution of light on chelate stability is obviously dependent of the source used to transferring the photons.

Three light sources were employed to study their contribution on chelates stability during the irradiation after adding 0.59 mM of hydrogen peroxide (Figure 39).

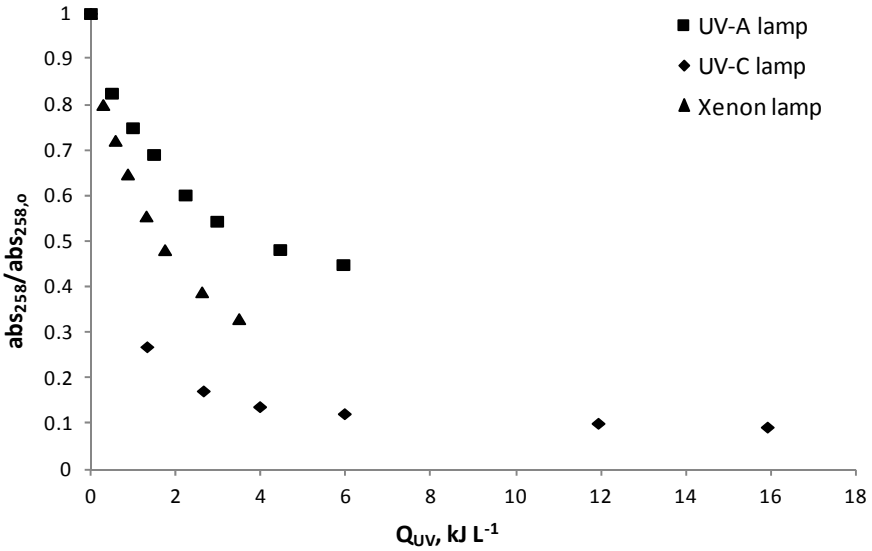


**Figure 39 Evaluation of the iron chelate stability under oxidation with $[H_2O_2]_0$=0.59 mM at standard temperature (T=25 °C) and under different source of UV irradiation.**

It was expected that the higher effect in terms of chelate decomposition would have been obtained by UV-C irradiation which wavelength of emitted radiation (254 nm) is the closest to

the maximum absorbance of the solution (258 nm). Moreover, the emission spectrum of UV-C lamps is also included in the range of absorbance of $H_2O_2$ (<310 nm) that involves a higher HO· radicals production. The experimental result remarks as, also in this case, the complete hydrogen peroxide consumption was achieved after only 10 minutes since the beginning of the irradiation. In this case the kinetic rate followed by the reaction assumed a pseudo-first order kinetic constant of 0.042 $min^{-1}$ and more than 70% of Fe(III)-NTA chelates were destroyed in only 10 minutes of reaction. Afterwards, the kinetic reaction showed a strong reduction when the chelates decomposition was entirely attributable to the only action of the organic radicals. Thus, the reaction totally ended after 30 minutes of irradiation (which correspond to a UV dose of 4 kJ $L^{-1}$) when less than 10% of the initial chelates contents remained available.

On the other hand, a great similarity was observed between the results exhibited when UV-A lamps and solar simulator were used to irradiate the solution. The Xenon lamp, in fact, emits in a wider range of wavelengths (>280 nm) than the UV-A lamps but with intensity sensibly lower than them which emission is instead totally concentrated at 356 nm. The reactions followed a kinetics rate which the pseudo-first order kinetic constants assumed the values of 0.007 and 0.008 $min^{-1}$ respectively. After the total hydrogen peroxide consumption (at 10 minutes) the kinetic slowly reduced overtime reaction. The wider emission spectrum of the Xenon lamp was probably responsible of the higher instability arisen with respect to what happened when UV-A lamps were employed. After 120 minutes of irradiation, in fact, the 67% of chelates destruction was caused but a 55% was instead obtained under UV-A irradiation corresponding to a UV dose of 3 and 6 kJ $L^{-1}$ respectively. It seems clear as, overlooking in this context the characteristic of contamination, UV-A light could represent the more adequate choice of irradiation to better preserve the chelates during the reaction.

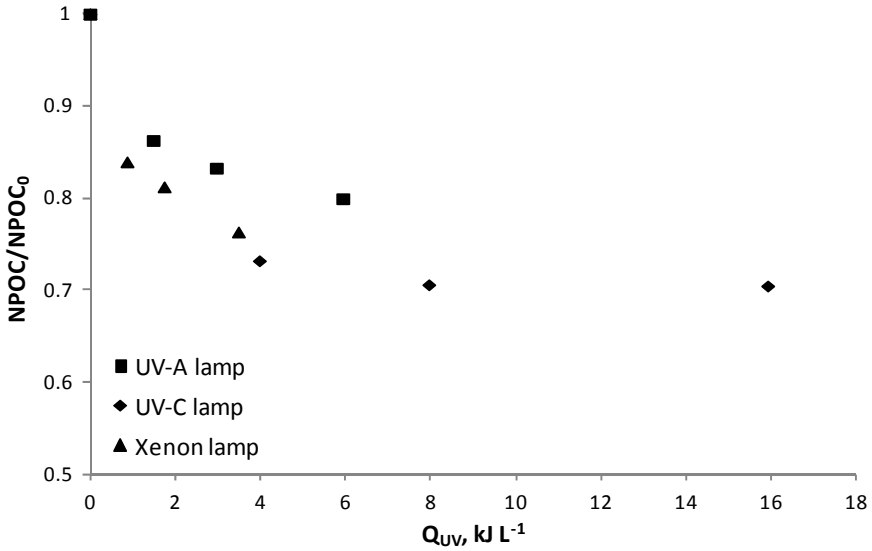


**Figure 40 Mineralization of iron chelate solution under oxidation with $[H_2O_2]_0$=0.59 mM at standard temperature (T=25 °C) and under different source of UV irradiation.**

Finally, the efficiency obtained in terms of solution mineralization is shown in Figure 40. No correlation between the higher level of Fe(III)-NTA decomposition and solution mineralization was found under UV-C irradiation. The efficiency registered for the solution mineralization was of almost 30% which was not so higher if compared to what instead obtained in the other two

cases analyzed (20% and 24% with UV-A and Xenon lamps respectively). Thus, after the total consumption of $H_2O_2$, the organic radicals generated were strongly responsible for the breakage of the bonds in chelates structure but their contribution was not enough to produce the mineralization of the effluent. Furthermore, the photochemical activity of the organic radicals could not allow the achievement of a higher mineralization. Therefore, the use of such a high energetic light could be more counterproductive than useful in terms of prolonging the lifetime of the chelates.

## 6.6 Conclusions

An analysis of the stability of the chelate solution under different combination of the most important operating parameters that influence photo-Fenton like at neutral pH was carried out. Three operating parameters were considered as stress factor for the chelate solution (i.e. photochemical stress, oxidative stress and thermal stress).

It was found out that:

- The control of temperature is unnecessary if performed in absence of any other stress factors for the solution. During 9 days without temperature control, no changes were observed in the absorbance exhibited by the chelate solution which demonstrates a good stability of the complexes under aging.

- Under UV-A irradiation the chelates solution showed a temporary stability before exhibiting a gradual damage and subsequent iron release. Nevertheless, the possibility of delaying the beginning of the instability phenomena by temperature control was demonstrated. In fact, the decomposition of chelates started as soon as higher the temperature of the solution was kept. In spite of that, the release of iron from the structure of the complex was completely avoided during two hours of irradiation when keeping the temperature at 10-15 °C. Particularly interesting is the evidence that shows no release of iron before 45 minutes of irradiation under the whole temperature test range.

- Under UV-A irradiation a slow mineralization of the solution was also achieved (≤16%). Likewise, NPOC removal curves showed a first step in which the solution remained stable followed by a gradual decline due to the action of the organic radicals produced by the breakage of the chelates.

- By combining photochemical and oxidative stresses, the chelate decomposition with subsequent iron release was unavoidable. Thus, by adding $H_2O_2$ (0.59 mM) the absorbance reduction curves of the solution showed a gradual decline since the beginning of the irradiation. Regardless, once again by controlling the temperature solution was still possible the achievement of a chelates lifetime extension (from 60% of reduction to 42% in two hours turning the temperature down 20 °C). Besides, similarly to what observed in chelates content reduction, the mineralization of the solution started simultaneously with the beginning of the irradiation. Thus, the extra oxidation attributable to the generation of hydroxyl radicals allowed an only slight enhancement in NPOC removal (≤20%).

- The effect on chelates stability of different hydrogen peroxides doses showed a direct proportional correlation between the hydrogen peroxide dose and the destruction of Fe(III)-NTA. Also the efficiency in mineralization exhibited a progressive increment according to the increment of the hydrogen peroxide dose applied (from 20% to 44% when increasing $H_2O_2$ by five times).

- The influence of the emission spectrum of the lamps employed for irradiation was finally confirmed. As it was expected UV-C lamps were the most unfavourable for applications in photo-Fenton like at neutral pH catalysed by iron chelates. The solution, in fact, suffered an unbearable stress because the proximity of its peak absorbance wavelength to the peak emission wavelength of the UV-C lamps. More than 90% of reduction in chelates content was, in fact, registered after only 30 minutes of UV-C irradiation by adding 0.59 mM $H_2O_2$. In spite of that, 55% and 67% of reduction of the chelates available for the reaction was registered after two hours under irradiation with UV-A and Xe lamps by adding 0.59 mM $H_2O_2$. The wider range of Xenon lamp emission wavelength than UV-A lamps was responsible of the higher instability produced in the chelates solution during the exposure. Finally, to ensure as long as possible the preservation of the chelates and the subsequent catalytic activity of the solution, UV-A irradiation could be recommended.

## 6.7 Appendix

Applied Catalysis B: Environmental 179 (2015) 372–379

Contents lists available at ScienceDirect

Applied Catalysis B: Environmental

journal homepage: www.elsevier.com/locate/apcatb

# Study of Fe(III)-NTA chelates stability for applicability in photo-Fenton at neutral pH

Antonella De Luca[a,*], Renato F. Dantas[b], Santiago Esplugas[a]

[a] Department of Chemical Engineering, University of Barcelona, Martí i Franquès 1, 08028 Barcelona, Spain
[b] School of Technology, University of Campinas, Paschoal Marmo 1888, 13484332 Limeira, Brazil

ARTICLE INFO

*Article history:*
Received 6 February 2015
Received in revised form 7 May 2015
Accepted 12 May 2015
Available online 14 May 2015

*Keywords:*
Chelating agent
NTA
Iron
Neutral pH
Stability
AOPs

ABSTRACT

The stability of ferric nitrilotriacetate chelates (Fe(III)-NTA) was studied under thermal, oxidative and photochemical stress. The knowledge of chelate stability is fundamental to correctly implement the management system of wastewater treatment plant for application of chelates as catalyst in photo-Fenton process at neutral pH. Fe(III)-NTA solution stability was monitored under different temperature conditions ($T$ = 10–30 °C), in presence and absence of UV-A irradiation and by adding three different concentrations of $H_2O_2$. The additional effect on chelate stability caused by different irradiation source (UV-A, UV-C and Xenon lamps) was also evaluated. Although the complexes were stable under the temperature test range, temperature control is crucial when stressing the solution by irradiation or by adding hydrogen peroxide. The solution was kept stable during two hours of reaction under UV-A irradiation only when temperature was set at 10–15 °C while in presence of hydroxyl radicals (HO•) the temperature control could only reduce the chelates decomposition. Fe(III)-NTA solution mineralization could be obtained under irradiation and radical strain. Thus, the production of organic radical from free ligands was also demonstrated. Finally, the suitableness of UV-C lamps as light source for the process application was questioned since they caused a strong degradation of the chelate solution. Indeed, only 30 min of UV-C irradiation by adding 0.59 mM of hydrogen peroxide caused almost 90% reduction of the chelate content in the solution.

# 7 Effect of water composition on iron chelate based photo-Fenton process efficiency

## 7.1 Introduction

The effectiveness of chelate based photo-Fenton like at neutral and circumneutral pH in recalcitrant compounds removal has been already corroborated by the results showed in the previous chapters. The main operational parameters that influence the stability of the chelate solution, that means the removal efficiency of the treatment, have been also analyzed. UV-A irradiation has been identified as the best light source to carry out the treatment. In fact, the possibility of ensure ferric ion reconversion into ferrous ion and the capability to enhance the Fenton like reaction while safeguarding the lifetime of the chelates make UV-A light the good compromise required for the treatment.

Nevertheless, the results showed in the previous chapters keep assuming the hallmarks of theoretical results if overlooking the effect that the water composition could provoke on the global efficiency. The presence in the treating solution of other cationic species, the carbonate and bicarbonate content and the natural organic matter are in fact elements that cannot be ignored. In this chapter the effect of the initial water quality on the development of the treatment has been evaluated. At this purpose, several natural aqueous matrixes have been spiked with the target compound (SMX) and treated by means of Fe(III)-NTA based photo-Fenton like at circumneutral pH. The natural aqueous water matrixes chosen for this study (tap water, secondary effluent from municipal wastewater treatment plant, well water) were significantly different in terms of initial composition in order to better determine their influence in the treatment. The experiments have been also carried out in Milli-Q water for an easier comparison.

Additionally, with the intention of making the study more realistic in terms of possible real application, the chelating process was carried out separately from the treating solution and then spiked just before the treatment. In the previous studies, the chelating process was carried out directly in the solution to be treated. In large scale treatment unit, this should be obtained by adding iron and the chelating agents in the solution, adjusting the pH and then waiting a reasonable time to ensure the proper formation of the iron chelate. This process would significantly increase the volume required for the unit of treatment and increase the amount of reagents required to control the pH. The intention of find out a modified treatment in order to overcome the large amount of reagent needed for pH adjustment and to reduce the process' cost would be completely vanished. The suitability of the iron chelate solution to be stored within at least 9 days has been already demonstrated in the Chapter 6. Avoiding carry out the chelation directly inside the treating solution and adding it as reagent before the treatment could then ensure an easier management of process. Moreover, this strategy gives an additional benefit related to the effectiveness of the process. In fact, avoiding the contact of the chelating agent with the others cationic species in the solution could limit the competition for chelation.

Some strategies to enhance the effectiveness of the treatment were also considered. Keeping longer iron chelates stable under the attack of radicals and photons could determine better performance if considering the global effect on SMX removal and iron sludge production. In this chapter, the results obtained when dosing the iron chelate solution over reaction, to reduce the exposition to the oxidative and photochemical stress, are also discussed. The addition of $Mn^{2+}$ for mediated photo-Fenton like at circumneutral pH catalyzed by Fe(III)-NTA chelates was also investigated. Moreover, the possibility to enhance the process by applying a selective oxidation of the target compound was also considered. Hydrogen peroxide was substituted by persulfate when treating SMX in Milli-Q water in order to study its possible activation by iron chelate under UV-A irradiation.

## 7.2 Sample preparation and experimental setup

Ferric ion solution 35.8 mM was prepared fresh daily dissolving anhydrous $FeCl_3$ in 0.1 M HCl to minimize iron(III) hydrolysis and polymerization (Flynn 1984). Iron chelate solution 1.79 mM of $Fe^{3+}$ was prepared by mixing the ferric ion solution with a solution 2.68 mM of NTA in Milli-Q water (1.5:1 NTA:Fe). After approximately 15 minutes of stirring, the pH solution was slowly adjusted to 8.0 to allow the chelating agent's dissolution. The treating solution was then prepared by adding SMX in concentration of 0.079 mM (20 mg $L^{-1}$, TOC= 12.3 mg $L^{-1}$, COD= 25.2 mg $L^{-1}$) in the aqueous matrix used to carry out the experiments (Milli-Q water, tap water, secondary effluent from wastewater treatment plant, well water). Before treatment, 100 mL of chelate solution was added to ensure a concentration of iron of 0.089 mM (5 mg $L^{-1}$ of $Fe^{3+}$ as Fe(III)-NTA). Hydrogen peroxide was then added in concentration of 0.294 mM (10 mg $L^{-1}$) immediately before to start the experiment.

To perform the experiment with dosage of iron chelate, to limit the dilution of the treating volume, a more concentrated iron chelate solution was prepared. The methodology followed for the preparation was the same described before. At this purpose, ferric ion solution 71.6 mM in 0.1 M HCl was prepared. Thus, iron chelate solution 3.58 mM of $Fe^{3+}$ was prepared by mixing ferric ion solution with 5.37 mM NTA (1.5:1 NTA:Fe). The scheme of iron dosage over reaction is showed in Figure 41:

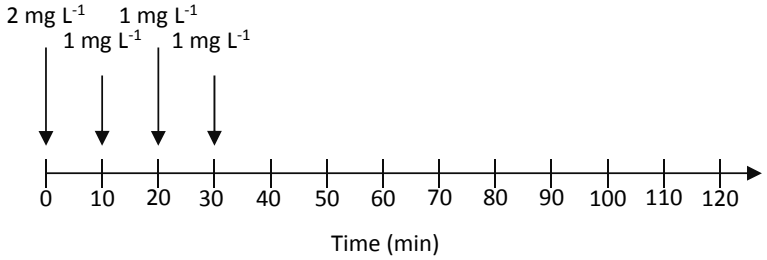


**Figure 41 Iron chelate dosage scheme**

In the experiment in which hydrogen peroxide was substituted with persulfate, the same molar concentration of oxidant was added to the solution (0.294 mM $S_2O_8^{2-}$ corresponding to 70 mg $L^{-1}$).

For the $Mn^{2+}$_mediated photo-Fenton like catalyzed by Fe(III)-NTA, $Mn^{2+}$ as $MnSO_4 \cdot H_2O$ was added in molar ratio of 0.5:1 Mn:Fe (0.047 mM of $Mn^{2+}$ corresponding to 2.45 mg $L^{-1}$). The

rationale of adopting this molar ratio lies in the theoretical amount of NTA free for chelation. In fact, being 1:1 the stoichiometric NTA:Fe molar ratio for chelation, it can be assumed that the a $Mn^{2+}$ content respecting the 0.5:1 Mn:Fe was the exact stoichiometric molar concentration of Mn(II)-NTA chelate of possible formation.

All the Photo-Fenton like experiments were performed under UV-A irradiation. At this purpose the experimental device used to carry out the experiment was the UV-A Photo-reactor described in the Chapter 3 (Section 3.3.1).

In Table 21 are summarized the experimental condition adopted for the experiments:

**Table 31 Operating condition adopted in Photo-Fenton like at circumneutral pH for SMX removal**

| | V (L) | T (°C) | $[SMX]_0$ | $[H_2O_2]_0$ | $[S_2O_8^{2-}]_0$ | $[Fe^{3+}]$ 1.5:1 NTA:Fe | $[Mn^{2+}]$ 0.5:1 Mn:Fe |
|---|---|---|---|---|---|---|---|
| **UV-A/$H_2O_2$/FeNTA** | 2 | 25 | 0.079 mM (20 mg $L^{-1}$) | 0.294 mM (10 mg $L^{-1}$) | - | 0.089 mM (5 mg $L^{-1}$) | - |
| **UV-A/$H_2O_2$/$FeNTA_{dosed}$** | 2 | 25 | 0.079 mM (20 mg $L^{-1}$) | 0.294 mM (10 mg $L^{-1}$) | - | Total 0.089 mM (5 mg $L^{-1}$) | - |
| **UV-A/$H_2O_2$/FeNTA_$Mn^{2+}$** | 2 | 25 | 0.079 mM (20 mg $L^{-1}$) | 0.294 mM (10 mg $L^{-1}$) | - | 0.089 mM (5 mg $L^{-1}$) | 0.047 mM (2.46 mg $L^{-1}$) |
| **UV-A/PS/FeNTA** | 2 | 25 | 0.079 mM (20 mg $L^{-1}$) | - | 0.294 mM (70 mg $L^{-1}$) | 0.089 mM (5 mg $L^{-1}$) | - |

The four aqueous matrixes spiked with the target compound derived from different sources and were characterized by different values of the main water quality's parameters. In Table 32 are indicated the most important parameter of characterization of the aqueous solutions used for the study:

**Table 32 Aqueous matrixes characterization.**

| | Milli-Q (MQ) | Tap water (TW) | Wastewater (WW) | Well water (HW) |
|---|---|---|---|---|
| **Origin** | Merk-Millipore | Barcelona (Catalunya, Spain) | WWTP Calafell (Catalunya, Spain) | Pacs del Penedès (Catalunya, Spain) |
| **pH** | 5.3 | 7.5 | 7.4 ± 0.02 | 7.9 |
| **NPOC (mg $L^{-1}$)** | «1 | 3.7± 2.9 | 7.2 ± 1.7 | 1.6± 0.7 |
| **IC (mg $L^{-1}$)** | «1 | 31.6± 4.1 | 78.7 ± 5.1 | 35.5± 0.6 |
| **TN (mg $L^{-1}$)** | «1 | 1.8± 0.6 | 22.7 ± 15.1 | 22.4± 0.4 |
| **$Na^+$ (mg $L^{-1}$)** | «1 | 66.7 ± 40.1 | 392.2 ± 35.7 | 41.3 ± 9.5 |
| **$NH_4^+$ (mg $L^{-1}$)** | «1 | <LOD | 20.1 ± 28.5 | <LOD |
| **$K^+$ (mg $L^{-1}$)** | «1 | 11.9 ± 6.6 | 22.9 ± 0.4 | 1.4 ± 1.4 |
| **$Ca^{2+}$ (mg $L^{-1}$)** | «1 | 35.7 ± 6.9 | 71.5 ± 11.2 | 55.9 ± 0.9 |
| **$Mg^{2+}$ (mg $L^{-1}$)** | «1 | 16.2 ± 5.1 | 59.7 ± 8.5 | 66.4 ± 2.7 |
| **Alkalinity ($mg_{CaCO3}$ $L^{-1}$)** | «1 | 143.29 ± 16.2 | 209.7 ± 14.2 | 158.6± 2.8 |

## 7.3 Results and discussions

### *7.3.1 Effect of the water composition*

In order to compare the influence of the water composition on the efficiency of the process, the same treatment was applied for treating four different water solutions. Carry out the

chelating process separately from the solution to be treated, represents an useful tool to correctly evaluate this effect. Thus, the competition for the chelating agents due to the presence of other cationic species can be then neglected in this step and limited at the phase of treatment. Despite this, after the addition of the volume of chelate solution required to reach the desired catalyst concentration, the chelated central cation can equally be exchanged. In Table 33 are listed the real initial $Fe_{tot}$ concentrations (as Fe(III)-NTA) achieved after addition of the chelate solution in the treating volume:

**Table 33 $Fe_{tot}$ initial concentration as Fe(III)-NTA after adding the iron chelate solution to the treating solution**

| | $Fe_{tot,0}$ [mg $L^{-1}$] |
|---|---|
| **Milli-Q (MQ)** | 4.6 |
| **Tap water (TW)** | 4.6 |
| **Wastewater (WW)** | 2.6 |
| **Well water (HW)** | 2.8 |

It appears evident, that even improving the chelating process, the competition exhibited by other ionic species present into the solution cannot be completely avoided. Thus, chelates of other ion species can be eventually formed. Between the four, wastewater and well water were, in fact, the two matrixes characterized by the highest content in ions of $Ca^{2+}$ and $Mg^{2+}$. Therefore, these two matrixes exhibited the lower Fe(III)-NTA content after adding iron chelate solution to the treating volume.

After the addition of $H_2O_2$, UVA light was switched on. Photo-Fenton like reaction started to take place in the four aqueous matrixes and the SMX degradation was obtained following the trend observable in Figure 42(a)).

SMX degradation occurred faster in Milli-Q water, then in tap water and significantly slower in well water and wastewater (almost 10 times slower), as it is also observable from the calculated pseudo-first order kinetic constants ($k_{obs}$). These assumed the value of $(1.46\pm0.29) \times 10^{-2}$ $min^{-1}$, $(7.91\pm1.00) \times 10^{-3}$ $min^{-1}$, $(4.26\pm0.60) \times 10^{-3}$ $min^{-1}$, $(3.84\pm1.52) \times 10^{-3}$ $min^{-1}$ respectively when treating SMX in Milli-Q water, tap water, well water and wastewater.

By correlation of the experimental results obtained, it is possible to observe that the faster kinetic rates correspond to the reactions occurring in the solution in which the initial iron content was higher (Figure 42(b)). In fact, in the case of Milli-Q water and tap water, higher $H_2O_2$ consumption was also observed after 120 minutes of reaction. The higher production of radicals was not only observable in terms of SMX degradation but also in the chelates decomposition. In fact, after 45 minutes of irradiation a gradual iron loss was observed in Milli-Q water. The same effect started a little before in tap water, which the curve of iron content showed the same slope than in Milli-Q water. This experimental evidence shows as, under the same condition of stress, the iron chelate decomposition follows a similar trend.

On the other hand, in well and wastewater, which showed the lowest reaction rates in term of SMX removal, no significant iron lost was observed within 120 minutes of reaction. At that time, almost 25% of the initial content of $H_2O_2$ was still remaining into the solution.

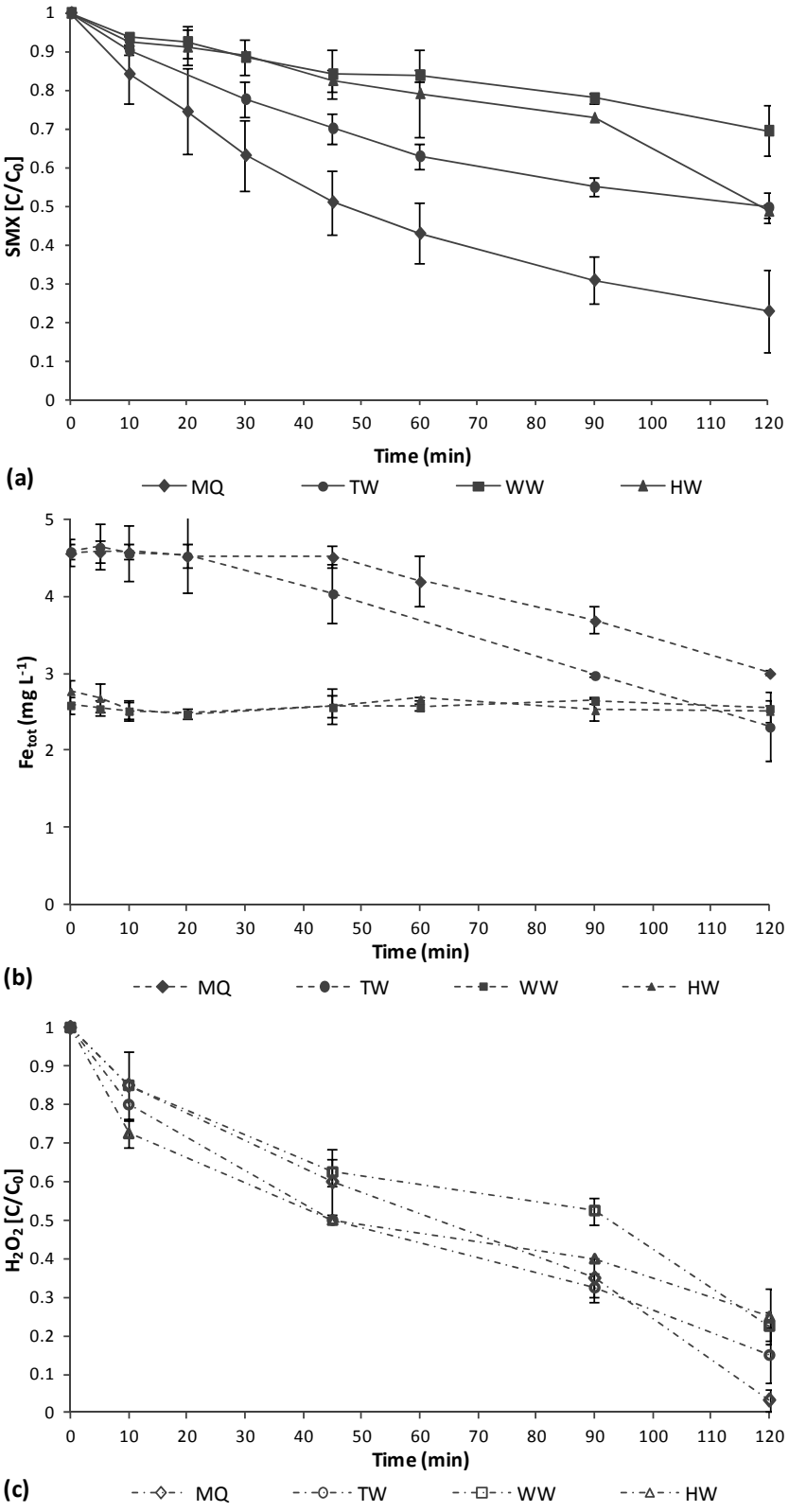


**Figure 42 (a) SMX removal by photo-Fenton like at circumneutral pH catalyzed by Fe(III)-NTA chelates (NTA:Fe=1.5:1); (b) trend of Fe content over reaction; (c) $H_2O_2$ consumption.**

However, Figure 42(c) also shows as, the kinetics rates exhibited in $H_2O_2$ consumption do not show a real correlation to what obtained in terms of SMX removal. In fact, when treating the contaminant in wastewater and well water, SMX degradation was significantly lower and the

breakage of the chelates almost null. In spite of that, the $H_2O_2$ consumptions showed a tendency analogue to what observed in tap and Milli-Q water. This result can be better understood if taking into consideration the specific quality of each matrix spiked with the contaminant. Wastewater was the matrix characterized by the highest alkalinity and organic matter content. Thus, considering the rate constant for reaction of the reactive species in solution, the scavenging effect operated by the carbonate species on the hydroxyl radicals can be easily understood (Table 34). Moreover, the higher content in organic matter in wastewater could have contributed in the formation of other iron chelates species photo chemically inactive. Then, their contribution in radical production was null while limiting the loss of the iron content. Concerning well and tap water, in this case the contribution of the carbonates content in the scavenging well effect of the radicals might be almost comparable. The two matrixes, in fact, are characterized by an almost equal alkalinity while tap water was also characterized by a higher content of organic matter. However SMX removal was significantly lower when treated in well water. The lower efficiency in SMX degradation in the case of well water would be then rather imputable to the lower content in iron chelates.

**Table 34 Constant rate for reaction with HO· of the main species present in the solution**

| | $K_{HO\cdot}$ ($M^{-1} s^{-1}$) | |
|---|---|---|
| **SMX** | $3.70 \times 10^9$ | (Lam and Mabury 2005) |
| **Fe(III)-NTA** | $1.60 \times 10^8$ | (Buxton et al. 1988) |
| **Fe(II)-NTA** | $5.0 \times 10^9$ | (Buxton et al. 1988) |
| **NTA** | $5.50 \times 10^8$ | (De Laat et al. 2011) |
| **$CO_3^{2-}$** | $3.90 \times 10^8$ | (Buxton et al. 1988) |
| **$HCO_3^-$** | $8.50 \times 10^6$ | (Buxton et al. 1988) |
| **NOM** | $1.9 \times 10^4$ to $1.3 \times 10^5$ $(mg\ L^{-1})^{-1} s^{-1}$ | (Peyton et al. 1998) |

Additionally, the results in Figure 42(b) shows as, when iron loss was registered, the beginning of the iron chelate decomposition coincided with a change in the degradation rate of the target contaminant. In Table 35 are summarized the percentages of SMX removal, iron loss and hydrogen peroxide consumption, together with the data of pH and pseudo first-order rate constant in the considered aqueous matrixes:

**Table 35 Fe(III)-NTA based photo-Fenton like at circumneutral pH: experimental results**

| | $pH_0$ | $pH_f$ | SMX | $k_{obs}$ | $Fe_{lost}$ | $H_2O_{2,cons}$ |
|---|---|---|---|---|---|---|
| | - | - | % | $min^{-1}$ | % | % |
| **MQ** | 7.35±0.17 | 6.61±0.92 | 77.1 | $(1.46\pm0.29) \times 10^{-2}$ | 34.1 | 96.7 |
| **TW** | 7.21±0.06 | 7.35±0.08 | 50.3 | $(7.91\pm1.00) \times 10^{-3}$ | 49.6 | 85.0 |
| **WW** | 7.33±0.10 | 7.49±0.06 | 30.5 | $(3.84\pm1.52) \times 10^{-3}$ | 1.6 | 77.5 |
| **HW** | 7.39±0.01 | 7.20±0.04 | 51.2 | $(4.26\pm0.60) \times 10^{-3}$ | 9.2 | 75.0 |

These results remark the importance of keeping soluble the reaction's catalyst the longer as possible. In the previous chapters it has been also demonstrated as the resistance of the chelate solution under oxidative and photochemical stress does not persist until the complete hydrogen peroxide consumption. Some strategies could be then adopted in order to extend the lifetime of the chelates. Dosing the addition of chelate solution over reaction could represent an useful strategy to extend the durability of the chelates. Depending of the dose, a

slower reaction rate would be eventually expected but the possibility to limit iron precipitation and the amount of sludge produced could be equally attractive.

### *7.3.2 Iron chelate dosage*

In order to extend the stability of the chelate solution, a strategy to reduce the exposition under oxidative and photochemical stress was developed. Thus, dosage of chelate solution was performed when treating SMX in the water matrixes considered in this chapter. The scheme of iron chelate dosage has been already shown in Figure 41.

Figure 43 shows the degradation curve of SMX exhibited in tap water when adding iron chelate solution in one unique addition and when dosing the chelates as by scheme represented before. Iron content as Fe(III)-NTA during the reaction is also showed. As it is possible to observe, when dosing over reaction the iron chelate solution, at the beginning, the reaction rate showed a slower kinetic than when added entirely in one unique dose. On the other hand by dosing Fe(III)-NTA, around 45 minutes of reaction, it was possible to achieve higher concentration of iron. Then, the kinetic of SMX removal also showed a significant increment. However, though the concentration of iron after 120 minutes of reaction was higher by almost 1 mg $L^{-1}$ than in the case of the unique addition, the kinetic rate of SMX removal showed a more drastic decrease. This result can be probably explained considering the decomposition of hydrogen peroxide, which showed a completely analogue tendency in the two experiments (Figure 44).

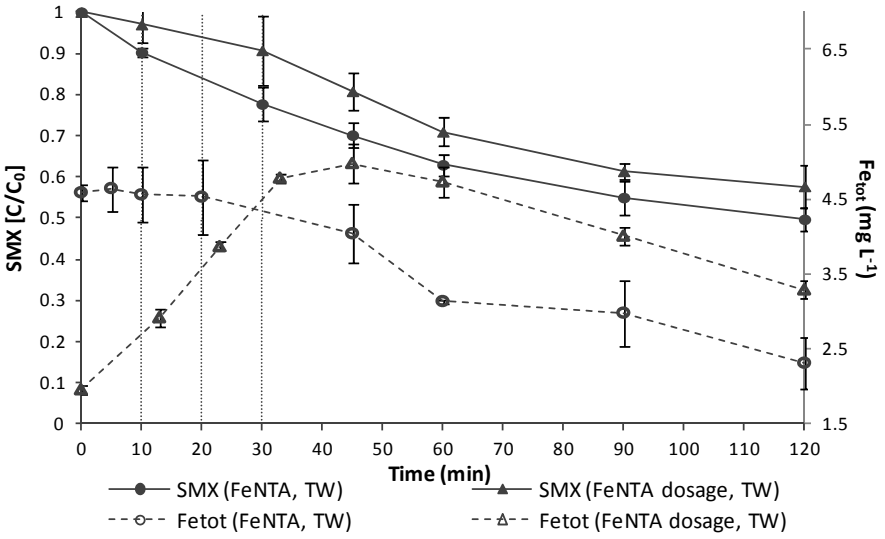


**Figure 43 SMX removal in tap water by photo-Fenton like at circumneutral pH with Fe(III)-L chelates (NTA:Fe=1.5:1) by unique addition ($pH_0$=7.21±0.06, $pH_f$=7.35±0.08) and by chelate dosage ($pH_0$=7.39±0.12, $pH_f$=7.33±0.16) with trend of iron content.**

After the achievement of the concentration's peak of iron chelate (around 45 minutes of reaction), the chelate solution showed a reduction in iron content following exactly the tendency of the experiment with unique addition of chelates (curves almost parallels). This result points out the effect of the iron chelate breakage which, as showed in Chapter 6, seems to follow a specific kinetic for the experimental condition adopted.

In the first 10 minutes of reaction, $H_2O_2$ consumption followed the same trand for both the two different strategies of iron chelate addition. Afterwards, the consumption decreased in the experiment where iron chelate solution was dosed. Due to the higher content of catalyst available for the decomposition reaction, the kinetic of hydrogen peroxide consumption would have been expected to be higher in iron chelate dosage. However, this showed to be slightly slower.

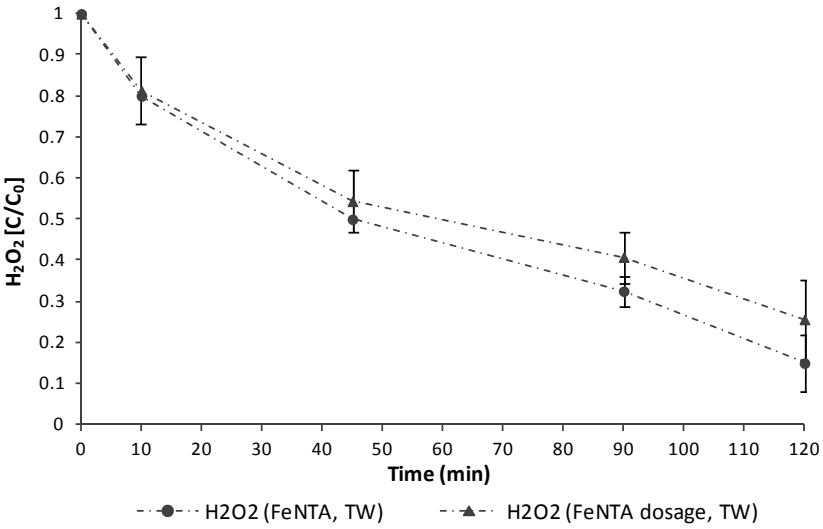


**Figure 44 Trend of $H_2O_2$ consumption over reaction when treating SMX in tap water by means of photo-Fenton like at circumneutral pH catalyzed by Fe(III)-NTA chelates (NTA:Fe=1.5:1)**

The same strategy was also applied when treating SMX in secondary effluent from (WWTP). In this case, when dosing the iron chelate addition, in the first 30 minutes of reaction an increment of the iron content was observed and a peak in concentration was achieved around 35 minutes. Nevertheless, no significant improvement was registered. Moreover, iron chelate started to quickly decompose after the achievement of the highest concentration. Around 60 minutes from the beginning of the experiment, the iron chelate decomposition slowed down. Thus, the concentration of iron available to catalyze Fenton like reaction settled at lower values than in the case of the single addition of Fe(III)-chelates (Figure 45).

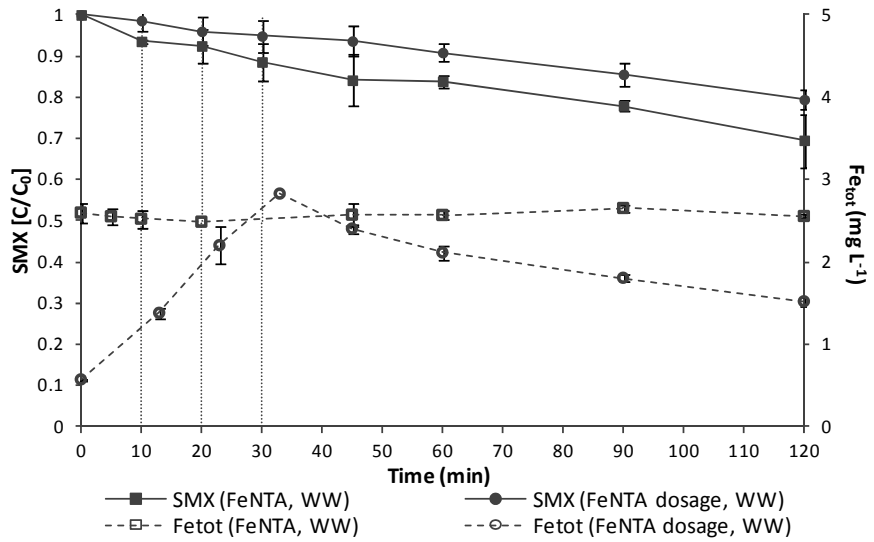

**Figure 45 SMX removal in secondary effluent form WWTP by photo-Fenton like at circumneutral pH with Fe(III)-L chelates (NTA:Fe=1.5:1) by unique addition ($pH_0$=7.21±0.06, $pH_f$=7.35±0.08) and by chelate dosage ($pH_0$=7.92±0.05, $pH_f$=7.70±0.02) with trend of iron content.**

No enhancement in term of SMX removal was achieved when dosing the iron chelate solution. Moreover, since no significant difference in term of iron chelates content was observable when adopting the two different strategies, no change in the kinetic rate of SMX removal could be either observed. Concerning the hydrogen peroxide consumption, this showed a tendency completely comparable in the case of the two different strategies (Figure 46).

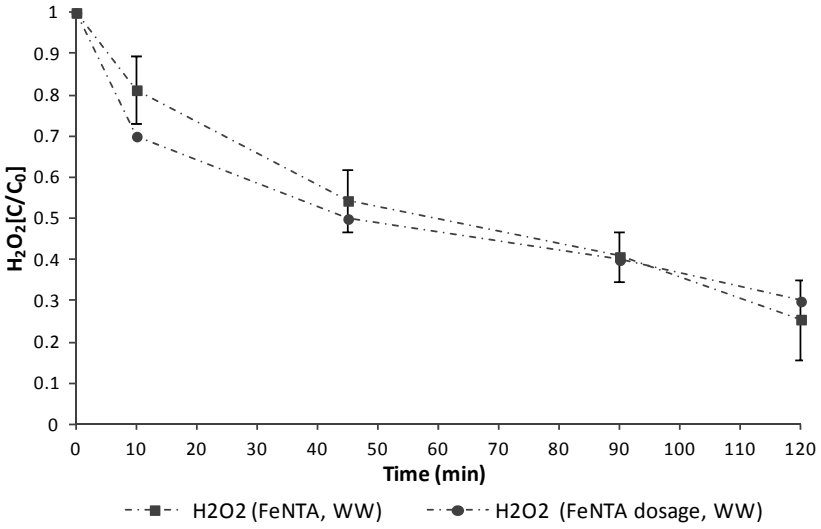


**Figure 46 Trend of $H_2O_2$ consumption over reaction when treating SMX in secondary effluent from WWTP by means of photo-Fenton like at circumneutral pH catalyzed by Fe(III)-NTA chelates (NTA:Fe=1.5:1).**

More in detail, in the first minutes of reaction (30-40 minutes), due to the higher content in iron chelate, the decomposition's kinetic was slightly higher in the case of the single addition of iron chelate solution. Afterwards, the decomposition kept following the same kinetic rate and no significant difference of $H_2O_2$ was observable at the end of the experiment. These results demonstrate that the enhancement of SMX removal achievable by dosing iron chlate solution is limited (in the configuration considered in this study) by the presence of high contents of carbonates and organic matter.

When treating SMX in well water, the results were more characteristic. Figure 47 shows as the strategy of iron chelate dosage was successful to overcome the competition for chelation established by the presence of the high content in ionic species. After 30 minutes of reaction, in fact, the iron content as Fe(III)-NTA overcome the value of 4.5 mg $L^{-1}$. However, this enhancement of chelate concentration available to catalyze Fenton like reaction was not replicated in SMX removal efficiency. No additional SMX removal was in fact observable after 120 minutes of reaction (Figure 47).

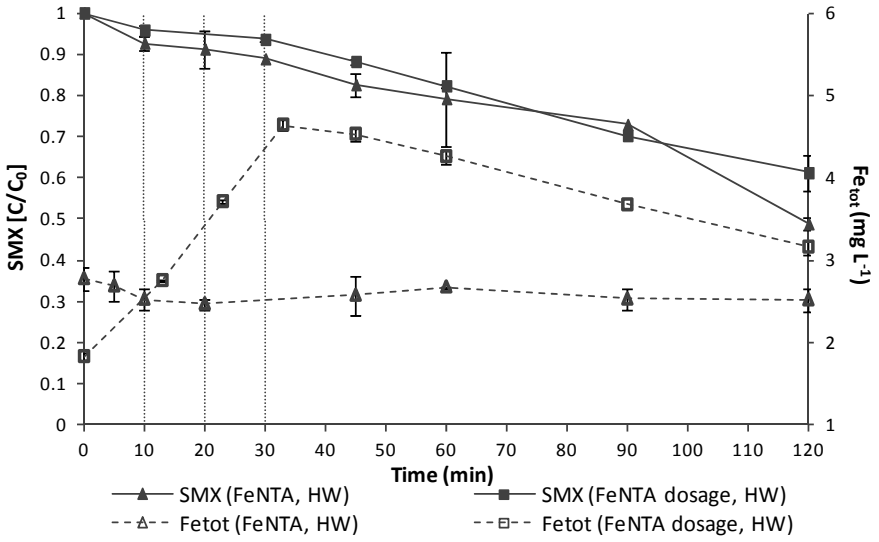


**Figure 47 SMX removal in well water by photo-Fenton like at circumneutral pH with Fe(III)-L chelates (NTA:Fe=1.5:1) by unique addition ($pH_0$=7.39±0.01, $pH_f$=7.20±0.04) and by chelate dosage ($pH_0$=7.45±0.14, $pH_f$=7.46±0.14) with trend of iron content.**

Similarly, the trend showed by the curve of hydrogen peroxide decomposition was exactly the same for both the adopted strategy (Figure 48).

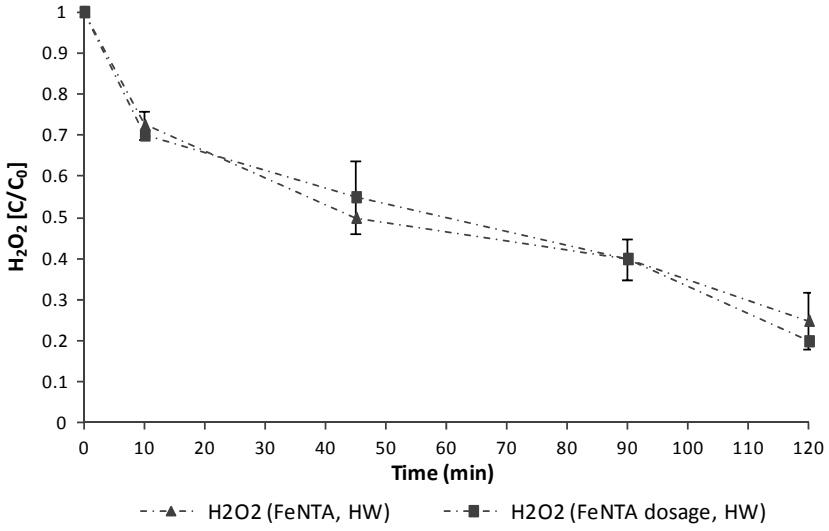


**Figure 48 Trend of $H_2O_2$ consumption over reaction when treating SMX in well water by means of photo-Fenton like at circumneutral pH catalyzed by Fe(III)-NTA chelates (NTA:Fe=1.5:1).**

In Table 36 are summarized the essential results of the comparison between iron addition strategies in the water matrixes considered in this study. For the experiment with dosage of iron chelate solution, the percentage of iron lost is calculated by the highest concentration achieved.

**Table 36 Strategies of iron chelate dosage Fe(III)-NTA based photo-Fenton like at circumneutral pH: experimental results.**

| | | $pH_0$ - | $pH_f$ - | SMX % | $k_{obs}$ $min^{-1}$ | $Fe_{lost}$ % | $H_2O_{2,cons}$ % |
|---|---|---|---|---|---|---|---|
| **TW** | Fe(III)-NTA Single addition | 7.21±0.06 | 7.35±0.08 | 50.3 | (7.91±1.00) x $10^{-3}$ | 49.6 | 85.0 |
| | Fe(III)-NTA dosage | 7.39±0.12 | 7.33±0.16 | 42.3 | (5.67±0.88) x $10^{-3}$ | 33.9 | 74.4 |
| **WW** | Fe(III)-NTA Single addition | 7.33±0.10 | 7.49±0.06 | 30.5 | (3.84±1.52) x $10^{-3}$ | 1.6 | 77.5 |
| | Fe(III)-NTA dosage | 7.92±0.05 | 7.70±0.02 | 20.6 | (2.70±0.79) x $10^{-3}$ | 46.3 | 70.0 |
| **HW** | Fe(III)-NTA Single addition | 7.39±0.01 | 7.20±0.04 | 51.2 | (4.26±0.60) x $10^{-3}$ | 9.2 | 75.0 |
| | Fe(III)-NTA dosage | 7.45±0.14 | 7.46±0.14 | 38.8 | (3.13±0.06) x $10^{-3}$ | 31.9 | 80.0 |

Finally, as already showed in Chapter 5, with the experimental condition adopted in this study, no significant effect in mineralization could be observed.

### *7.3.3 Fe(III)-NTA driven persulfate activation and other strategies for SMX removal in Milli-Q water*

The effectiveness of Fe(III)-NTA chelates based Photo-Fenton like for SMX removal has been largely demonstrated in the previous chapters. However, the removal efficiency could be still enhanced. At this purpose, some additional strategies were assessed in order to find out the possible modification of the process.

It has been already described as several parameters are able to influence the effectiveness of the process. Between them, the presence of other ionic specie plays a key role. In fact, though the stability constant for chelation of $Ca^{2+}$ and $Mg^{2+}$ with NTA are significantly lower than with $Fe^{3+}$, high content of these species in solution can equally compromise the chelation process through the establishment of a competition kinetic. Complexes as Ca(II)-NTA and Mg(II)-NTA do not show activity in catalyzing $H_2O_2$ to generate highly active oxidants (Li et al. 2016). However, other competing metal ions could show catalytic activity in radical production. Li et al. (2016) showed as the presence of $Mn^{2+}$ together with Fe(III)-NTA resulted in more than 99% of crotamiton (CRMT) removal after 15 minutes of reaction respect the 10 % obtained when in presence of the only Fe(III)-NTA (Li et al. 2016). From this study, it can be deduced as the mixture of Fe(III)-NTA and Mn(II)-NTA complexes showed significant spectral changes after the addition of $H_2O_2$. The absorbance profile, in fact, extended to the visible light region (e.g., starting from 380 nm versus 500 nm before and after the addition of $H_2O_2$), and also showed a large decrease in UV absorbance. The results suggested that new compounds were formed from the mixture of Fe(III)-NTA and Mn(II)-NTA complexes in the presence of $H_2O_2$ which were supposed to be responsible of the observed enhancement in efficiency. It was also proven that the new species chelate catalyzed the production of $O_2{\cdot}^-$.

Another strategy that could represent an useful implemented tool to enhance the efficiency of the process is to exchange the Fenton's oxidant ($H_2O_2$) for $S_2O_8^{2-}$ (PS) which allows the

combined production of sulfate and hydroxyl radicals. The high oxidation potential of sulfate radicals together with their selective oxidation could bring to better efficiency in terms of SMX removal. However, though the possibility of catalyze the decomposition of PS by means of iron chelate has been already discussed in the introduction, the radical production will be surely reduced by the presence of the transition metal in the chelate form. A strong increase of radical production by irradiation cannot be equally expected. In fact, the molar extinction coefficients of PS at 248, 308, and 351 nm are 27.5 ± 1.1, 1.18 ± 0.05, and 0.25 ± 1.01 $mol^{-1}$ $cm^{-1}$, respectively, suggesting the high energy of short wavelength UV (Herrmann 2007). The radical production under UV-A irradiation would result particularly reduced.

In Figure 49 are shown the experimental results obtained by applying the strategies previously described for SMX removal in Milli-Q water. These results can be easier explained by looking at the most significant data summarized in Table 37.

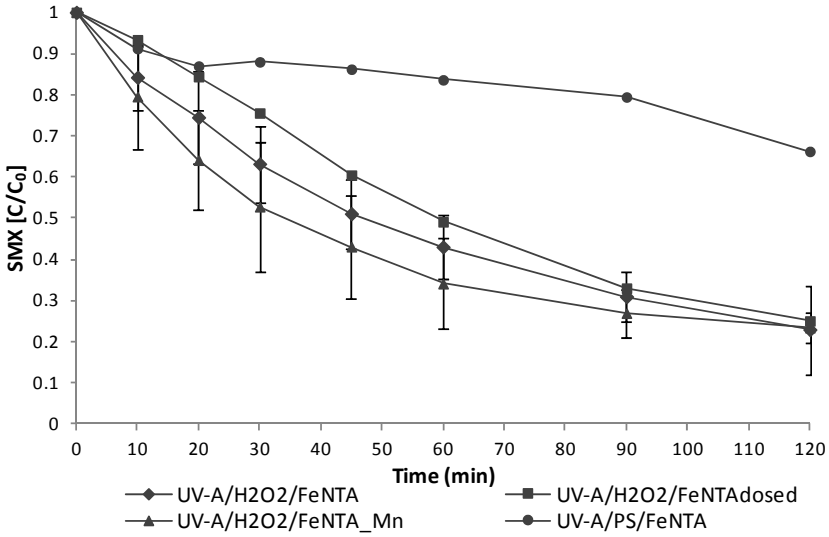


**Figure 49 SMX removal in Milli-Q water by four different configurations of photo-Fenton like at circumneutral pH with Fe(III)-L chelates in molar ratio NTA:Fe=1.5:1. UV-A/$H_2O_2$/FeNTA ($pH_0$=7.35±0.17, $pH_f$=6.61±0.92), UV-A/$H_2O_2$/$FeNTA_{dosed}$ ($pH_0$=7.56, $pH_f$=5.88), UV-A/$H_2O_2$/$FeNTA\_Mn^{2+}$ ($pH_0$=7.34±0.14, $pH_f$=5.86±0.51), UV-A/PS/FeNTA ($pH_0$=7.4, $pH_f$=3.66).**

It can be observed as when applying UV-A/PS/FeNTA low efficiency in term of SMX removal could be obtained (only 28% of SMX removal was obtained after 120 minutes of reaction). Though the initial rate for reaction (6.99 x $10^{-3}$ $min^{-1}$) was almost comparable to what obtained in the other experiments, the final SMX removal percentage was not really significant if compared with the others. This result was quite predictable if taking into consideration the aspects previously remarked. Since iron in chelated form is not as reactive as the free ion, the catalytic effect in PS decomposition is obviously reduced. Moreover, due to the much lower molar extinction coefficient than under UV-C irradiation, UV-A irradiation cannot ensure a proper PS activation. However, at it has been also described in Chapter 6, UV-C irradiation strongly compromises the stability of iron chelate. Thus, UV-C irradiation does not represent a favorable source of irradiation when employing iron chelates. On the other hand, iron chelate stability resulted compromised since the beginning of the reaction showing a probably higher reactivity with $SO_4^{\cdot -}$ radicals (Figure 50). Nevertheless, the low radical production resulted in a final iron loss percentage not higher than in the other experimental conditions (32.7%).

The results obtained when applying UV-A/$H_2O_2$/FeNTA by single addition or by dosage of the iron chelate solution appear rather comparable. A first step can be identified in which a slower kinetic was exhibited by SMX removal during iron chelate dosage (8.48 x $10^{-3}$ $min^{-1}$ while (2.20±0.82) x $10^{-2}$ $min^{-1}$ in case of the single addition of catalyst). This result is easily explained if considering the initial lower content of iron in the first 30 minutes of reaction. Afterwards, a slight improvement was observed and after 120 minutes of reaction almost the same percentage of SMX removal was obtained (75% when dosing the iron chelate solution and 78% when adding the catalyst at the beginning).

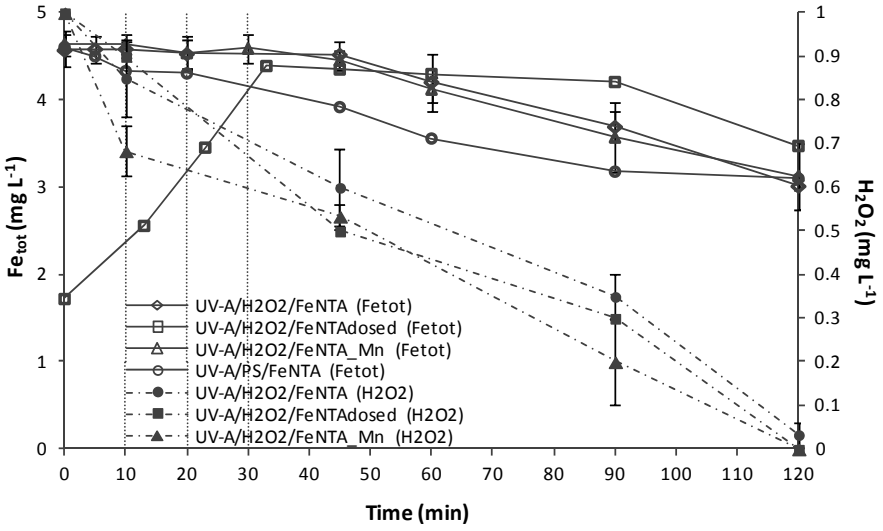


**Figure 50 Trend of iron content and hydrogen peroxide consumption over reaction for SMX removal in Milli-Q water by four different configurations of photo-Fenton like at circumneutral pH with Fe(III)-L chelates in molar ratio NTA:Fe=1.5:1. (UV-A/$H_2O_2$/FeNTA ($pH_0$=7.35±0.17, $pH_f$=6.61±0.92), UV-A/$H_2O_2$/$FeNTA_{dosed}$ ($pH_0$=7.56, $pH_f$=5.88), UV-A/$H_2O_2$/FeNTA_$Mn^{2+}$ ($pH_0$=7.34±0.14, $pH_f$=5.86±0.51), UV-A/PS/FeNTA ($pH_0$=7.4, $pH_f$=3.66)**

Once again, as previously observed when applying this strategy in more complexes aqueous solutions, iron chelate dosage seems to be an useful strategy to extend the lifetime of iron chelates. Nevertheless, this benefit does not have confirmation in terms of contaminant removal.

Finally, adopting $Mn^{2+}$_mediated Photo-Fenton like, a slight improvement in SMX removal was obtained. More considerable was the rate removal exhibited at the beginning of the reaction ((2.20±0.82) x $10^{-2}$ $min^{-1}$), the highest between those registered in the set of experiments carried out in this section. Thus, though the percentage of SMX removal after 120 minutes of reaction did not result significantly enhanced respect to the other experiments, the higher initial rate makes this strategy particularly interesting. The trend showed in iron chelate decomposition and the initial content of iron chelate demonstrated that the presence of $Mn^{2+}$ does not compromise the chelation process of iron. The stability constant for chelation of Fe(III)-NTA is in fact significantly higher than Mn(II)-NTA (log K= 15.87 and 7.44 respectively). Additionally the stoichiometric amount of $Mn^{2+}$ ion added to the solution was not high enough to move the equilibrium of chelating reaction toward an higher formation of Mn(II)-NTA.

The results discussed in this section are now summarized in Table 37:

**Table 37 Fe(III)-NTA based photo-Fenton like at circumneutral pH in Milli-Q water: experimental results**

| | $pH_0$ | $pH_f$ | SMX | $k_{obs}$ | $Fe_{lost}$ | $H_2O_{2,cons}$ |
|---|---|---|---|---|---|---|
| | - | - | % | $min^{-1}$ | % | % |
| **UV-A/$H_2O_2$/FeNTA** | 7.35±0.17 | 6.61±0.92 | 77.1 | (1.46±0.29) x $10^{-2}$ | 34.1 | 97.7 |
| **UV-A/$H_2O_2$/$FeNTA_{dosed}$** | 7.56 | 5.88 | 74.9 | 8.48 x $10^{-3}$ | 20.9 | 95.0 |
| **UV-A/$H_2O_2$/FeNTA_$Mn^{2+}$** | 7.34±0.14 | 5.86±0.51 | 78.1 | (2.20±0.82) x $10^{-2}$ | 32.5 | 100 |
| **UV-A/PS/FeNTA** | 7.40 | 3.66 | 27.9 | 6.99 x $10^{-3}$ | 32.7 | - |

Finally, by carrying out the treatment in all the condition showed in this chapter, any significant mineralization could be achieved.

## 7.4 Conclusions

From this study it results as the quality of the treating solution strongly influences the trend of the reaction. Highest content of competing ions can drastically reduce the efficiency of the chelation process resulting in a minor amount of catalyst available for the Fenton like reaction. On the other hand, alkalinity plays a fundamental role during the treatment, when carbonates species act as scavengers for radicals reactions with the target compounds. Further investigation could be carried out to find a rule able to make predictable the average efficiency obtainable if knowing the quality of the treating water.

- Iron chelate dosage, in Milli-Q water as by the scheme assessed in this study, demonstrated to be useful to extend the lifetime of the chelates (in almost all the real matrixes used as well). This effect was, however, not combined with a higher SMX removal. Nevertheless, the results showed in this section cannot be considered sufficient to exclude the possibility that iron chelate dosage could be successful in improving the efficiency of the process. At this purpose, further investigation would be required to find out the optimum scheme of dosage to reach the combined effect of extending the lifetime of the chelate and enhance the target compound removal.

- UV-A/PS/FeNTA treatment was between all those considered in this study, the one that showed the lowest eficiency in terms of SMX removal. Though, as discussed in the introduction, some studies have demonstrated that chelate driven persulfate activation is possible, under the experimental conditions adopted in this study, the result was not satisfactory. The low concentration of the reagents adopted were probably not enough to ensure the proper persulfate decomposition. Increase production could have been obtained by coupling metal activation and UV irradiation. However, by the intent of extending the lifetime of the chelates, UV-C irradiation should be avoided. On the other hand, persulfate activation is more effective when under UV-C irradiation. Thus, also in this case, further investigation might be carried out in order to find out the optimum conditions to be adopted.

- Finally, $Mn^{2+}$_mediated Photo-Fenton like catalyzed by Fe(III)-NTA chelates was, between the processes considered, the most promising strategy of this study. Even though the enhancement obtained by adding $Mn^{2+}$ was not as resounding as from other studies by literature, higher pseudo-first order constant was exhibited by the

SMX removal curve. The possibility to increase the additional removal percentage should be carefully assessed by modifying the set up parameters adopted.

# 8 Effect of Bromide on the degradation of organic contaminants with UV and $Fe^{2+}$ Activated Persulfate

## 8.1 Introduction

In Chapter 7 has been introduced the possibility to activate persulfate by means of transition metal in the chelate form. It has been largely demonstrated as sulfate radical based AOPs are suitable processes to be applied in recalcitrant compounds treatment.

In this chapter, the results of a study carried out at the University of Cincinnati (Ohio, USA) under the supervision of the Professor Dionysios D. Dionysiou are discussed. The aim of this study was to evaluate the effect of the presence of halide anions as bromide ($Br^-$) and chloride ($Cl^-$) when applying UV and $Fe^{2+}$ activated persulfate (PS) treatment for the removal of recalcitrant organic compounds.

The chosen compounds in this study are benzophenone-4 (BZ4), nitrobenzene (NB), nitrobenzoic acid (NBA), atrazine (ATZ) and ampicillin (AMP), structures of which are shown in Table 38.

**Table 38 Structure of the studied compounds.**

| Benzophenone-4 (**BZ4**, $C_{14}H_{12}O_6S$) | Nitrobenzene (**NB**, $C_6H_5NO_2$) | Nitrobenzoic acid (**NBA**, $C_7H_5NO_4$) |
|---|---|---|
| 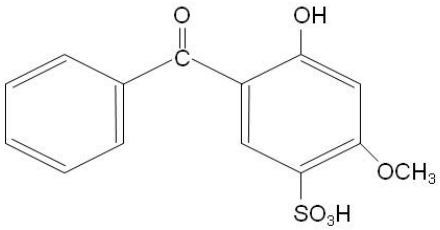 | 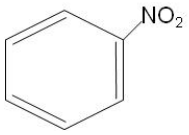 | 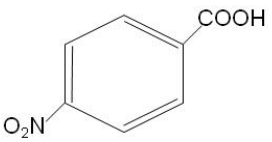 |
| Atrazine (**ATZ**, $C_8H_{14}ClN_5$) | Ampicillin (**AMP**, $C_{16}H_{18}N_3NaO_4S$) | |
| 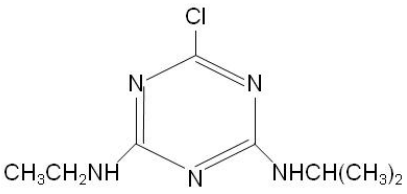 | 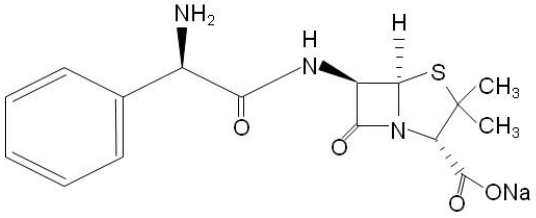 | |

BZ4 is primarily used as an organic UV filter. Because of its wide application, BZ4 can be easily found in the environment after its release through swimming and bathing (Giokas et al. 2007). It has a documented perturbation risk on the ecosystem via interruption of sexual hormone system of fish and other aquatic organisms (Zucchi et al. 2011). NB is a nitrite product of the chemical industry often used in glazing agents or solvents (Agrawal et al. 2011). Several studies published in the last decades have proven the presence of NB in natural environment and organs of many animals and human beings due to oil spills, industrial and municipal effluents (Rimkus et al. 1994; Gatermann et al. 1995). Because of the high toxicity of this compound, the Environmental Protection Agencies (EPAs) of many nations have classified NB as a “pollutant of main concern” (Zhao et al. 2003). NBA is a derivative of benzoic acid employed as a synthetic reagent in industrial applications. Degradation of nitroaromatics may form a group of

compounds showing different levels of toxicity and acting as carcinogens and mutagens (Yinon 1990; Spain et al. 2000). ATZ is an herbicide of the triazine class mainly applied to remove broadleaf and grassy weeds in corn or crops. Agricultural runoff as well as dumped pesticide wastes from pesticide manufacturing industry can both result in the presence of this compound in aquatic systems (Gosh and Philip 2006). Since 2003, atrazine has been banned for agricultural use by EU though its use is still allowed in countries such as China and USA (Bethsass and Colangelo 2006). Over 60 million pounds of atrazine have been applied annually in the United States (Acosta et al. 2004). Persistence of ATZ in the environment makes it a Priority A chemical for potential groundwater contamination by US EPA (US Environmental Protection Agency 1985). AMP is a semi-synthetic penicillin largely used as an antibiotic in human and veterinary medicine (Elmolla and Chaudhuri 2009a). The most significant problem concerning the presence of antibiotics in the environment is probably the development of antibiotic resistant bacteria and pathogens (Walter and Vennes 1985).

These model compounds have different reactivity with hydroxyl/sulfate radicals and thus can represent a wide range of organic contaminants toward the degradation by the studied AOPs in the absence/presence of halides, especially bromide. In this study, we focused on the impact of bromide and chloride on their kinetic removal by UV-254 nm/PS/$Fe^{2+}$. Whether pH is as an efficiency determining factor in this iron catalyzed process was evaluated. The outcome of this study presents useful scientific information on the effectiveness of UV-254 nm/PS/$Fe^{2+}$ on the degradation of various organic compounds, especially in the absence/presence of halides.

## 8.2 Materials and methods

### *8.2.1 Materials*

Major compounds, benzophenone-4 (BZ4) (Fluka), ampicillin (AMP, sodium salt, Fisher), atrazine (ATZ, Sigma Aldrich), nitrobenzene (NB, Baker Analyzed Reagent), nitrobenzoic acid (NBA, MCB Reagents, Merck), potassium persulfate ($K_2S_2O_8$, Sigma Aldrich), potassium bromide (KBr, Fisher) and ferrous sulfate ($FeSO_4 \cdot 7H_2O$, Fisher), were of analytical grade.

### *8.2.2 Analysis*

The concentration of organic compounds was determined by HPLC with a diode array detector (Agilent 1100 Series quaternary LC). Mainly two different methods were applied. For BZ4, ATZ, NB and NBA, a C18 Discovery HS (Supelco) column (4.6 x 150 mm, 5 µm) was utilized. The column temperature was set at 25 °C. The mobile phase constituted of 0.1% acetic acid in Milli-Q water and ethanol in a ratio of 60:40 (v:v) with a flow rate of 0.2 mL $min^{-1}$ and an injection volume of 50 µL (Method no.1). The second method employed for AMP detection (Method no.2) involved a Nova-Pak C18 Waters column (3.9 x 150 mm, 5 µm). The mobile phase constituted of 0.1% acetic acid in Milli-Q water and acetonitrile in a ratio of 80:20 (v:v). The temperature column was set at 25 °C, with the flow rate at 0.5 mL $min^{-1}$ and the injection volume at 20 µL. The detection wavelength, retention time, limits of detection and quantification (LOD and LOQ) for each model contaminant are listed in Table 39 (Ripp and Program 1996). A third method was applied in order to determine the concentration of para-

chlorobenzoic acid (pCBA) and m-toluic acid (m-methylbenzoic acid, TA) which were used as a competitor for determining second-order rate constants of BZ4 with hydroxyl radical and sulfate radical, respectively. In this case the same column employed for BZ4 detection was utilized but with a different mobile phase of 0.05% trifluoroacetic acid (TFA) in acetonitrile solution and 0.05% TFA in Milli-Q water in a ratio of 40:60 (v:v). A flow rate of 0.2 mL $min^{-1}$, an injection volume of 25 µL and a column temperature of 40 °C were applied with a detection wavelength set at 238 nm for both compounds.

**Table 39 Limit of detection and quantification for studied compounds.**

| | Method no. | Detection wavelength | Retention time | Limit of detection LOD | Limit of quantification LOQ |
|---|---|---|---|---|---|
| | | (nm) | (min) | (x$10^{-6}$ M) | (x$10^{-6}$ M) |
| **BZ4** | 1 | 226.0 | 3.8 | 0.19 | 0.62 |
| **NBA** | 1 | 286.4 | 5.7 | 0.10 | 0.32 |
| **NB** | 1 | 286.4 | 7.0 | 0.17 | 0.57 |
| **ATZ** | 1 | 226.0 | 7.4 | 0.07 | 0.24 |
| **AMP** | 2 | 196.4 | 6.0 | 2.32 | 7.72 |

Total organic carbon (TOC), as non-purgeable organic carbon (NPOC), was measured by a Shimadzu VCSH-ASI TOC Analyzer.

### *8.2.3 Photolytic experiments*

Experiments were carried out in a collimated beam system using two 15 W low-pressure UV lamps (Cole-Parmer) with monochromatic emission at $\lambda_{max}$=254 nm. The reactor consisted of a Pyrex® glass Petri dish (60x15 mm) with a quartz cover. The average UV fluence rate in 10 mL water solution was determined to be 0.1 mW $cm^{-2}$ by ferrioxalate actinometry, $I^-/IO_3^-$ actinometry, and a calibrated radiometer (Model IL 1700, XRD (XRL) 140T254 low profile germicidal probe, International Light, Co., Newburyport, MA) (He et al. 2012).

General concentrations of 500 µM persulfate, 40 µM contaminants, 20 µM catalyst $Fe^{2+}$ and 5 mM bromide were spiked into 10 mL Mill-Q water. Low persulfate concentration can prevent the necessity of an additional sulphur removal or the reductive formation of sulphide in an anaerobic process. The release of iron into the environment is not regulated in Europe or in USA, though US EPA has established a Secondary Maximum Contaminant Level of 0.3 mg $L^{-1}$ for this metal. The low iron concentration used in this study could therefore limit the release of iron. Due to the limit of the analytical methods, a high initial contaminant concentration of 40 µM was chosen so that the kinetics could be compared in terms of both the degradation of the parent compound and its mineralization extent. A high initial halide concentration of 5 mM was used aiming to observe its direct impact on the proposed UV-254 nm/PS/$Fe^{2+}$ process. Sulfuric acid or sodium hydroxide was used when pH adjustment was required.

In competition study for the determination of second-order rate constants, the initial concentrations of BZ4, pCBA ($k_{HO\cdot/pCBA}$=5 x $10^9$ $M^{-1}$ $s^{-1}$ (Buxton et al. 1988)), and $H_2O_2$ were 4 µM, 4 µM, and 500 µM, respectively, for $k_{HO\cdot}$ determination; while those of BZ4, TA ($k_{SO4\cdot-/TA}$=2.0 x $10^9$ $M^{-1}$ $s^{-1}$(Neta et al. 1977)), $K_2S_2O_8$, and t-BuOH were 4 µM, 4 µM, 500 µM and 500 mM, respectively, for $k_{SO4\cdot-}$ determination. No significant UV direct photolysis of BZ4, pCBA

or TA was observed. Any observed degradation of these compounds would therefore be resulted from radical reactions. The rate constant of t-BuOH with hydroxyl radical ($k_{HO\cdot/t\text{-}BuOH}$= 6.0 x $10^8$ $M^{-1}$ $s^{-1}$ (Buxton et al. 1988)) is around three-order higher than with sulfate radical ($k_{SO4\cdot-/\ t\text{-}BuOH}$ = 8.4 x $10^5$ $M^{-1}$ $s^{-1}$(Clifton and Huie 1989)). Thus, the addition of an excessive amount of t-BuOH allowed a strong suppression of the reaction of target compounds with hydroxyl radical (Rickman and Mezyk 2010; Toth et al. 2012; He et al. 2014). Though the presence of the competitors and t-BuOH influenced the steady-state radical concentrations, without the radical concentration values, the second order rate constant of BZ4 with the radical species could still be calculated according to the following equation (Eq. 94) without knowledge of the radical concentrations (Dantas et al. 2007) which is in fact an integrated equation for eq (8)-(11) in Gonzalez-Olmos (Gonzalez-Olmos et al. 2011):

$$\ln\left(\frac{[\mathrm{BZ4}]}{[\mathrm{BZ4}]_0}\right) = \ln\left(\frac{[\mathrm{reference}]}{[\mathrm{reference}]_0}\right)\frac{k_{\mathrm{radical/BZ4}}}{k_{\mathrm{radical/reference}}} \qquad (94)$$

At each predetermined UV irradiation time interval, 100 µL of the solution was sampled and, without adding any quenching agent, injected into the HPLC within a short period of time. In the case of TOC measurement, no quenching substance was added either. Instead, the samples were analyzed immediately after irradiation. Experiments were carried out in triplicate, unless noted otherwise. The error bars in the figures represent the standard error of the mean.

## 8.3 Results and discussion

### *8.3.1 Degradation of BZ4 under different operating conditions*

In order to evaluate the influence of the operating parameters on contaminant removal, different concentrations of $Fe^{2+}$, PS and $Br^-$ were employed.

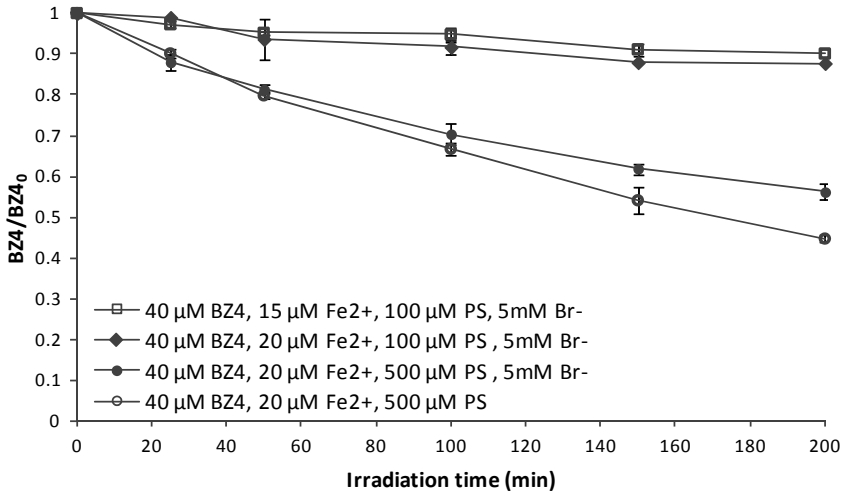


**Figure 51 Influence of $Fe^{2+}$, PS and $Br^-$ on BZ4 degradation. $[BZ4]_0$=40 µM; $[Fe^{2+}]$=15 or 20 µM; $[S_2O_8^{2-}]_0$=100 or 500 µM; $[Br^-]_0$=0 or 5 mM ($pH_0$=6.0±0.8; $pH_f$=5.3±0.5).**

As shown in Figure 51, by increasing the iron concentration from 15 µM to 20 µM in the presence of 100 µM PS and 5 mM $Br^-$, no significant enhancement was observed, i.e., 10% vs 13% BZ4 removal, respectively, after up to 200 min reaction. On the other hand, a PS

concentration increase from 100 µM to 500 µM resulted in a much higher efficiency on BZ4 removal, which could be attributed to the generation of more radicals according to reactions (59) and (62) in Table 13. Finally, with initial concentrations of 40 µM BZ4, 20 µM $Fe^{2+}$, and 500 µM PS, the absence and presence of 5 mM bromide resulted in comparable pseudo first-order rate constants ($k_{obs}$) of (4.4±0.2) x $10^{-3}$ $min^{-1}$ and (4.3±0.1) x $10^{-3}$ $min^{-1}$, respectively.

To better understand the influence of the catalyst and bromide on BZ4 removal, further studies were carried out. As can be deduced from Figure 52, in either presence or absence of bromide, there was a slight improvement in the percentage degradation of BZ4 with the addition of 20 µM $Fe^{2+}$. The pH adjustment in the presence of 20 µM $Fe^{2+}$ did not show any significant influence, as indicated by 41% and 44% BZ4 removal, at pH=3 and without pH adjustment ($pH_0$=6.0±0.8, $pH_f$=5.3±0.5), respectively. These results clearly suggest UV/PS/$Fe^{2+}$ was advantageous by enhancing photo-regeneration of $Fe^{2+}$ for catalytic radical generation and therefore became less significantly impacted by water pH.

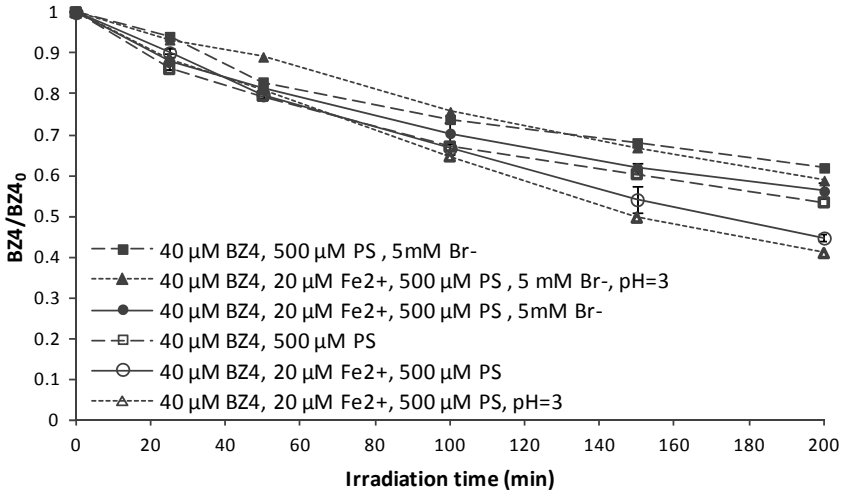


**Figure 52 Influence of $Fe^{2+}$, pH and $Br^-$ on BZ4 degradation. $[BZ4]_0$=40 µM; $[Fe^{2+}]$=0 or 20 µM; $[S_2O_8^{2-}]_0$=500 µM; $[Br^-]_0$=0 or 5 mM ($pH_0$=6.0±0.8; $pH_f$=5.3±0.5 or pH=2.8±0.2).**

In this study, the second-order rate constant of BZ4 with HO· or $SO_4^{\cdot-}$ were determined through competition kinetics and found to be $k_{HO\cdot/BZ4}$=4.86 x $10^9$ $M^{-1}s^{-1}$ and $k_{SO4^{\cdot-}/BZ4}$=5.90 x $10^8$ $M^{-1}$ $s^{-1}$, respectively, according to Eq (94) (Figure 53). Due to the higher rate constants of $Br^-$ with the radical species, i.e., $k_{HO\cdot/Br^-}$=1.10 x $10^{10}$ $M^{-1}s^{-1}$ (Buxton et al. 1988) and $k_{SO4^{\cdot-}/Br^-}$=3.50 x $10^9$ $M^{-1}$ $s^{-1}$ (Neta et al. 1988), and the much higher concentration of $Br^-$ in the reaction solution (5 mM $Br^-$ versus 40 µM BZ4), the competition of Br- for the radicals led to a reduced BZ4 removal effectiveness. To better understand this result, the quenching ratio based on the second-order rate constants of BZ4 and $Br^-$ with the two main radicals can be calculated, following the equations proposed by Gonzales-Olmos et al. (2011) (Gonzalez-Olmos et al. 2011):

$$\frac{R_{HO\cdot}}{R_{SO_4^{\cdot-}}} = \frac{1+(k_{SO_4^{\cdot-}/Br^-}/\,k_{SO_4^{\cdot-}/BZ4})([Br^-]/[BZ4])}{1+(k_{HO\cdot/Br^-}/\,k_{HO\cdot/BZ4})([Br^-]/[BZ4])} \quad (95)$$

The obtained $R_{HO\cdot}/R_{SO4^{\cdot-}}$=2.62 (>1, Table 40) suggests the reaction of sulfate radicals with BZ4 was more suppressed by the presence of $Br^-$. Considering the higher $k_{HO\cdot/BZ4}$ than $k_{SO4^{\cdot-}/BZ4}$, a non-significant inhibition of the BZ4 removal could therefore be explained.

**Table 40 Second-order rate constant for the reaction of the studied compounds and $Br^-$ with hydroxyl radical and sulfate radical, $R_{HO\cdot}/R_{SO4\cdot}$- calculated according to Eq. (95) and compound percentage removal after 200 min of treatment.**

| | k ($M^{-1}s^{-1}$) | | | | $R_{HO\cdot}/R_{SO4\cdot}^{-}$ (*) | η (%) (**) | |
|---|---|---|---|---|---|---|---|
| | HO· | | $SO_4\cdot^-$ | | | with $Br^-$ | without $Br^-$ |
| **BZ4** | $4.86 \times 10^9$ | | $5.90 \times 10^8$ | | 2.62 | 44 | 55 |
| **NBA** | $2.60 \times 10^9$ | (Buxton et al. 1988) | $\leq 10^6$ | (Neta et al. 1977) | 825.7 | 8 | 37 |
| **NB** | $3.90 \times 10^9$ | (Buxton et al. 1988) | $\leq 10^6$ | (Neta et al. 1977) | 1237.4 | 79 | 53 |
| **ATZ** | $(2.60\pm0.4) \times 10^9$ | (Haag and Yao 1992) | $2.59 \times 10^9$ | (Khan et al. 2014) | 0.32 | 58 | 100 |
| **AMP** | $4.87 \times 10^9$ | (He et al. 2014) | $2.00 \times 10^9$ | (He et al. 2014) | 0.76 | 66 | 100 |
| **$Br^-$** | $1.10 \times 10^{10}$ | (Buxton et al. 1988) | $3.50 \times 10^9$ | (Neta et al. 1977) | - | | - |

(*) quenching ratio based on the second-order rate constants of the compound and $Br^-$ with the two main radicals species in solution (equation 2, section 3.1).
(**) compound percentage removal after 200 min of treatment in presence and absence of bromide ions.

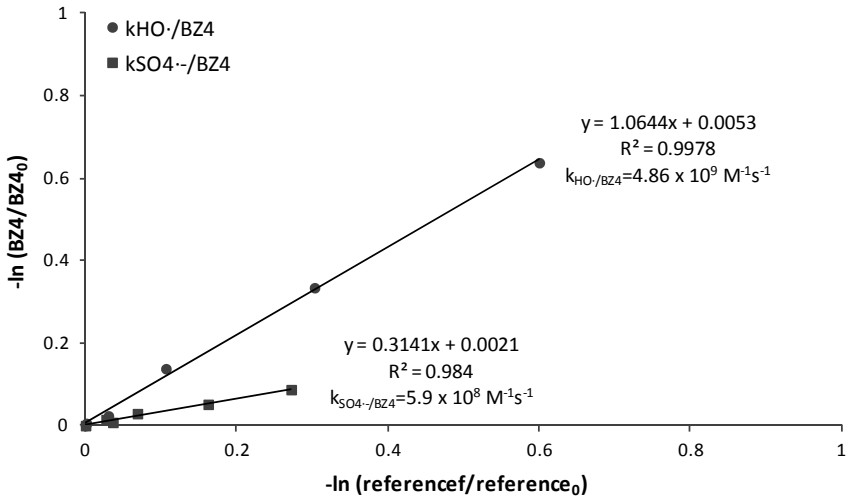


**Figure 53 Determination of the second-order rate constants of BZ4 with hydroxyl radical and sulfate radical.**

### *8.3.2 Degradation of different organic compounds - influence of bromide ions*

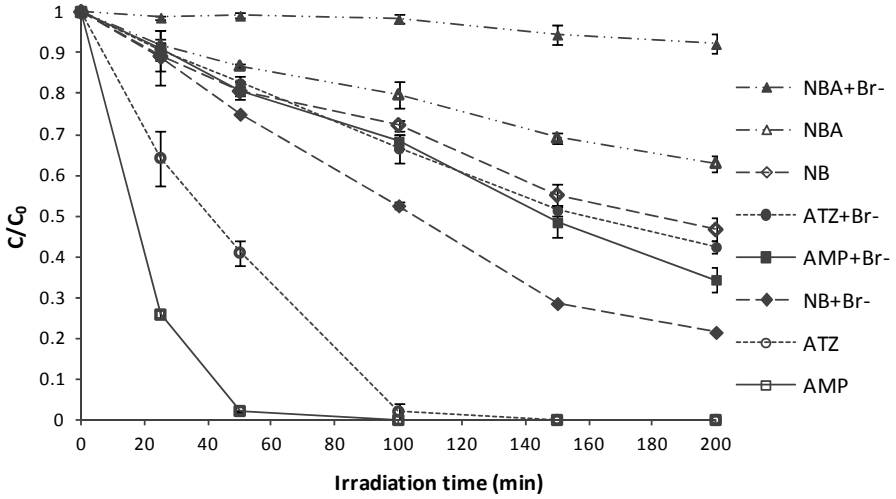


**Figure 54 Degradation of different organic compounds by UV/PS/$Fe^{2+}$ in the presence or absence of bromide. $[BZ4]_0=[AMP]_0=[ATZ]_0=[NBA]_0=[NB]_0$=40 µM; $[Fe^{2+}]$=20 µM; $[S_2O_8^{2-}]_0$=500 µM; $[Br^-]_0$= 5 mM (BZ4 results are shown in Figures 51 and 52).**

Table 40 also summarizes the rate constants for the reaction of the studied compounds with hydroxyl and sulfate radicals. As previously described, the reactions which allow the conversion of $SO_4^{\cdot-}$ to HO· are affected by solution pH (reaction 62) and characterized by slow kinetics (reaction 63), as shown in Table 13. However, even at lower pH of 2 or 3, NB, which has a low second order rate constant of ≤ $10^6$ $M^{-1}$ $s^{-1}$ with $SO_4^{\cdot-}$, was still found to be significantly degraded by UV/PS process (He et al. 2014). Thus the contribution of hydroxyl radical at low pH conditions may not be neglected. The degradation efficiency of all these compounds in Figure 54 followed well with their relative reactivity with the hydroxyl radical and sulfate radical in the absence of bromide. When the concentration of Br- (5 mM) was more than 100 times higher than those of the target compounds and its reactivity with the hydroxyl and sulfate radicals were also higher, a significant inhibition should be observed if only hydroxyl and sulfate radicals were mainly responsible for the degradation. The quenching ratio $R_{HO\cdot}/R_{SO4\cdot-}$ was again calculated (Table 40). For AMP and ATZ, second order rate constants of which with HO· were comparable to those with $SO_4^{\cdot-}$, the more affected reaction was found to be HO· reaction ($R_{HO\cdot}/R_{SO4\cdot-}$<1). For all the other compounds with $R_{HO\cdot}/R_{SO4\cdot-}$>1, the quenching effect was probably due to suppressions on sulfate radical reaction. This effect is experimentally confirmed except for NB. The presence of $Br^-$ significantly enhanced the degradation rate of NB, indicating that Br- acted as a promoter of the degradation of NB (Wu et al. 2015). After 200 min treatment, the percentage removal of NB increased from 53% to 79% along with $k_{obs}$ of (4.4±0.3) x $10^{-3}$ $min^{-1}$ in water and (6.2±0.1) x $10^{-3}$ $min^{-1}$ in bromide containing water. In order to obtain further insights on the degradation kinetics of NB, an additional set of experiments on the degradation of NB was carried out. Experiments were also performed on substituted NB (i.e., NBA) as a comparison.

Another consideration can be done on the effect of scavenging radicals operated by bromide ions. Studies have demonstrated the possible bromate formation from bromide oxidation in $SO_4^{\cdot-}$ based AOPs. Thus, radicals involved in the reaction with $Br^-$ can form bromine atoms (Br·) which can go through a series of reactions with $Br^-$ and $H_2O$ to form HOBr/$OBr^-$ (Table 14). On

the basis of studies reported in the literature (Fang and Shang 2012; Lutze et al. 2014), it seems reasonable to expect $HOBr/OBr^-$ as intermediate of the stepwise conversion of $Br^-$ to $BrO_3^-$ by radical oxidation and UV photolysis. Nevertheless, additional investigation is required in order to provide more accurate information on this aspect.

### *8.3.3 Degradation of NB*

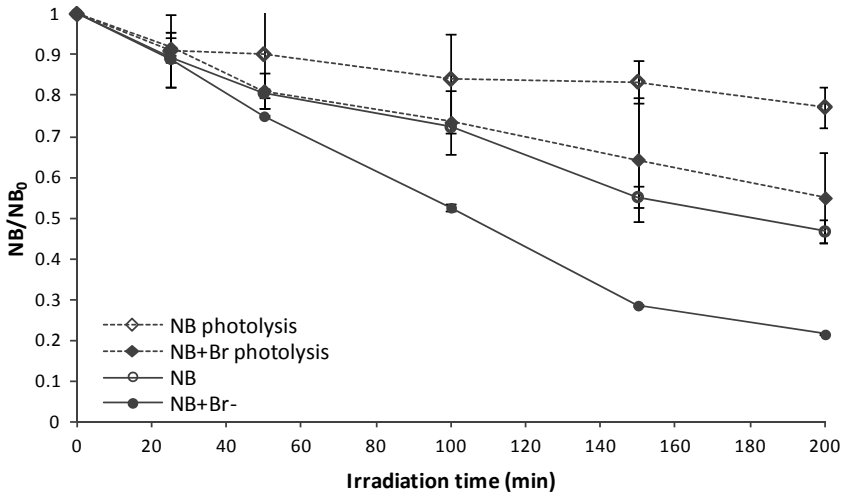


**Figure 55 Degradation of NB by UV/PS/$Fe^{2+}$ (shown already in Figure 54) and UV direct photolysis. $[NB]_0$=40 µM; $[Fe^{2+}]$=20 µM; $[S_2O_8^{2-}]_0$=500 µM; $[Br^-]_0$=0 or 5 mM ($pH_0$=6.0±0.3; $pH_f$=5.5±0.5).**

As shown in Figure 55, the enhancement attributable to the presence of bromide ions was clearly observed even during the direct photolysis of NB, with 23% and 45% removal, respectively, in the absence and presence of bromide ions in 200 min ($pH_0$=6.0±0.3, $pH_f$=5.5±0.5). Comparatively, there was no significant difference in the presence or absence of bromide by UV/PS/$Fe^{2+}$ at pH 3 (Figure 56). No adverse impact on the removal of NB at different pH conditions may indicate an advantage of UV/PS/$Fe^{2+}$ over Fenton and Photo Fenton reactions.

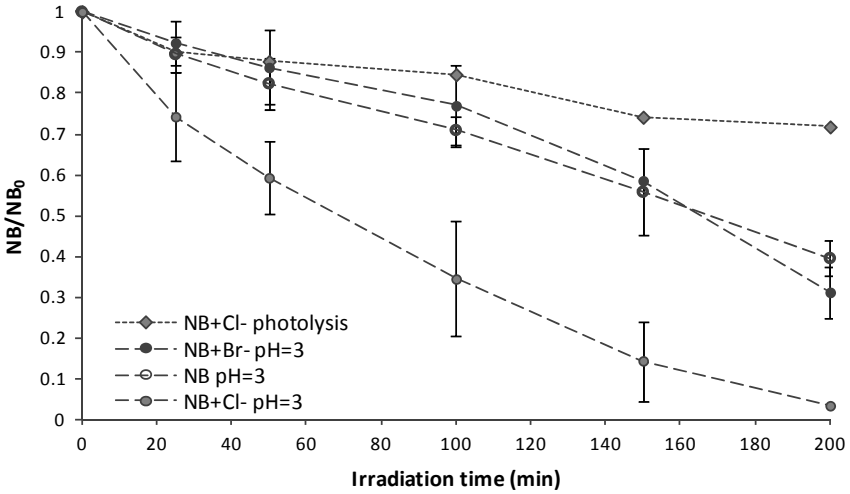


**Figure 56 Degradation of NB by UV/PS/$Fe^{2+}$ and UV direct photolysis in the presence or absence of halides (pH=2.8±0.2 and $pH_0$=6.0±0.3; $pH_f$=5.5±0.5). $[NB]_0$=40 µM; $[Fe^{2+}]$=20 µM; $[S_2O_8^{2-}]_0$=500 µM; $[Br^-]_0$=$[Cl^-]_0$=0 or 5 mM.**

In chloride containing water, there was a 28% removal of NB, which was comparable to the direct photolysis of NB. However, the presence of chloride ions in UV/PS/$Fe^{2+}$ (pH=3) was found to promote significantly the treatment efficiency reaching 97%, as shown in Figure 56. Several studies have demonstrated in $SO_4^{\cdot -}$ based treatment systems the involvement of various $Cl^-$ related chain reactions leading to the generation of chlorine based radicals such as $Cl^{\cdot}$ and $Cl_2^{\cdot -}$ to participate in the degradation of the contaminants (Anipsitakis et al. 2006; Wang et al. 2011; Yuan et al. 2014).

The positive effect of bromide on degradation kinetics could be extended to the mineralization of NB, as shown in Figure 57. Despite the promising result obtained in terms of NB degradation, the contribution of chloride to the mineralization was minimal, which may indicate the strong selectivity of the associated active chlorine species. In this study, we showed varied promoting effects from bromide and chloride ions on the photolysis, photochemical degradation, and mineralization of NB. More studies are still needed for a better understanding of the actual role of bromide (and chloride) on the degradation of NB.

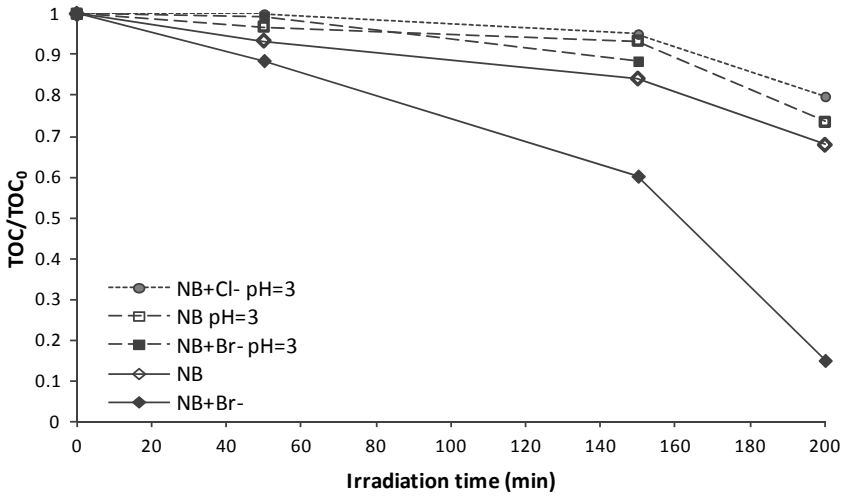


**Figure 57 TOC removal by UV/PS/$Fe^{2+}$ at different pH conditions (pH=2.8±0.2; $pH_0$=6.0±0.3 and $pH_f$=5.5±0.5). $[NB]_0$=40 µM ($TOC_0$=2.07±0.12); $[Fe^{2+}]$=20 µM; $[S_2O_8^{2-}]_0$=500 µM; $[Br^-]_0$=$[Cl^-]_0$=5 mM.**

### *8.3.4 Degradation of NBA*

The nitrobenzene structure may be of significant importance for those particular observations in the presence of halides. A similar study was, therefore, carried out using a substituted nitrobenzene, i.e., nitrobenzoic acid (NBA). Figure 58 shows no direct photolysis of NBA in the presence or absence of bromide. Thus, different from what was observed for NB, the presence of bromide played an inhibitor role for the removal of substituted nitrobenzene. Meanwhile, the presence of chloride had no significant influence on direct photolysis or photochemical degradation of NBA (Figure 59).

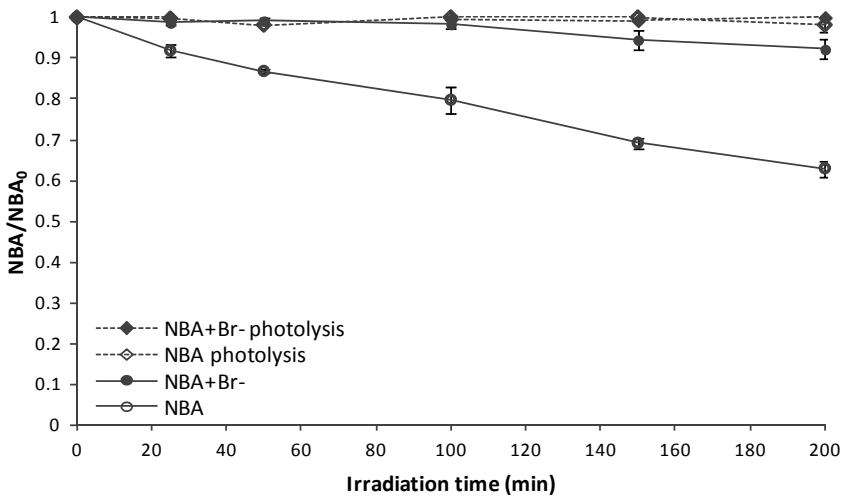


**Figure 58 Degradation of NBA by UV/PS/$Fe^{2+}$ (shown in Figure 54) and UV direct photolysis in the presence or absence of bromide (pH=6.0±0.5). $[NBA]_0$=40 μM; $[Fe^{2+}]$=20 μM; $[S_2O_8^{2-}]_0$=500 μM; $[Br^-]_0$=5 mM.**

In the absence of halide, only 37% of NBA removal was obtained after 200 min of irradiation without an initial pH adjustment ($pH_0$=6.0±0.5, $pH_f$=5.8±0.5, Figure 58 and 52% in acidic solution (Figure 59), showing limited efficiency of UV/PS/$Fe^{2+}$ for the removal of this compound, consistent with its reactivity with hydroxyl radical and sulfate radical (as shown in Table 40). In fact, there has been several reported studies on the contaminant-specific scavenging effect of halides (Westerhoff et al. 2004; Echigo and Minear 2006; Heeb et al. 2014). The two strong electron withdrawing functional groups for NBA probably limited its transformation by bromine related radical species which are reactive with electron rich compounds (Grebel et al. 2010).

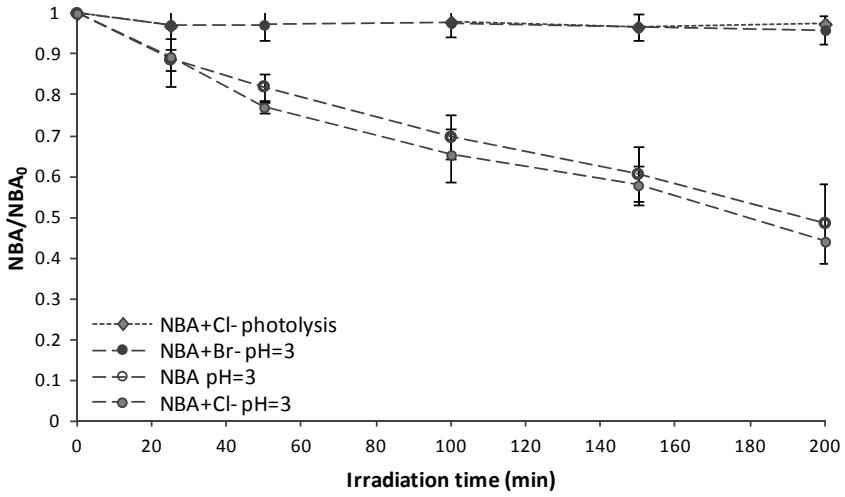


**Figure 59 Degradation of NBA by UV/PS/$Fe^{2+}$ and UV direct photolysis in the presence and absence of halides (pH=2.8±0.2 and $pH_0$=6.0±0.5; $pH_f$=5.8±0.5). $[NBA]_0$=40 μM; $[Fe^{2+}]$=20 μM; $[S_2O_8^{2-}]_0$=500 μM; $[Br^-]_0$=$[Cl^-]_0$=5 mM.**

Similar observation was found in terms of TOC removal, with the presence of bromide significantly inhibited the mineralization of NBA (Figure 60). In the presence of bromide, there was no more than 10% of mineralization while in the absence of bromide, 28% and 37% TOC removal was observed at natural pH and in acidic media, respectively.

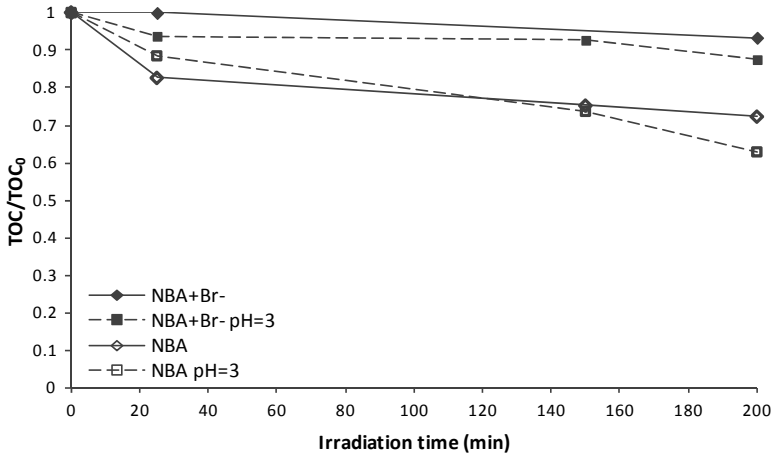


**Figure 60 TOC removal by UV/PS/$Fe^{2+}$ in the presence and absence of halides at different pH conditions (pH=2.8±0.2; $pH_0$=6.0±0.5 and $pH_f$=5.8±0.5). $[NBA]_0$=40 μM ($TOC_0$=3.58±0.05); $[Fe^{2+}]$=20 μM; $[S_2O_8^{2-}]_0$=500 μM; $[Br^-]_0$=5 mM.**

## 8.4 Conclusions

This study evaluated the effects of bromide on the removal rates of organic compounds (benzophenone-4, atrazine, ampicillin, nitrobenzene and nitrobenzoic acid) by AOPs, especially UV/PS/$Fe^{2+}$.

- As expected, the addition of $Fe^{2+}$ and the increase in oxidant dosage enhanced the photochemical degradation of model compounds.
- The inhibition effect due to the presence of bromide ions was confirmed in most cases except for NB.
- NB was the only compound studied to be positively affected by the presence of bromide ions. Similar results were observed by the treatment of NB in chloride containing waters. No such influence was observed for the treatment of substituted nitrobenzene (i.e., NBA). The specific behavior shown for NB requires further investigation in order to better understand the mechanism that governs its degradation.
- The study demonstrated the different reactivity of organic compounds toward UV/PS/$Fe^{2+}$ process in the presence and absence of halides, providing useful information for their role in water decontamination using such processes.

## 8.5 Appendix

Accepted Manuscript


Effects of Bromide on the Degradation of Organic Contaminants with UV and $Fe^{2+}$ Activated Persulfate

Antonella De Luca, Xuexiang He, Dionysios D. Dionysiou, Renato F. Dantas, Santiago Esplugas

PII: S1385-8947(16)30873-7
DOI: http://dx.doi.org/10.1016/j.cej.2016.06.066
Reference: CEJ 15376

To appear in: *Chemical Engineering Journal*

Please cite this article as: A. De Luca, X. He, D.D. Dionysiou, R.F. Dantas, S. Esplugas, Effects of Bromide on the Degradation of Organic Contaminants with UV and $Fe^{2+}$ Activated Persulfate, *Chemical Engineering Journal* (2016), doi: http://dx.doi.org/10.1016/j.cej.2016.06.066

# 9 Conclusions and Recommendations

## 9.1 Conclusions

The main objective of this study was to define the proper set up of photo-Fenton like at neutral pH catalyzed by iron chelate. The aim was the assessment of the suitability of chelate based processes in the degradation of recalcitrant contaminant.

Though specific conclusions have been provided at the end of each chapter, the main results obtained can be here summarized.

From **Chapter 4** it could be concluded:

- ✓ Under the experimental conditions adopted in the study (1 mg $L^{-1}$ of $Fe^{2+}$ and 5 mg $L^{-1}$ of $H_2O_2$), Fenton did not allow significant atrazine removal when treated in SE from WWTP in initial concentration of 0.1 mg $L^{-1}$ and at 2.8±0.1.
- ✓ The enhancement due to the UV-A irradiation was confirmed by treating atrazine (0.1 mg $L^{-1}$) in SE from WWTP under the experimental conditions adopted for the study (1 mg $L^{-1}$ of $Fe^{2+}$ and 5 mg $L^{-1}$ of $H_2O_2$ at pH=2.8±0.1). 50% of the initial content of atrazine could be removed within 120 minutes of reaction.
- ✓ The combined contribution of the photolysis together with the higher production of HO· due to the shortest wavelength of irradiation (254 nm), allowed a significantly enhanced atrazine removal when treating the solution with UV-C photo-Fenton. Under the experimental conditions of this study (1 mg $L^{-1}$ of $Fe^{2+}$ and 1 mg $L^{-1}$ of $H_2O_2$ at pH=2.8±0.1) almost the 100% of atrazine was removed alter only 20 minutes of reaction. The biodegradability of the effluent was also improved and no toxic transformation products were produced.
- ✓ UV-C Photo-Fenton can be identified as useful technique for atrazine degradation.

From the **Chapter 5** it can be highlighted:

- ✓ $Fe^{3+}$ is preferable for iron chelation since, as the higher stability constant also shows, it ensures better chelates stability respect to $Fe^{2+}$.
- ✓ The stoichiometric L:Fe molar ratio 1:1 is generally not enough to ensure the complete chelation of the iron content. Higher amount of chelating agents generally promote higher and faster degradation of the target compound.
- ✓ The optimum ratio L:Fe has to be established taking under consideration the balance between chelation efficiency, environmental suitability and lower costs.
- ✓ Chelates of EDTA and NTA showed great catalytic activity and significant amount of SMX could be removed with minimal addition of chelating agent.
- ✓ Oxalic acid has to be added in high concentration to reach good efficiency for iron chelation. Fe(III)-OA did not show anyway important catalytic activity.
- ✓ Chelates of tartaric acid showed minimal catalytic activity demonstrating its not suitability as ligand for the purpose of the study.

- ✓ Considering its biodegradability, low toxicity and best suitability among the chelating agents tested, NTA (in 1.5:1 NTA:Fe molar ratio) can be considered a good strategy to carry out photo-Fenton like at circumneutral pH.

From **Chapter 6** on the stability of Fe(III)-NTA chelates it can be pointed out that:

- ✓ The control of temperature is unnecessary if performed in absence of any other stress factors. Chelate solution can be stored without temperature control at least during 9 days, since no changes were observed when monitoring the solution within this time.
- ✓ Under UV-A irradiation the chelates solution showed a temporary stability before exhibiting a gradual damage and subsequent iron release. This effect could be delayed by controlling the temperature of the solution. No iron release was registered before 45 minutes of irradiation under the whole temperature test range.
- ✓ By combining photochemical and oxidative stresses, the chelate decomposition with subsequent iron release was unavoidable. Thus, by adding $H_2O_2$ the iron chelates content gradually decreased since the beginning of the irradiation. Temperature control promoted the extension of the chelates lifetime (from 60% of reduction to 42% in two hours turning the temperature down 20 °C).
- ✓ A direct proportional correlation between the hydrogen peroxide dose and the destruction of Fe(III)-NTA could be identified.
- ✓ Emission spectrum of the lamps employed for irradiation influences the stability of the chelates. UV-C lamps were identified as the most unfavorable for applications in photo-Fenton like at neutral pH catalyzed by iron chelates. More than 90% of reduction in chelates content was, in fact, registered after only 30 minutes of UV-C irradiation by adding 0.59 mM $H_2O_2$. In spite of that, 55% and 67% of reduction of the chelates available for the reaction was registered after two hours under irradiation with UV-A and Xe lamps by adding 0.59 mM $H_2O_2$. The wider range of Xenon lamp emission wavelength than UV-A lamps was responsible of the higher instability produced in the chelates solution during the exposure.
- ✓ Finally, UV-A irradiation was identified as the more suitable to ensure as long as possible the preservation of the chelates and the subsequent catalytic activity of the solution.

**Chapter 7** purchased useful information as:

- ✓ High content of competing ions can drastically reduce the efficiency of the chelation process resulting in a minor amount of catalyst available for the reaction.
- ✓ Alkalinity and high content in organic matter also influence the efficiency of the process by scavenging the radical available for the reaction.
- ✓ Under the experimental conditions adopted in the study, iron chelate dosage generally allowed extending the chelates' lifetime but it did not promote higher SMX removal.
- ✓ Even though the enhancement obtained by adding $Mn^{2+}$ was not as resounding as from other studies by literature. The addition of $Mn^{2+}$ for mediated photo-Fenton like at neutral pH catalyzed by Fe(III)-NTA, , higher pseudo-first order constant was exhibited by the SMX removal curve.

- ✓ Under UV-A irradiation and the experimental parameters set for this study, UV-A/PS/FeNTA demonstrated to be not suitable for recalcitrant contaminant removal.

From **Chapter 8** it can be pointed out as:

- ✓ The addition of $Fe^{2+}$ and the increase in oxidant dosage enhanced the photochemical degradation of model compounds.
- ✓ The inhibition effect due to the presence of bromide ions was also confirmed in most cases except for NB.
- ✓ While in water free of $Br^-$, AMP and ATZ were fast and completely degraded under the experimental condition adopted, their removal was significantly reduced when in presence of $Br^-$.
- ✓ BZ4 and NBA, which showed a higher recalcitrant behavior under the radical attack, also suffered the inhibition operated by the presence of bromide. NBA, in particular exhibited an almost null removal in bromide containing water.
- ✓ NB removal resulted enhanced when treated in bromide containing water. Similar results were observed by the treatment of NB in chloride containing waters.
- ✓ No such influence was observed for the treatment of substituted nitrobenzene (i.e., NBA). Finally, this study demonstrated the different reactivity of organic compounds toward UV/PS/$Fe^{2+}$ process in the presence and absence of halides, providing useful information for their role in water decontamination using such processes.

## 9.2 Recommendations

From the results obtained by the study presented in Chapter 7 derivate the main recommendation for further investigation on the applicability of chelate based Photo-Fenton like at neutral pH. In fact, since the influence of the treating water quality was clearly demonstrated, it would be important to carry out additional testes in order to make possible an approximated prediction of the efficiency achievable when knowing the characteristic of treating effluent.

Moreover, even though iron chelate dosage did not allow an improvement of SMX removal, the results showed Chapter 7 cannot be considered sufficient to exclude the possibility that this strategy could be successful in improving the efficiency of the process. At this purpose, further investigation would be required to find out the optimum scheme of dosage to reach the combined effect of extending the lifetime of the chelate and enhance the target compound removal.

Regarding the possibility of persulfate activation by iron chelate, in this study the results obtained were completely unsatisfactory. However, the low concentration of the reagents adopted were probably not enough to ensure the proper persulfate decomposition. Also the possibility to combine the process with UV-C irradiation should be better evaluated. It has been, in fact demonstrated as UV-C might be avoided in order to keep longer the chelate stable under reaction stress. However, the required lifetime is strongly dependent of the efficiency of the process.

Finally, $Mn^{2+}$_mediated Photo-Fenton like catalyzed by Fe(III)-NTA appeared promising for improving the process. Higher initial kinetic was exhibited by SMX removal when adding $Mn^{2+}$. However, the global efficiency exhibited after 120 minutes did not keep this improvement. Nevertheless, only one ratio Mn:Fe has been tested in this study. Other combination might be tested in order to evaluate the possibility of increase the extra efficiency.

Verify the suitability of the process when treating streams characterized by the presence of pollutant in more realistic concentrations also represent an important step for future investigation.

From Chapter 8, some additional study could be also carried out in order, for example to better explain the specific behavior shown for NB. Moreover, the possible formation of bromate also requires further investigation.

## References


Abida O, Mailhot G, Litter M, Bolte M (2006) Impact of iron-complex (Fe(III)-NTA) on photoinduced degradation of 4-chlorophenol in aqueous solution. *Photochem Photobiol Sci* 5: 395–402. doi: 10.1039/b518211e

Acosta EJ†, Steffensen MB†, Tichy SE, Simanek* EE (2004) Removal of Atrazine from Water Using Covalent Sequestration. *J Agric Food Chem* 53: 545–549.

Agrawal A, Gutch M, Arora R, Jain N (2011) Acute cardiogenic pulmonary oedema with multiorgan dysfunction--still to learn more about nitrobenzene poisoning. BMJ Case Rep. doi: 10.1136/bcr.10.2011.5026

Ahmad M, Teel AL, Furman OS, Reed JI, Watts RJ (2012) Oxidative and Reductive Pathways in Iron-Ethylenediaminetetraacetic Acid–Activated Persulfate Systems. *J Environ Eng* 138: 411–418. doi: 10.1061/(ASCE)EE.1943-7870.0000496

An J, Zhu L, Zhang Y, Tang H (2013) Efficient visible light photo-fenton-like degradation of organic pollutants using in situ surface-modified $BiFeO_3$ as a catalyst. *J Environ Sci* (China) 25: 1213–1225.

Andrianirinaharivelo SL, Pilichowski J-F, Bolte M (1993) Nitrilotriacetic acid transformation photo-induced by complexation with iron(III) in aqueous solution. *Transit Met Chem* 18: 37–41. doi: 10.1007/BF00136046

Anipsitakis GP, Dionysiou DD (2004) Radical Generation by the Interaction of Transition Metals with Common Oxidants. *Environ Sci Technol* 38: 3705–3712. doi: 10.1021/es035121o

Anipsitakis GP, Dionysiou DD, Gonzalez MA (2006) Cobalt-Mediated Activation of Peroxymonosulfate and Sulfate Radical Attack on Phenolic Compounds. Implications of Chloride Ions. *Environ Sci Technol* 40: 1000–1007. doi: 10.1021/es050634b

APHA APHA, AWWA AWWA, Rice EW, Bridgewater L (2012) Standard methods for the examination of water and wastewater, 22nd ed. Washington, DC: American Public Health Association, Washington, DC, USA

Arnold SM, Hickey WJ, Harris RF (1995) Degradation of Atrazine by Fenton's Reagent: Condition Optimization and Product Quantification. *Environ Sci Technol* 29: 2083–2089. doi: 10.1021/es00008a030

Ayodele OB, Lim JK, Hameed BH (2012) Degradation of phenol in photo-Fenton process by phosphoric acid modified kaolin supported ferric-oxalate catalyst: Optimization and kinetic modeling. *Chem Eng J* 197: 181–192. doi: 10.1016/j.cej.2012.04.053

Ballesteros Martín MM, Sánchez Pérez JA, Casas López JL, Oller I, Malato RS et al (2009) Degradation of a four-pesticide mixture by combined photo-Fenton and biological oxidation. *Water Res* 43: 653–660. doi: 10.1016/j.watres.2008.11.020

Balzani V, Carassiti V (1970) In: Photochemistry of coordination compound. Academic Press, London, pp 145–192

Batista APS, Nogueira RFP (2012) Parameters affecting sulfonamide photo-Fenton degradation – Iron complexation and substituent group. *J Photochem Photobiol A Chem* 232: 8–13. doi: 10.1016/j.jphotochem.2012.01.016

Bautitz IR, Nogueira RFP (2010) Photodegradation of lincomycin and diazepam in sewage treatment plant effluent by photo-Fenton process. *Catal Today* 151: 94–99. doi: 10.1016/j.cattod.2010.02.018

Baxendale JH, Wilson JA (1957) The photolysis of hydrogen peroxide at high light intensities. *Trans Faraday Soc* 53: 344. doi: 10.1039/tf9575300344

Beckwith RC, Wang TX, Margerum DW (1996) Equilibrium and Kinetics of Bromine Hydrolysis. *Inorg Chem* 35: 995–1000. doi: 10.1021/ic950909w

Bennedsen LR, Muff J, Søgaard EG (2012) Influence of chloride and carbonates on the reactivity of activated persulfate. *Chemosphere* 86: 1092–1097. doi: 10.1016/j.chemosphere.2011.12.011

Bethsass J, Colangelo A (2006) European Union bans atrazine, while the United States negotiates continued use. *Int J Occup Environ Health* 12: 260–267.

Bielski BHJ, Cabelli DE, Arudi RL, Ross AB (1985) Reactivity of $HO_2/O_2^-$ Radicals in Aqueous Solution. *J Phys Chem Ref Data* 14: 1041–1100. doi: 10.1063/1.555739

Blesa MA, Borghi EB, Maroto AJ., Regazzoni AE (1984) Adsorption of EDTA and iron—EDTA complexes on magnetite and the mechanism of dissolution of magnetite by EDTA. *J Colloid Interface Sci* 98: 295–305. doi: 10.1016/0021-9797(84)90155-3

Bolton JR, Bircher KG, Tumas W, Tolman CA (2001) Figures-of-merit for the technical development and application of advanced oxidation technologies for both electric- and solar-driven systems (IUPAC Technical Report). *Pure Appl Chem* 73: 627–637. doi: 10.1351/pac200173040627

Bottoni P, Funari E (1992) Criteria for evaluating the impact of pesticides on groundwater quality. *Sci Total Environ* 123-124: 581–590. doi: 10.1016/0048-9697(92)90180-Z

Bouki C, Venieri D, Diamadopoulos E (2013) Detection and fate of antibiotic resistant bacteria in wastewater treatment plants: a review. *Ecotoxicol Environ Saf* 91: 1–9. doi: 10.1016/j.ecoenv.2013.01.016

Boxall ABA, Rudd MA, Brooks BW, Caldwell DJ, Choi K, Hickmann S, Innes E, Ostapyk K, Staveley JP, Verslycke T, Ankley GT, Beazley KF, Belanger SE, Berninger JP, Carriquiriborde P, Coors A, Deleo PC, Dyer SD, Ericson JF, Gagné F, Giesy JP, Gouin T, Hallstrom L, Karlsson MV, Larsson DGJ, Lazorchak JM, Mastrocco F, McLaughlin A, McMaster ME, Meyerhoff RD, Moore R, Parrott JL, Snape JR, Murray-Smith R, Servos MR, Sibley PK, Straub JO, Szabo ND, Topp E, Tetreault GR, Trudeau VL, Van Der Kraak G (2012) Pharmaceuticals and personal care products in the environment: what are the big questions? *Environ Health Perspect* 120: 1221–1229. doi: 10.1289/ehp.1104477

Brack W, Dulio V, Slobodnik J, von der Ohe PC, Prioritisation WGN, Deckere ED, Kuhne R, Ebert RU, Ginebreda A, Cooman WD, Schuurmann G, Piha H, Hanke G, Koschorreck J, Schwesig D, Leonards P, Schwesig D, Borchers U, Chancerelle L, Eriksson U, Farre M, Goksoyr A, Lamoree M, Leonards P, Lepom P, Vrana B, Vermeirssen ELM, Allan IJ, Kohoutek J, Kennedy K, Mills GA, Greenwood R, Leeuwen S, Strub MP, Cofino W, Lindström G, Bavel B, Horai H, Arita M, Kanaya S, Nihei Y, Ikeda T, Suwa K, Ojima Y, Tanaka K, Tanaka S, Aoshima K, Schulze T, Schymanski E, Stravs M, Neumann S, Krauss M, Singer H, Hug C, Gallampois C, Hollender J, Slobodnik J, Hildebrandt C, Wolf W, Neumann, S (2012) The NORMAN Network and its activities on emerging environmental substances with a focus on effect-directed analysis of complex environmental contamination. *Environ Sci Eur* 24: 29. doi: 10.1186/2190-4715-24-29

Brooks BW, Turner PK, Stanley JK, Weston JJ, Glidewell EA, Foran CM, Slattery M, La Point TW,Huggett DB (2003) Waterborne and sediment toxicity of fluoxetine to select organisms. *Chemosphere* 52: 135–142. doi: 10.1016/S0045-6535(03)00103-6

Bucheli-Witschel M, Egli T (2001) Environmental fate and microbial degradation of aminopolycarboxylic acids. *FEMS Microbiol Rev* 25: 69–106. doi: 10.1111/j.1574-6976.2001.tb00572.x

Bunescu A, Besse-Hoggan P, Sancelme M, MailhotG, Delort AM (2008) Fate of the nitrilotriacetic acid-Fe(III) complex during photodegradation and biodegradation by Rhodococcus rhodochrous. *Appl Environ Microbiol* 74: 6320–6326. doi: 10.1128/AEM.00537-08

Buxton G V., Dainton FS (1968) The Radiolysis of aqueous Solutions of Oxybromine Compounds; the Spectra and Reactions of BrO and $BrO_2$. *Proc R Soc A Math Phys Eng Sci* 304: 427–439. doi: 10.1098/rspa.1968.0095

Buxton G V., Greenstock CL, Helman WP, Ross AB, Tsang W (1988) Critical Review of rate constants for reactions of Hydrated Electrons, Hydrogen Atoms and Hydroxyl radicals ($\cdot OH/\cdot O^-$) in Aqueous Solution. *J Phys Chem Ref Data* 17: 513–886. doi: 10.1063/1.555805

Calvin M, Wilson KW (1945) Stability of Chelate Compounds. J Am Chem Soc 67:2003–2007. doi: 10.1021/ja01227a043

Carra I, Malato S, Jiménez M, Maldonado MI, Sánchez Pérez JA (2014) Microcontaminant removal by solar photo-Fenton at natural pH run with sequential and continuous iron additions. *Chem Eng J* 235: 132–140. doi: 10.1016/j.cej.2013.09.029

Cavalcante RP, da Rocha Sandim L, Bogo D, Barbosa AMJ, Osugi ME, Blanco M, de Oliveira SC, de Fatima CMM, Machulek A, Ferreira VS (2013) Application of Fenton, photo-Fenton, solar photo-Fenton, and UV/$H_2O_2$ to degradation of the antineoplastic agent mitoxantrone and toxicological evaluation. *Environ Sci Pollut Res Int* 20: 2352–2361. doi: 10.1007/s11356-012-1110-y

Chan KH, Chu W (2003) Modeling the reaction kinetics of Fenton's process on the removal of atrazine. *Chemosphere* 51: 305–311. doi: 10.1016/S0045-6535(02)00812-3

Christensen H, Sehested K, Corfitzen H (1982) Reactions of hydroxyl radicals with hydrogen peroxide at ambient and elevated temperatures. *J Phys Chem* 86: 1588–1590. doi: 10.1021/j100206a023

Chu W, Chan KH, Kwan CY, Choi KY (2007) Degradation of atrazine by modified stepwise-Fenton's processes. *Chemosphere* 67: 755–761. doi: 10.1016/j.chemosphere.2006.10.039

Clara M, Strenn B, Gans O, Martinez E, Kreuzinger N, Kroiss H (2005) Removal of selected pharmaceuticals, fragrances and endocrine disrupting compounds in a membrane bioreactor and conventional wastewater treatment plants. *Water Res* 39: 4797–4807. doi: 10.1016/j.watres.2005.09.015

Clifton CL, Huie RE (1989) Rate constants for hydrogen abstraction reactions of the sulfate radical, $SO_4^-$. Alcohols. *Int J Chem Kinet* 21: 677–687. doi: 10.1002/kin.550210807

Coddington JW, Hurst JK, Lymar S V. (1999) Hydroxyl Radical Formation during Peroxynitrous Acid Decomposition. *J Am Chem Soc* 121: 2438–2443. doi: 10.1021/ja982887t

Coelho A, Castro A V, Dezotti M, Sant'Anna GL (2006) Treatment of petroleum refinery sourwater by advanced oxidation processes. *J Hazard Mater* 137: 178–184. doi: 10.1016/j.jhazmat.2006.01.051

Comninellis C, Kapalka A, Malato S, Parsons SA, Poulios I, Mantzavinos D (2008) Advanced oxidation processes for water treatment: advances and trends for R&D. *J Chem Technol Biotechnol* 83: 769–776. doi: 10.1002/jctb.1873

Cooper GD, DeGraff BA (1972) Photochemistry of the monoxalatoiron(III) ion. *J Phys Chem* 76: 2618–2625. doi: 10.1021/j100662a027

Crane M, Watts C, Boucard T (2006) Chronic aquatic environmental risks from exposure to human pharmaceuticals. *Sci Total Environ* 367: 23–41. doi: 10.1016/j.scitotenv.2006.04.010

Crittenden JC, Zhang Y, Hand DW, Perram DL, Marchand EG (1996) Solar detoxification of fuel-contaminated groundwater using fixed-bed photocatalysts. *Water Environ Res* 68: 270–279.

da Silva SS, Chiavone-Filho O, de Barros Neto EL, Nascimento CAO (2012) Integration of processes induced air flotation and photo-Fenton for treatment of residual waters contaminated with xylene. *J Hazard Mater* 199-200: 151–157. doi: 10.1016/j.jhazmat.2011.10.070

Dantas RF, Canterino M, Marotta R, Sans C, Esplugas S, Andreozzi R (2007) Bezafibrate removal by means of ozonation: Primary intermediates, kinetics, and toxicity assessment. *Water Res* 41: 2525–2532. doi: 10.1016/j.watres.2007.03.011

Dantas RF, Contreras S, Sans C, Esplugas S (2008) Sulfamethoxazole abatement by means of ozonation. *J Hazard Mater* 150: 790–794. doi: 10.1016/j.jhazmat.2007.05.034

Dao YH, De Laat J (2011) Hydroxyl radical involvement in the decomposition of hydrogen peroxide by ferrous and ferric-nitrilotriacetate complexes at neutral pH. *Water Res* 45: 3309–3317. doi: 10.1016/j.watres.2011.03.043

De la Cruz N, Romero V, Dantas RF, Marco P, Bayarri B, Giménez J, Esplugas S (2013) o-Nitrobenzaldehyde actinometry in the presence of suspended $TiO_2$ for photocatalytic reactors. *Catal Today* 209: 209–214. doi: 10.1016/j.cattod.2012.08.035

De Laat J, Dao YH, Hamdi El Najjar N, Daou C (2011) Effect of some parameters on the rate of the catalysed decomposition of hydrogen peroxide by iron(III)-nitrilotriacetate in water. *Water Res* 45: 5654–5664. doi: 10.1016/j.watres.2011.08.028

De Laat J, Gallard H, Ancelin S, Legube B (1999) Comparative study of the oxidation of atrazine and acetone by $H_2O_2$/UV, Fe(III)/UV, Fe(III)/$H_2O_2$/UV and Fe(II) or Fe(III)/$H_2O_2$. *Chemosphere* 39: 2693–2706. doi: 10.1016/S0045-6535(99)00204-0

de Lima Perini JA, Perez-Moya M, Nogueira RFP (2013) Photo-Fenton degradation kinetics of low ciprofloxacin concentration using different iron sources and pH. *J Photochem Photobiol A Chem* 259: 53–58. doi: 10.1016/j.jphotochem.2013.03.002

De Luca A, Dantas RF, Esplugas S (2014) Assessment of iron chelates efficiency for photo-Fenton at neutral pH. *Water Res* 61: 232–242. doi: 10.1016/j.watres.2014.05.033

Echigo S, Minear RA (2006) Kinetics of the reaction of hypobromous acid and organic matters in water treatment processes. *Water Sci Technol* 53: 235–243. doi: 10.2166/wst.2006.358

Egli T (2001) Biodegradation of metal-complexing aminopolycarboxylic acids. *J Biosci Bioeng* 92: 89–97. doi: 10.1016/S1389-1723(01)80207-3

Elmolla E, Chaudhuri M (2009a) Optimization of Fenton process for treatment of amoxicillin, ampicillin and cloxacillin antibiotics in aqueous solution. *J Hazard Mater* 170: 666–672. doi: 10.1016/j.jhazmat.2009.05.013

Elmolla ES, Chaudhuri M (2009b) Degradation of the antibiotics amoxicillin, ampicillin and cloxacillin in aqueous solution by the photo-Fenton process. *J Hazard Mater* 172: 1476–1481. doi: 10.1016/j.jhazmat.2009.08.015

Elmolla ES, Chaudhuri M (2011) Combined photo-Fenton-SBR process for antibiotic wastewater treatment. *J Hazard Mater* 192: 1418–1426. doi: 10.1016/j.jhazmat.2011.06.057

Emilio CA, Jardim WF, Litter MI, Mansilla HD (2002) EDTA destruction using the solar ferrioxalate advanced oxidation technology (AOT): Comparison with solar photo-Fenton treatment. *J Photochem Photobiol A Chem* 151: 121–127. doi: 10.1016/S1010-6030(02)00173-9

European Commission. Directive 2000/60/EC, Pub. L. No. DOUE, L 327 (2000). Diario Oficial de las Comunidades Europeas.

European Commission. Error correction Regulation (EC) 850/2004, Pub. L. No. DOUE, L 229 (2004). Diario oficial de la Unión europea.

European Commission. Regulation (EC) 850/2004, Pub. L. No. DOUE, L 158 (2004). Diario oficial de la Unión europea.

European Commission. 2006/507/EC, Pub. L. No. DOUE, L 209 (2006).

European Commission. Regulation (EC) 1195/2006, Pub. L. No. DOUE, L 217 (2006). Diario oficial de la Unión europea.

European Commission. Error correction Regulation (EC) 850/2004, Pub. L. No. DOUE, L 204 (2007). Diario oficial de la Unión europea.

European Commission. Regulation (EC) 172/2007, Pub. L. No. DOUE, L 55 (2007). Diario oficial de la Unión europea.

European Commission. Regulation (EC) 323/2007, Pub. L. No. DOUE, L 85 (2007). Diario oficial de la Unión europea.

European Commission. Directive 2008/105/EC, Pub. L. No. DOUE, L348 (2008). Diario oficial de la Unión europea.

European Commission. Directive 2009/90/EC, Pub. L. No. DOUE, L201 (2009). Diario oficial de la Unión europea.

European Commission. Regulation (EC) 304/2009, Pub. L. No. DOUE, L 96 (2009). Diario oficial de la Unión europea.

European Commission. Regulation (EU) 756/2010, Pub. L. No. DOUE, L 223 (2010). Diario oficial de la Unión europea.

European Commission. Regulation (EU) 757/2010, Pub. L. No. DOUE, L223 (2010). Diario oficial de la Unión europea.

European Commission. Regulation (EU) 519/2012, Pub. L. No. DOUE, L159 (2012). Diario oficial de la Unión europea.

European Commission. Regulation (EU) No 1342/2014, Pub. L. No. DOUE, L363 (2014). Diario oficial de la Unión europea.

European Commission (2014a) Water http://ec.europa.eu/environment/water/index_en.htm

European Environment Agency. (2012). Water resources in Europe in the context of vulnerability (pp. 1–96).

European Federation of Pharmaceutical Industry and Associations. (EFPIA). (2014). The pharmaceutical industry in figures. Retrieved from http://www.efpia.eu/uploads/Figures_2014_Final.pdf

European Union. Decisión 2007/639, Pub. L. No. DOUE, L 258 (2007). Diario oficial de la Unión europea.

European Union. Decisión 2009/63, Pub. L. No. DOUE, L 23 (2009).

Fang J-Y, Shang C (2012) Bromate formation from bromide oxidation by the UV/persulfate process. *Environ Sci Technol* 46: 8976–8983. doi: 10.1021/es300658u

Farré MJ, Doménech X, Peral J (2006) Assessment of photo-Fenton and biological treatment coupling for Diuron and Linuron removal from water. *Water Res* 40: 2533–2540. doi: 10.1016/j.watres.2006.04.034

Fatta-Kassinos D, Dionysiou DD, Kümmerer K (2016) Advanced Treatment Technologies for Urban Wastewater Reuse. Springer International Publishing, Berlin (Germany).

Faust BC, Hoigné J (1990) Photolysis of Fe (III)-hydroxy complexes as sources of OH radicals in clouds, fog and rain. *Atmos Environ Part A Gen Top* 24: 79–89. doi: 10.1016/0960-1686(90)90443-Q

Feng J, Hu X, Yue PL, Zhu HY, Lu GQ (2003) Discoloration and mineralization of Reactive Red HE-3B by heterogeneous photo-Fenton reaction. *Water Res* 37: 3776–3784. doi: 10.1016/S0043-1354(03)00268-9

Flynn CM (1984) Hydrolysis of inorganic iron(III) salts. *Chem Rev* 84: 31–41. doi: 10.1021/cr00059a003

Furia TE (1973) CRC Handbook of Food Additives, Second Edition, Boca Raton (FL,USA) Volum 1.

Furman OS, Teel AL, Watts RJ (2010) Mechanism of Base Activation of Persulfate. *Environ Sci Technol* 44: 6423–6428. doi: 10.1021/es1013714

Gallard H (2000) Kinetic modelling of Fe(III)/$H_2O_2$ oxidation reactions in dilute aqueous solution using atrazine as a model organic compound. *Water Res* 34: 3107–3116. doi: 10.1016/S0043-1354(00)00074-9

Galvão SAO, Mota ALN, Silva DN, Moraes JEF, Nascimento CAO, Chiavone FO (2006) Application of the photo-Fenton process to the treatment of wastewaters contaminated with diesel. *Sci Total Environ* 367: 42–49. doi: 10.1016/j.scitotenv.2006.01.014

Garrido-Ramírez EG, Theng BK., Mora ML (2010) Clays and oxide minerals as catalysts and nanocatalysts in Fenton-like reactions — A review. *Appl Clay Sci* 47: 182–192. doi: 10.1016/j.clay.2009.11.044

Gatermann R, Hühnerfuss H, Rimkus G, Wolf M, Franke S (1995) The distribution of nitrobenzene and other nitroaromatic compounds in the North Sea. *Mar Pollut Bull* 30: 221–227. doi: 10.1016/0025-326X(94)00161-2

Gavrilescu M (2005) Fate of pesticides in the environment and its bioremediation. *Eng Life Sci* 5: 497–526.

Generalitat de Catalunya Preus de l'energia. Institut Català d'Energia. http://icaen.gencat.cat/ca/pice_serveis/pice_estadistiques_energetiques/pice_resultats/pice_preus_de_l_energia/. Accessed 2 Jun 2016

Gennaro A (1995) Remington: The Science and Practice of Pharmacy19th. Mack Publishing Company, Easton, PA, pp 1276–1277

Gerecke AC, Schärer M, Singer HP, Müller SR, Schwarzenbach RP, Sägesser M, Ochsenbein U, Popow G (2002) Sources of pesticides in surface waters in Switzerland: pesticide load through waste water treatment plants—current situation and reduction potential. *Chemosphere* 48: 307–315. doi: 10.1016/S0045-6535(02)00080-2

Gfrerer M, Wenzl T, Quan X, Platzer B. Lankmayr E (2002) Occurrence of triazines in surface and drinking water of Liaoning Province in Eastern China. *J Biochem Biophys Methods* 53: 217–228. doi: 10.1016/S0165-022X(02)00110-0

Ghosh PK, Philip L (2006) Environmental significance of atrazine in aqueous systems and its removal by biological processes: an overview. *Glob NEST J* 8: 159–178.

Ginebreda A, Muñoz I, de Alda ML, Brix R, López-Doval J, Barceló D (2010) Environmental risk assessment of pharmaceuticals in rivers: relationships between hazard indexes and aquatic macroinvertebrate diversity indexes in the Llobregat River (NE Spain). *Environ Int* 36: 153–162. doi: 10.1016/j.envint.2009.10.003

Giokas DL, Salvador A, Chisvert A (2007) UV filters: From sunscreens to human body and the environment. *TrAC Trends Anal Chem* 26: 360–374. doi: 10.1016/j.trac.2007.02.012

Glassmeyer ST, Furlong ET, Kolpin DW, Cahill JD, Zaugg SD, Werner SL, Meyer MT, Kryak DD (2005) Transport of Chemical and Microbial Compounds from Known Wastewater Discharges: Potential for Use as Indicators of Human Fecal Contamination. *Environ Sci Technol* 39: 5157–5169. doi: 10.1021/es048120k

Glaze WH (1987) Drinking-water treatment with ozone. *Environ Sci Technol* 21: 224–230. doi: 10.1021/es00157a001

Glaze WH, Kang J-W, Chapin DH (1987) The Chemistry of Water Treatment Processes Involving Ozone, Hydrogen Peroxide and Ultraviolet Radiation. *Ozone Sci Eng* 9: 335–352. doi: 10.1080/01919518708552148

Göbel A, Thomsen A, McArdell CS, Joss A, Giger W (2005) Occurrence and Sorption Behavior of Sulfonamides, Macrolides, and Trimethoprim in Activated Sludge Treatment. *Environ Sci Technol* 39: 3981–3989. doi: 10.1021/es048550a

Gogate PR, Pandit AB (2004) A review of imperative technologies for wastewater treatment I: oxidation technologies at ambient conditions. *Adv Environ Res* 8: 501–551. doi: 10.1016/S1093-0191(03)00032-7

Gojković SL, Gupta S, Savinell R. (1999) Heat-treated iron(III) tetramethoxyphenyl porphyrin chloride supported on high-area carbon as an electrocatalyst for oxygen reduction. *J Electroanal Chem* 462: 63–72. doi: 10.1016/S0022-0728(98)00390-8

González O, Sans C, Esplugas S (2007) Sulfamethoxazole abatement by photo-Fenton toxicity, inhibition and biodegradability assessment of intermediates. *J Hazard Mater* 146: 459–464. doi: 10.1016/j.jhazmat.2007.04.055

Gonzalez-Olmos R, Holzer F, Kopinke F-D, Georgi A (2011) Indications of the reactive species in a heterogeneous Fenton-like reaction using Fe-containing zeolites. *Appl Catal A Gen* 398: 44–53. doi: 10.1016/j.apcata.2011.03.005

Gosh PK, Philip L (2006) Environmental significance of atrazine in aqueous systems and its removal by biological processes: an overview. *Glob NEST J* 8: 159–178.

Gozzi F, Machulek A, Ferreira VS, Osugi ME, Santos APF, Nogueira JA, Dantas RF, Esplugas S, de Oliveira SC (2012) Investigation of chlorimuron-ethyl degradation by Fenton, photo-Fenton and ozonation processes. *Chem Eng J* 210: 444–450. doi: 10.1016/j.cej.2012.09.008

Grebel JE, Pignatello JJ, Mitch WA (2010) Effect of halide ions and carbonates on organic contaminant degradation by hydroxyl radical-based advanced oxidation processes in saline waters. *Environ Sci Technol* 44: 6822–6828. doi: 10.1021/es1010225

Gu X, Lu S, Qiu Z, Sui Q, Banks CJ, Imai T, Lin , Luo Q (2013) Photodegradation performance of 1,1,1-trichloroethane in aqueous solution: In the presence and absence of persulfate. *Chem Eng J* 215: 29–35. doi: 10.1016/j.cej.2012.09.132

Guenter Kari F, Hilger S, Canonica S (1995) Determination of the Reaction Quantum Yield for the Photochemical Degradation of Fe(III)-EDTA: Implications for the Environmental Fate of EDTA in Surface Waters. *Environ Sci Technol* 29: 1008–1017. doi: 10.1021/es00004a022

Haag WR, Hoigne J (1983) Ozonation of bromide-containing waters: kinetics of formation of hypobromous acid and bromate. *Environ Sci Technol* 17: 261–267. doi: 10.1021/es00111a004

Haag WR, Yao CCD (1992) Rate Constants for Reaction of Hydroxyl Radicals with Several Drinking Water Contaminants. *Environ Sci Technol* 26: 1005–1013.

Hanna K, Chiron S, Oturan MA (2005) Coupling enhanced water solubilization with cyclodextrin to indirect electrochemical treatment for pentachlorophenol contaminated soil remediation. *Water Res* 39: 2763–2773. doi: 10.1016/j.watres.2005.04.057

Hatchard CG, Parker CA (1956a) A New Sensitive Chemical Actinometer. II. Potassium Ferrioxalate as a Standard Chemical Actinometer. *Proc R Soc A Math Phys Eng Sci* 235: 518–536. doi: 10.1098/rspa.1956.0102

Hatchard CG, Parker CA (1956b) A New Sensitive Chemical Actinometer. II. Potassium Ferrioxalate as a Standard Chemical Actinometer. *Proc R Soc A Math Phys Eng Sci* 235: 518–536. doi: 10.1098/rspa.1956.0102

He X, Mezyk SP, Michael I, Fatta-Kassinos, Dionysiou DD (2014) Degradation kinetics and mechanism of β-lactam antibiotics by the activation of $H_2O_2$ and $Na_2S_2O_8$ under UV-254nm irradiation. *J Hazard Mater* 279: 375–383. doi: 10.1016/j.jhazmat.2014.07.008

He X, Pelaez M, Westrick JA, O'Shea, Kevin E, Hiskia A, Triantis T, Kaloudis T, Stefan MI, de la Cruz AA, Dionysiou DD (2012) Efficient removal of microcystin-LR by UV-C/$H_2O_2$ in synthetic and natural water samples. *Water Res* 46: 1501–1510. doi: 10.1016/j.watres.2011.11.009

Heberer T (2002) Occurrence, fate, and removal of pharmaceutical residues in the aquatic environment: a review of recent research data. *Toxicol Lett* 131: 5–17. doi: 10.1016/S0378-4274(02)00041-3

Heeb MB, Criquet J, Zimmermann-Steffens SG, von Gunten U (2014) Oxidative treatment of bromide-containing waters: formation of bromine and its reactions with inorganic and organic compounds--a critical review. *Water Res* 48: 15–42. doi: 10.1016/j.watres.2013.08.030

Hernando MD, Gómez MJ, Agüera A, Fernández-Alba AR (2007) LC-MS analysis of basic pharmaceuticals (beta-blockers and anti-ulcer agents) in wastewater and surface water. *TrAC Trends Anal Chem* 26: 581–594. doi: 10.1016/j.trac.2007.03.005

Herrmann H (2007) On the photolysis of simple anions and neutral molecules as sources of O-/OH, SO(x)- and Cl in aqueous solution. *Phys Chem Chem Phys* 9: 3935–3964. doi: 10.1039/b618565g

Hislop KA, Bolton JR (1999) The Photochemical Generation of Hydroxyl Radicals in the UV−vis/Ferrioxalate/$H_2O_2$ System. *Environ Sci Technol* 33: 3119–3126. doi: 10.1021/es9810134

Hişmioğullari ŞE, Yarsan E (2009) Spectrophotometric determination and stability studies of sulfamethoxazole and trimethoprim in oral suspension by classical least square calibration method. *Hacettepe Univ J Fac Pharm* 29: 95–104.

Hoigné J (1998) Chemistry of Aqueous Ozone and Transformation of Pollutants by Ozonation and Advanced Oxidation Processes. In: Hrubec J (ed) Quality and Treatment of Drinking Water II. Springer Berlin Heidelberg, Berlin, Heidelberg, pp 83–141

Hoigné J, Bader H (1976) The role of hydroxyl radical reactions in ozonation processes in aqueous solutions. *Water Res* 10: 377–386. doi: 10.1016/0043-1354(76)90055-5

Homem V, Santos L (2011) Degradation and removal methods of antibiotics from aqueous matrices--a review. *J Environ Manage* 92: 2304–2347. doi: 10.1016/j.jenvman.2011.05.023

Howsawkeng J, Watts RJ, Washington DL, Teel AL, Hess TF, Crawford RL (2001) Evidence for Simultaneous Abiotic−Biotic Oxidations in a Microbial-Fenton's System. *Environ Sci Technol* 35: 2961–2966. doi: 10.1021/es001802x

Huang K-C, Zhao Z, Hoag GE, Dahmani A, Block PA (2005) Degradation of volatile organic compounds with thermally activated persulfate oxidation. *Chemosphere* 61: 551–560. doi: 10.1016/j.chemosphere.2005.02.032

Huang W, Brigante M, Wu F, Mousty C, Hanna K, Mailhot G (2013) Assessment of the Fe(III)–EDDS Complex in Fenton-Like Processes: From the Radical Formation to the Degradation of Bisphenol A. *Environ Sci Technol* 47: 1952–1959. doi: 10.1021/es304502y

Huang W, Brigante M, Wu F, Hanna K, Mailhot G (2012) Development of a new homogenous photo-Fenton process using Fe(III)-EDDS complexes. *J Photochem Photobiol A Chem* 239: 17–23. doi: 10.1016/j.jphotochem.2012.04.018

Huang Y-H, Huang Y-J, Tsai H-C, Chen H-T (2010) Degradation of phenol using low concentration of ferric ions by the photo-Fenton process. *J Taiwan Inst Chem Eng* 41: 699–704. doi: 10.1016/j.jtice.2010.01.012

Huston PL, Pignatello JJ (1999) Degradation of selected pesticide active ingredients and commercial formulations in water by the photo-assisted Fenton reaction. *Water Res* 33: 1238–1246. doi: 10.1016/S0043-1354(98)00330-3

Iglesias Esteban R, Ortega de Miguel E (2008) Present and future of wastewater reuse in Spain. *Desalination* 218: 105–119. doi: 10.1016/j.desal.2006.09.031

Iglesias R, Ortega E, Batanero G, Quintas L (2010) Water reuse in Spain: Data overview and costs estimation of suitable treatment trains. *Desalination* 263: 1–10. doi: 10.1016/j.desal.2010.06.038

Ikehata K, El-Din MG (2006) Aqueous pesticide degradation by hydrogen peroxide/ultraviolet irradiation and Fenton-type advanced oxidation processes: a review. *J Environ Eng Sci* 5: 81–135. doi: 10.1139/s05-046

International Organization for Standardization (1988) ISO 6332: Water quality — Determination of iron — Spectrometric method using 1,10-phenanthroline.

Jeong J, Yoon J (2005) pH effect on OH radical production in photo/ferrioxalate system. *Water Res* 39: 2893–2900. doi: 10.1016/j.watres.2005.05.014

Jiang X, Wu Y, Wang P, Li H, Dong W (2013) Degradation of bisphenol A in aqueous solution by persulfate activated with ferrous ion. *Environ Sci Pollut Res* 20: 4947–4953. doi: 10.1007/s11356-013-1468-5

Jo Y-H, Do S-H, Kong S-H (2014) Persulfate activation by iron oxide-immobilized $MnO_2$ composite: Identification of iron oxide and the optimum pH for degradations. *Chemosphere* 95: 550–555. doi: 10.1016/j.chemosphere.2013.10.010

Kari FG, Giger W (1996) Speciation and fate of ethylenediaminetetraacetate (EDTA) in municipal wastewater treatment. *Water Res* 30: 122–134. doi: 10.1016/0043-1354(95)00125-5

Kasprzyk-Hordern B, Dinsdale RM, Guwy AJ (2008) The occurrence of pharmaceuticals, personal care products, endocrine disruptors and illicit drugs in surface water in South Wales, UK. *Water Res* 42: 3498–518. doi: 10.1016/j.watres.2008.04.026

Kassinos D, Varnava N, Michael C, Piera P (2009) Homogeneous oxidation of aqueous solutions of atrazine and fenitrothion through dark and photo-Fenton reactions. *Chemosphere* 74: 866–72. doi: 10.1016/j.chemosphere.2008.10.008

Katsumata H, Kaneco S, Suzuki T, Ohta K, Yobiko Y (2005) Degradation of linuron in aqueous solution by the photo-Fenton reaction. *Chem Eng J* 108: 269–276. doi: 10.1016/j.cej.2005.02.029

Kearney PC, Roberts T (1998) Pesticide remediation in soils and water. Wiley, New York (NY, USA).

Khan JA, He X, Shah NS, Khan HM, Hapeshi E, Fatta-Kassinos D, Dionysiou DD. (2014) Kinetic and mechanism investigation on the photochemical degradation of atrazine with activated $H_2O_2$, $S_2O_8^{2-}$ and $HSO_5^-$. *Chem Eng J* 252: 393–403. doi: 10.1016/j.cej.2014.04.104

Kim SD, Cho J, Kim IS, Vanderford BJ, Snyder SA (2007) Occurrence and removal of pharmaceuticals and endocrine disruptors in South Korean surface, drinking, and waste waters. *Water Res* 41: 1013–1021. doi: 10.1016/j.watres.2006.06.034

Klamerth N, Malato S, Agüera A, Fernández-Alba A (2013) Photo-Fenton and modified photo-Fenton at neutral pH for the treatment of emerging contaminants in wastewater treatment plant effluents: A comparison. *Water Res* 47: 833–840. doi: 10.1016/j.watres.2012.11.008

Klaning UK, Sehested K, Appelman EH (1991) Laser flash photolysis and pulse radiolysis of aqueous solutions of the fluoroxysulfate ion, $SO_4F_.$. *Inorg Chem* 30: 3582–3584. doi: 10.1021/ic00018a040

Kläning UK, Wolff T (1985) Laser Flash Photolysis of HClO, $ClO_2^-$, HBrO, and $BrO_2^-$ in Aqueous Solution. Reactions of Cl- and Br-Atoms. *Berichte der Bunsengesellschaft für Phys Chemie* 89: 243–245. doi: 10.1002/bbpc.19850890309

Kolpin DW, Furlong ET, Meyer MT, Thurman EM, Zaugg SD, Barber LB, Buxton HT (2002) Pharmaceuticals, Hormones, and Other Organic Wastewater Contaminants in U.S. Streams, 1999−2000: A National Reconnaissance. *Environ Sci Technol* 36: 1202–1211. doi: 10.1021/es011055j

Kolthoff IM, Medalia AI, Raaen HP (1951) The reaction between ferrous iron and peroxides. IV. Reaction with potassium persulfate. J Am Chem Soc 73:1733–1739.

Ku Y, Wang L-S, Shen Y-S (1998) Decomposition of EDTA in aqueous solution by UV/H2O2 process. *J Hazard Mater* 60: 41–55. doi: 10.1016/S0304-3894(97)00153-2

Kuhn HJ, Braslavsky SE, Schmidt R (2004) Chemical actinometry ( IUPAC Technical Report ). *Pure Appl Chem* 76: 2105–2146.

Lam MW, Mabury SA (2005) Photodegradation of the pharmaceuticals atorvastatin, carbamazepine, levofloxacin, and sulfamethoxazole in natural waters. *Aquat Sci* 67: 177–188. doi: 10.1007/s00027-004-0768-8

Lapworth DJ, Baran N, Stuart ME, Ward RS (2012) Emerging organic contaminants in groundwater: A review of sources, fate and occurrence. *Environ Pollut* 163:287–303. doi: 10.1016/j.envpol.2011.12.034

Li Y, Sun J, Sun S-P (2016) $Mn^{2+}$-mediated homogeneous Fenton-like reaction of Fe(III)-NTA complex for efficient degradation of organic contaminants under neutral conditions. *J Hazard Mater* 313: 193–200. doi: 10.1016/j.jhazmat.2016.04.003

Liang C, Guo Y (2010) Mass Transfer and Chemical Oxidation of Naphthalene Particles with Zerovalent Iron Activated Persulfate. *Environ Sci Technol* 44: 8203–8208. doi: 10.1021/es903411a

Liang C, Liang C-P, Chen C-C (2009) pH dependence of persulfate activation by EDTA/Fe(III) for degradation of trichloroethylene. *J Contam Hydrol* 106: 173–182. doi: 10.1016/j.jconhyd.2009.02.008

Libert B, Franceschi VR (1987) Oxalate in crop plants. *J Agric Food Chem* 35: 926–938. doi: 10.1021/jf00078a019

Lindsey ME, Meyer M, Thurman EM (2001) Analysis of Trace Levels of Sulfonamide and Tetracycline Antimicrobials in Groundwater and Surface Water Using Solid-Phase Extraction and Liquid Chromatography/Mass Spectrometry. *Anal Chem* 73: 4640–4646. doi: 10.1021/ac010514w

Lipczynska-Kochany E, Sprah G, Harms S (1995) Influence of some groundwater and surface waters constituents on the degradation of 4-chlorophenol by the Fenton reaction. *Chemosphere* 30: 9–20. doi: 10.1016/0045-6535(94)00371-Z

Litter MI, Quici N (2010) Photochemical Advanced Oxidation Processes for Water and Wastewater Treatment. *Recent Patents Eng* 4: 217–241.

Luo Y, Guo W, Ngo HH, Nghiem LD, Hai FI, Zhang J, Liang S, Wang XC (2014) A review on the occurrence of micropollutants in the aquatic environment and their fate and removal during wastewater treatment. *Sci Total Environ* 473-474: 619–641. doi: 10.1016/j.scitotenv.2013.12.065

Lutze H V, Bakkour R, Kerlin N, von Sonntag C, Schmidt TC (2014) Formation of bromate in sulfate radical based oxidation: mechanistic aspects and suppression by dissolved organic matter. *Water Res* 53: 370–377. doi: 10.1016/j.watres.2014.01.001

Ma WT, Fu KK, Cai Z, Jiang GB (2003) Gas chromatography/mass spectrometry applied for the analysis of triazine herbicides in environmental waters. *Chemosphere* 52: 1627–1632. doi: 10.1016/S0045-6535(03)00502-2

Mamou A, Rabani J, Behar D (1977) Oxidation of aqueous $Br^-$ by OH radicals, studied by pulse radiolysis. [Electrons]. *J. Phys. Chem.* 81 (15): 1447-1448.

Manning PG, Ramamoorthy S (1973) Equilibrium studies of metal-ion complexes of interest to natural waters — VII Mixed-ligand complexes of Cu(II) involving fulvic acid as primary ligand. *J Inorg Nucl Chem* 35: 1577–1581. doi: 10.1016/0022-1902(73)80248-9

Marchini S, Passerini L, Cesareo D, Tosato ML (1988) Herbicidal triazines: Acute toxicity onDaphnia, fish, and plants and analysis of its relationships with structural factors. *Ecotoxicol Environ Saf* 16: 148–157. doi: 10.1016/0147-6513(88)90029-2

Mark G, Schuchmann MN, Schuchmann H-P, von Sonntag C (1990) The photolysis of potassium peroxodisulphate in aqueous solution in the presence of tert-butanol: a simple actinometer for 254 nm radiation. *J Photochem Photobiol A Chem* 55: 157–168. doi: 10.1016/1010-6030(90)80028-V

Maruthamuthu P, Neta P (1978) Phosphate radicals. Spectra, acid-base equilibriums, and reactions with inorganic compounds. *J Phys Chem* 82: 710–713. doi: 10.1021/j100495a019

Matos TAF, Dias ALN, Reis ADP, da Silva MRA, Kondo MM (2012) Degradation of Abamectin Using the Photo-Fenton Process. *Int J Chem Eng* 7.

Matthew BM, Anastasio C (2006) A chemical probe technique for the determination of reactive halogen species in aqueous solution: Part 1 – bromide solutions. *Atmos Chem Phys* 6: 2423–2437. doi: 10.5194/acp-6-2423-2006

Means JL, Kucak T, Crerar DA (1980) Relative degradation rates of NTA, EDTA and DTPA and environmental implications. *Environ Pollut Ser B, Chem Phys* 1: 45–60. doi: 10.1016/0143-148X(80)90020-8

Meneses M, Pasqualino JC, Castells F (2010) Environmental assessment of urban wastewater reuse: treatment alternatives and applications. *Chemosphere* 81: 266–272. doi: 10.1016/j.chemosphere.2010.05.053

Min G, Wang S, Zhu H, Fang G, Zhang Y (2008) Multi-walled carbon nanotubes as solid-phase extraction adsorbents for determination of atrazine and its principal metabolites in water and soil samples by gas chromatography-mass spectrometry. *Sci Total Environ* 396: 79–85. doi: 10.1016/j.scitotenv.2008.02.016

Ministerio de Agricultura A y MA Plan Nacional de Reutilización de Aguas - Participación pública - Participación pública - Agua - magrama.es. http://www.magrama.gob.es/es/agua/participacion-publica/pnra.aspx#. Accessed 31 May 2016

Miranda-García N, Maldonado MI, Coronado JM, Malato S (2010) Degradation study of 15 emerging contaminants at low concentration by immobilized TiO2 in a pilot plant. *Catal Today* 151: 107–113. doi: 10.1016/j.cattod.2010.02.044

Miró P, Arques A, Amat AM, Marín García ML, Miranda Alonso MA (2013) A mechanistic study on the oxidative photodegradation of 2,6-dichlorodiphenylamine-derived drugs: Photo-Fenton versus photocatalysis with a triphenylpyrylium salt. *Appl Catal B Environ* 140-141: 412–418. doi: 10.1016/j.apcatb.2013.04.042

Monteagudo JM, Durán A, Aguirre M, San Martín I (2011) Optimization of the mineralization of a mixture of phenolic pollutants under a ferrioxalate-induced solar photo-Fenton process. *J Hazard Mater* 185: 131–139. doi: 10.1016/j.jhazmat.2010.09.007

Monteagudo JM, Durán A, Culebradas R, San Martín I, Carnicer A (2013) Optimization of pharmaceutical wastewater treatment by solar/ferrioxalate photo-catalysis. *J Environ Manage* 128: 210–219. doi: 10.1016/j.jenvman.2013.05.013

Monteith HD, Parker WJ, Bell JP, Melcer H (1995) Modeling the fate of pesticides in municipal wastewater treatment. *Water Environ Res* 67: 964–970. doi: 10.2175/106143095X133194

Morel FMM, Hering JG (1993) Principles and Applications of Aquatic Chemistry. Wiley, New York (NY, USA).

Muñoz I, Gómez-Ramos MJ, Agüera A, Fernández-Alba AR, García-Reyes JF, Molina-Díaz A (2009) Chemical evaluation of contaminants in wastewater effluents and the environmental risk of reusing effluents in agriculture. *TrAC Trends Anal Chem* 28: 676–694. doi: 10.1016/j.trac.2009.03.007

Navarro S, Vela N, Giménez MJ, Navarro G (2004) Persistence of four s-triazine herbicides in river, sea and groundwater samples exposed to sunlight and darkness under laboratory conditions. *Sci Total Environ* 329: 87–97. doi: 10.1016/j.scitotenv.2004.03.013

Nentwig G (2007) Effects of pharmaceuticals on aquatic invertebrates. Part II: the antidepressant drug fluoxetine. *Arch Environ Contam Toxicol* 52: 163–170. doi: 10.1007/s00244-005-7190-7

Neta P, Huie RE, Ross AB (1988) Rate Constants for Reactions of Inorganic Radicals in Aqueous Solution. *J Phys Chem Ref Data* 17: 1027–1284. doi: 10.1063/1.555808

Neta P, Madhavan V, Zemel H, Fessenden RW (1977) Rate constants and mechanism of reaction of sulfate radical anion with aromatic compounds. *J Am Chem Soc* 99: 163–164. doi: 10.1021/ja00443a030

Neyens E, Baeyens J (2003) A review of classic Fenton's peroxidation as an advanced oxidation technique. *J Hazard Mater* 98: 33–50. doi: 10.1016/S0304-3894(02)00282-0

Nitoi I, Oncescu T, Oancea P (2013) Mechanism and kinetic study for the degradation of lindane by photo-Fenton process. *J Ind Eng Chem* 19: 305–309. doi: 10.1016/j.jiec.2012.08.016

Nogueira KRB, Teixeira ACSC, Nascimento CAO, Guardani R (2008) Use of solar energy in the treatment of water contaminated with phenol by photochemical processes. *Brazilian J Chem Eng* 25: 671–682. doi: 10.1590/S0104-66322008000400005

Nogueira RFP, Oliveira MC, Paterlini WC (2005a) Simple and fast spectrophotometric determination of $H_2O_2$ in photo-Fenton reactions using metavanadate. *Talanta* 66: 86–91. doi: 10.1016/j.talanta.2004.10.001

Nogueira RFP, Silva MRA, Trovó AG (2005b) Influence of the iron source on the solar photo-Fenton degradation of different classes of organic compounds. *Sol Energy* 79: 384–392. doi: 10.1016/j.solener.2005.02.019

Nowack B, Stone AT (2002) Homogeneous and Heterogeneous Oxidation of Nitrilotrismethylenephosphonic Acid (NTMP) in the Presence of Manganese(II, III) and Molecular Oxygen. *J Phys Chem B* 106: 6227–6233. doi: 10.1021/jp014293+

Park S, Choi K (2008) Hazard assessment of commonly used agricultural antibiotics on aquatic ecosystems. *Ecotoxicology* 17: 526–538. doi: 10.1007/s10646-008-0209-x

Pera-Titus M, García-Molina V, Baños MA, Giménez J, Esplugas S (2004) Degradation of chlorophenols by means of advanced oxidation processes: a general review. *Appl Catal B Environ* 47: 219–256. doi: 10.1016/j.apcatb.2003.09.010

Pérez M, Torrades F, Domènech X, Peral J (2002) Fenton and photo-Fenton oxidation of textile effluents. *Water Res* 36: 2703–2710. doi: 10.1016/S0043-1354(01)00506-1

Petala M, Tsiridis V, Samaras P, Zouboulis A, Sakellaropoulos GP (2006) Wastewater reclamation by advanced treatment of secondary effluents. *Desalination* 195: 109–118. doi: 10.1016/j.desal.2005.10.037

Petrovic M, Barceló D (2006) Application of liquid chromatography/quadrupole time-of-flight mass spectrometry (LC-QqTOF-MS) in the environmental analysis. *J Mass Spectrom* 41: 1259–1267. doi: 10.1002/jms.1103

Petrovic M, Radjenovic J, Barcelo D (2011) Advanced oxidation processes (AOPs) applied for wastewater and drinking water treatment. Elimination of pharmaceuticals. *Holist Approach to Environ* 1: 63–74.

Peyton GR, Bell OJ, Girin E, LeFaivre MH, Sanders J (1998) Effect of Bicarbonate Alkalinity on Performance of Advanced Oxidations Processes (Project# 533). http://www.waterrf.org/ExecutiveSummaryLibrary/90737_533_profile.pdf

Phillips PJ, Smith SG, Kolpin DW, Zaugg SD, Buxton HT, Furlong ET, Esposito K, Stinson B (2010) Pharmaceutical formulation facilities as sources of opioids and other pharmaceuticals to wastewater treatment plant effluents. *Environ Sci Technol* 44: 4910–4916. doi: 10.1021/es100356f

Pignatello JJ (1992) Dark and photoassisted iron$^{3+}$-catalyzed degradation of chlorophenoxy herbicides by hydrogen peroxide. *Environ Sci Technol* 26: 944–951. doi: 10.1021/es00029a012

Pignatello JJ, Oliveros E, MacKay A (2006) Advanced Oxidation Processes for Organic Contaminant Destruction Based on the Fenton Reaction and Related Chemistry. *Crit Rev Environ Sci Technol* 36: 1–84. doi: 10.1080/10643380500326564

Pirkanniemi K, Sillanpää M, Sorokin A (2003) Degradative hydrogen peroxide oxidation of chelates catalysed by metallophthalocyanines. *Sci Total Environ* 307: 11–18. doi: 10.1016/S0048-9697(02)00499-0

Planas C, Caixach J, Santos FJ, Rivera J (1997) Occurrence of pesticides in Spanish surface waters. Analysis by high resolution gas chromatography coupled to mass spectrometry. *Chemosphere* 34: 2393–2406. doi: 10.1016/S0045-6535(97)00085-4

Pupo Nogueira RF, Guimarães JR (2000) Photodegradation of dichloroacetic acid and 2,4-dichlorophenol by ferrioxalate/H2O2 system. *Water Res* 34: 895–901. doi: 10.1016/S0043-1354(99)00193-1

Quinn B, Gagné F, Blaise C (2008) An investigation into the acute and chronic toxicity of eleven pharmaceuticals (and their solvents) found in wastewater effluent on the

cnidarian, Hydra attenuata. *Sci Total Environ* 389: 306–314. doi: 10.1016/j.scitotenv.2007.08.038

Rahim Pouran S, Abdul Aziz AR, Wan Daud WMA (2015) Review on the main advances in photo-Fenton oxidation system for recalcitrant wastewaters. *J Ind Eng Chem* 21: 53–69. doi: 10.1016/j.jiec.2014.05.005

Ramamoorthy S, Manning PG (1974) Inorganic phosphate and the uptake of mineral nutrients by plants. *Inorg Nucl Chem Lett* 10: 623–628. doi: 10.1016/0020-1650(74)80004-8

Rastogi A, Al-Abed SR, Dionysiou DD (2009) Sulfate radical-based ferrous–peroxymonosulfate oxidative system for PCBs degradation in aqueous and sediment systems. *Appl Catal B Environ* 85: 171–179. doi: 10.1016/j.apcatb.2008.07.010

Redpath JL, Willson RL (1975) Chain Reactions and Radiosensitization: Model Enzyme Studies. *Int J Radiat Biol* 27: 389–398. doi: 10.1080/09553007514550361

Richardson SD (2008) Environmental mass spectrometry: emerging contaminants and current issues. *Anal Chem* 80: 4373–4402. doi: 10.1021/ac800660d

Richardson SD, Ternes TA (2011) Water analysis: emerging contaminants and current issues. *Anal Chem* 83: 4614–4648. doi: 10.1021/ac200915r

Rickman KA, Mezyk SP (2010) Kinetics and mechanisms of sulfate radical oxidation of β-lactam antibiotics in water. *Chemosphere* 81: 359–365. doi: 10.1016/j.chemosphere.2010.07.015

Rigg T, Taylor W, Weiss J (1954) The Rate Constant of the Reaction between Hydrogen Peroxide and Ferrous Ions. *J Chem Phys* 22: 575. doi: 10.1063/1.1740127

Rimkus G, Rimkus B, Wolf M (1994) Nitro musks in human adipose tissue and breast milk. *Chemosphere* 28: 421–432. doi: 10.1016/0045-6535(94)90138-4

Ripp J, Program WLC& R (1996) Analytical Detection Limit Guidance & Laboratory Guide for Determining Method Detection Limits. Wisconsin Department of Natural Resources, Laboratory Certification Program

Rocha ORS da, Dantas RF, Duarte MMMB, Duarte MML, Silva VL (2013) Solar photo-Fenton treatment of petroleum extraction wastewater.

Rosales E, Pazos M, Sanromán MA (2012) Advances in the Electro-Fenton Process for Remediation of Recalcitrant Organic Compounds. *Chem Eng Technol* 35: 609–617. doi: 10.1002/ceat.201100321

Sanchiz J, Esparza P, Domínguez S, Brito F, Mederos A (1999) Solution studies of complexes of iron(III) with iminodiacetic, alkyl-substituted iminodiacetic and nitrilotriacetic acids by potentiometry and cyclic voltammetry. *Inorganica Chim Acta* 291: 158–165. doi: 10.1016/S0020-1693(99)00125-5

Santos-Juanes Jordá L, Ballesteros Martín MM, Ortega Gómez ECRA, Román Sánchez IM, Casas López JL, Sánchez Pérez JA (2011) Economic evaluation of the photo-Fenton process. Mineralization level and reaction time: the keys for increasing plant efficiency. *J Hazard Mater* 186: 1924–1929. doi: 10.1016/j.jhazmat.2010.12.100

Sathiakumar N, Delzell E (2010) A Review of Epidemiologic Studies of Triazine Herbicides and Cancer. *Crit Rev Toxicol* 27: 599–612. doi: 10.3109/10408449709084405

Schnitzer RJ (1978) IARC monographs on the evaluation of the carcinogenic risk of chemicals to man: Vol. 15: Some Fumigants, the Herbicides 2, 4-D and 2, 4, 5-T, Chlorinated Dibenzodioxins and Miscellaneous Industrial Chemicals. WHO Press. International Agency for Research on Cancer, L.

Schultz MM, Furlong ET, Kolpin DW, Werner SL, Schoenfuss HL, Barber LB, Blazer VS, Norris DO, Vajda ALM(2010) Antidepressant pharmaceuticals in two U.S. effluent-impacted streams: occurrence and fate in water and sediment, and selective uptake in fish neural tissue. *Environ Sci Technol* 44: 1918–1925. doi: 10.1021/es9022706

Sedlak DL, Hoigné J (1993) The role of copper and oxalate in the redox cycling of iron in atmospheric waters. *Atmos Environ Part A Gen Top* 27: 2173–2185. doi: 10.1016/0960-1686(93)90047-3

Segura PA, François M, Gagnon C, Sauvé S (2009) Review of the occurrence of anti-infectives in contaminated wastewaters and natural and drinking waters. *Environ Health Perspect* 117: 675–684. doi: 10.1289/ehp.11776

Selvam K, Muruganandham M, Swaminathan M (2005) Enhanced heterogeneous ferrioxalate photo-fenton degradation of reactive orange 4 by solar light. *Sol Energy Mater Sol Cells* 89: 61–74. doi: 10.1016/j.solmat.2005.01.002

SES (1994) The UV oxidation handbook. Solarchem Environmental Systems, Markham (ON, CAN).

Shah NS, He X, Khan JA, Khan HM, Boccelli DL, Dionysiou DD (2015) Comparative studies of various iron-mediated oxidative systems for the photochemical degradation of endosulfan in aqueous solution. *J Photochem Photobiol A Chem* 306: 80–86. doi: 10.1016/j.jphotochem.2015.03.014

Sillanpää M (1997) Reviews of Environmental Contamination and Toxicology: Continuation of Residue Reviews. In: Ware GW (ed). Springer New York, New York, NY, pp 85–111

Sillanpää M, Oikari A (1996) Assessing the impact of complexation by EDTA and DTPA on heavy metal toxicity using microtox bioassay. *Chemosphere* 32: 1485–1497. doi: 10.1016/0045-6535(96)00057-4

Sillanpää M, Pirkanniemi K, Dhondup P (2003) The Acute Toxicity of Gluconic Acid, ?-Alaninediacetic Acid, Diethylenetriaminepentakismethylenephosphonic Acid, and Nitrilotriacetic Acid Determined by Daphnia magna, Raphidocelis subcapitata , and Photobacterium phosphoreum. *Arch Environ Contam Toxicol* 44: 332–335. doi: 10.1007/s00244-002-1220-5

Sillanpää MET, Kurniawan TA, Lo W (2011) Degradation of chelating agents in aqueous solution using advanced oxidation process (AOP). *Chemosphere* 83: 1443–1460. doi: 10.1016/j.chemosphere.2011.01.007

Silva AMT, Zilhão NR, Segundo RA, Azenha M, Fidalgo F, Silva AF, Faria JL, Teixeira J (2012) Photo-Fenton plus Solanum nigrum L. weed plants integrated process for the abatement of highly concentrated metalaxyl on waste waters. *Chem Eng J* 184: 213–220. doi: 10.1016/j.cej.2012.01.038

Simunovic M, Kusic H, Koprivanac N, Bozic AL (2011) Treatment of simulated industrial wastewater by photo-Fenton process: Part II. The development of mechanistic model. *Chem Eng J* 173: 280–289. doi: 10.1016/j.cej.2010.09.030

Sirtori C, Zapata A, Gernjak W, Malato S, Lopez A, Agüera A (2011) Solar photo-Fenton degradation of nalidixic acid in waters and wastewaters of different composition.

Analytical assessment by LC-TOF-MS. *Water Res* 45: 1736–1744. doi: 10.1016/j.watres.2010.11.023

Sorvari J, Sillanpää M (1996) Influence of metal complex formation on heavy metal and free EDTA and DTPA acute toxicity determined by Daphnia magna. *Chemosphere* 33: 1119–1127. doi: 10.1016/0045-6535(96)00251-2

Spain JC, Hughes JB, Knackmuss H-J (2000) Biodegradation of Nitroaromatic Compounds and Explosives. Lewis Publishers, Boca Raton, FL

Spanish Goverment. Real Decreto Legislativo 1/2001, Pub. L. No. BOE no 176 (2001).

Spanish Goverment. Real Decreto 606/2003, Pub. L. No. BOE no 135 (2003). Spain.

Spanish Goverment. Real Decreto 60/2011, Pub. L. No. BOE no 19 (2011).

Spanish Goverment. Real Decreto 670/2013, Pub. L. No. BOE no 227 (2013).

Spanish Goverment. Resolution 2013, Pub. L. No. BOE no 103 (2013). Spain: Diario oficial del Estado.

Stasicka Z (2011) Transition metal complexes as solar photocatalysis in the environment: a short review of recent development. In: van Eldik R, Stochel G (eds) Inorganic Photochemistry, 63. Academic Press, London (UK), pp 291–343.

Stolzberg RJ, Hume DN (1975) Rapid formation of iminodiacetate from photochemical degradation of iron(III) nitrilotriacetate solutions. *Environ Sci Technol* 9: 654–656. doi: 10.1021/es60105a001

Stumm W, Morgan JJ (2012) Aquatic Chemistry: Chemical Equilibria and Rates in Natural Waters.

Sun J-H, Sun S-P, Fan M-H, Guo HQ, Lee Y-F, Sun R-X (2008) Oxidative decomposition of p-nitroaniline in water by solar photo-Fenton advanced oxidation process. *J Hazard Mater* 153: 187–193. doi: 10.1016/j.jhazmat.2007.08.037

Sun S-P, Zeng X, Lemley AT (2013) Kinetics and mechanism of carbamazepine degradation by a modified Fenton-like reaction with ferric-nitrilotriacetate complexes. *J Hazard Mater* 252: 155–165. doi: 10.1016/j.jhazmat.2013.02.045

Sun S-P, Zeng X, Li C, Lemley AT (2014) Enhanced heterogeneous and homogeneous Fenton-like degradation of carbamazepine by nano-$Fe_3O_4$/$H_2O_2$ with nitrilotriacetic acid. *Chem Eng J* 244: 44–49. doi: 10.1016/j.cej.2014.01.039

Sun Y, Pignatello JJ (1993) Photochemical reactions involved in the total mineralization of 2,4-D by iron(3+)/hydrogen peroxide/UV. *Environ Sci Technol* 27: 304–310. doi: 10.1021/es00039a010

Sun Y, Pignatello JJ (1992) Chemical treatment of pesticide wastes. Evaluation of iron(III) chelates for catalytic hydrogen peroxide oxidation of 2,4-D at circumneutral pH. *J Agric Food Chem* 40: 322–327. doi: 10.1021/jf00014a031

Svenson A, Kaj L, Björndal H (1989) Aqueous photolysis of the iron (III) complexes of NTA, EDTA and DTPA. *Chemosphere* 18: 1805–1808. doi: 10.1016/0045-6535(89)90464-5

Tamimi M, Qourzal S, Barka N, Assabbane A, Aitichou Y (2008) Methomyl degradation in aqueous solutions by Fenton's reagent and the photo-Fenton system. *Sep Purif Technol* 61: 103–108. doi: 10.1016/j.seppur.2007.09.017

Tang W (1997) Oxidation kinetics and mechanisms of trihalomethanes by Fenton's reagent. *Water Res* 31: 1117–1125. doi: 10.1016/S0043-1354(96)00348-X

Teijon G, Candela L, Tamoh K, Molina-Díaz A, Fernández-Alba AR (2010) Occurrence of emerging contaminants, priority substances (2008/105/CE) and heavy metals in treated wastewater and groundwater at Depurbaix facility (Barcelona, Spain). *Sci Total Environ* 408: 3584–3595. doi: 10.1016/j.scitotenv.2010.04.041

Toth JE, Rickman KA, Venter AR, Kiddle JJ, Mezyk SP (2012) Reaction kinetics and efficiencies for the hydroxyl and sulfate radical based oxidation of artificial sweeteners in water. *J Phys Chem A* 116: 9819–9824. doi: 10.1021/jp3047246

Trovo' A, Pupo Nogueira RF, Aguera A, Fernandez-Alba AR, Malato S (2011) Degradation of the antibiotic amoxicillin by photo-Fenton process e Chemical and toxicological assessment. *Water Res* 45: 1394–1402. doi: 10.1016/j.watres.2010.10.029

Tsang DCW, Lo IMC, Surampalli RY (2012) Chelating agents for land decontamination technologies.

Tuulos-tikka S, Sillanpää M, Rämö J (2000) Determination of Nitrilotriacetic Acid in Waste and Natural Waters. *Int J Environ Anal Chem* 77: 221–232. doi: 10.1080/03067310008032684

Ukrainczyk M, Stelling J, Vučak M, Neumann T (2013) Influence of etidronic acid and tartaric acid on the growth of different calcite morphologies. *J Cryst Growth* 369: 21–31. doi: 10.1016/j.jcrysgro.2013.01.037

UNESCO, WWAP (2012) United Nations World Water Development Report 4. Volume 1: Managing Water under Uncertainty and Risk.

US Environmental Protection Agency (1985) EPA draft final list of recommendations for chemicals in the National Survey for Pesticides in Groundwater. *Chem Regul Rep* 9: 1033.

US EPA National Center for Environmental (1986) Guidelines for Carcinogen Risk Assessment (1986). http://cfpub.epa.gov/ncea/risk/recordisplay.cfm?deid=54933&CFID=43868260&CFTOKEN=58847449. Accessed 15 Jan 2016

Vedrenne M, Vasquez-Medrano R, Prato-Garcia D, Frontana-Uribe BA, Hernandez-Esparza M, de Andrés JM (2012) A ferrous oxalate mediated photo-Fenton system: Toward an increased biodegradability of indigo dyed wastewaters. *J Hazard Mater* 243: 292–301. doi: 10.1016/j.jhazmat.2012.10.032

Von Gunten U (2003) Ozonation of drinking water: part II. Disinfection and by-product formation in presence of bromide, iodide or chlorine. *Water Res* 37: 1469–1487. doi: 10.1016/S0043-1354(02)00458-X

Von Gunten U, Oliveras Y (1998) Advanced Oxidation of Bromide-Containing Waters: Bromate Formation Mechanisms. *Environ Sci Technol* 32: 63–70. doi: 10.1021/es970477j

Wagner I, Strehlow H (1987) On the flash photolysis of bromide ions in aqueous solutions. *Berichte der Bunsengesellschaft für Phys Chemie* 91: 1317–1321. doi: 10.1002/bbpc.19870911203

Walling C (1975) Fenton's reagent revisited. *Acc Chem Res* 8: 125–131. doi: 10.1021/ar50088a003

Walling C, Goosen A (1973) Mechanism of the ferric ion catalyzed decomposition of hydrogen peroxide. Effect of organic substrates. *J Am Chem Soc* 95: 2987–2991. doi: 10.1021/ja00790a042

Walter M V, Vennes JW (1985) Occurrence of multiple-antibiotic-resistant enteric bacteria in domestic sewage and oxidation lagoons. *Appl Envir Microbiol* 50: 930–933.

Wang Z, Yuan R, Guo Y, Xu L, Liu J (2011) Effects of chloride ions on bleaching of azo dyes by $Co^{2+}$/oxone reagent: kinetic analysis. *J Hazard Mater* 190: 1083–1087. doi: 10.1016/j.jhazmat.2011.04.016

Ward TM, Weber JB (1968) Aqueous solubility of alkylamino-s-triazine as a function of pH and molecular structure. *J Agric Food Chem* 16: 959–961. doi: 10.1021/jf60160a034

Westerhoff P, Chao P, Mash H (2004) Reactivity of natural organic matter with aqueous chlorine and bromine. *Water Res* 38: 1502–1513. doi: 10.1016/j.watres.2003.12.014

White VE, Knowles CJ (2003) Degradation of copper-NTA by Mesorhizobium sp. NCIMB 13524. *Int Biodeterior Biodegradation* 52: 143–150. doi: http://dx.doi.org/10.1016/S0964-8305(03)00049-0

WHO/UNICEF (2014) World Health Organization, Progress on drinking water and sanitation. World Health Organization, South-East Asia Regional Office

Willett KL, Hites RA (2000) Chemical Actinometry: Using o-Nitrobenzaldehyde to Measure Lamp Intensity in Photochemical Experiments. *J Chem Educ* 77: 900. doi: 10.1021/ed077p900

Wols BA, Hofman-Caris CHM (2012) Review of photochemical reaction constants of organic micropollutants required for UV advanced oxidation processes in water. *Water Res* 46: 2815–2827. doi: 10.1016/j.watres.2012.03.036

Wols BA, Hofman-Caris CHM, Harmsen DJH, Beerendonk EF (2013) Degradation of 40 selected pharmaceuticals by UV/H2O2. *Water Res* 47: 5876–5888. doi: 10.1016/j.watres.2013.07.008

World Health Organization (WHO) WHO | World Health Organization. http://www.who.int/en/. Accessed 24 May 2016

World Water Council World Water Council - Water Crisis. http://www.worldwatercouncil.org/library/archives/water-crisis/. Accessed 31 May 2016

World Water Council (2015) Delivering a pact for water security World Water Council 2013-2015 Triennial Report.

Wu X, Gu X, Lu S, Xu M, Zang X, Miao Z, Qiu Z, Sui Q (2014) Degradation of trichloroethylene in aqueous solution by persulfate activated with citric acid chelated ferrous ion. *Chem Eng J* 255: 585–592. doi: 10.1016/j.cej.2014.06.085

Wu Y, Bianco A, Brigante M, Dong W, de Sainte-Claire P, Hanna K, Mailhot G (2015) Sulfate Radical Photogeneration Using Fe-EDDS: Influence of Critical Parameters and Naturally Occurring Scavengers. *Environ Sci Technol* 49: 14343–14349. doi: 10.1021/acs.est.5b03316

Xue X, Hanna K, Despas C, Wu F, Deng N (2009) Effect of chelating agent on the oxidation rate of PCP in the magnetite/$H_2O_2$ system at neutral pH. *J Mol Catal A Chem* 311: 29–35. doi: 10.1016/j.molcata.2009.06.016

Yang H, Abbaspour KC (2007) Analysis of wastewater reuse potential in Beijing. *Desalination* 212: 238–250. doi: 10.1016/j.desal.2006.10.012

Yang S, Wang P, Yang X, Shan L, Zhang W, Shao X, Niu R (2010) Degradation efficiencies of azo dye Acid Orange 7 by the interaction of heat, UV and anions with common oxidants: Persulfate, peroxymonosulfate and hydrogen peroxide. *J Hazard Mater* 179: 552–558. doi: 10.1016/j.jhazmat.2010.03.039

Yinon J (1990) Toxicity and Metabolism of Explosives. CRC Press, Boca Raton, FL

Yuan R, Wang Z, Hu Y, Wang B, Gao S (2014) Probing the radical chemistry in UV/persulfate-based saline wastewater treatment: kinetics modeling and byproducts identification. *Chemosphere* 109: 106–112. doi: 10.1016/j.chemosphere.2014.03.007

Zehavi D, Rabani J (1972) Oxidation of aqueous bromide ions by hydroxyl radicals. Pulse radiolytic investigation. *J Phys Chem* 76: 312–319. doi: 10.1021/j100647a006

Zepp RG, Faust BC, Hoigne J (1992) Hydroxyl radical formation in aqueous reactions (pH 3-8) of iron(II) with hydrogen peroxide: the photo-Fenton reaction. *Environ Sci Technol* 26: 313–319. doi: 10.1021/es00026a011

Zhang Y, Pagilla K (2010) Treatment of malathion pesticide wastewater with nanofiltration and photo-Fenton oxidation. *Desalination* 263: 36–44. doi: 10.1016/j.desal.2010.06.031

Zhao X-K, Yang G-P, Gao X-C (2003) Studies on the sorption behaviors of nitrobenzene on marine sediments. *Chemosphere* 52: 917–925. doi: 10.1016/S0045-6535(03)00258-3

Zucchi S, Blüthgen N, Ieronimo A, Fent K (2011) The UV-absorber benzophenone-4 alters transcripts of genes involved in hormonal pathways in zebrafish (Danio rerio) eleuthero-embryos and adult males. *Toxicol Appl Pharmacol* 250: 137–146. doi: 10.1016/j.taap.2010.10.001

# Congress communications

During the development of this thesis, the author took part in several conferences and meetings presenting different part of her work. The contributions given by the author are listed below.

***ORAL presentations:***

- Madrid – Spain (20-22 June 2016), **META 2016 (XII Spanish Round table on water treatment),** *Fe(III)-L chelates based Photo-Fenton at neutral pH: efficiency and process' strategies.* A. De Luca, R.F. Dantas, S. Esplugas.
- Athens - Greece (21-24 October 2015), **EAAOP4 – European Conference on Environmental Applications on Advanced Oxidation Processes**, *Effects of water composition of iron chelate based Photo-Fenton process efficiency.* A. De Luca, R.F. Dantas, S. Esplugas.
- Barcelona – Spain (28 June-3 July 2015), **IOA 22nd World Congress: Ozone and Advanced Oxidation: Leading –edge science and technologies,** *Assessment of Fe(III)-NTA use in Photo-Fenton at neutral pH.* A. De Luca, R.F. Dantas, S. Esplugas.
- Tarragona – Spain (10-12 June 2015), **EMChIE 2015 – 7th European Meeting on Chemical Industry and Environment,** *Iron chelate based Photo-Fenton process for antibiotic removal.* A. De Luca, R.F. Dantas, S. Esplugas.
- Alicante - Spain (18-20 June 2014), **META 2014 (XI Spanish Round table on water treatment),** *Utilización de procesos de Oxidación avanzada para el reuso de agua (Application of Advanced Oxidation Processes for water reuse).* M. Mercé, A. Justo, A. De Luca, A. Cruz, D.D. Ramos, O. Gonzales, R.F. Dantas, C. Sans, S. Esplugas.
- Recife – Brasil (15-18 October 2013), **1st Iberoamerican Congress of Advanced Oxidation,** *Photo-Fenton at neutral pH using Fe(III) complexes for micropollutant removal.* R.F. Dantas, A. De Luca, S. Esplugas.
- Almeria – Spain (4-6 October 2012), **META 2012 (X Spanish Round table on water treatment),** *Aplicación de Procesos de Oxidación Avanzada para el reúso de aguas (Application of Advanced Oxidation Processes for water reuse).* M.M. Micó, A. Justo, A. Cruz, A. De Luca, O. Gonzales, R.F. Dantas, C. Sans, S. Esplugas.

***POSTER presentations:***

- Barcelona – Spain (30 September- 3 October 2014), **13th MCCE - 13th Mediterranean Congress of Chemical Engineering,** *Assessment of iron chelates efficiency for Photo-Fenton at neutral pH.* A. De Luca, R.F. Dantas, S. Esplugas.
- Barcelona – Spain (25-28 June 2013), **ICCE 2013 - 14th EuCheMS International Conference on Chemistry and Environment,** *Atrazine removal in municipal secondary effluents by Fenton and photo-Fenton treatments.* A. De Luca, R.F. Dantas, S. Esplugas.

# Resumen en catellano

## Introducción

Aunque el nuevo informe publicado por el WHO/UNICEF indica que 2 mil millones de personas han ganado acceso a recursos de agua potable, 884 millones aún no disponen de los adecuados recursos hídricos (WHO/UNICEF, 2014). Esta disparidad en la accesibilidad es varía según se trate de ciudades o de zonas rurales, donde este problema es más evidente.

El difícil escenario de accesibilidad a los recursos hídricos se agrava por fenómenos como la escasez de agua disponible debido al cambio climático y la explotación de los recursos, realizado a menudo de manera no adecuada. En la superficie de la tierra hay suficiente agua dulce para satisfacer las necesidades de 8 mil millones de personas. Pero está mal repartida, mal gastada y frecuentemente contaminada (World Council 2105).

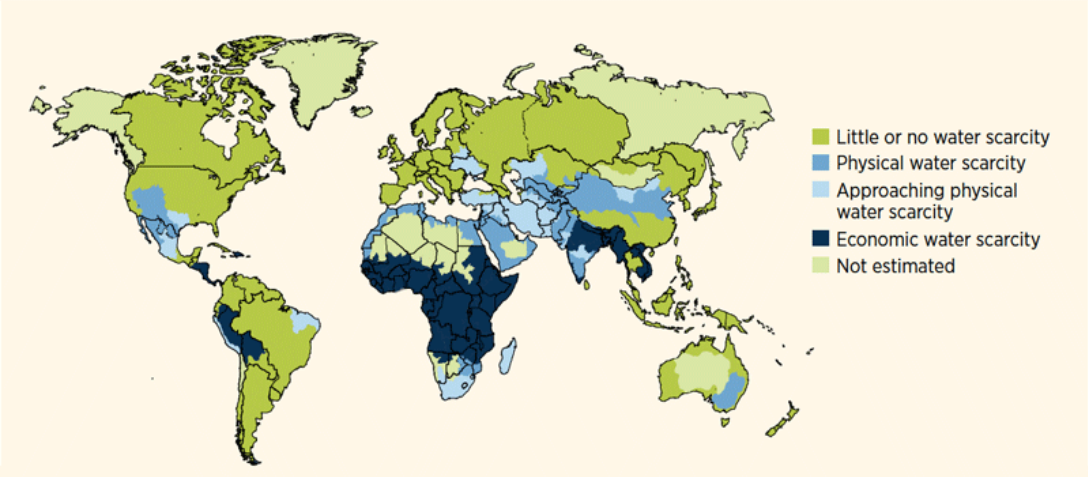


**Figura 1 Escasez de los recursos hídricos del mundo (UNESCO)**

Es evidente que se necesita de una gran participación para hacer frente a estos problemas y para que todos puedan disfrutar del derecho fundamental de disponer de recursos hídricos adecuados.

La descarga de contaminantes en los cuerpos hídricos representa un factor de gran riesgo para la salud humana y para la fauna en general. Las estaciones depuradoras de aguas residuales (EDAR) juegan en este caso un papel fundamental para reducir la amenaza de contacto humano con aguas contaminadas (Meneses 2010). Los afluentes a las EDAR pueden tener características muy variables por lo que una definición univoca de un plan de tratamiento no es posible. En consequencia, debido al inadecuado plan de tratamiento de algunas EDAR para hacer frente a determinadas características de contaminación, éstas representan una de las principales fuentes de contaminación de los cuerpos hídricos (Glassmeyer et al. 2005; Clara et al. 2005). En efecto, muchos contaminantes no pueden ser eliminados a través de procesos de tratamiento convencionales (Ginebreda et al. 2010; Teijon et al. 2010). Existe una clase de contaminantes identificada como contaminantes emergentes (CE) para los cuales se necesitan tratamientos específicos de degradación. Entre estos contaminantes se encuentran, medicamentos, hormonas, productos de cuidado personal, destructores endocrinos etc. A pesar de que estos contaminantes se detectan en concentraciones muy pequeñas, la preocupación está relacionada con sus propiedades de persistencia y bioacumulación (Kim et al. 2007; Hernando et al. 2007; Richardson 2008). Una posible solución a este problema pasa por la actualización de las EDARs a las nuevas exigencias de tratamiento, mediante tratamientos terciarios.

Los tratamientos terciarios pueden ser realizados por medio de varios tipos de procesos. Entre estos, de probada eficacia están los procesos de oxidación avanzada (POA). Los POA se definen como aquella clase de procesos caracterizados por la generación de radicales hidroxilo (HO·) en cantidades suficientes como para realizar la purificación del afluente.

En función de la fuente de la que derivan las especies oxidantes y el método empleado para su producción, una de las posibles clasificaciones de los POA podría ser:

- Basados la fotolisis:
  - UV fotolisis;
  - V-UV fotolisis;
- Basados en ozono:
  - Ozonización;
  - Ozonización + UV y/o $H_2O_2$;
  - Ozonización + catálisis;
- Basados en los radicales hidroxilos:
  - Fenton;
  - Fenton-like;
  - Foto-Fenton;
  - UV/ $H_2O_2$;
  - Electro-Fenton;
  - Foto catálisis;
- Basados en los radicales sulfato:
  - UV/PS y UV/PMS;
  - catalizador/PS y catalizador/PMS;
  - calor/PS y calor/PMS;
- Procesos térmicos:
  - oxidación supercrítica húmeda;
  - oxidación húmeda;
  - oxidación húmeda + $H_2O_2$;
- Basados en energía:
  - tecnologías de ultrasonidos;
  - oxidación electroquímica;
  - oxidación mediante haz de electrones;
  - procesos combinados con microondas.

Entre estos, Fenton y foto-Fenton representan tratamientos que han sido largamente estudiados y identificados como buenas tecnologías para la eliminación de contaminantes. Con el tiempo, la utilización de Fenton y foto-Fenton se ha visto limitada por una serie de desventajas, como la necesidad de acidificar el medio de reacción para favorecer la solubilización del hierro, que es el catalizador de la reacción. Para minimizar estas desventajas, la comunidad científica está trabajando para conseguir aplicar el proceso sin modificar el pH de la solución. De estas modificaciones, nacen nuevos procesos identificados como Fenton-like. Fenton y Foto-Fenton like a pH neutro que pueden ser llevados a cabo de manera heterogénea o homogénea dependiendo de la fase en la que se encuentra el catalizador (Sun et al., 2014; Tao et al., 2008; Garrido-Ramírez et al., 2010). La utilización de agentes quelantes permite la solubilización del hierro aunque a pH neutro (foto-Fenton like de tipo homogéneo) a través de la formación de complejos de hierro fotoactivos ($Fe^{3+}L$) útiles para la catalización de la reacción de Fenton (Pignatello et al., 2006).

En esta tesis se busca la posible aplicación de foto-Fenton like a pH neutro catalizado por quelados de hierro en condiciones de pH cercano a la neutralidad. También se presentan los principales resultados experimentales de la influencia de la composición de la matriz a tratar en las eficiencias del proceso. Finalmente, se comentará sobre la posible aplicación de algunas estrategias para promover una mejor eficiencia de estos procesos.

## Objetivos

Los principales objetivos de esta tesis son:

- ✓ La determinación de la idoneidad de la aplicación del proceso de Fenton y foto-Fenton (con radiación UV-A y UV-C) en el tratamiento de compuestos recalcitrantes y la evaluación de la posibilidad de realizar la modificación del proceso para su aplicación en condiciones de pH cercanos a la neutralidad.

- ✓ La evaluación de la idoneidad de algunos agentes para formar complejos con el hierro y que puedan ser utilizados como foto catalizadores del proceso de foto-Fenton like a pH neutro. La identificación del ratio molar L:Fe más adecuada para asegurar la completa quelacion del contenido de hierro en solución para cada uno de los compuestos quelantes utilizados (EDTA, NTA, acido oxálico y acido tartárico). Finalmente la evaluación de la eficacia de estos catalizadores en la degradación de sulfametoxazol (SMX) por medio de foto-Fenton like a pH próximo a la neutralidad y la identificación del más adecuado para la aplicación.

- ✓ Conseguir un conocimiento detallado de la estabilidad del quelado de hierro (Fe(III)-NTA). Para lo cual se estudiara la estabilidad de los quelados bajo estrés térmico, oxidativo y foto químico.

- ✓ La evaluación de la eficiencia de tratamiento alcanzable con el tratamiento de foto-Fenton like catalizado por Fe (III)-NTA aplicado a diferentes matrices acuosas. El estudio de la influencia sobre el proceso operada por los parámetros característicos de la cualidad del agua.

- ✓ La identificación de posibles estrategias para la optimización del proceso en vías a reducir la influencia de la composición del agua sobre las eficiencias de proceso. Diferentes estrategias para promover la degradación del SMX han sido consideradas (dosificación de quelados, adición de $Mn^{2+}$ para favorecer la producción de otras especies radicales cuales $O_2^{\cdot -}$; adición de persulfato para producir radicales $SO_4^{\cdot -}$).

## Materiales, métodos analíticos y procedimiento experimental

Los contaminantes modelos utilizados para llevar cabo los estudios que son objetos de esta tesis son: Atrazina (Fluka, pureza 98%), Sulfametoxazole (SMX, Sigma-Aldrich). Las estructuras químicas y las principales características químicas de los compuestos se hallan resumidos en la siguiente Tabla 1:

**Tabla 1 Compuestos modelo utilizados en este estudio**

| Atrazina (ATZ) | | Sulfametoxazole (SMX) | |
|---|---|---|---|
| **Formula química** | $C_8H_{14}ClN_5$ | **Formula química** | $C_{10}H_{11}N_3O_3S$ |
| **Estructura química** | 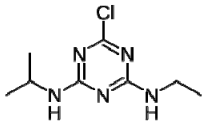 | **Estructura química** | 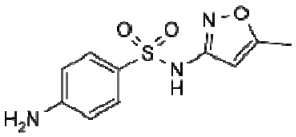 |
| **Masa molar** | 215.68 g/mol | **Masa molar** | 253.28 g/mol |
| **Numero CAS** | 1912-24-9 | **Numero CAS** | 723-46-6 |

Los agentes quelantes usados en este estudio son: ácido nitrilotriacetico (NTA, Alfa Aesar), ácido etilendiammintetraacetico (EDTA, Panreac), ácido oxálico en forma hidratada (Panreac), DL-ácido tartárico (Alfa Aesar). Las principales características químicas de los compuestos quelantes están resumidos en Tabla 2:

**Tabla 2 Compuestos quelantes usados en este estudio**

| Acido nitrilotriacetico (NTA) | | Acido etilendiamminotetraacetico (EDTA) | |
|---|---|---|---|
| **Formula química** | $C_6H_9NO_6$ | **Formula química** | $C_{10}H_{16}N_2O_8$ |
| **Estructura química** | 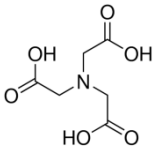 | **Estructura química** | 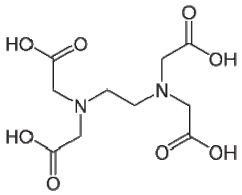 |
| **Masa molar** | 191.12 g/mol | **Masa molar** | 292.24 g/mol |
| **Numero CAS** | 139-13-9 | **Numero CAS** | 60-00-4 |
| **Acido oxálico** | | **DL-acido tartárico** | |
| **Formula química** | $C_2H_2O_4{\cdot}2H_2O$ | **Formula química** | $C_4H_6O_6$ |
| **Estructura química** | 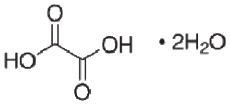 | **Estructura química** | 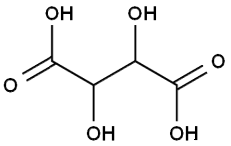 |
| **Masa molar** | 126.07 g/mol | **Masa molar** | 150.09 g/mol |
| **Numero CAS** | 6153-56-6 | **Numero CAS** | 133-37-9 |

Las principales técnicas analíticas utilizadas fueron:

- Cromatografía liquida de elevada precisión (HPLC) para la determinación del contenido de atrazina(ATZ) y sulfametoxazole (SMX);
- Método estándar que emplea 1,10- fenantrolina (ISO 6332, (International Organization for Standardization 1988)) para la determinación del contenido de hierro en solución;
- Método espectrofotométrico que emplea metavanadato (Nogueira et al. 2005) para la determinación del contenido de peróxido de hidrogeno;
- Determinación del Carbono Orgánico Total (COT);
- Determinación de la Demanda Química de Oxigeno (DQO);
- Determinación de la Demanda Bioquímica de Oxigeno (DBO);
- Medida de absorbancia a 254 nm para la monitorización de la descomposición de los anillos aromáticos;
- Cromatografía iónica para la cuantificación del contenido iónicos del agua;

- Microtox y Luminotox para los ensayos biológico de toxicidad;
- Medidas actinométricas para a determinación de los flujos fotónicos característicos de los reactores utilizados para la irradiación.

Los rectores foto catalíticos empleados para los experimentos de foto-Fenton y foto-Fenton like fueron:

- Foto-reactor de luz UV-A

Para la irradiación de la solución de experimento con luz UV-A se utilizó un reactor encamisado de 2 L equipado con tres lámparas de luz negra (Philips TL 8W, 08 FAM) en tubos de vidrio Duran. La emisión máxima de las lámparas utilizadas es a 365 nm cuyo flujo fotónico, medido a la longitud de emisión de máxima potencia con método actinométrico basado en la medición de o-nitrobenzaldeide (Kuhn et al. 2004; De la Cruz et al. 2013), es de $5.05 \times 10^{-6}$ Einstein $s^{-1}$. El diseño esquemático del reactor está representado en Figura 2:

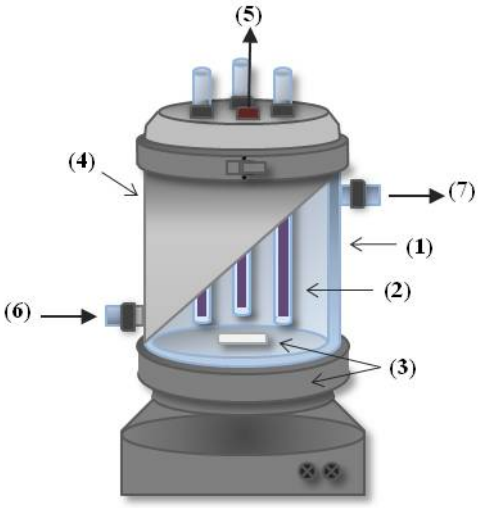


**Figura 2 Esquema del foto-reactor UV-A. (1) reactor de vidrio encamisado de 2L, (2) Lámparas UV-A, (3) agitación magnética, (4) cobertura, (5) punto de muestreo. (6) baño termostático (IN), (7) baño termostático (OUT)**

- Foto-reactor de luz UV-C

El reactor foto-químico utilizado para la irradiación de la solución con luz UV-C es del todo parecido al reactor foto-químico de luz UV-A. La única diferencia reside en el tipo de lámparas utilizadas. En este caso el reactor foto-químico está equipado con tres lámparas de luz fluorescente (Philips TUV 8W, G8T5) en tubo de cuarzo. El flujo fotónico medido con método actinométrico (Kuhn et al. 2004) es de $0.94 \times 10^{-5}$ Einstein $s^{-1}$a 254 nm. El diseño esquemático del reactor está representado en Figura 3:

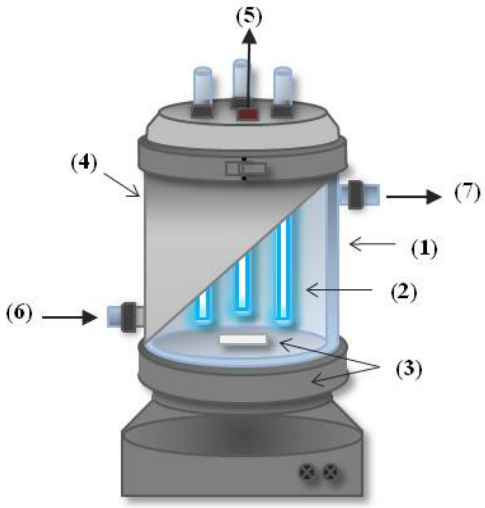


**Figura 3 Esquema del Foto-reactor UV-C. (1) reactor de vidrio encamisado de 2L, (2) Lámparas UV-A, (3) agitación magnética, (4) cobertura, (5) punto de muestreo. (6) baño termostático (IN), (7) baño termostático (OUT)**

- Simulador solar

La irradiación por luz solar se llevó a cabo en un simulador solar (Solarbox Co.Fo.Me.Gra, 220 v, 50 Hz). A este propósito, la solución de tratamiento fue bombeada desde un reactor externo de 1 L conectado con un baño termostático a un foto-reactor tubular de vidrio Duran (24 cm de longitud, 2.11 cm de diámetro, 0.078 L) dispuesto en el simulador solar. Aquí la solución se irradia por medio de una lámpara de Xenón de 1 kW (Philips XOP 15-OF 1CT). El flujo fotónico fue medido con método actinométrico de o-nitrobenzaldeide (Kuhn et al. 2004; De la Cruz et al. 2013) que resultó ser $2.68 \times 10^{-6}$ Einstein $s^{-1}$. Un esquema del simulador solar está representado en Figura 4:

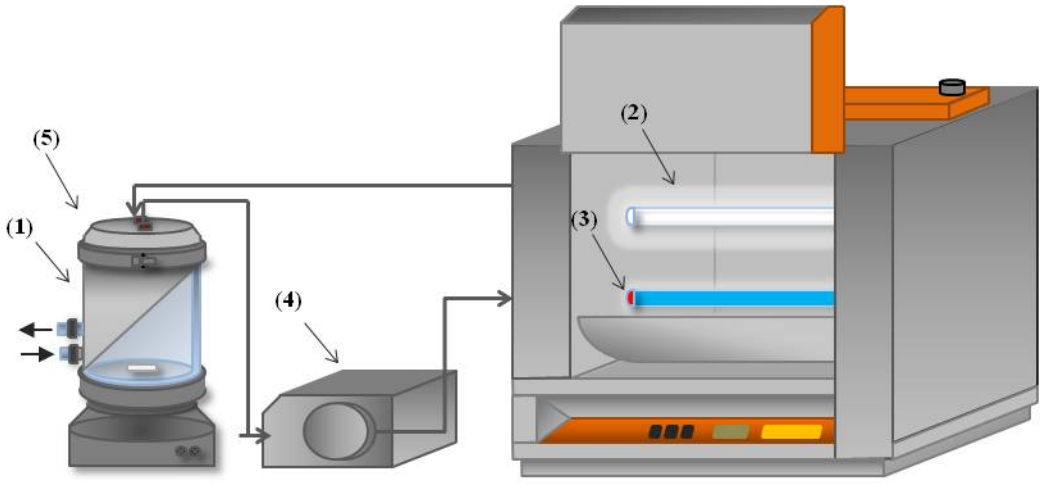


**Figura 4 Simulador solar. (1) Reactor encamisado de vidrio de 1 L, (2) lámpara de Xenon, (3) foto-reactor tubular (24 cm de longitud, 2.11 cm de diámetro, 0.078 L), (4) bomba peristáltica, (5) punto de muestreo,**

## Resultados y discusiones

- **Capítulo 4: "Tratamiento de atrazina en efluente secundario procedente de EDAR por medio de tratamiento de Fenton y foto-Fenton"**

El estudio presentado en el capítulo 4 busca confirmar la elevada eficacia del proceso de tratamiento de Fenton y foto-Fenton en el tratamiento de compuestos recalcitrantes. De esta forma, el capítulo se enfoca como un estudio preliminar que será ampliamente comentado en los capítulos siguientes.

Para este estudio se utilizó un efluente secundario procedente de EDAR (TOC variable entre 11 and 18 mg $L^{-1}$) dopado con atrazina en concentración de 0.1 mg $L^{-1}$. Los tratamientos aplicados para la comparación de las eficiencias de degradación fueron: Fenton, UV-A foto-Fenton y UV-C foto-Fenton. Los experimentos se realizaron en condiciones de pH acido (2.8±0.1). Las principales características del efluente secundario utilizado para llevar a cabo los experimentos se encuentran resumidos en la siguiente Tabla 3:

**Tabla 3 Características del efluente secundario procedente de EDAR filtrado con filtro 10 µm**

| **Parámetro** | |
|---|---|
| **pH** | 7.85 |
| **Turbidez (NTU)** | 0.90 |
| **COD (mg $L^{-1}$)** | 11-18 |
| **DQO (mg$O_2$ $L^{-1}$)** | 33-34 |
| **$DBO_5$ (mg $O_2$ $L^{-1}$)** | 8.5 |

Los experimentos fueron realizados tras añadir los reactivos de Fenton con concentraciones de 1 mg $L^{-1}$ de $Fe^{2+}$ para Fenton y UV-C foto-Fenton y 5 mg $L^{-1}$ para UV-A foto-Fenton, mientras para los tres experimentos, 5 mg $L^{-1}$ de $H_2O_2$ fueron también añadidos. La mayor concentración de hierro añadido en el caso de UV-A foto-Fenton se debe a la consideración del efecto añadido de fotolisis en el caso de UV-C foto-Fenton.

Los resultados más significativos en término de eliminación de atrazina se indican a continuación. En el caso de Fenton solo se pudo alcanzar un 20% de degradación de atrazina (Figura 5). Una mayor velocidad de reacción se pudo observar en los primeros minutos de reacción después de los cuales esta se redujo drásticamente así como el consumo de peróxido de hidrogeno. La mínima cantidad de catalizador disponible para la reacción de Fenton puede significativamente haber comprometido el desarrollo del proceso y las consiguientes eficiencias obtenidas.

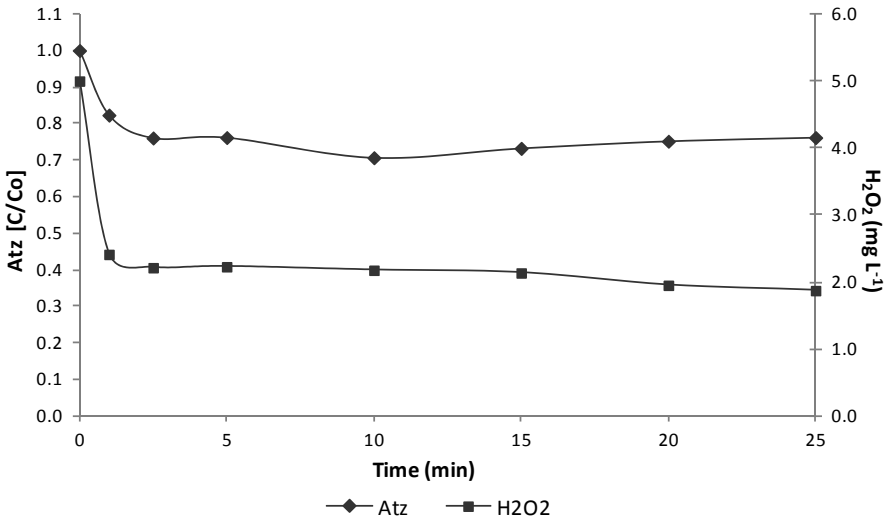


**Figura 5 Degradación de atrazina por Fenton: $[ATZ]_0$ = 0.1 mg $L^{-1}$; $[H_2O_2]_0$ = 5 mg $L^{-1}$; $[Fe^{2+}]_0$ = 1 mg $L^{-1}$; pH = 2.7 ± 0.1.**

En el caso de UV-A foto-Fenton, el mayor contenido en catalizador unido a la recuperación de $Fe^{2+}$ por efecto de la irradiación permitió alcanzar eficiencias mayores de degradación. Después de 120 minutos de reacción, cuando ya no había oxidante disponible para la producción de radicales, se consiguió alcanzar 60% de degradación de atrazina (Figura 6). El significativo cambio de cinética observado después lo primeros minutos de reacción corresponde al momento en el que se obtuvo el 90% de oxidación del contenido en $Fe^{2+}$.

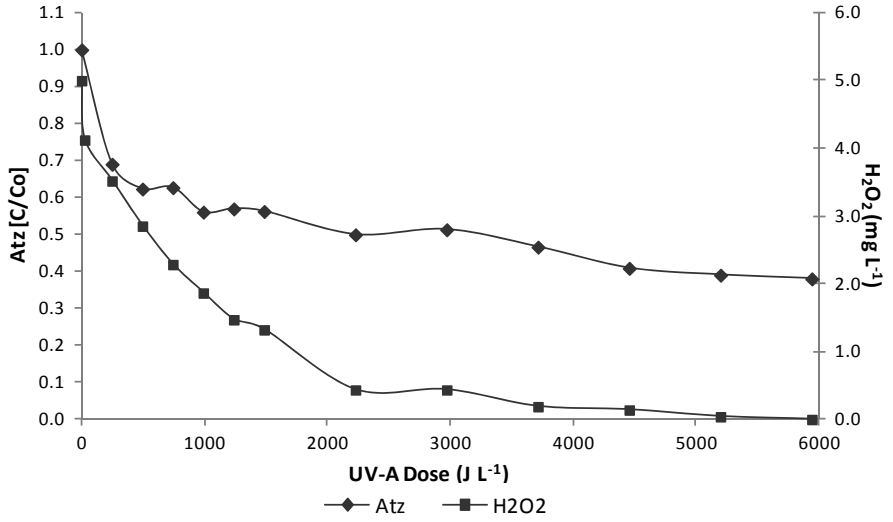


**Figura 6 Degradación de atrazina por UV-A foto-Fenton: [ATZ]0 = 0.1 mg L-1; $[H_2O_2]_0$ = 5 mg L-1; [Fe2+]0 = 5 mg L-1; pH = 2.7 ± 0.1.**

Finalmente, cuando el proceso de foto-Fenton se llevó a cabo con irradiación UV-C, el proceso de degradación de atrazina se vió significativamente promovido y se alcanzó la completa degradación del compuesto modelo después de tan solo 20 minutos. Este resultado se puede explicar teniendo en cuenta la mayor contribución en término de producción de radical hidroxilo y a la más adecuada longitud de onda de emisión de la radiación luminosa. Adicionalmente, la contribución en término de fotolisis para la desaparición de atrazina no puede ser no considerada. La curva de degradación de atrazina por medio de UV-C foto-Fenton está representada en Figura 7:

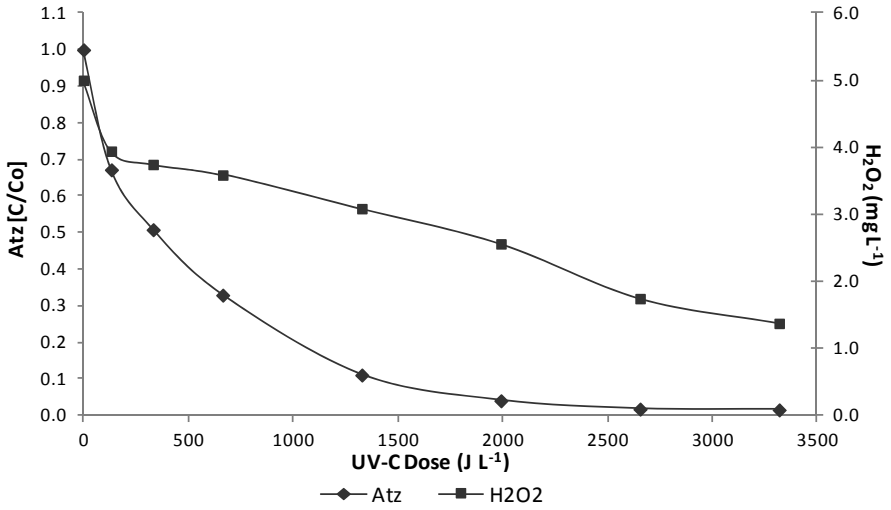


**Figura 7 Degradación de atrazina por UV-C foto-Fenton: $[ATZ]_0$ = 0.1 mg $L^{-1}$; $[H_2O_2]_0$ = 5 mg $L^{-1}$; $[Fe^{2+}]_0$ = 1 mg $L^{-1}$; pH = 2.7 ± 0.1.**

Respecto a la mineralización, aplicando el proceso de Fenton no se pudo observar reducción de contenido orgánico de la solución a lo largo del proceso, solo el 18% pudo ser alcanzado aplicando irradiación UV-A y 40% de mineralización se obtuvo aplicando radiación UV-C.

Finalmente, tras un estudio de costes teniendo en cuenta las eficiencias de tratamiento conseguidas mediante la aplicación de los tres procesos, se pudo identificar el proceso UV-C foto-Fenton como particularmente atractivo para el tratamiento de compuestos recalcitrantes en agua de efluente secundario. La idoneidad del uso de luz UV-C para la irradiación en el caso de proceso modificado y su aplicación a pH neutro aún tiene que ser demostrada.

- **Capítulo 5: "Foto-Fenton a pH próximo a la neutralidad catalizado por quelados de hierro: actividad catalítica y aplicabilidad de cuatro quelados de hierro"**

El estudio presentado en el capítulo 5 se basa en la evaluación de la posible aplicación a pH cercanos a la neutralidad del proceso de foto-Fenton like catalizado por quelados de hierro. Con esta finalidad, la idoneidad por la aplicación de cuatro diferentes agentes quelantes (EDTA, NTA, acido oxálico y acido tartárico) ha sido evaluada. El sulfametoxazole se utilizó como compuesto modelo para la evaluación de la actividad fotocatalítica de los compuestos quelantes en la producción de radicales hidroxilos. Los experimentos se llevaron a cabo bajo irradiación UV-A con el utilizo de 5 mg $L^{-1}$ en forma quelada, 10 mg $L^{-1}$ de $H_2O_2$ para la degradación de 20 mg $L^{-1}$ de SMX.

El primer resultado importante de este estudio se obtuvo tras un análisis de la búsqueda del ratio molar óptimo L:Fe para obtener la completa quelacion del contenido en hierro en solución. Se demostró que el ratio estequiometrico de quelación no permite alcanzar la completa quelación del hierro añadido. Claramente, dependiendo de la estructura química de los compuestos quelados y de la capacidad exhibida para establecer enlaces estables con el $Fe^{3+}$, la cantidad de agente quelante requerido se presenta significativamente variable (Figura 9):

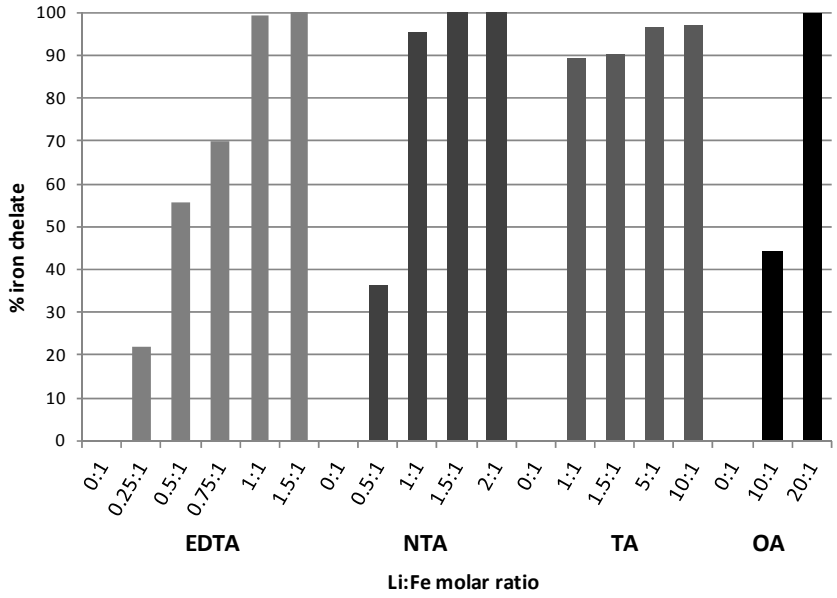


**Figura 8 Porcentaje de quelados de hierro producido en función de L:Fe(III)**

La Tabla 4 resume los ratios molares óptimos del estudio de quelación:

**Tabla 4 Ratios molares óptimos de quelación para los agentes quelantes analizados**

| | L:Fe molar ratio |
|---|---|
| **Fe(III)-EDTA** | 1.5:1 |
| **Fe(III)-NTA** | 1.5:1 |
| **Fe(III)-TA** | 10:1 |
| **Fe(III)-OA** | 20:1 |

Los ratios molares así determinados han sido aplicados en el tratamiento de foto-Fenton like a pH cercano a la neutralidad para la degradación del SMX. Los resultados obtenidos están representados en Figura 10:

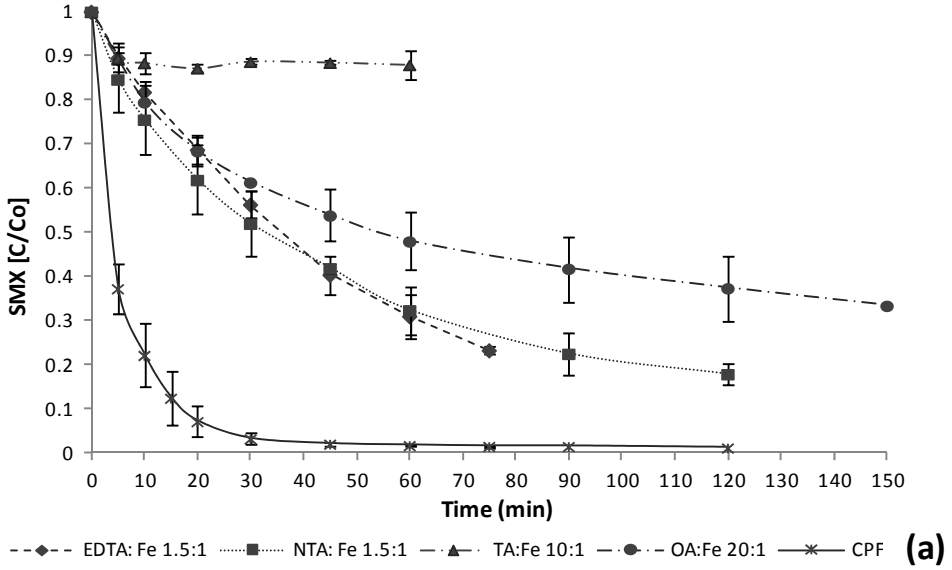


**Figura 9 (a) Degradación de SMX por aplicación de foto-Fenton like a pH neutro catalizado por Fe(III)-L ($Fe^{3+}$ 0.089 mM as Fe(III)-L, pH= 7.0 ±0.7) respecto al obtenido por medio de foto-Fenton convencional (CPF) ($Fe^{2+}$ 0.089 mM as $Fe_2SO_4 \cdot 7H_2O$, pH= 2.8 ±0.1)**

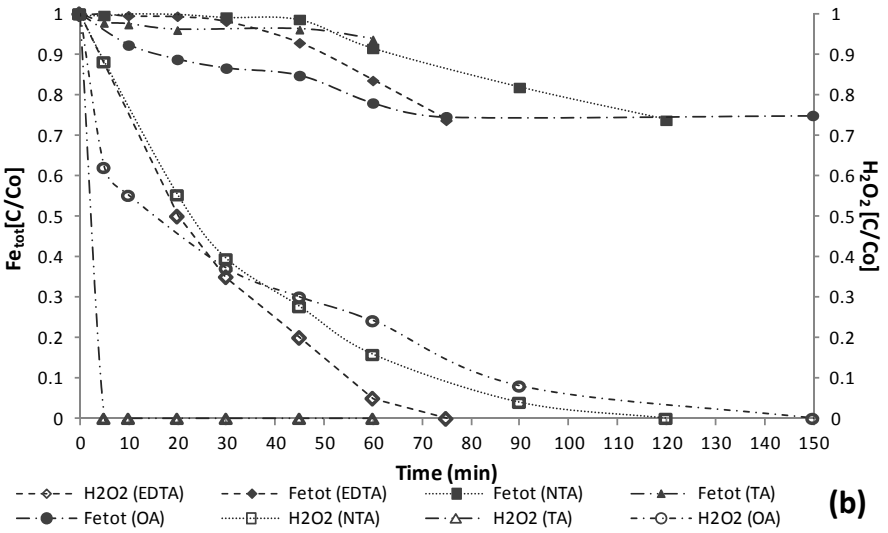


**Figura 9 (b) variación del contenido de hierro durante la reacción frente al consumo de $H_2O_2$**

Los resultados experimentales evidenciaron que el uso de quelados de Fe(III)-EDTA permiten alcanzar un porcentaje de degradación del SMX superior al 77% en un tiempo de reacción de 75 minutos tiempo en el que el $H_2O_2$ resultó completamente consumido. Quelados de Fe(III)-NTA, permitieron alcanzar porcentajes de degradación incluso mayores (83%) aunque en tiempos de reacción ligeramente superiores a los requeridos por el uso de EDTA como agente quelante. Por otro lado, el uso de NTA como agente quelante del hierro se demostró ventajoso por la posibilidad de alcanzar cinéticas de degradación del SMX mayores en los primeros minutos de la reacción. Adoptando quelados Fe(III)-OA, el 66% de eliminación de SMX pudo ser obtenido solo después de 150 minutos de reacción. El elevando contenido de agente quelante utilizado por alcanzar la completa quelación de hierro no fue suficiente a promover una cinética comparable a la obtenida utilizando quelados de EDTA y NTA. Finalmente, los resultados experimentales también pusieron en evidencia como los quelados de acido tartárico (Fe(III)-TA) demostraron ser totalmente ineficaces para alcanzar el objetivo. La degradación del SMX, de hecho no superó el 14% de degradación del contaminante modelo. Conviene destacar, de todas formas, que este dado tiene que ser considerado conjuntamente con el dado experimental que evidencio la drástica desaparición del $H_2O_2$ durante los primeros minutos de reacción. Este resultado esta probablemente relacionado con la presencia de una elevada concentración de ácido tartárico libre que posiblemente actúa como secuestrante de los radicales hidroxilos.

Hay otros resultados muy importantes que conviene comentar y que son apreciables en la Figura 9(b). Respecto a la estabilidad de los quelados a lo largo de la oxidación, se pudo observar cómo, excepto en el caso de Fe(III)-OA, los quelados de hierro son estables durante los primero 45 minutos de reacción. Posteriormente, una gradual perdida en contenido de hierro pudo ser observada. En el caso del ácido oxálico, ya desde el principio de la reacción se pudo observar una reducción gradual en contenido de hierro evidenciando la menor estabilidad de estos respecto a los de EDTA y NTA.

Otro resultado destacable está relacionado con la posibilidad de mayor porcentaje de degradación de SMX cuando se aplican dosis ligeramente superiores a lo estrictamente necesario para la completa quelación del hierro. Es el caso, por ejemplo, de los quelados de

EDTA, un ratio molar de 1:1 L:Fe, prácticamente conduce al 100 % de quelacion. De todas formas una concentración añadida ligeramente superior a la ratio molar 1:1 conduce a mayores degradaciones de SMX. Este resultado es claramente visible en la Figura 10:

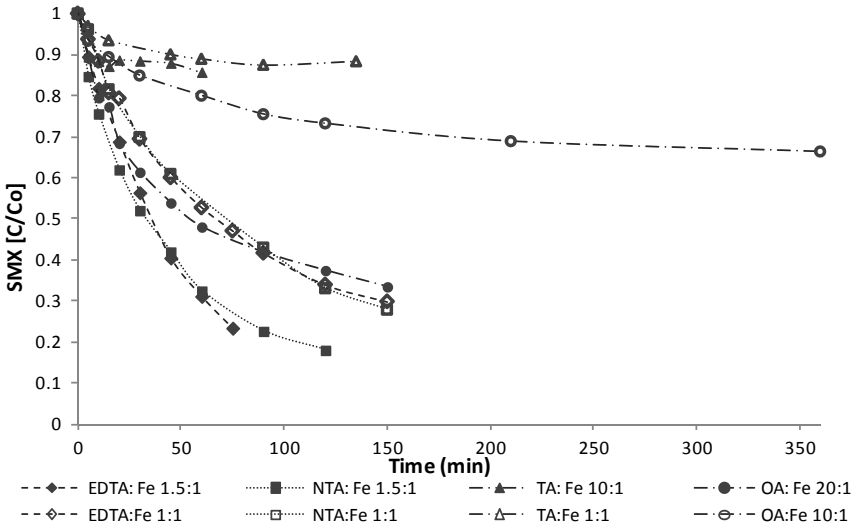


**Figura 10 Evaluación de la actividad catalítica de la degradación del SMX aplicando diferentes L:Fe ratios molares.**

Hay una serie de resultados interesantes que pueden ser obtenidos por el análisis de la figura anterior. Aunque un ratio molar 1:1 L:Fe permite alcanzar un valor muy próximo al 100% de quelación, en el caso de NTA y EDTA, la reducción de los ratio molares determinaron una indiscutible reducción en cinética por la degradación del SMX. Este efecto fue tanto más evidente en el caso del ácido oxálico. En este caso, reduciendo el ratio molar de quelación a valores de 10:1, los quelados de Fe(III)-OA solo permitieron alcanzar una reducción de SMX de 30% aproximativamente en un tiempo de reacción de 350 minutos. Finalmente reduciendo el ratio molar de quelación TA:Fe a 1:1 como indicado por estudio de literatura (Sun and Pignatello 1992) se pudo observar que el efecto secuestrante no pudo ser igualmente limitado y así como observado anteriormente, la completa desaparición del $H_2O_2$ fue apreciada inmediatamente en los primeros minutos.

Desde el punto de vista de la actividad catalítica, estos resultados evidenciaron que el NTA es el compuesto quelante más indicado para la aplicación de entre los agentes quelantes considerados en este estudio. Teniendo en cuenta la mayor biodegradabilidad y la menor toxicidad del NTA respecto al EDTA, se refuerza su idoneidad. La mayor idoneidad respecto a los otros agentes quelantes utilizados, también fue evaluado desde un punto de vista económico y de sostenibilidad ambiental. Conviene señalar que los agentes quelantes son compuestos orgánicos cuya adición al medio puede determinar una fuente de contaminación adicional. Es por esta razón que su uso no puede realizarse sin condiciones. La contribución en término de carbono orgánico total (COT) correspondiente a los ratios molares adoptados, ha sido entonces calculada. Además el mayor costo debido a su utilización ha sido también calculado utilizando el método propuesto por Bolton et al. (2001) basado en el coste eléctrico por orden de magnitud. En la Figura 12 se han representado el incremento de COT frente al coste por cada uno de los ratios molares L:Fe considerados en este capítulo.

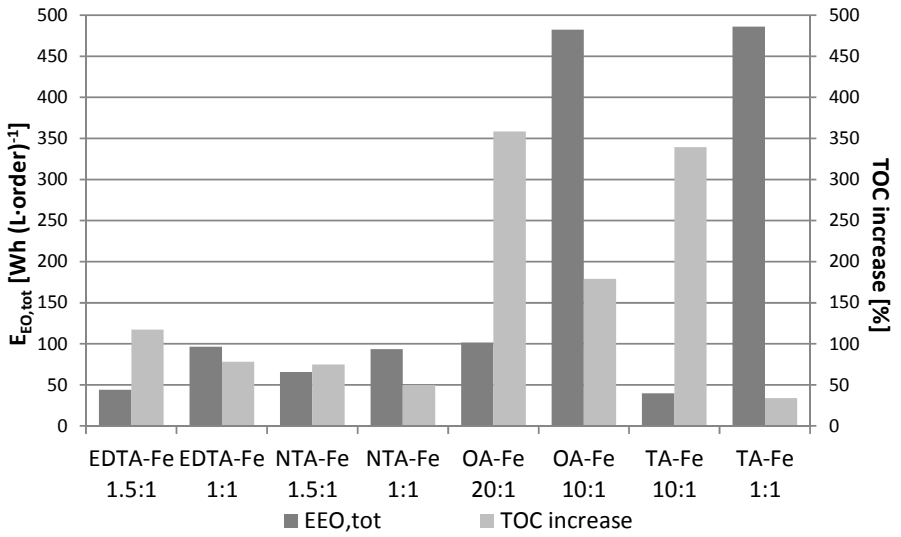


**Figura 11 Estimación de costes frente el incremento de COT debido a la aplicación del proceso de foto-Fenton catalizado por quelados de hierro en diferentes ratios molares.**

Del estudio económico y de sostenibilidad así realizado se puede, entonces, deducir como efectivamente la aplicación de los quelados de Fe(III)-NTA en el ratio molar 1.5:1 destaque como la solución más sostenible entre todas las que se han evaluado.

- **Capítulo 6: "Quelados de Fe(III)-NTA: estabilidad y aplicabilidad en el proceso foto-Fenton a pH neutro"**

En el capítulo anterior, se ha evidenciado como entre los quelados considerados por aplicación en foto-Fenton like a pH neutro, el NTA resulta el más atractivo desde el punto de vista de su actividad catalítica y desde el punto de vista económico y de sostenibilidad ambiental. El capítulo 6, se ha dedicado a la discusión de los resultados experimentales obtenidos mediante un estudio de estabilidad sobre los quelados Fe(III)-NTA. El conocimiento de la respuesta de los quelados de hierro debido a su exposición a los factores de estrés por la aplicación del proceso se traduce en un instrumento útil para la previsión de la durabilidad de los quelados y como consecuencia de la actividad catalítica esperable.

La estabilidad de los quelados ha sido evaluada bajo estrés térmico, oxidativo y fotoquímico. Para esto, la estabilidad de la solución de quelados ha sido monitoreada bajo diferentes condiciones de temperatura, bajo la aplicación de diferentes dosis de $H_2O_2$ y también bajo irradiación realizada por medio de diferentes fuentes (lámparas UV-A, UV-C y Xenón).

Los resultados experimentales demostraron que la temperatura por sí solo no determina la aparición de fenómenos de inestabilidad de los quelados. También se ha demostrado que durante los 9 días en el que la solución ha sido monitoreada, ningún cambio en el contenido de hierro ha sido detectado. Este resultado es particularmente importante desde un punto de vista operativo, ya que permite la posibilidad de poder mantener almacenada la solución de quelados en tiempo en el caso de una real aplicación en planta.

Mediante la Irradiación de la solución de quelados con luz UV-A (Figura 12) se pudieron seguir los fenómenos de inestabilidad de los quelados. También se constató que controlando la

temperatura de la solución los efectos debido a la irradiación podían ser reducidos. En particular, cuando la temperatura se mantuvo entre 10 y 15 °C, no se registró ninguna pérdida de hierro, lo que constituye una demostración de que los quelados de hierro no subieron ninguna descomposición en las dos horas en las que se monitoreo la solución. Pero cuando la temperatura de la solución se mantuvo constante entre los valores de 20-25°C, se apreció una gradual perdida de hierro que empezó a tener lugar a los 60 minutos de irradiación. Finalmente, controlando la temperatura de la solución a valores de 30°C, la ruptura de los quelados de hierro se realizó a partir de los 45 minutos de reacción. Bajo los efectos de la irradiación, también pudo apreciarse una gradual mineralización de la solución.

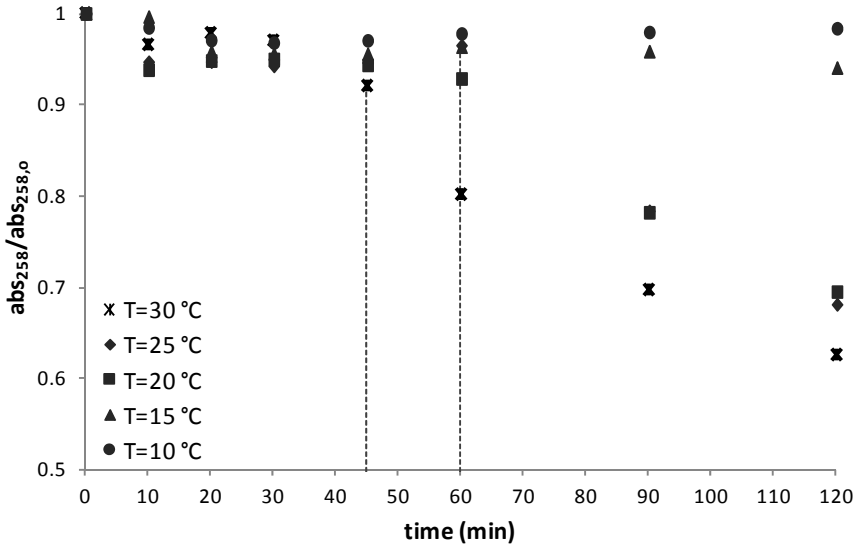


**Figura 12 Estabilidad de la solución de quelados bajo irradiación UV-A y diferentes temperaturas**

Con la adición de $H_2O_2$ en concentración de 0.59 mM (Figura 13), se apreció una gradual reducción en contenido de hierro ya desde los primeros minutos de reacción. La reducción de temperatura, en este caso, no permitió posponer el instaurarse de fenómenos de inestabilidad pero si consintió reducir el porcentaje de pérdida total. También en este caso se registró una gradual mineralización de la solución, que así como se había registrado por la perdida en contenido de hierro, empezó ya desde los primeros minutos de reacción.

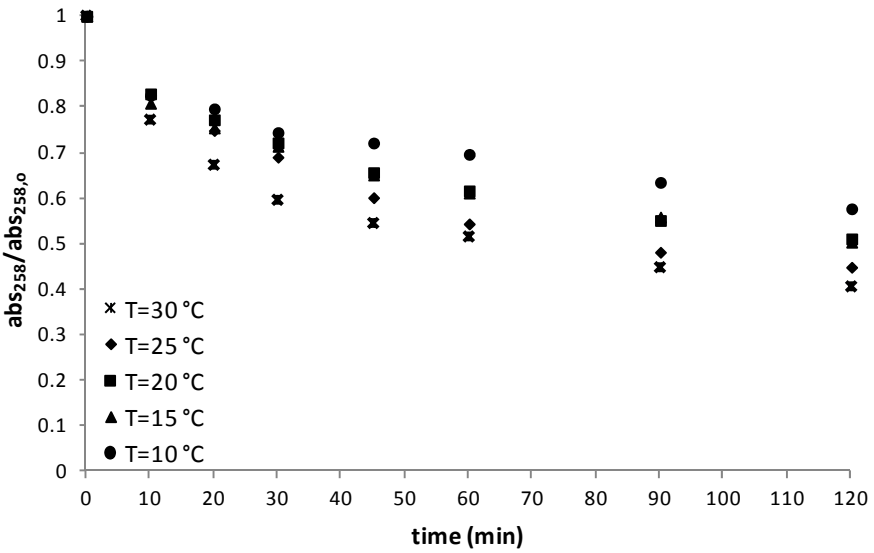


**Figura 13 Estabilidad de la solución de quelados a diferentes temperaturas en presencia de 0.59 mM H2O2 y irradiación UV-A**

Variando la dosis de $H_2O_2$ desde el valor de 0.59 a 2.94 mM se pudo determinar una correlación de tipo linear entre la perdida de hierro y la concentración añadida (Figura 14).

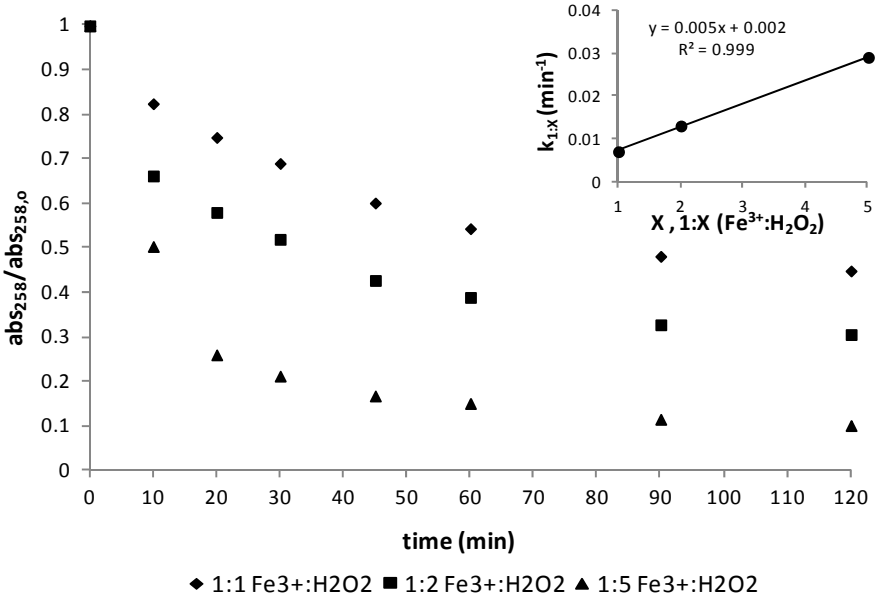


**Figura 14 Relacion linear entre la dosis de $H_2O_2$ y roptura de los quelados**

Finalmentese usaron tres diferentes fuentes de radiación con el objetivo de determinar aquella que permitiera extender la vida útil de los quelados. Por esta razón, en presencia de $H_2O_2$ 0.59 mM se irradió la solución con lámparas UV-A, UV-C y de Xenón. Lo que se observó, es que debido a la mayor absorbancia de la solución en correspondencia a la máxima emisión de las lámparas de tipo UV-C, una reducción de casi el 80 % pudo ser obtenida con una dosis de 1.5 kJ $L^{-1}$. En el caso de irradiación con lámpara de Xenón, la ruptura de los quelados de hierro se produjo en menor medida respecto a lo que se había obtenido en el caso del utilizo de lámparas UV-C pero de contra el efecto fue mucho más marcado que en el caso del uso de

lámpara UV-A. Estas demostraron ser las más indicadas, desde el punto de vista de la estabilidad de los quelados, para llevar a cabo el proceso de foto-Fenton like a pH neutro.

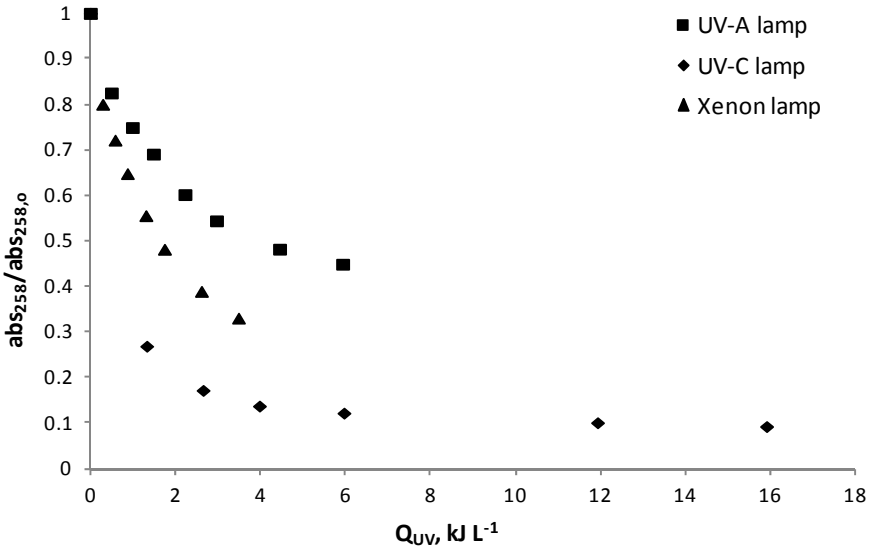


**Figura 15 Influencia del tipo de irradiación aplicada sobre la estabilidad de los quelados**

- **Capítulo 7: "Influencia de la composición del afluente en las eficiencias de degradación"**

En el capítulo anterior se ha demostrado como los parámetros operativos de proceso pueden influir significativamente en las eficiencias de proceso. Parámetros externos al proceso, como por ejemplo la calidad de la matriz a tratar, también pueden determinar una significativa reducción de las eficiencias. Este capítulo se ha dedicado al estudio de como los parámetros más significativos de la matriz acuosa influyen en el rendimiento del proceso. Por esta razón cuatro matrices diferentes han sido dopadas con el contaminante modelo (SMX) para estudiar su degradación. Las matrices utilizadas han sido: agua Milli-Q, agua procedente de la rete de distribución urbana de Barcelona (tap water, TW), efluente secundario procedente de una estación de depuración de agua residual (wastewater, WW) y agua de pozo (well water, HW). Las principales características de estos efluentes están resumidas en Tabla 5:

**Tabla 5 Caracteristicas de las matrices acuosas utilizadas para los experimentos**

| | **Milli-Q (MQ)** | **Agua de red (TW)** | **Agua residual (WW)** | **Agua de pozo (HW)** |
|---|---|---|---|---|
| **Origen** | Merk-Millipore | Barcelona (Catalunya) | WWTP Calafell (Catalunya) | Pacs del Penedès (Catalunya) |
| **pH** | 5.3 | 7.5 | 7.4 ± 0.02 | 7.9 |
| **NPOC (mg $L^{-1}$)** | «1 | 3.7± 2.9 | 7.2 ± 1.7 | 1.6± 0.7 |
| **IC (mg $L^{-1}$)** | «1 | 31.6± 4.1 | 78.7 ± 5.1 | 35.5± 0.6 |
| **TN (mg $L^{-1}$)** | «1 | 1.8± 0.6 | 22.7 ± 15.1 | 22.4± 0.4 |
| **$Na^+$ (mg $L^{-1}$)** | «1 | 66.7 ± 40.1 | 392.2 ± 35.7 | 41.3 ± 9.5 |
| **$NH_4^+$ (mg $L^{-1}$)** | «1 | <LOD | 20.1 ± 28.5 | <LOD |
| **$K^+$ (mg $L^{-1}$)** | «1 | 11.9 ± 6.6 | 22.9 ± 0.4 | 1.4 ± 1.4 |
| **$Ca^{2+}$ (mg $L^{-1}$)** | «1 | 35.7 ± 6.9 | 71.5 ± 11.2 | 55.9 ± 0.9 |
| **$Mg^{2+}$ (mg $L^{-1}$)** | «1 | 16.2 ± 5.1 | 59.7 ± 8.5 | 66.4 ± 2.7 |
| **Alcalinidad ($mg_{CaCO3}$ $L^{-1}$)** | «1 | 143.29 ± 16.2 | 209.7 ± 14.2 | 158.6± 2.8 |

La elevada concentración de calcio y magnesio, sobretodo en el caso de WW y HW generaron un fenómeno de competición para la formación de complejos con el NTA. Aunque las constante de estabilidad de los quelados Fe(III))-NTA sean mayores de las de los quelados Ca(II)-NTA y Mg(II)-NTA, las elevadas concentraciones de estos cationes, evidentemente, favorecen el intercambio del ion central del quelado, determinando así una pérdida de hierro por precipitación. Las concentraciones iniciales de hierro en forma quelada para las diferentes matrices se hallan indicadas en la Tabla 6.

**Tabla 6 Concentración de hierro en forma quelada en las matrices consideradas**

| | $Fe_{tot,0}$ [mg $L^{-1}$] |
|---|---|
| **Milli-Q (MQ)** | 4.6 |
| **Agua de red (TW)** | 4.6 |
| **Agua residual (WW)** | 2.6 |
| **Agua de Pozo (HW)** | 2.8 |

La degradación de SMX en las matrices reales obtenida aplicando el proceso de foto-Fenton con las concentraciones iniciales de hierro así definidas se encuentran representadas en la Figura 16.

Tal como se esperaba, el mayor porcentaje de SMX eliminado correspondió al agua Milli-q, mientras los porcentaje de degradaciónes registrados por tratamiento en las otras matrices fueron particularmente reducidos. El 50% de degradación fue obtenido en TW y HW mientras en WW no fue posible alcanzar eficiencias superiores a 30%. La menor eficiencia registrada en la degradación de SMX en las matrices reales se debe al mayor contenido en carbonatos y materia orgánica, que actúan como secuestrantes de los radicales, reduciendo así la cantidad disponible para la oxidación del SMX. En las dos matrices en las que no fue posible alcanzar la quelación del contenido total de hierro, no se observó perdida de hierro durante los 120 minutos de reacción. En este caso, la menor concentración en quelados, catalizadores de la reacción de descomposición del peróxido de hidrogeno, fue responsable de una menor producción de radicales y, en consecuencia de un menor ataque oxidativo a los quelados. Una gradual perdida de hierro fue a su vez registrada cuando la reacción se llevó a cabo en MQ y TW. En el primer caso, los quelados fueron estables hasta los 45 minutos de reacción mientras en TW la perdida de hierro tuvo lugar a partir de los 20 minutos de reacción. El mayor contenido en iones de calcio y magnesio en este caso, pudo determinar el establecimiento de unas condiciones menos favorables para la estabilidad de los quelados, favoreciendo probablemente el intercambio del metal central con las otras especies iónicas presentes en solución.

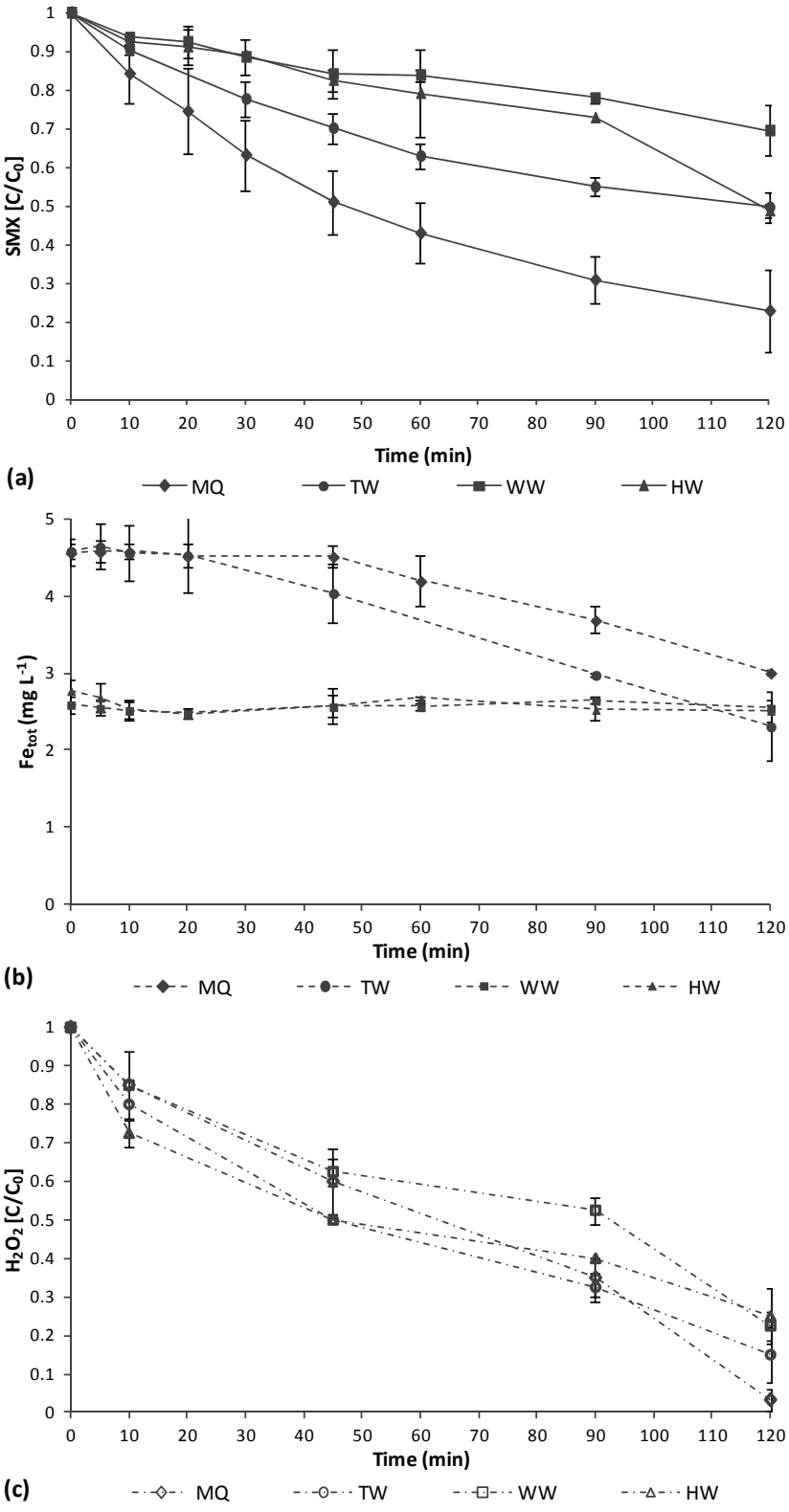


**Figura 16 (a) Degradación de SMX por Fe(III)-NTA/$H_2O_2$/UV en las matrices reales consideradas. (b) Estabilidad de los quelados a lo largo de la reacción. (c) Concentración Consumo de peróxido de hidrógeno en la degradación de SMX por Fe(III)-NTA/$H_2O_2$/UV en las matrices reales consideradas.**

En el intento de obtener una mejor degradación del contaminante modelo y de extender la vida útil de los quelados, se aplicó una estrategia para limitar la exposición de los complejos a

los estreses de tipo oxidativo y fotoquímico. Para esta finalidad, se realizó una dosificación de los complejos. Los resultados obtenidos no fueron satisfactorios. Con esta estrategia, pudo ser obtenida la zona de mayor estabilidad de los quelados, pero esto no se tradujo en una mejora en términos de degradación de SMX. Un diferente esquema de dosificación podría, probablemente, permitir degradaciones mayores.

También se adoptaron otras estrategias para la degradación de SMX en agua Milli-Q. La degradación adicional debida a la adición de iones de $Mn^{2+}$ fue evaluada. Li et al. (2016) demostraron que la mediación de $Mn^{2+}$ promueve la producción de radicales $O_2\cdot^-$ con consiguiente mejora de las eficiencias de degradación (Li et al. 2016). Además, el peróxido de hidrogeno fue sustituido por persulfato $S_2O_8^{2-}$ para promover su activación por medio de Fe(III)-NTA y formación de radicales $SO_4\cdot^-$. Finalmente la dosificación de quelados de hierro también fue aplicada en agua Milli-Q.

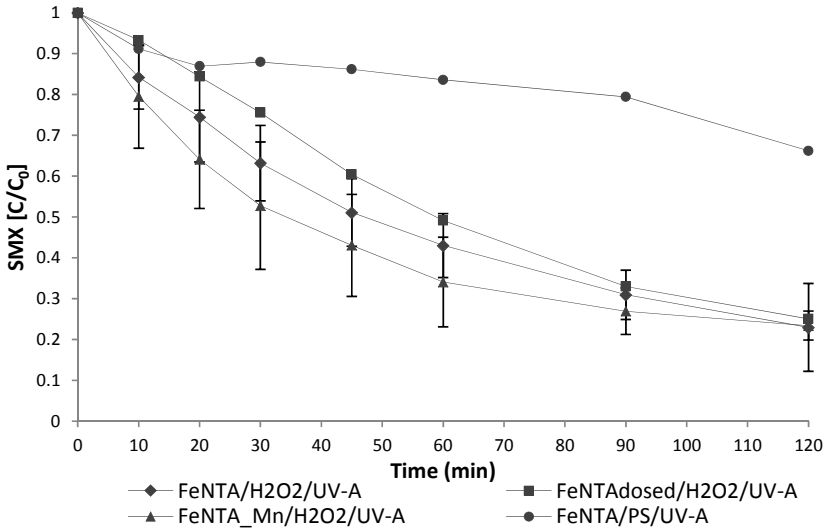


**Figura 17 Degradación de SMX obtenida tras aplicación de diferentes estrategias de tratamiento**

Los resultados mostraron como, aunque en los experimentos con y sin adición de $Mn^{2+}$, el porcentaje final de degradación fuese del todo comparable (78% y 77% respectivamente), la curva de degradación de SMX en presencia de $Mn^{2+}$ exhibió una mayor degradación en los primeros minutos de reacción. La sustitución de $H_2O_2$ por $S_2O_8^{2-}$ se demostró del todo ineficaz bajo estas condiciones operativas y de irradiación UV-A.

- **Capítulo 8: "Degradación de contaminantes orgánicos por medio de UV/$Fe^{2+}$/PS en presencia de bromatos"**

El capítulo experimental final de la tesis doctoral se dedica a la discusión de los resultados obtenidos de un estudio llevado a cabo en la Universidad de Cincinnati, bajo la supervisión del Prof. Dionisyou.

El objetivo de este estudio era la determinación de los efectos que la presencia de bromatos determina en la degradación de contaminantes orgánicos por aplicación del proceso de UV/PS y UV/$Fe^{2+}$/PS. Por esta razón, compuestos tales como benzophenone-4 (BZ4), nitrobenzene (NB), ácido nitrobenzoico (NBA), atrazina (ATZ) y ampicilina (AMP) en concentración de 40 µM

fueron utilizados para dopar soluciones sintéticas en presencia de PS 500 µM, $Fe^{2+}$ 20 µM y $Br^-$ 5 mM.

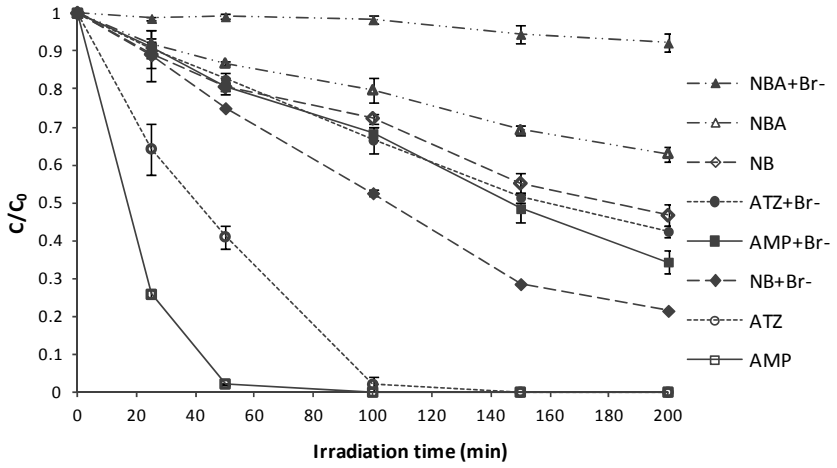


**Figura 18 Efecto de la presencia de $Br^-$ en la degradación de diferentes compuestos orgánicos**

Los resultados mostraron como la degradación de casi todos los compuestos (todos menos NB) se vio inhibida por la presencia de $Br^-$ (Figura 18). Este efecto se debe a un efecto de competición por los radicales disponibles para la reacción en presencia de $Br^-$, altamente reactivo con las especies radicales en solución (Tabla 7).

**Tabla 7 Constantes cinéticas de reacción con los radicales HO· y $SO_4^{\cdot -}$ de los compuestos en solución frente a las eficiencias obtenidas por la aplicación del tratamiento**

| | k ($M^{-1}s^{-1}$) | | | | η (%) (**) | |
|---|---|---|---|---|---|---|
| | HO· | | $SO_4^{\cdot -}$ | | con $Br^-$ | Sin $Br^-$ |
| **BZ4** | $4.86 \times 10^9$ | | $5.90 \times 10^8$ | | 44 | 55 |
| **NBA** | $2.60 \times 10^9$ | (Buxton et al. 1988) | $\leq 10^6$ | (Neta et al. 1977) | 8 | 37 |
| **NB** | $3.90 \times 10^9$ | (Buxton et al. 1988) | $\leq 10^6$ | (Neta et al. 1977) | 79 | 53 |
| **ATZ** | $(2.60 \pm 0.4) \times 10^9$ | (Haag and Yao 1992) | $2.59 \times 10^9$ | (Khan et al. 2014) | 58 | 100 |
| **AMP** | $4.87 \times 10^9$ | (He et al. 2014) | $2.00 \times 10^9$ | (He et al. 2014) | 66 | 100 |
| **$Br^-$** | $1.10 \times 10^{10}$ | (Buxton et al. 1988) | $3.50 \times 10^9$ | (Neta et al. 1977) | - | - |

Respecto a lo que se observó en el caso de los otros contaminantes orgánicos considerados, el ión Br- favoreció la degradación de NB. Este efecto ya habia sido observado en otros estudios (Wu et al. 2015), aunque no pudo ser reproducido en otros compuesto con características químicas similares como el NBA.

Aunque se requieran estudios adicionales para la interpretación de los efectos beneficiosos en la degradación de NB debido a la presencia de $Br^-$, los resultados presentados en este capítulo reiteran la evidencia que la composición de la solución de tratamiento puede significativamente influenciar las eficiencias de proceso obtenible. Además, estudios adicionales también deberían de ser focalizados en la determinación de la posible formación

de bromuros por efecto de la oxidación de los bromatos. Este punto representa un elemento fundamental para la evaluación de la idoneidad de aplicación de procesos basados en radicales sulfatos en el tratamiento de afluente contenientes bromatos.

## Conclusiones

Las conclusiones más importantes que pueden ser deducidas desde esta tesis, pueden ser resumidas como sigue:

- El Fe(III)-NTA se distinguió por una mayor actividad catalítica junto con una mejor idoneidad desde el punto de vista medio ambiental. Así que, entre los quelados de hierro analizados, Fe(III)-NTA se identifica como el más adecuado para llevar a cabo el proceso de foro-Fenton like a pH neutro.
- El control de temperatura de los quelados de hierro puede representar una herramienta importante para extender la vida útil de los complejos de hierro cuando son expuestos a estrés oxidativo fotoquímico durante el tratamiento.
- Una correlación de tipo linear existe entre la concentración de oxidante utilizado y la pérdida de hierro exhibida.
- La Irradiación UV-A limita la aparición de fenómenos de inestabilidad durante el tratamiento.
- La presencia de iones de $Ca^{2+}$ y $Mg^{2+}$ afectan de manera significativa el contenido en quelados de hierro disponible para la reacción.
- Elevados valores de alcalinidad y COT se traducen en una menor eficiencia de degradación del contaminante SMX debido al secuestro de los radicales hidroxilos.
- La dosificación del hierro permitió extender la vida útil de los quelados, pero en las condiciones experimentales consideradas no produjo una eliminación adicional del SMX.
- La adición de $Mn^{2+}$ para favorecer la producción de radicales $O_2{\cdot}^-$ se demostró prometedora para mejorar la cinética de la degradación aunque, en las condiciones experimentales adoptadas, no pudo conseguirse una mayor degradación del SMX.
- La aplicación de Fe(III)-NTA/PS/UV-A demostró no ser una estrategia válida para el tratamiento SMX bajo las condiciones consideradas en este estudio.
- En los tratamientos $Fe^{2+}$/PS/UV, la presencia de bromatos presenta una gran influencia en la degradación de contaminantes emergentes.

## Bibliografia

Bolton JR, Bircher KG, Tumas W, Tolman CA (2001) Figures-of-merit for the technical development and application of advanced oxidation technologies for both electric- and solar-driven systems (IUPAC Technical Report). Pure Appl Chem 73:627–637. doi: 10.1351/pac200173040627

Buxton G V., Greenstock CL, Helman WP, Ross, AB, Tsang, W (1988) Critical Review of rate constants for reactions of Hydrated Electrons, Hydrogen Atoms and Hydroxyl radicals (·OH/·O-) in Aqueous Solution. J Phys Chem Ref Data 17:513–886. doi: 10.1063/1.555805

Clara M, Strenn B, Gans O, Martinez, E, Kreuzinger, N, Kroiss, H (2005) Removal of selected pharmaceuticals, fragrances and endocrine disrupting compounds in a membrane

bioreactor and conventional wastewater treatment plants. Water Res 39:4797–807. doi: 10.1016/j.watres.2005.09.015

De la Cruz N, Romero V, Dantas RF, Marco P, Bayarri B, Giménez J, Esplugas S (2013) o-Nitrobenzaldehyde actinometry in the presence of suspended TiO2 for photocatalytic reactors. Catal Today 209:209–214. doi: 10.1016/j.cattod.2012.08.035

Garrido-Ramírez EG, Theng BK., Mora ML (2010) Clays and oxide minerals as catalysts and nanocatalysts in Fenton-like reactions — A review. Appl Clay Sci 47:182–192. doi: 10.1016/j.clay.2009.11.044

Ginebreda A, Muñoz I, de Alda ML, Brix R, López-Doval J, Barceló D (2010) Environmental risk assessment of pharmaceuticals in rivers: relationships between hazard indexes and aquatic macroinvertebrate diversity indexes in the Llobregat River (NE Spain). Environ Int 36:153–62. doi: 10.1016/j.envint.2009.10.003

Glassmeyer ST, Furlong ET, Kolpin DW, Cahill JD, Zaugg SD, Werner SL, Meyer MT, Kryak DD (2005) Transport of Chemical and Microbial Compounds from Known Wastewater Discharges: Potential for Use as Indicators of Human Fecal Contamination. Environ Sci Technol 39:5157–5169. doi: 10.1021/es048120k

Haag WR, Yao CCD (1992) Rate Constants for Reaction of Hydroxyl Radicals with Several Drinking Water Contaminants. Environ Sci Technol 26:1005–1013.

He X, Mezyk SP, Michael I, Fatta-Kassinos D, Dionysiou DD (2014) Degradation kinetics and mechanism of β-lactam antibiotics by the activation of $H_2O_2$ and Na2S2O8 under UV-254nm irradiation. J Hazard Mater 279:375–383. doi: 10.1016/j.jhazmat.2014.07.008

Khan JA, He X, Shah NS, Khan HM, Hapeshi E, Fatta-Kassinos D, Dionysiou DD (2014) Kinetic and mechanism investigation on the photochemical degradation of atrazine with activated $H_2O_2$, S2O82− and HSO5−. Chem Eng J 252:393–403.

Kim SD, Cho J, Kim IS, Vanderford BJ, Snyder SA (2007) Occurrence and removal of pharmaceuticals and endocrine disruptors in South Korean surface, drinking, and waste waters. Water Res 41:1013–21. doi: 10.1016/j.watres.2006.06.034

Kuhn HJ, Braslavsky SE, Schmidt R (2004) Chemical actinometry ( IUPAC Technical Report ). Pure Appl Chem 76:2105–2146.

Li Y, Sun J, Sun S-P (2016) Mn2+-mediated homogeneous Fenton-like reaction of Fe(III)-NTA complex for efficient degradation of organic contaminants under neutral conditions. J Hazard Mater 313:193–200. doi: 10.1016/j.jhazmat.2016.04.003

Meneses M, Pasqualino JC, Castells F (2010) Environmental assessment of urban wastewater reuse: treatment alternatives and applications. Chemosphere 81:266–72. doi: 10.1016/j.chemosphere.2010.05.053

Neta P, Madhavan V, Zemel H, Fessenden RW (1977) Rate constants and mechanism of reaction of sulfate radical anion with aromatic compounds. J Am Chem Soc 99:163–164. doi: 10.1021/ja00443a030

Nogueira RFP, Oliveira MC, Paterlini WC (2005a) Simple and fast spectrophotometric determination of $H_2O_2$ in photo-Fenton reactions using metavanadate. Talanta 66:86–91. doi: 10.1016/j.talanta.2004.10.001

Pignatello JJ, Oliveros E, MacKay A (2006) Advanced Oxidation Processes for Organic Contaminant Destruction Based on the Fenton Reaction and Related Chemistry. Crit Rev Environ Sci Technol 36:1–84. doi: 10.1080/10643380500326564

Richardson SD (2008) Environmental mass spectrometry: emerging contaminants and current issues. Anal Chem 80:4373–4402. doi: 10.1021/ac800660d

Sun Y, Pignatello JJ (1992) Chemical treatment of pesticide wastes. Evaluation of iron(III) chelates for catalytic hydrogen peroxide oxidation of 2,4-D at circumneutral pH. J Agric Food Chem 40:322–327. doi: 10.1021/jf00014a031

Sun S-P, Zeng X, Li C, Lemley AT (2014) Enhanced heterogeneous and homogeneous Fenton-like degradation of carbamazepine by nano-Fe3O4/ $H_2O_2$ with nitrilotriacetic acid. Chem Eng J 244:44–49. doi: 10.1016/j.cej.2014.01.039

Tao, X., Su, J., Wang, L., Chen, JF., (2008) A new heterogeneous catalytic system for wastewater treatment: Fe-immobilized polyelectrolyte microshells for accumulation and visible light-assisted Fotooxidative degradation of dye pollutants. J. Mol. Catal. A: Chem., 280 (1-2), 186-193.

Teijon G, Candela L, Tamoh K, et al (2010) Occurrence of emerging contaminants, priority substances (2008/105/CE) and heavy metals in treated wastewater and groundwater at Depurbaix facility (Barcelona, Spain). Sci Total Environ 408:3584–95. doi: 10.1016/j.scitotenv.2010.04.041

WHO/UNICEF (2014) World Health Organization, Progress on drinking water and sanitation. World Health Organization, South-East Asia Regional Office

World Water Council (2015) Delivering a pact for water security World Water Council 2013-2015 Triennial Report.

Wu Y, Bianco A, Brigante M, et al (2015) Sulfate Radical Photogeneration Using Fe-EDDS: Influence of Critical Parameters and Naturally Occurring Scavengers. Environ Sci Technol 49:14343–9. doi: 10.1021/acs.est.5b03316